UNIVERSITY OF CALIFORNIA, SAN DIEGO

The distribution of suspended microplastics and nanoplastics in the Northeast Pacific and their effects on zooplankton consumers

A dissertation submitted in partial satisfaction of the requirements for the degree Doctor of Philosophy

in

Oceanography

by

Jennifer Anne Brandon

Committee in charge:

Professor Mark D. Ohman, Chair
Professor Lihini I. Aluwihare
Professor Amro Hamdoun
Professor Michael R. Landry
Professor Michael Sailor

2017

The Dissertation of Jennifer Anne Brandon is approved, and it is acceptable in quality and form for publication on microfilm and electronically:

Chair

University of California, San Diego

2017

DEDICATION

To Mom, Dad, and Kristi, for all the phone calls. And to Jeanne and Aunt Ruth, for all the cards. You kept me sane, you reminded me I was loved, and you believed in me when I didn't.

TABLE OF CONTENTS

LIST OF FIGURES

LIST OF TABLES

ACKNOWLEDGEMENTS

Many people have told me over these five and a half years, “your PhD isn’t a sprint, it’s a marathon.” I don’t think it's either. I think grad school is a team sport. There are so many people that have their handprints on this dissertation and have deeply impacted the last half decade of my life, and I am so thankful for all of them.

I must start with Mark Ohman. Mark, thank you for making me a better scientist than I thought I could be. Thank you for pushing me to be better and work harder every single day, and for always reminding me what it looks like to truly love coming to work everyday.

Mike Landry, thank you for your calming presence and your big perspective, and for allowing me to move into your lab and your grad students’ office and do two of my chapters as a defacto Landry lab member. Mike Sailor, thank you for all your knowledge and chemistry expertise – this dissertation truly could not have happened without you. And thank you for letting me do my other two chapters in your laboratory. Amro Hamdoun, thank you for always reminding me our work is more important and has a bigger impact than just some data, and inspiring me to think about my science in unique ways. Lihini Aluwihare, thank you for being a badass woman scientist, answering every chemistry question I had, and for always believing in me and my love for life outside academia. I’m sorry I had to be the one to tell you that Prince died.

To the #uhOhman lab, thank you for going down the rabbit hole of grad school with me these last five years. To the older cohort of Ohman lab members – Alison, Miriam, and Jesse – thank you for imparting so much knowledge and wisdom to me right as you were leaving. You didn’t have to invest any time in this perky, excited first year,

but you did and you made my life so much easier because of it. Amanda, thank you for joining the lab. I needed you. Thank you for being so cool, and being the best officemate, and reminding me that it's never too late to get fully out of my comfort zone. To Cat, thank you for being my friend, and bonding with me over so many things outside the world of science. I'm so glad we'll both be around next year. To Bengineer, thank you for all the sports, all the hugs, all the long, long days at sea. I'll sing country with you while flipping ethanol any day buddy. To Jeff, you are honestly one of the smartest people I have ever met, but also one of the nicest and most humble. I am so glad you found us. To Laura, you never stop moving and I'm so inspired by it. To Stephanie, I can't wait to see where you go.

I would be remiss to not thank Miriam again, because I never would have come to grad school if it weren't for you and your brilliance in research and science outreach. Reading about plastic in People magazine got me here, where I studied the very SEAPLEX samples I read about as a wide-eyed junior in college, and now I'm off to do a career in science outreach myself. Thank you for teaching me about plastic and science communication and answering my 10,000 emails over the last 5 years. And thanks for going from being a scientific hero of mine to my good friend.

To all of my undergrads, Linda, Alicia, Eric, Emily, India, Sara, and Eliya, and my volunteer Sam, thank you for putting in all the countless hours of labwork. Without you, so much of this work couldn't have been possible. You are all incredible and I am looking forward to seeing where your career paths take you. To my coauthors, Ali Freibott and Bill Jones, thank you for sharing your scientific expertise and overlapping your experimental worlds with the world of marine debris.

To my BO cohort of ladies, Eiren, Natasha, Lynn, and Heather, it is a privilege to be surrounded by such incredible, accomplished, badass women daily. I can't count how many ways you have all inspired me as scientists, coworkers, and friends. The things I have learned from you about life, work-life balance, science, and relationships are invaluable. Can't wait until you all are running the scientific world someday. To my entire 2012 cohort, you are all so brilliant, so fun, and so nice. From first-year classes, catching up at TGs, nights on the town, and now watching each other publish incredible papers and sign the rafters in Surfside, it is a privilege to know you all. To so many other Scripps friends: Belli, Bryce, Jess, Amy, Stephanie, Christian, Julia, Alain, Noelle, Emily, and so many others, I will miss you all so much. Scripps has been a hard road for me, but you have all made it worthwhile.

To all the people that help make Scripps students lives livable, thank you. To the communications office, thank you for helping me disseminate my science while also being a buffer when I needed you to be. To the development office, thank you for always being so excited about what I had to offer. Thank you to the grad office and IOD for everything – for answering all my questions, for believing in us, and for advocating for us. Your smiling faces have been so important to me.

To the staff of Birch Aquarium, you have always been such an important part of my experience at Scripps. I have loved every experience getting to volunteer with you and be a part of the numerous activities happening at the Aquarium. Thank you for everything you have taught me, and for always being such a breath of fresh air. I am so excited to become a part of the Birch family.

Finally, to my team. To Kelsey, Kayla, Emma, and Linsey, you are all the

powerful ladies I wish I could be. Thank you all for choosing to be in the Ohman Lab when you didn't even need to. To Kelsey, thank you for listening to all my early-20s drama, when I was young and dumb and didn't know what I was doing in science or life. To Emma, you inspire me everyday to speak up for myself and to take no prisoners. To Kayla, you are quite simply one of the coolest people I know. Thank you for being undeniably yourself at all times, and for liking me for just who I am. Linsey, it is one of my greatest accomplishments of grad school that Kayla and I went from having a friend crush on the coolest girl at Scripps to being actual great friends with you. I literally could not have done it without you. Don't ever forget how invaluable you are. To Ali, thank you for every single minute of our friendship. Thank you for all the commiseration, all the moments at sea, all the long days in your office, all the shots of whiskey, all the texts since you left, all the everything. From the very first SKrillEx when Team JenniAli was born, you have been one of the brightest lights of grad school. Mike Navarro, thank you for being such an incredible officemate, and for getting past seeing me as a spoiled sorority girl. I miss you everyday buddy. Amanda, thank you for taking over Mike's spot and being the best officemate and labmate and friend. Lauren, you are the ultimate Mirada neighbor, shopping buddy, happy hour partner, and general gal pal I needed. Thank you for all the shenanigans.

To my family, there is far too much to say, so I'll just say, thank you for always believing I had a unique story worth telling, and for listening through the hard last five years. You have all put in more than your fair share of TLC. It has never escaped me how lucky I am to have you. Thank you for the fun vacations, the endless phone calls, and for bragging about me to all our friends because you're so genuinely proud of me. To Jack

and Abby, thanks for arriving during this adventure. And to my CPC family, thanks for always making me want to come home.

And to my families at Flood and at YoungLife, thank you so much for coming into my life when you did. Thank you for growing me and maturing me and reminding me how wonderfully beautiful life is outside the lab. Molly, from the moment I met you, I knew I had to be best friends with the chick with a white streak in her hair. You have shown me more love and taught me more about living life well than you will ever know. To Ashley, there are no words to express how grateful I am for our heart bond. You pour wisdom into me like water, and you have taught me so much about self-care. And to Dora, thank you for being my silver lining in the darkest days, and going out of your way to show me love always. There are endless more people to thank from both Flood and YoungLife. Without you all, San Diego could have just been a city where I worked too hard and slept too little. Because of all of you, it became home.

Chapter 2, in full, is a reprint of the material as it appears in Marine Pollution Bulletin, 2016. Brandon, Jennifer; Goldstein, Miriam; Ohman, Mark D., 2016. The dissertation author was the primary investigator and author of this paper.

Chapter 3, in part is currently being prepared for submission for publication of the material. Brandon, Jennifer; Freibott, Alexandra. The dissertation author was the primary investigator and author of this material.

Chapter 4, in part is currently being prepared for submission for publication of the material. Brandon, Jennifer. The dissertation author was the primary investigator and author of this material.

Chapter 5, in part is currently being prepared for submission for publication of the

material. Brandon, Jennifer; Jones, William. The dissertation author was the primary investigator and author of this material.

VITA

2011 Bachelor of Science, Biology, Duke University

2011 Bachelor of Arts, English, Duke University

2014 Master of Science, Marine Biology, Scripps Institution of Oceanography, University of California, San Diego

2017 Doctor of Philosophy, Oceanography, Scripps Institution of Oceanography, University of California, San Diego

PUBLICATIONS

Brandon, J.A, Goldstein, M. and Ohman, M.D., 2016. Long-term aging and degradation of microplastic particles: Comparing in situ oceanic and experimental weathering patterns. *Marine Pollution Bulletin*, *110*:299-308.

Colton, M.D., Kwok, K.W., Brandon, J.A., Warren, I.H., Ryde, I.T., Cooper, E.M., Hinton, D.E., Rittschof, D. and Meyer, J.N., 2014. Developmental toxicity and DNA damage from exposure to parking lot runoff retention pond samples in the Japanese medaka (*Oryzias latipes*). *Marine Environmental Research*, *99*:117-124.

ABSTRACT OF THE DISSERTATION

The distribution of suspended microplastics and nanoplastics in the Northeast Pacific and their effects on zooplankton consumers

by

Jennifer Anne Brandon

Doctor of Philosophy in Oceanography

University of California, San Diego, 2017

Professor Mark D. Ohman, Chair

Plastic marine debris has been a cause of concern for decades, especially in the Northeast Pacific Ocean. Recent research has shown that the vast majority of plastic in the ocean is not easily noticeable large pieces, but microplastic (< 5 mm). The distribution and abundance of microplastic in the ocean is relatively understudied, especially the subcategory nanoplastic (< 333 μm), because its size makes it difficult to accurately sample and enumerate. The goal of this dissertation is to better quantify the distribution, abundance, and ecological impacts of microplastics in the Northeast Pacific, and to assess utilization of suspended plastic particles by planktonic consumers. I examined the degradation of microplastic over time, the oceanic distribution of nanoplastic particles,

and the chronology of microplastic deposition in coastal sediments throughout the past century.

I performed a laboratory weathering experiment and compared the chemical degradation of laboratory and open ocean samples to determine how long microplastic had been aging and degrading in the ocean. I found that carbonyl, hydroxyl, and carbon-oxygen bonds change progressively with weathering, but in a nonlinear manner. Weathering time can nevertheless be roughly approximated over large time periods. I found that microplastics from the North Pacific Subtropical Gyre had weathered longer than coastal plastics.

I introduced the use of epifluorescence microscopy to enumerate nanoplastics. By sampling surface waters in a transect from Seattle to Honolulu, I found concentrations of nanoplastics to be ~5-7 orders of magnitude higher than previous studies that analyzed larger microplastics. Nanoplastics are most likely to affect suspension-feeding zooplankton at the surface of the ocean. I analyzed multiple species of salps sampled in oceanic waters to determine whether they had ingested nanoplastics; every salp analyzed had ingested nanoplastics, regardless of species, life history stage, or oceanic region sampled in. The average plastic they had ingested was significantly smaller than the average ambient surface nanoplastic available to them.

I examined the temporal accumulation of microplastics in sediments over the past 72 years. By analyzing a box core from anoxic bottom waters in the Santa Barbara Basin off the coast of California, I found an exponential increase in plastic deposition in sediment since 1945. This increase in plastic deposition rate was tightly correlated with

exponential increases in Southern California population and worldwide plastic production over the same period.

This dissertation found that microplastics and nanoplastics are more abundant, temporally persistent, and spatially widespread than previously thought. These plastics are being consumed by suspension-feeding pelagic tunicates, and thus could be entering much of the pelagic food web.

CHAPTER 1: Introduction

Plastics are a ubiquitous part of modern consumer culture. Synthetic plastics (derived from fossil fuels, rather than plants and animals) were invented only 110 years ago, with the advent of Bakelite (Fig. 1.1; American Chemistry Council 2014a). They became much more commercially popular in the 1940s (Jambeck et al. 2015). In the 72 years since World War II, plastic consumption has steadily risen in America and worldwide, and shows no signs of slowing (Fig. 1.2; Jambeck et al. 2015).

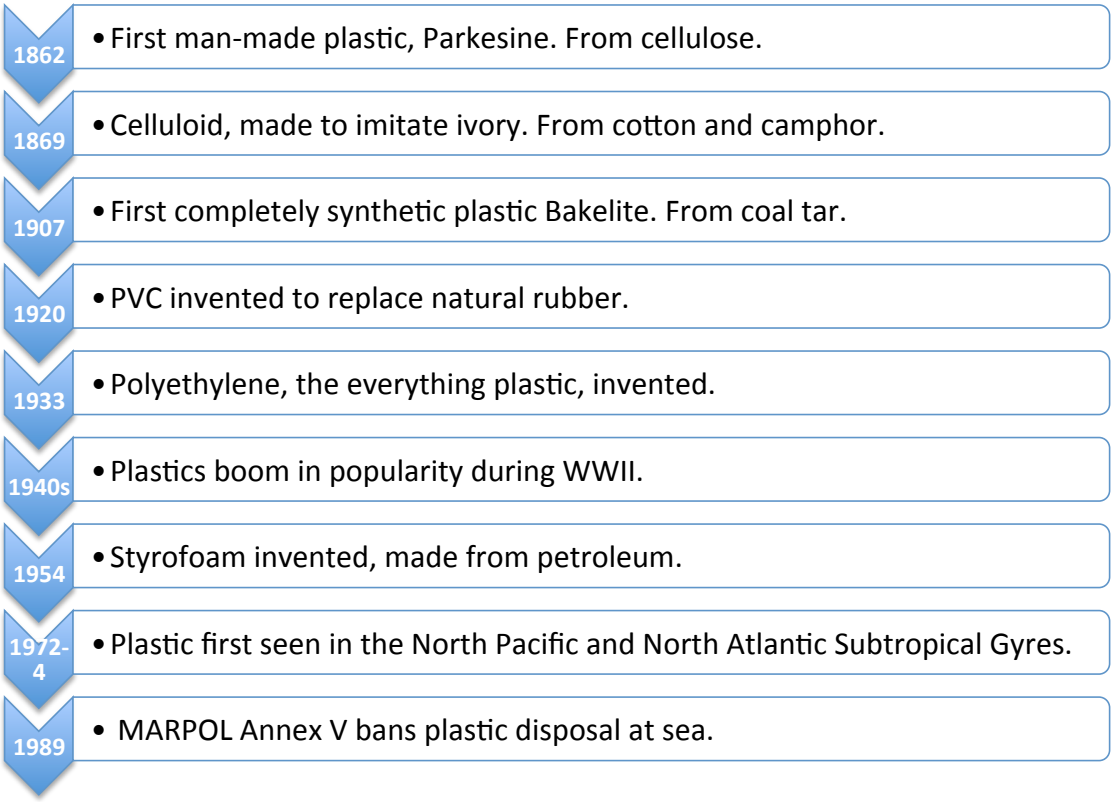

Figure 1.1: Timeline of plastic history. Adapted from *The History of Plastic: From Billiards to Bibs* from NPR.org, Carpenter and Smith 1972, Venrick et al. 1973, Colton et al. 1974, Wong et al. 1974, and Miriam Goldstein's PhD dissertation, 2012, unpublished.

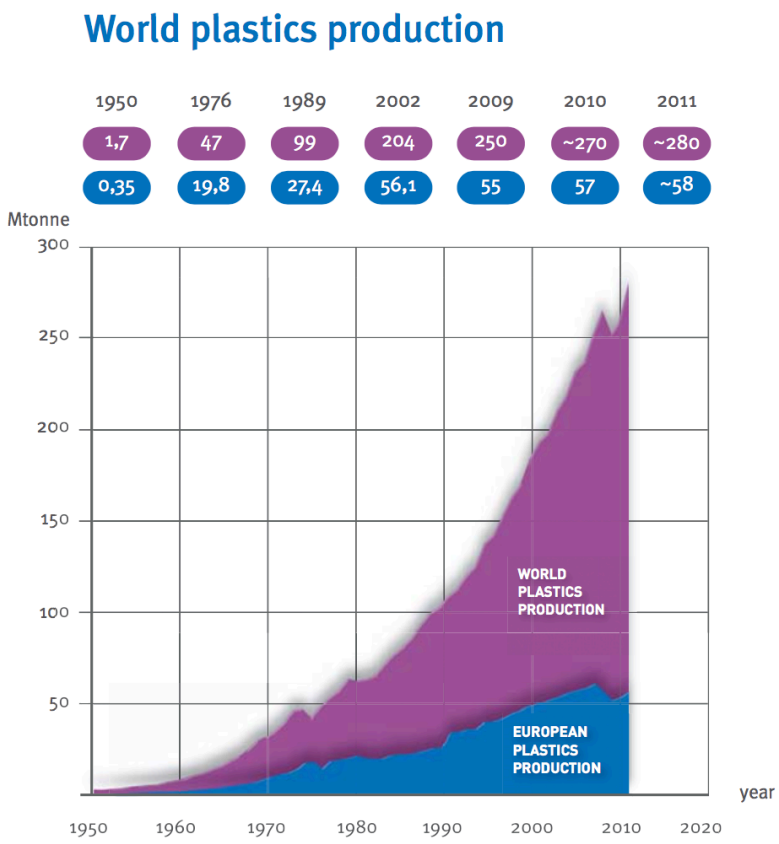

Figure 1.2: World plastics production 1950-2011. Includes thermoplastics, polyurethanes, thermosets, elastomers, adhesives, coatings and sealants and polypropylene fibers. Not included: Polyethylene Terephthalate -, Polyamide-, and Polyacryl-Fibers. From PlasticsEurope Market Research Group (PEMRG).

Annual global plastic production reached 311 million tons in 2014 (GESAMP 2016) and that number is steadily growing. Not only is plastic use and production increasing, but it is increasingly part of the waste stream: from < 1% of American municipal solid waste by mass in 1960 to 12.9% in 2014 (Jambeck et al. 2015, EPA 2016). Mismanaged plastic waste is reaching the ocean, with an estimated 4.8-12.7 million metric tons of plastic entering the ocean every year (Jambeck et al. 2015, EPA 2016). Population size and quality of waste management systems largely determine which coastal nations contribute the most marine debris (Jambeck et al. 2015). The world population is increasing, and higher human density is projected to especially impact coastal areas and coastal ecosystems. Nearly all growth is

predicted to take place in developing countries and most will occur along the coasts (Fig. 1.3; Browne et al. 2011). Both of these characteristics will likely lead to more marine debris, as developing countries tend to have higher percentages of mismanaged waste, and areas of higher populations produce more waste. Thus, the problem of marine debris is likely to only worsen in the future.

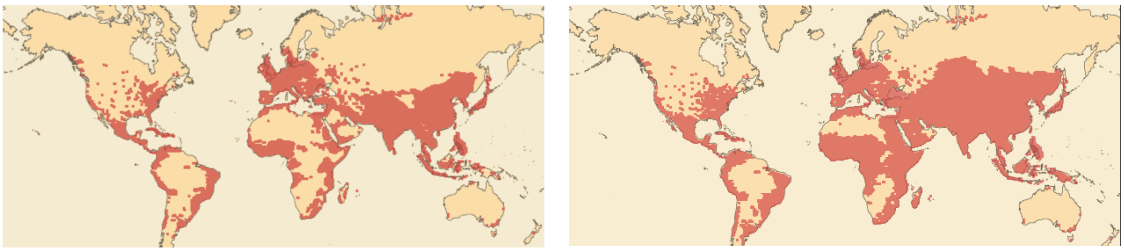

Figure 1.3: World population in A) 1999 and B) estimated in 2050. Adapted from *World Population: A Graphic Simulation of the History of Human Population Growth*. A) 1999, when 6 billionth person born. B) Depicts the predicted world population of nine billion people in 2050. Every red dot on the map equals one million people.

Types of Plastics

There are six main consumer plastics used today, which correspond to the recycling codes 1-6 commonly printed on plastic items. Plastic number 7 does not exist as a single entity, but denotes assorted or miscellaneous plastic types. Table 1.1 (end of chapter) lists the most common consumer plastics, their densities, and some of their most common uses. I will often use the acronyms from column two of Table 1.1 in the rest of this dissertation.

Areas Impacted by Plastic Marine Debris

Plastics are found in virtually all aquatic environments sampled to date. Starting in the 1970s, only a few decades after the surge in plastic consumption, scientists began finding plastics in the open ocean, specifically in the subtropical gyres (Venrick et al. 1973, Colton et al. 1974, Wong et al. 1974). Microdebris, generally defined as debris smaller than 5 mm

in its longest dimension (Arthur 2009), has been found in open ocean gyres (Goldstein et al. 2012), coastal waters (Gilfillan et al. 2009), shorelines (Browne et al. 2011), the deep sea (Van Cauwenberghe et al. 2013), rivers (Lechner et al. 2014), and in the Great Lakes (Eriksen et al. 2013).

The high concentrations of plastics in subtropical gyres are due to the entrainment of drifting, positively buoyant plastics into gyres by the large-scale ocean circulation (Fig. 1.4; Meehl 1982). The edges and center of a gyre acts as a convergence zone of surface waters, where plastics from the edges of the ocean basin converge and aggregate, and then circulate there, potentially indefinitely (Maximenko et al. 2012).

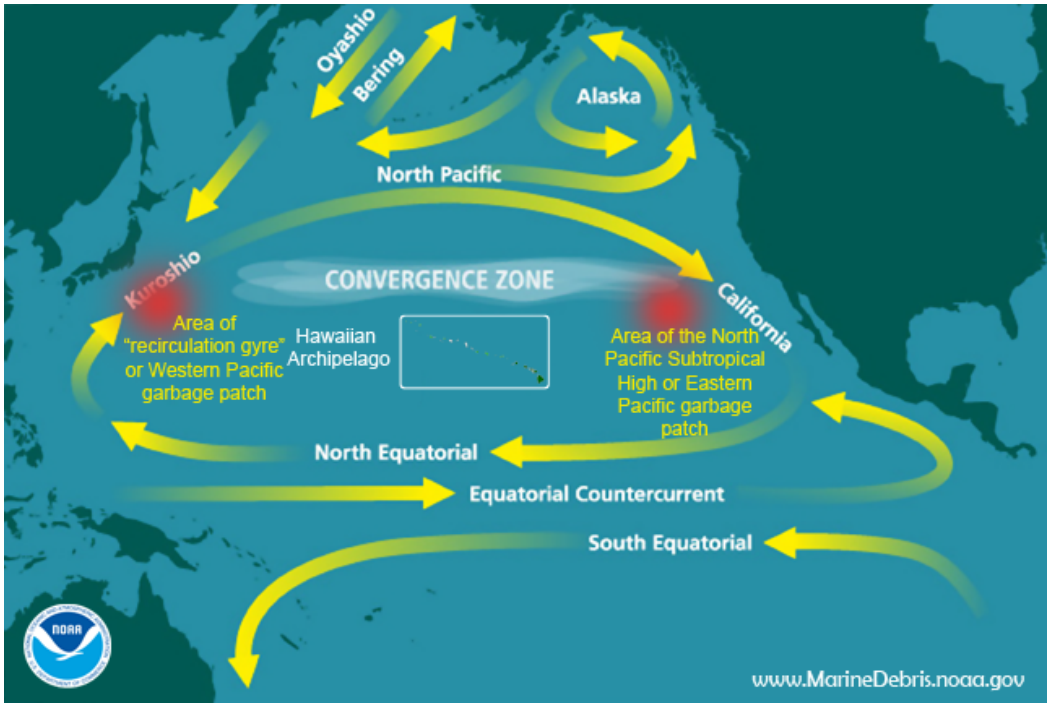

Figure 1.4: The North Pacific Subtropical Gyre, illustrating that gyre circulation leads to accumulation of buoyant plastics in convergence zones. Similar convergences are found in all five subtropical gyres. From NOAA Marine Debris Program.

The abundance of microplastics in the center of gyres may be increasing, as Goldstein et al. (2012) found a two order of magnitude increase in abundance from 1972-1987 to 1999-2010 in the Northeast Pacific. However, Law et al. (2014) did not find a

robust positive trend of plastic accumulation in the same area from 2001 to 2012, and found only a ten-fold increase between 1972-1987 and 1999-2010 when incorporating their data with results from Goldstein et al. An earlier study found no significant increase in plastic in the subtropical latitudes of the Northeast Atlantic from 1986 to 2008 (Law et al. 2010). Although the spatial and temporal trends of plastic accumulation do not seem to follow a consistent pattern in the world's gyres, it is approximated that about half of all floating microplastic lies in the five subtropical gyres (GESAMP 2016).

An estimated 60-80% of plastic that ends up in the ocean comes from land-based sources, instead of originating from ships (Ocean Conservancy 2010). Many of the first marine debris studies focused only on sampling open-ocean plastic, rather than nearshore plastic debris or plastic in sediment, and thus probably under-sampled coastal plastics. Some isolated studies on coastal debris have documented benthic plastics in sandy habitats (Abu-Hilal and Al-Najjar 2009), estuaries (Browne et al. 2010), and subtidal habitats (Backhurst and Cole 2000) around the world, but the sampling has been sporadic and the methodology has not always been uniform (Hidalgo-Ruz et al. 2012). Furthermore, nearshore water column sampling has been sparse.

Coastal regions of high population density have significantly more plastic in their local marine sediments (Fig. 1.5a,b; Browne et al. 2011). Browne et al. (2011) identified the majority of the plastics they found as synthetic clothing fibers from wastewater effluent. They also found 250% more microplastic pieces in areas of sewage disposal, despite the fact that sites in both the North Sea and English Channel had not been active disposal sites for more than ten years (Fig. 1.5c). Along with the increase in general plastic consumption and production, synthetic fabrics, such as nylon and acrylic, are rising in prevalence (Browne et

al. 2011). A single synthetic fleece jacket can release an average of 1,174 mg of microfibers per washing (Hartline et al. 2016), or an average of 300 microfibers L^{-1} (Browne et al. 2011). This pattern of highest abundance near populated areas also applies to inland waters. Eriksen et al. (2013) collected an average of 43,000 microplastic particles km^{-2} in the Great Lakes, but the sampling station directly downstream of Cleveland, OH and Erie, PA had 466,000 particles km^{-2}, more than all other stations combined. As coastal populations grow and clothes are increasingly produced from synthetic substances, effluent-derived fibers will likely become a larger concern in nearshore areas (Browne et al. 2011). This thesis will quantify the abundances of plastics in both nearshore surface waters and sediments, as well as open ocean surface waters.

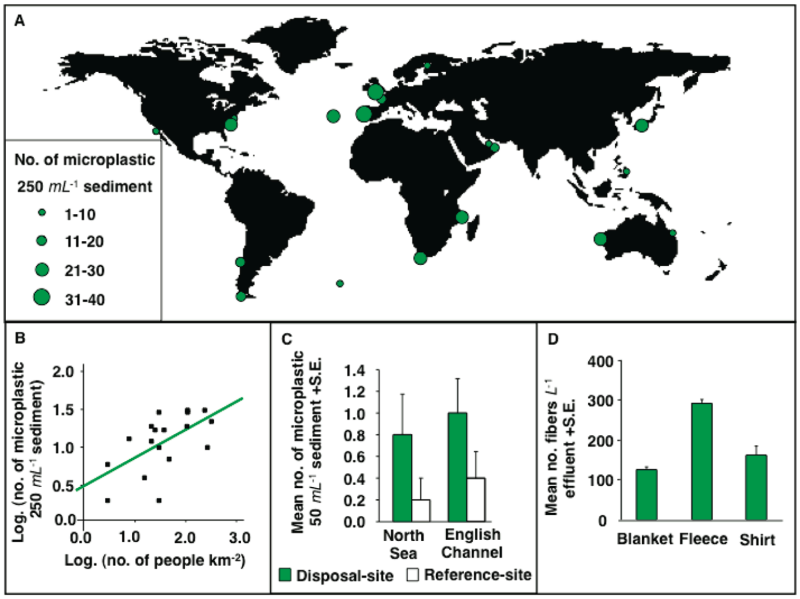

Figure 1.5: Microplastic in sediments around the world. From Browne et al. 2011.A) Global extent of microplastic in sediments from 18 sandy shores and identified as plastic by Fourier Transform Infrared (FTIR) spectroscopy. The size of filled-circles represents number of microplastic particles found. B) Relationship between population-density and number of microplastic particles in sediment from sandy beaches. C) Number of particles of microplastic in sediments from sewage disposal-sites and reference-sites at two locations in U.K. D) Number of polyester fibers discharged into wastewater from the use of washing machines with blankets, fleeces, and shirts (all polyester).

Even with the high abundances recorded in the center of gyres and in nearshore sediments, multiple studies predict there is actually even more plastic in the ocean than previously reported (Cózar et al. 2014, Jambeck et al. 2015). Jambeck et al. (2015)'s model of land-based plastic input is 1-3 orders of magnitude higher than most ocean abundance estimates (Law et al. 2010, Cózar et al. 2014, Eriksen et al. 2014, Law et al. 2014), suggesting much more plastic is entering the ocean than marine debris studies are finding. Jambeck et al. (2015) even note that their model does not include plastic inputs from natural disasters, losses at sea, or fishing gear. One possible reason for this mismatch in numbers is that microplastics have only been an area of concern in marine debris studies in recent years (Thompson et al. 2004), and microplastics, and nanoplastics especially, are still highly undersampled in marine debris studies (Goldstein et al. 2013). Another reason is that almost all abundance studies only sample buoyant plastics in surface water (Law et al. 2010, Cózar et al. 2014, Eriksen et al. 2014, Law et al. 2014), leaving negatively buoyant plastic and the benthos heavily undersampled. Plastics may be removed from surface waters, and thus current abundance estimates, for multiple reasons including nano-fragmentation, predation, biofouling, and shore deposition (Thompson et al. 2004, Law et al. 2010, Andrady 2011, Cózar et al. 2014). This dissertation attempts to close these abundance gaps, by developing a method of sampling nanoplastics, and by analyzing marine debris in both sediments and zooplankton that may act as a vector to carry marine debris from surface waters to the benthos. In so doing, this dissertation will attempt to close the gap between modeled and measured estimates of marine debris abundance.

How Long Do Plastics Remain in the Ocean?

In order to develop models of microplastic abundance and distribution, or to develop policy to mitigate the marine debris problem, it is important to know how long marine debris has been in the ocean, how long it has accumulated in a certain region, and where it originated. Unfortunately, all of these questions are difficult to answer. For large pieces of debris, written characters, such as product expiration dates, can sometimes help (Stefatos et al. 1999), but even text cannot always provide a point source of origin in today's worldwide maritime economy (Goldstein et al. 2014). Rafting species can sometimes be tied to a specific area of origin (Gregory 2009, Goldstein et al. 2014, Carlton et al. 2017), and their age can give a minimum length of time in the ocean, but no maximum (Hoffman 1989). There are anecdotal stories of WWII supplies or action figures from the 1970s washing up on beaches (Moody 2010), but it generally cannot be proven that these items remained in the ocean continuously. Currently, there is no method to estimate how long a given microplastic particle has been in the ocean. The small size of fragmented, weathered microplastics makes it impossible to trace these particles to their source (Jambeck et al. 2015). Knowing how long a particle has been in the ocean is critical for calculating the residence time of particles in different oceanic regions, testing the accuracy of models, calculating the residence time of sorbed pollutants in the ocean, and assessing the efficacy of marine debris mitigation policy. This thesis attempts to decipher the aging and degradation patterns of individual pieces of plastic, in order to try to develop a method to assess the amount of time a piece of debris has been in the ocean.

Accumulation of Plastics in the Ocean Over Time

Although it is important to know how long individual pieces of marine debris have been in the ocean, it is even more important to understand patterns of spatial and temporal accumulation of marine debris. Knowing areas that are prone to large collections of marine debris and knowing how long marine debris has been accumulating in certain regions is essential for mitigation and policy efforts, as well as studying which animals are the most affected by debris. However, as stated before, plastic is a relatively new material and marine debris is an even newer area of study, so few studies have quantified the accumulation of marine debris over time. The few temporal studies of marine debris accumulation have focused on buoyant marine debris in surface waters (Law et al. 2010, Goldstein et al. 2012, Law et al. 2014). But marine debris has been recorded in many other marine habitats, including in benthic sediments (Thompson et al. 2004, Ryan et al. 2009, Browne et al. 2011, Hidalgo-Ruz et al. 2012, Van Cauwenberghe et al. 2013, Woodall et al. 2014). Analyzing sediment cores, like Kasten or box cores, makes it possible to measure the accumulation rate of a certain item, like microplastics, in specific regions of the ocean over time. The Santa Barbara Basin has intermittently anoxic bottom water and varved sediment layers, a result of productive summers and non-productive winters (Hendy et al. 2013, Schimmelmann et al. 2013). These varved sediment layer couplets allow the fine-scale resolution (on the order of 1-2 years) that is required to calculate the deposition rate of microplastic over the relatively short time frame that synthetic plastic has been in existence – i.e. the last 110 years (Fig. 1.1; American Chemistry Council 2014a). By analogy with previous literature from different ocean regions, it is likely that sediment cores from the Santa Barbara Basin, a nearshore area of high urban population, will have high plastic abundances, dominated by fibers of mixed densities (Browne et al. 2011, Eriksen et al. 2013, Woodall et al. 2014, GESAMP 2016).

This thesis analyzes a box core from the Santa Barbara Basin for plastic deposition from before and after the advent of plastic in order to calculate the rate of plastic deposition in the sedimentary record; it compares the deposition rate from pre- and post-1945 to correct for processing contamination. This part of the study not only evaluates temporal trends of microplastic accumulation in sediments, which has important ecological consequences and is important for understanding plastics' abundance in the understudied benthos, but it also ties into a larger discussion of the use of manmade objects, like plastics, as sedimentary markers for proxies of the new geological epoch, the Anthropocene (Zalasiewicz et al. 2016, Zalasiewicz et al. 2017).

The Effects of Microplastics on Pelagic Animals

The impacts of large marine debris on megafauna are well-studied (Derraik 2002). Large debris, termed macrodebris (> 5 mm), can cause animal entanglement (Henderson 2001), be ingested (Derraik 2002), and can obstruct gastrointestinal tracts (Fry et al. 1987). It can also allow invasive organisms to raft long distances (Goldstein et al. 2014, Carlton et al. 2017) and entangle and damage corals and other benthic animals (Donohue et al. 2001, Schlining et al. 2013).

Studies on the impacts of microplastics on the abundant planktonic suspension-feeding species in the ocean are sparse. Suspension-feeders have the potential to be especially affected by micro- and nanoplastic because so many species are non-selective feeders, and can ingest a significant amount of inorganic material (Moore et al. 2001). Among epipelagic suspension-feeding zooplankton, salps in particular have the potential to come into contact with a large amount of microplastic due to their cosmopolitan distribution,

especially in tropical and temperate regions such as gyres, where plastic is the most concentrated (Bone 1998, Goldstein et al. 2013). Salps are particularly vulnerable to microplastic because they are non-selective generalist feeders, they have very high clearance rates, and their size range of prey overlaps with the most numerically abundant plastic particles in the ocean (Chan and Witting 2012, Goldstein et al. 2013).

Salps are known to go through occasional "boom and bust" cycles, when they can swarm to intense densities and consume all, or almost all, of the phytoplankton in the water, potentially outcompeting the other grazers in the area (Alldredge and Madin 1982). These swarms could filter out a large amount of microplastic from the top of the water column. Salps are noted for their role in the carbon cycle; both their large, fast-sinking fecal pellets and their dead tunics are key to transporting carbon to the benthos (Bruland and Silver 1981, Smith et al. 2014). If salps are found to be ingesting plastic particles *in situ*, they could be a key vector of microplastic from surface water to the benthos, and a key pathway of missing oceanic microplastic in surface abundance estimates.

Many marine animals have been fed microplastics in laboratory experiments in recent years with differing results. Some animals, including lugworms, amphipods, and barnacles, ingested microplastics within a few days of exposure (Thompson et al. 2004). Some, like chaetognaths, were offered plastic spheres and did not ingest them (Cole et al. 2013). And some, like sea cucumbers, selectively fed on microplastic particles over natural food (Graham and Thompson 2009). Far fewer studies have found microplastic in animals' guts *in situ*, but plastics have been found *in situ* in barnacles (Goldstein and Goodwin 2013), Norwegian lobster (Murray and Cowie 2011), mesopelagic fish (Davison and Asch 2011)

and many species of megafauna. Notably the Laysan albatross has shown increased starvation and fledgling mortality due to plastic ingestion (Fry et al. 1987).

Some animals, like mesopelagic fish, have been found with microplastics in their stomachs (Davison and Asch 2011), but it is unclear whether the microplastics were eaten by the fish or by their prey. I am focusing on salps, a zooplankton consumer near the bottom of the food web, because it is essential to understand how these base consumers are interacting with plastic. This information will improve our understanding of the greater ecological consequences of microplastics on the open ocean and gyre systems.

The effects of plastics on pelagic ecosystems extend beyond direct ingestion. Plastics are rarely just a simple hydrocarbon chain; the plastic debris being consumed in the ocean often incorporates bisphenol A (BPA), phthalates, plasticizers, colorants, flame retardants and other compounds that can enter the food web and accumulate in animal tissue (Browne et al. 2013, Rochman et al. 2013b, Jang et al. 2016). Plastics are hydrophobic, and as such can sorb polyaromatic hydrocarbons (PAHs), polychlorinated biphenyls (PCBs), and other persistent, bioaccumulative, and toxic substances (PBTs) from the atmosphere and ocean, which can become bioavailable once consumed (Ogata et al. 2009, Browne et al. 2011, Rochman et al. 2013b). Rochman et al. (2013) examined Japanese medaka that were fed low-density polyethylene (LDPE) that had sorbed PBTs from the marine environment. Not only had the fish concentrated these compounds in their tissues but they also exhibited hepatic stress and liver tumors. There has been documented reduced survival, feeding, and immunity (Browne et al. 2013), and weight loss (Besseling et al. 2012) in lugworms fed microplastics. Fish that fed on zooplankton that were fed nanoparticles not only transported the nanoplastic particles up the food chain, but the nanoplastic particles were found in the

fishes' brain tissue and brain damage and behavioral disorders were observed in the fish (Mattsson et al. 2017). Ogata et al. (2009) collected beached plastic resin pellets around the world (Fig. 1.6) and tested them for environmental pollutants that had sorbed to the pellets from the environment. The highest values of PCBs are in industrialized, populated places, like the US coast and Japan (Fig. 1.6).

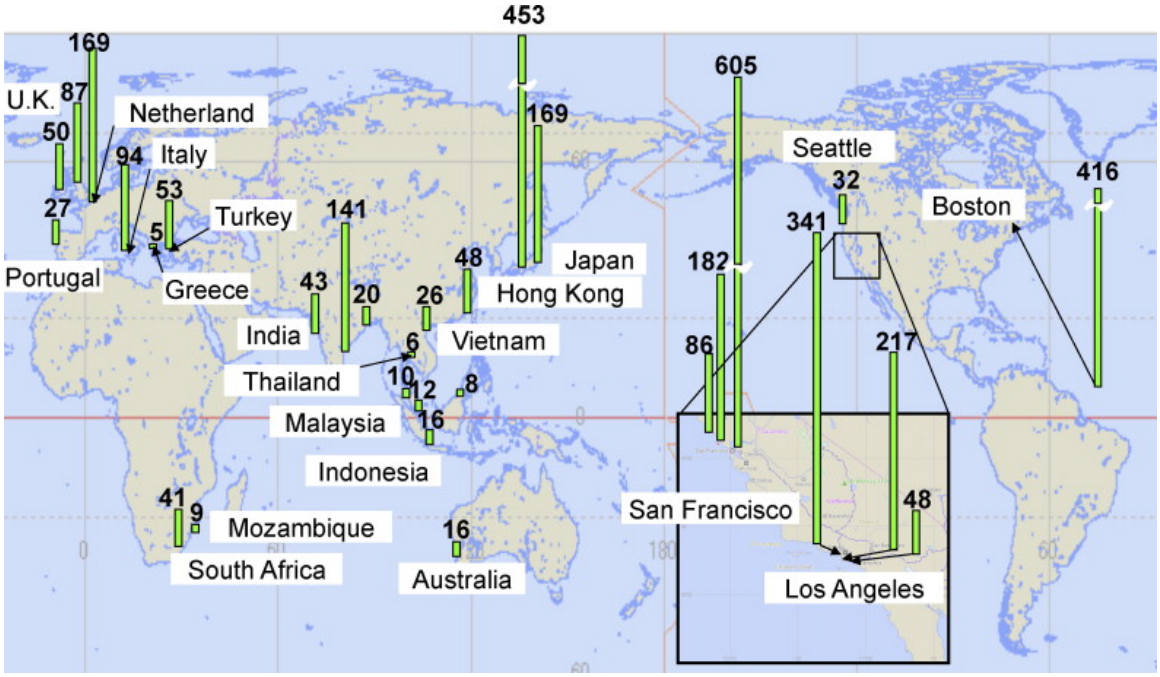

Figure 1.6: Median concentrations of ∑13 polychlorinated biphenyls (PCBs) (ng/g-pellet) in beached plastic pellets. ∑13 PCBs = sum of concentrations of CB# 66, 101, 110, 149, 118, 105, 153, 138, 128, 187, 180, 170, 206. From Ogata et al. 2009.

Types of Marine Microplastics

Microplastics (< 5 mm) come from multiple sources, and their appearance can reveal their point of origin. Knowing microplastics' point of origin is important to determine what products are most commonly ending up as marine debris, and which regions are sources of the most plastic. Linking of plastics to source materials can have important implications for policy and mitigation efforts. Microplastics can come from synthetic clothing fibers, and often be brightly colored and elongate (Browne et al. 2011). They can derive from

macroplastics (> 5 mm) that have been physically and photo-degraded into this size range, and will thus have more jagged, irregular edges (Browne et al. 2010). If the microplastics originated as round 'microscrubbers' or 'microbeads' in cleaning products and cosmetics, they will be mostly polyethylene spheres or fragments (Browne et al. 2011).

Many microplastics, especially in sediment, are covered in a biofilm and resemble biotic material. Though Browne et al. (2011) found mostly synthetic clothing fibers in their samples, they admit that they probably under-sampled other plastics due to their visual techniques for identification. For microplastics, there is a need to positively identify samples by methods other than just visual appearance.

Sorting, Identifying, and Quantifying Microplastics

Plastics can also be sorted and identified by their densities (Table 1.1, Column 3), which affect their buoyancies and location in the water column, but the results are not always intuitive (Hidalgo-Ruz et al. 2012). Law et al. (2010) found 99% of plastic in manta (neuston) tows in the North Atlantic Subtropical Gyre to be less dense than seawater, but nearshore plankton tows (using a Continuous Plankton Recorder) contained both positively and negatively buoyant plastics (Thompson et al. 2004). Positively buoyant plastics can also be found in benthic sediments, although at lower percentages than negatively buoyant plastics (Browne et al. 2011). Fig. 1.7A illustrates that negatively buoyant plastics can also be found in surface tows and beach sediments at very low rates of occurrence. Nonetheless, it is important to recognize the differences in buoyancy between plastic types, as only 46% of manufactured plastic is positively buoyant (USEPA 1992). One study found that fibers were four orders of magnitude more abundant in deep-sea sediment than in surface waters,

so the debris composition in samples from different parts of the water column may vary (Woodall et al. 2014, GESAMP 2016).

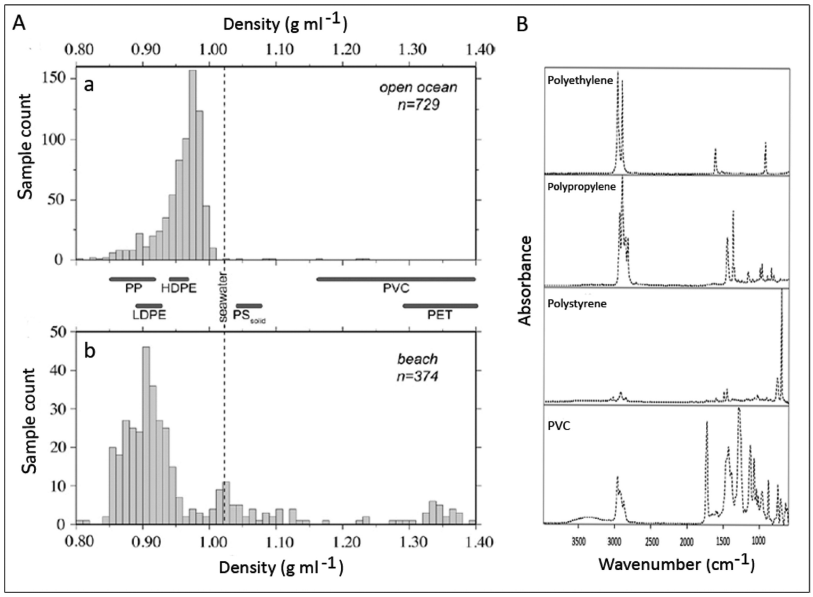

Figure 1.7: A) Frequency of microplastics of different densities found at a) the sea surface and b) in beach sediment. Vertical dashed line equals average density of seawater; horizontal bold lines indicate densities of polymers. **B) FTIR spectra of common plastic polymers.** From Hidalgo-Ruiz et al. 2012.

In addition to the density of plastics, it has been observed that the larger an item is, the more likely it is to stay buoyant, even if it has developed a large rafting community (Thiel and Gutow 2005). Small objects, even if positively buoyant, may become negatively buoyant if covered with enough rafting organisms or biofilm. This may explain how some positively buoyant plastics reach the seafloor (Thiel and Gutow 2005, Kaiser et al. 2017). There is also the possibility that positively buoyant microplastics enter the ocean via sewage outfall pipes so near the sea floor that they are immediately incorporated into the sediments. There is also the possibility, explored in this thesis, of animals consuming buoyant particles at the surface and transporting them to the benthos via fecal transport or diel vertical migration.

In order to properly identify plastics, it is important to identify plastic not just by visual inspection, but also by spectral identity, especially considering they are not always distributed according to their density. In this dissertation, I use Fourier Transform Infrared (FTIR) Spectroscopy to identify microplastics found in my surface and sediment samples and epifluorescence microscopy to identify nanoplastics (< 333 μm) in surface and zooplankton gut contents samples. FTIR spectroscopy gives a unique spectral reading for each plastic type (Fig. 1.7b), and can thus identify small particles to type that could not otherwise be categorized.

Nanoplastics

The distribution of small plastic particles is of concern in the modern ocean, due to the fact that microplastics are in the right size range for ingestion by so many planktonic consumers. There are unknown food web consequences if the base consumers are ingesting large amounts of synthetic plastic. However, the smallest size classes of microplastics have not been well assessed in most studies of plastic abundance (Goldstein et al. 2013). Many of the studies that have surveyed plastic in the North Pacific Subtropical Gyre, and other areas, have used nets with 333 μm mesh (Hidalgo-Ruz et al. 2012, Eriksen et al. 2013, Goldstein et al. 2013), potentially dramatically undersampling plastics smaller than 333 μm. In van Sebille et al. (2015), the mesh of 11,000+ surface plankton tows ranged from 150 μm to 3.0 mm, but over 90% of the tows used 333 or 335 μm mesh. Goldstein et al. (2013) quantified the spatial heterogeneity of plastic debris in the North Pacific Ocean. Their results, (Fig. 1.8), illustrate that over 90% of the plastic they counted and measured (n=32,090 pieces) on two extensive scientific expeditions was smaller than 1 cm^2 in surface area. However, due to the

mesh size of the collecting net (333 μm), they were not able to assess the abundance of still smaller particles.

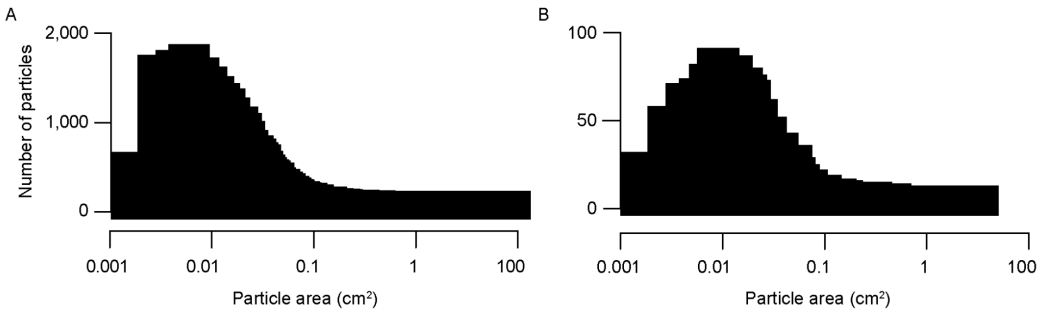

Figure 1.8: Plastic size spectra. All plastic collected by surface manta tows. From Goldstein et al., 2013. A) Summer 2009, n=30,518 pieces; B) Fall 2010, n=1,572 pieces.

It is likely that plastic < 333 μm (referred to in the plastics literature and in this dissertation as nanoplastic) is far more numerous than larger microplastics because plastic continues to physically degrade into smaller and smaller pieces over time (Gilfillan et al. 2009), and models simulate that smaller plastic particles degrade and fragment into smaller pieces at faster rates than larger pieces (Gerritse 2015, GESAMP 2016).

When sampling with 80 μm mesh instead of 450 μm mesh in the Northeast Atlantic, Lozano and Mouat (2009) collected up to 100,000 times more plastic particles. There is a compelling need to quantify the amount of plastic in the ecologically important size range of 0-333 μm, which is the size range of particles ingested by many suspension-feeders, including salps, copepods, mussels, clams, larvaceans, and echinoderm larvae (Wilson 1973, Harbison and McAlister 1979, Hart 1991, Defossez and Hawkins 1997, Browne et al. 2008, Katija et al. 2017). Some studies state that nanoplastics (< 333 μm) have never even been detected *in situ* in the marine environment, mainly due to the difficulties in identifying them, and thus their abundance and ecological significance is relatively unknown (GESAMP 2015, Koelmans et al. 2015, GESAMP 2016). This thesis contributes a new approach to

identifying nanoplastic particles, using their autofluorescent properties as detected by epifluorescent microscopy.

Study Areas of this Thesis

I am interested in the North Pacific Subtropical Gyre (NPSG) because of its large spatial extent (Karl 1999), the way its circulation causes large amounts of plastic to aggregate (Fig. 1.4; Maximenko et al. 2012), and the immense amount of marine debris chronicled there (Moore et al. 2001, Goldstein et al. 2012). Chapters 2, 3 and 4 of this dissertation sample from the NPSG. However, I am also interested in the spatial distribution, size composition, and utilization of nearshore marine plastics and the differences between nearshore and open ocean plastic concentrations. Chapters 2, 3, 4, and 5 sample nearshore water or sediment of the California Current System. Nearshore sediment and surface water off of Southern California should be heavily impacted by marine debris due to proximity to areas of high population density (Browne et al. 2011, Eriksen et al. 2013).

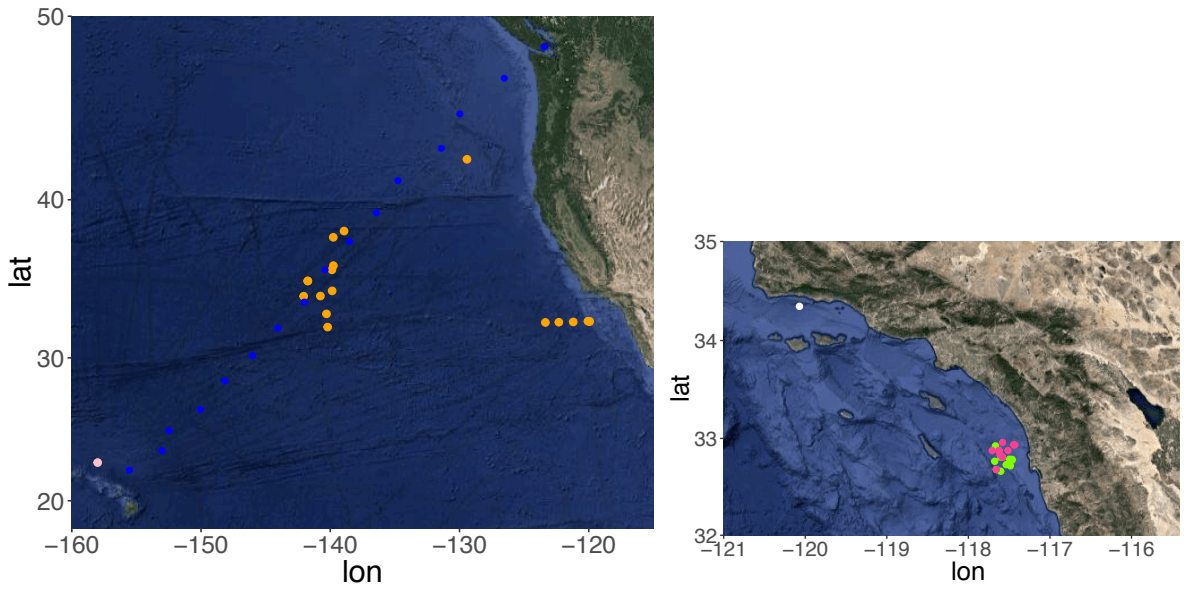

Figure 1.9: Maps of study regions for this dissertation. A) Study regions in nearshore California Current Ecosystem and North Pacific Subtropical Gyre. Red: SEAPLEX (Chapter 2, 3 and 4). Yellow: *Falkor* (Chapter 3). Green: SKrillEx I and SKrillEx II (Chapter 3,4). White: Santa Barbara Basin (Chapter 5). B) Inset of nearshore study regions. Green: SKrillEx I (Chapter 3,4). Pink: SKrillEx II (Chapter 3). White: Santa Barbara Basin (Chapter 5).

Guiding Questions

I am interested in the spatial and temporal abundance and variability of microplastics (< 5 mm) and the subcategory nanoplastics (< 333 μm). They are a relatively under-studied component of marine debris, but have the potential to be the most ecologically important type of marine debris. The goal of this dissertation is to improve understanding of the distribution of microplastics and nanoplastics in the Northeast Pacific, and the utilization of suspended plastic particles by planktonic consumers. I focus my dissertation on the following central questions:

1. Can the age of microplastic collected from the open ocean be determined? How do sunlight and seawater affect the aging of the most common plastics?

2. What are the ambient concentrations and ecological consequences of the previously undersampled nanoplastic (< 333 μm) in the surface ocean?
3. Do neustonic suspension-feeding zooplankton ingest nanoplastic particles *in situ*?
4. How have sedimentation rates of microplastics changed in the Santa Barbara Basin over the last century?

I address Question 1 by comparing the chemical structure of experimentally weathered plastics with microplastics collected in the open ocean using Fourier Transform Infrared (FTIR) spectroscopy. This chapter is published in Marine Pollution Bulletin. I address Question 2 by sampling for nanoplastics in different regions of the NE Pacific, and quantifying and identifying the particles with epifluorescence microscopy. I answer Question 3 by analyzing ingestion of microplastics by salps, using them as model organisms of neustonic suspension-feeders. I answer Question 4 by examining a box core from the Santa Barbara Basin for microplastic and identifying a subset of the identified microplastics by FTIR. This dissertation concludes with Chapter 6, which discusses these findings in their greater ecological context and their importance for application in future marine debris mitigation and policy work.

Table 1.1: Common Consumer Plastics and Applications

Resin ID[1]	Plastic Type[1]	Density[2, 3] (g/cm^3)	Date of first manufacture[4-6]	Common Applications[1, 5-7]
1	Polyethylene Terephthalate (PET)	1.35	Early 1970s	Disposable clear plastic drink bottles, food jars
2	High Density Polyethylene (HDPE)	0.94-0.965	1955	Milk containers, detergent bottles, toys
3	Polyvinyl Chloride (PVC)	1.35	Late 1920s	Pipes and fittings, vinyl siding, synthetic-leather products, shampoo bottles
4	Low Density Polyethylene (LDPE)	0.91-0.925	1935	Shrink wrap, dry cleaning bags, freezer bags
5	Polypropylene (PP)	0.89-0.91	1957	Flexible containers, bottle caps, drink cups
6	Polystyrene (PS)	1.0-1.1	1937	Disposable cutlery, packing peanuts, CD
7	Assorted; nylon	1.11-1.18	1939	Stockings, parachutes, tents, guitar strings
7	Assorted; Poly(acrylonitrile): acrylic	1.20	1941	Sweaters, boot linings, carpets, upholstery

This table was adapted from Miriam Goldstein's PhD dissertation, 2012, unpublished.

1) American Chemistry Council 2014b
2) Freund Container and Supply 2010
3) Dotmar 2014
4) Andrady and Neal 2009
5) Dupont 2014a
6) Dupont 2014b
7) American Chemistry Council 2014c

REFERENCES:

Abu-Hilal, A. H., and T. H. Al-Najjar. 2009. Plastic pellets on the beaches of the northern Gulf of Aqaba, Red Sea. Aquatic Ecosystem Health & Management **12**:461-470.

Alldredge, A., and L. Madin. 1982. Pelagic tunicates: unique herbivores in the marine plankton. Bioscience **32**:655-663.

Andrady, A. L. 2011. Microplastics in the marine environment. Marine Pollution Bulletin **62**:1596-1605.

Arthur, C., Baker, J., and Bamford, H. (Eds.). 2009. Proceedings of the International Research Workshop on the Occurrence, Effects, and Fate of Microplastic Marine Debris, September 9-11, 2008, University of Washington Tacoma, Tacoma, WA, USA. U.S. Dept. of Commerce, National Oceanic and Atmospheric Administration, National Ocean Service, Office of Response & Restoration, Silver Spring, Md.

Backhurst, M. K., and R. G. Cole. 2000. Subtidal benthic marine litter at Kawau Island, north-eastern New Zealand. Journal of Environmental Management **60**:227-237.

Besseling, E., A. Wegner, E. M. Foekema, M. J. Van Den Heuvel-Greve, and A. A. Koelmans. 2012. Effects of microplastic on fitness and PCB bioaccumulation by the lugworm Arenicola marina (L.). Environmental science & technology **47**:593-600.

Bone, Q. 1998. The biology of pelagic tunicates. Oxford University Press, Oxford.

Browne, M. A., P. Crump, S. J. Niven, E. Teuten, A. Tonkin, T. Galloway, and R. Thompson. 2011. Accumulation of microplastic on shorelines worldwide: sources and sinks. Environmental science & technology **45**:9175-9179.

Browne, M. A., A. Dissanayake, T. S. Galloway, D. M. Lowe, and R. C. Thompson. 2008. Ingested microscopic plastic translocates to the circulatory system of the mussel, Mytilus edulis (L.). Environmental science & technology **42**:5026-5031.

Browne, M. A., T. S. Galloway, and R. C. Thompson. 2010. Spatial patterns of plastic debris along estuarine shorelines. Environmental science & technology **44**:3404-3409.

Browne, Mark A., Stewart J. Niven, Tamara S. Galloway, Steve J. Rowland, and Richard C. Thompson. 2013. Microplastic moves pollutants and additives to worms, reducing functions linked to health and biodiversity. Current Biology **23**:2388-2392.

Bruland, K., and M. Silver. 1981. Sinking rates of fecal pellets from gelatinous zooplankton (salps, pteropods, doliolids). Marine Biology **63**:295-300.

Carlton, J. T., J. W. Chapman, J. B. Geller, J. A. Miller, D. A. Carlton, M. I. McCuller, N. C. Treneman, B. P. Steves, and G. M. Ruiz. 2017. Tsunami-driven rafting: Transoceanic species dispersal and implications for marine biogeography. Science **357**:1402-1406.

Carpenter, E. J., and K. Smith. 1972. Plastics on the Sargasso Sea surface. Science **175**:1240-1241.

Chan, W. Y., and J. Witting. 2012. The impact of microplastics on salp feeding in the tropical Pacific. Australian National University Undergraduate Research Journal **4**.

Cole, M., P. Lindeque, E. Fileman, C. Halsband, R. Goodhead, J. Moger, and T. S. Galloway. 2013. Microplastic ingestion by zooplankton. Environmental science & technology **47**:6646-6655.

Colton, J. B., F. D. Knapp, and B. R. Burns. 1974. Plastic particles in surface waters of the northwestern Atlantic. Science **185**:491-497.

Connection, Population. 2003. World Population: A Graphic Simulation of the History of Human Population Growth. PBS NOVA, http://www.pbs.org/wgbh/nova/earth/global-population-growth.html.

Conservancy, Ocean. 2010. Trash Travels. International Coastal Cleanup 25th Anniversary report.

Council, American Chemistry. 2014a. History of Polymers & Plastics for Teachers. http://www.americanchemistry.com/hops/intro_to_plastics/teachers.html.

Council, American Chemistry. 2014b. Life Cycle of a Plastic Product. http://www.americanchemistry.com/s_plastics/doc.asp?CID=1571&DID=5972.

Council, American Chemistry. 2014c. Resin Identification Codes. http://plastics.americanchemistry.com/Plastic-Resin-Codes-PDF.

Cózar, A., F. Echevarría, J. I. González-Gordillo, X. Irigoien, B. Úbeda, S. Hernández-León, Á. T. Palma, S. Navarro, J. García-de-Lomas, and A. Ruiz. 2014. Plastic debris in the open ocean. Proceedings of the National Academy of Sciences **111**:10239-10244.

Davison, P., and R. G. Asch. 2011. Plastic ingestion by mesopelagic fishes in the North Pacific Subtropical Gyre. Marine Ecology Progress Series **432**:173-180.

Defossez, J.-M., and A. Hawkins. 1997. Selective feeding in shellfish: size-dependent rejection of large particles within pseudofaeces from *Mytilus edulis*, *Ruditapes philippinarum* and *Tapes decussatus*. Marine Biology **129**:139-147.

Derraik, J. G. B. 2002. The pollution of the marine environment by plastic debris: a review. Marine Pollution Bulletin **44**:842-852.

Donohue, M. J., R. C. Boland, C. M. Sramek, and G. A. Antonelis. 2001. Derelict Fishing Gear in the Northwestern Hawaiian Islands: Diving Surveys and Debris Removal in

1999 Confirm Threat to Coral Reef Ecosystems. Marine Pollution Bulletin **42**:1301-1312.

Dotmar. 2014. Density of Plastics. http://www.dotmar.com.au/density.html.

Dupont. 2014a. Dupont Heritage Timeline: 1939 Nylon. History, http://www2.dupont.com/Phoenix_Heritage/en_US/1939_c_detail.html.

Dupont. 2014b. Dupont Heritage Timeline: 1941 Orlon. History, http://www2.dupont.com/Phoenix_Heritage/en_US/1941_detail.html.

EPA. 2016. Advancing Sustainable Materials Management: 2014 Fact Sheet. Advancing Sustainable Materials Management. U.S. Environmental Protection Agency.

Eriksen, M., L. C. Lebreton, H. S. Carson, M. Thiel, C. J. Moore, J. C. Borerro, F. Galgani, P. G. Ryan, and J. Reisser. 2014. Plastic Pollution in the World's Oceans: More than 5 Trillion Plastic Pieces Weighing over 250,000 Tons Afloat at Sea. PloS one **9**:e111913.

Eriksen, M., S. Mason, S. Wilson, C. Box, A. Zellers, W. Edwards, H. Farley, and S. Amato. 2013. Microplastic pollution in the surface waters of the Laurentian Great Lakes. Marine Pollution Bulletin **77**:177-182.

Fry, D. M., S. I. Fefer, and L. Sileo. 1987. Ingestion of plastic debris by Laysan albatrosses and wedge-tailed shearwaters in the Hawaiian Islands. Marine Pollution Bulletin **18**:339-343.

Gerritse, L. J., and D.Vethaak. 2015. CLEANSEA Special Newsletter. CLEANSEA.

GESAMP. 2015. Sources, fate and effects of microplastics in the marine environment: a global assessment. IMO/FAO/UNESCO-IOC/UNIDO/WMO/IAEA/UN/ UNEP/UNDP Joint Group of Experts on the Scientific Aspects of Marine Environmental Protection.

GESAMP. 2016. Sources, fates, and effects of microplastics in the marine environment: part two of a global assessment. IMO/FAO/UNESCO-IOC/UNIDO/WMO/IAEA/UN/ UNEP/UNDP Joint Group of Experts on the Scientific Aspects of Marine Environmental Protection.

Gilfillan, L. R., M. D. Ohman, M. J. Doyle, and W. Watson. 2009. Occurrence of plastic micro-debris in the southern California Current system. California Cooperative Oceanic Fisheries Investigations Reports **50**:123-133.

Goldstein, M. C., H. S. Carson, and M. Eriksen. 2014. Relationship of diversity and habitat area in North Pacific plastic-associated rafting communities. Marine Biology **161**:1441-1453.

Goldstein, M. C., and D. S. Goodwin. 2013. Gooseneck barnacles (*Lepas* spp.) ingest microplastic debris in the North Pacific Subtropical Gyre. PeerJ **1**:e184.

Goldstein, M. C., M. Rosenberg, and L. Cheng. 2012. Increased oceanic microplastic debris enhances oviposition in an endemic pelagic insect. Biology Letters **8**:817-820.

Goldstein, M. C., A. J. Titmus, and M. Ford. 2013. Scales of spatial heterogeneity of plastic marine debris in the northeast Pacific ocean. PloS one **8**:e80020.

Graham, E. R., and J. T. Thompson. 2009. Deposit- and suspension-feeding sea cucumbers (Echinodermata) ingest plastic fragments. Journal of Experimental Marine Biology and Ecology **368**:22-29.

Gregory, M. R. 2009. Environmental implications of plastic debris in marine settings—entanglement, ingestion, smothering, hangers-on, hitch-hiking and alien invasions. Philosophical Transactions of the Royal Society B: Biological Sciences **364**:2013-2025.

Harbison, G., and V. McAlister. 1979. The filter‐feeding rates and particle retention efficiencies of three species of *Cyclosalpa* (Tunicata, Thaliacea). Limnology and Oceanography **24**:875-892.

Hart, M. W. 1991. Particle captures and the method of suspension feeding by echinoderm larvae. The Biological Bulletin **180**:12-27.

Hartline, N. L., N. J. Bruce, S. N. Karba, E. O. Ruff, S. U. Sonar, and P. A. Holden. 2016. Microfiber masses recovered from conventional machine washing of new or aged garments. Environmental science & technology **50**:11532-11538.

Henderson, J. R. 2001. A pre- and post-MARPOL Annex V summary of Hawaiian monk seal entanglements and marine debris accumulation in the northwestern Hawaiian Islands, 1982–1998. Marine Pollution Bulletin **42**:584-589.

Hendy, I. L., L. Dunn, A. Schimmelmann, and D. Pak. 2013. Resolving varve and radiocarbon chronology differences during the last 2000 years in the Santa Barbara Basin sedimentary record, California. Quaternary International **310**:155-168.

Hidalgo-Ruz, V., L. Gutow, R. C. Thompson, and M. Thiel. 2012. Microplastics in the marine environment: a review of the methods used for identification and quantification. Environmental science & technology **46**:3060-3075.

Hoffman, D. L. 1989. Settlement and recruitment patterns of a pedunculate barnacle, *Pollicipes polymerus* (Sowerby), off La Jolla, California. Journal of Experimental Marine Biology and Ecology **125**:83-98.

Jambeck, J. R., R. Geyer, C. Wilcox, T. R. Siegler, M. Perryman, A. Andrady, R. Narayan, and K. L. Law. 2015. Plastic waste inputs from land into the ocean. Science **347**:768-771.

Jang, M., W. J. Shim, G. M. Han, M. Rani, Y. K. Song, and S. H. Hong. 2016. Styrofoam debris as a source of hazardous additives for marine organisms. Environmental science & technology **50**:4951-4960.

Kaiser, D., N. Kowalski, S. Oberbeckmann, and J. J. Waniek. 2017. Proving a paradigm: Biofilms enhance microplastic deposition.*in* ASLO 2017: Mountains to the Sea, Honolulu, HI.

Karl, D. M. 1999. A sea of change: biogeochemical variability in the North Pacific Subtropical Gyre. Ecosystems **2**:181-214.

Katija, K., C. A. Choy, R. E. Sherlock, A. D. Sherman, and B. H. Robison. 2017. From the surface to the seafloor: How giant larvaceans transport microplastics into the deep sea. Science Advances **3**:e1700715.

Koelmans, A. A., E. Besseling, and W. J. Shim. 2015. Nanoplastics in the aquatic environment. Critical review. Pages 325-340 Marine Anthropogenic Litter. Springer.

Law, K. L., S. Morét-Ferguson, N. A. Maximenko, G. Proskurowski, E. E. Peacock, J. Hafner, and C. M. Reddy. 2010. Plastic accumulation in the North Atlantic subtropical gyre. Science **329**:1185-1188.

Law, K. L., S. E. Morét-Ferguson, D. S. Goodwin, E. R. Zettler, E. DeForce, T. Kukulka, and G. Proskurowski. 2014. Distribution of surface plastic debris in the eastern Pacific Ocean from an 11-year data set. Environmental science & technology **48**:4732-4738.

Lechner, A., H. Keckeis, F. Lumesberger-Loisl, B. Zens, R. Krusch, M. Tritthart, M. Glas, and E. Schludermann. 2014. The Danube so colourful: A potpourri of plastic litter outnumbers fish larvae in Europe's second largest river. Environmental Pollution **188**:177-181.

Lozano, R., and J. Mouat. 2009. Marine Litter in the North-East Atlantic Region: Assessment and Priorities for Response. KIMO International. 9781906840266.

Masterson, K. 2009. The history of plastic: From billiards to bibs. Plastic Peril? NPR, http://www.npr.org/templates/story/story.php?storyId=114331762.

Mattsson, K., E. V. Johnson, A. Malmendal, S. Linse, L.-A. Hansson, and T. Cedervall. 2017. Brain damage and behavioural disorders in fish induced by plastic nanoparticles delivered through the food chain. Scientific Reports **7(1)**:11452.

Maximenko, N., J. Hafner, and P. Niiler. 2012. Pathways of marine debris derived from trajectories of Lagrangian drifters. Marine Pollution Bulletin **65**:51-62.

Meehl, G. A. 1982. Characteristics of surface current flow inferred from a global ocean current data set. Journal of Physical Oceanography **12**:538-555.

Moody, S. 2010. Washed Up: The curious journeys of flotsam and jetsam. Sasquatch Books.

Moore, C. J., S. L. Moore, M. K. Leecaster, and S. B. Weisberg. 2001. A comparison of plastic and plankton in the North Pacific central gyre. Marine Pollution Bulletin **42**:1297-1300.

Murray, F., and P. R. Cowie. 2011. Plastic contamination in the decapod crustacean *Nephrops norvegicus* (Linnaeus, 1758). Marine Pollution Bulletin **62**:1207-1217.

Ogata, Y., H. Takada, K. Mizukawa, H. Hirai, S. Iwasa, S. Endo, Y. Mato, M. Saha, K. Okuda, A. Nakashima, M. Murakami, N. Zurcher, R. Booyatumanondo, M. P. Zakaria, L. Q. Dung, M. Gordon, C. Miguez, S. Suzuki, C. Moore, H. K. Karapanagioti, S. Weerts, T. McClurg, E. Burres, W. Smith, M. V. Velkenburg, J. S. Lang, R. C. Lang, D. Laursen, B. Danner, N. Stewardson, and R. C. Thompson. 2009. International Pellet Watch: Global monitoring of persistent organic pollutants (POPs) in coastal waters. 1. Initial phase data on PCBs, DDTs, and HCHs. Marine Pollution Bulletin **58**:1437-1446.

PlasticsEurope. 2012. Plastics- The Facts 2012: An analysis of European plastics production, demand and waste data for 2011. http://www.plasticseurope.org/.

Rochman, C. M., E. Hoh, T. Kurobe, and S. J. Teh. 2013. Ingested plastic transfers hazardous chemicals to fish and induces hepatic stress. Scientific Reports **3**.

Ryan, P. G., C. J. Moore, J. A. van Franeker, and C. L. Moloney. 2009. Monitoring the abundance of plastic debris in the marine environment. Philosophical Transactions of the Royal Society of London B: Biological Sciences **364**:1999-2012.

Schimmelmann, A., I. L. Hendy, L. Dunn, D. K. Pak, and C. B. Lange. 2013. Revised~ 2000-year chronostratigraphy of partially varved marine sediment in Santa Barbara Basin, California. GFF **135**:258-264.

Schlining, K., S. von Thun, L. Kuhnz, B. Schlining, L. Lundsten, N. J. Stout, L. Chaney, and J. Connor. 2013. Debris in the deep: Using a 22-year video annotation database to survey marine litter in Monterey Canyon, central California, USA. Deep Sea Research Part I: Oceanographic Research Papers **79**:96-105.

Smith, K., A. Sherman, C. Huffard, P. McGill, R. Henthorn, S. Von Thun, H. Ruhl, M. Kahru, and M. Ohman. 2014. Large salp bloom export from the upper ocean and

benthic community response in the abyssal northeast Pacific: Day to week resolution. Limnology and Oceanography **59**:745-757.

Stefatos, A., M. Charalampakis, G. Papatheodorou, and G. Ferentinos. 1999. Marine debris on the seafloor of the Mediterranean Sea: Examples from two enclosed gulfs in western Greece. Marine Pollution Bulletin **38**:389-393.

Supply, Freund Container. 2010. Plastic Properties. Guide to Plastics.

Thiel, M., and L. Gutow. 2005. The ecology of rafting in the marine environment. II. The rafting organisms and community. Oceanography and Marine Biology: an annual review **43**:279-418.

Thompson, R. C., Y. Olsen, R. P. Mitchell, A. Davis, S. J. Rowland, A. W. John, D. McGonigle, and A. E. Russell. 2004. Lost at sea: where is all the plastic? Science **304**:838-838.

USEPA. 1992. Plastic pellets in the aquatic environment: Sources, and recommendations. Washington, DC.

Van Cauwenberghe, L., A. Vanreusel, J. Mees, and C. R. Janssen. 2013. Microplastic pollution in deep-sea sediments. Environmental Pollution **182**:495-499.

Venrick, E., T. Backman, W. Bartram, C. Platt, M. Thornhill, and R. Yates. 1973. Man-made objects on the surface of the central North Pacific Ocean. Nature **241**:271-271.

Wilson, D. S. 1973. Food size selection among copepods. Ecology **54**:909-914.

Wong, C., D. R. Green, and W. J. Cretney. 1974. Quantitative tar and plastic waste distributions in the Pacific Ocean. Nature **247**:30-32.

Woodall, L. C., A. Sanchez-Vidal, M. Canals, G. L. Paterson, R. Coppock, V. Sleight, A. Calafat, A. D. Rogers, B. E. Narayanaswamy, and R. C. Thompson. 2014. The deep sea is a major sink for microplastic debris. Royal Society open science **1**:140317.

Zalasiewicz, J., C. N. Waters, J. A. I. do Sul, P. L. Corcoran, A. D. Barnosky, A. Cearreta, M. Edgeworth, A. Gałuszka, C. Jeandel, and R. Leinfelder. 2016. The geological cycle of plastics and their use as a stratigraphic indicator of the Anthropocene. Anthropocene **13**:4-17.

Zalasiewicz, J., C. N. Waters, C. P. Summerhayes, A. P. Wolfe, A. D. Barnosky, A. Cearreta, P. Crutzen, E. Ellis, I. J. Fairchild, and A. Gałuszka. 2017. The Working Group on the Anthropocene: Summary of evidence and interim recommendations. Anthropocene. **19**:55-60.

CHAPTER 2

Contents lists available at ScienceDirect

Marine Pollution Bulletin

journal homepage: www.elsevier.com/locate/marpolbul

Long-term aging and degradation of microplastic particles: Comparing in situ oceanic and experimental weathering patterns

Jennifer Brandon *, Miriam Goldstein, Mark D. Ohman

Scripps Institution of Oceanography, University of California San Diego, La Jolla, CA 92093, USA

ARTICLE INFO

Article history:
Received 28 June 2015
Received in revised form 2 June 2016
Accepted 12 June 2016
Available online 22 June 2016

Keywords:
FTIR
Polyethylene (PE)
Polypropylene (PP)
North Pacific Subtropical Gyre
Weathering
Oceanic microplastic

ABSTRACT

Polypropylene, low-density polyethylene, and high-density polyethylene pre-production plastic pellets were weathered for three years in three experimental treatments: dry/sunlight, seawater/sunlight, and seawater/darkness. Changes in chemical bond structures (hydroxyl, carbonyl groups and carbon-oxygen) with weathering were measured via Fourier Transform Infrared (FTIR) spectroscopy. These indices from experimentally weathered particles were compared to microplastic particles collected from oceanic surface waters in the California Current, the North Pacific Subtropical Gyre, and the transition region between the two, in order to estimate the exposure time of the oceanic plastics. Although chemical bonds exhibited some nonlinear changes with environmental exposure, they can potentially approximate the weathering time of some plastics, especially high-density polyethylene. The majority of the North Pacific Subtropical Gyre polyethylene particles we measured have inferred exposure times > 18 months, with some >30 months. Inferred particle weathering times are consistent with ocean circulation models suggesting a long residence time in the open ocean.

1. Introduction

Plastics in the ocean, particularly in the North Pacific Subtropical Gyre, have been of concern for decades (Carpenter and Smith, 1972; Wong et al., 1974). Recent studies estimate that there may be approximately five trillion pieces of plastic in the global ocean, with an estimated 4.8 to 12.7 million metric tons entering the ocean annually (Eriksen et al., 2014; Jambeck et al., 2015). Eriksen et al. (2014), along with others (Hidalgo-Ruz et al., 2012; Goldstein et al., 2013), state that the vast numerical majority of plastics in the ocean are microplastic, or particles < 5 mm in diameter. However, there is currently no method that estimates how long a given microplastic particle has been in the ocean. The small size of fragmented, weathered particles also makes it impossible to trace these particles to their source (Jambeck et al., 2015). Knowing how long a particle has been in the ocean is critical for calculating the residence time of particles in different regions of the ocean, testing the accuracy of models, and assessing the efficacy of marine debris mitigation policy.

The small fragments of microplastic created by weathering are detrimental to ocean ecosystems for multiple reasons. Studies have shown gooseneck barnacles (Goldstein and Goodwin, 2013), mesopelagic fishes (Davison and Asch, 2011), Norway lobsters (Murray and Cowie, 2011), and other small animals can consume microplastics *in situ*, and other invertebrates have been shown to eat them in lab settings (Murray and Cowie, 2011; Cole et al., 2013; Wright et al., 2013). Synthetic microfibers and microplastics are small enough to physically accumulate and to translocate from an organism's gut into its circulatory system (Browne et al., 2008). Some plastics contain harmful chemical additives (e.g. PCBs – polychlorinated biphenyls) that can bioaccumulate in marine organisms, leading to liver toxicity and other deleterious physiological effects (Rochman et al., 2013). Since plastics' hydrophobicity causes them to sorb marine and atmospheric persistent organic pollutants, there is also concern for bioaccumulation of these pollutants from plastic ingestion (Ogata et al., 2009).

Microplastics are currently impossible to remove *en masse* from the open ocean due to their small size, chemical inertness, similar dimension and distribution as plankton and fish eggs, and their distribution over the vast extent of the oceanic gyres. Thus, it is essential to understand processes that lead to the accumulation and degradation of plastic particles, as well as to develop strategies to limit inputs into the ocean (Jambeck et al., 2015).

Although many studies have examined aging of polyethylene and polypropylene (Stark and Matuana, 2004; La Mantia and Morreale, 2008), almost all have been conducted in accelerated weathering devices that use much higher temperatures than natural weathering (Stark and Matuana, 2004). Elevated temperatures can lead to different chemical reactions than those that occur naturally (Lacoste and Carlsson, 1992; Tidjani, 2000).

There have been some studies of the natural weathering of plastics: Andrady et al. (1993) examined natural weathering of LDPE, and Rajakumar et al. (2009) examined natural weathering of PP; both experiments tested sheets of plastic film in ambient air and rain. Andrady (1990) compared the weathering of LDPE films in ambient

* Corresponding author.
E-mail address: jabrandon@ucsd.edu (J. Brandon).

http://dx.doi.org/10.1016/j.marpolbul.2016.06.048
0025-326X/

air and ambient seawater. Pegram and Andrady (1989) tested LDPE film, PP strapping tape, latex balloons and trawl netting in both ambient air and seawater. Though these studies are very useful, the numerical majority of marine debris is not intact films or objects but rather microplastic particles (Goldstein et al., 2013). Also, most previous studies extend for a maximum of three months, with some for only a few weeks (Lacoste and Carlsson, 1992; Andrady et al., 1993; La Mantia and Morreale, 2008), although Andrady (1990) and Pegram and Andrady (1989) weathered samples for a year. There is a need for greater understanding of the longer term, natural weathering of microplastics and the variables that interact in that weathering process (Tidjani, 2000). In addition, knowing how microplastic particles weather is important for understanding the ecological impacts of the most common type of marine debris.

The present study's unique results stem from longer term (i.e., 3 year) controlled exposure to natural sunlight and ambient seawater. It is therefore a more realistic proxy for the weathering processes that plastic particles experience in the open ocean than many previous studies. This is also the first study to directly compare naturally weathered plastic particles to particles collected from the ocean in an attempt to quantify the exposure time of the oceanic particles.

2. Materials and methods

2.1. Weathering experiment

Beginning in December 2010, preproduction pellets (or nurdles) of the six most common consumer plastics (Andrady, 2003) were exposed to three treatments: dry/sunlight, seawater/darkness, or seawater/sunlight, in comparison with dry/darkness control treatments. The dry/sunlight treatment roughly approximates the weathering conditions of dried plastic particles on beaches; seawater/darkness simulates conditions similar to those found in some benthic environments; seawater/sunlight simulates exposure of particles floating at the air-sea interface. The six consumer plastics were polyethylene terephthalate (PET; Resin ID #1), high density polyethylene (HDPE; Resin ID #2), polyvinyl chloride (PVC; Resin ID #3), low density polyethylene (LDPE; Resin ID #4), polypropylene (PP; Resin ID #5), and polystyrene (PS; Resin ID #6) (American Chemistry Council, 2010).

For the dry/sunlight treatment, 250 mL of each type of preproduction pellet were placed in Pyrex glass trays on the roof of Hubbs Hall at Scripps Institution of Oceanography, La Jolla, California, 32.867°N, 117.257°W. Each tray was covered by fiberglass screening (2 mm mesh size) to prevent pellet loss. Each type of plastic was placed in two trays on the roof (N = 2), except for PVC (N = 1 due to a shortage of supply pellets). The roof was covered in naturally colored pebbles, having a similar albedo effect as most beaches, and had unoccluded natural sunlight throughout daylight hours year-round.

For the seawater/darkness and seawater/sunlight treatments, 250 mL of each type of preproduction pellet were placed in 75.7 L (20 gal) aquaria with flowing seawater (N = 2 for each treatment, N = 1 for PVC). To separate plastic types, aquarium divider screens were installed. Each plastic type was randomly assigned to a location in the tank, with different locations in the two replicate tanks. Local seawater from the Scripps running seawater system (intake from the seaward end of the Scripps Pier) flowed continuously through a sprinkle bar placed over the tank, and drained through a screen-covered standpipe. The seawater/darkness treatment tanks were placed in an indoor experimental room and covered in opaque black plastic sheeting, which was only removed when the tanks were sampled. The seawater/sunlight tanks were placed side-by-side with the dry/sunlight treatments, and the tops of the aquaria were covered with fiberglass screening to prevent pellet loss.

From December 2010 to July 2012, the experiment was sampled monthly by removing ten pellets from each replicate. After July 2012, the tanks were all cleaned monthly, but the pellets were sampled bimonthly. After removal, pellets were gently wiped to remove epiphytes, rinsed with deionized water, dried at 60 °C for 24 h, and stored in glass vials in the dark at room temperature until Fourier-Transform Infrared Spectrometer (FTIR) analysis.

Seven time points were selected for analysis: T_0 = unweathered particles, T_5 = 5 months of weathering, T_9 = 9 months, T_{13} = 13 months, T_{18} = 18 months, T_{30} = 30 months, and T_{36} = 36 months. Only HDPE, LDPE and PP were analyzed for the experimental study because they are the most common plastics found at the ocean's surface, due to their common commercial use and positive buoyancy (Freund Container & Supply, 2010). In 2012, PE and PP accounted for 63% of the plastic waste in the United States (EPA, 2014).

2.2. Oceanic samples

In August 2009, samples were collected on the Scripps Environmental Accumulation of Plastic Expedition (SEAPLEX) cruise on the *R/V New Horizon* (Fig. 1). Samples were collected using a standard Manta net (0.86 m wide × 0.2 m high mouth opening) (Brown and Cheng, 1981) with 333 μm mesh, towed for 15 min at 0.7–1 m s^{-1}. Water volume flowing through the net was measured with a calibrated General Oceanics analog flowmeter. Samples were fixed in 1.8% formaldehyde buffered with sodium tetraborate.

Each sample was sorted for microplastic at 6–12× magnification under a Wild M-5 dissecting microscope. Plastic particles were removed, dried at 60 °C, and stored in glass vials in the dark at room temperature. If there were fewer than 50 particles per sample, the entire sample was analyzed. If there were >50 particles per sample, the sample was split using the quartering method (ASTM Standard C702/C702M-11, 2011) until an aliquot of 30–50 particles was obtained. Particles were then soaked for 12 h in 10% hydrochloric acid to remove calcium carbonate deposits, rinsed in deionized water, re-dried at 60 °C, and stored in glass vials in the dark at room temperature.

For the present study analysis, the California Current was defined as having a surface temperature < 19 °C and surface salinity < 33.5 (Lynn and Simpson, 1987). The North Pacific Subtropical Gyre (NPSG) was defined as having surface temperatures > 22 °C and salinity > 34.8 (Roden, 1980; Niiler and Reynolds, 1984). The transition region was defined as having a surface temperature of 19–22 °C and surface salinity of 33.5–34.8 (Roden, 1980; Lynn and Simpson, 1987). Because only surface data were used, these should be viewed as approximations rather than absolute oceanographic definitions (Goldstein et al., 2013). Fig. 1 reflects the sampling locations of the SEAPLEX cruise, with filled shapes indicating those sampling stations analyzed using FTIR in this study. These stations were chosen so that they were distributed throughout the cruise track, without reference to the abundance of plastic in each sample. Median bond indices (see below) from the three regions were

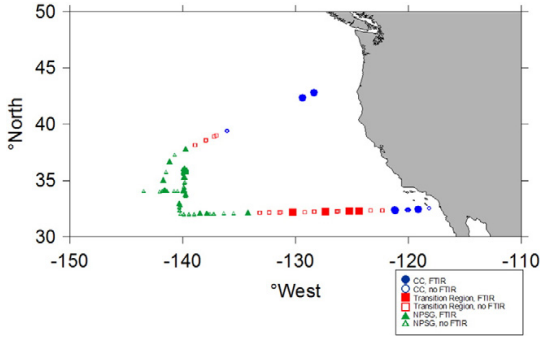

Fig. 1. SEAPLEX Manta net sampling locations. California Current (blue circles), transition region (red squares) North Pacific Subtropical Gyre (green triangles). Points indicate all locations sampled via Manta net; solid symbols are Manta samples analyzed by FTIR for this study.

compared by the Kruskal-Wallis test, then a multiple comparison test performed, adapted from Siegel and Castellan (1988), where significance between two regions was defined as $p < 0.05$.

2.3. FTIR

Both ocean-collected and weathering experiment samples were analyzed using a Fourier-Transform Infrared Spectrometer with an attenuated total reflectance (ATR) diamond crystal attachment (Nicolet 6700 with Smart-iTR). All spectra were recorded at 4 cm^{-1} resolution. The FTIR spectra for particles collected from the ocean were compared to both published standards (Forrest et al., 2007) and in-house standards for the 6 common consumer plastic types listed above. LDPE was distinguished from HDPE by the presence of a peak at 1377 cm^{-1}, with its presence indicating LDPE and absence HDPE (Fig. 2) (Lobo and Bonilla, 2003). If the type of polyethylene could not be positively determined, the sample was classified as unknown PE, which occurred in 30% of oceanic polyethylene samples.

For experimental weathering samples, 5 particles were randomly subsampled from the 10 particles collected at each time point. Depending on particle shape, either 2 or 3 spectra were obtained from different locations on each particle. For asymmetrical particles, especially LDPE which were often concave discs, the location of the spectra reading on the particle was determined to affect values due to the need for precise contact with the ATR crystal (Gulmine et al., 2002). Particles only demonstrated clean readings if the ATR crystal was completely, or almost completely, covered in plastic, and there was no trapped air between the plastic particle and the crystal. Clean spectra from different regions of a single particle were treated as independent and averaged. If a particle split into pieces or crumbled into powder while performing FTIR, readings of both the inside and outside of the pieces were taken and treated as independent, if readings were distinct.

Three likely areas of weathering-related change in infrared spectra were first identified from previous research: hydroxyl groups (broad peaks from 3100 to 3700, centered at 3300–3400 cm^{-1}), alkenes, or carbon double bonds (1600–1680 cm^{-1}), and carbonyls (1690–1810 cm^{-1}, centered at 1715 cm^{-1}) (Albertsson et al., 1987; Lacoste and Carlsson, 1992; Socrates, 2004; Pavia et al., 2008; Rajakumar et al., 2009). The

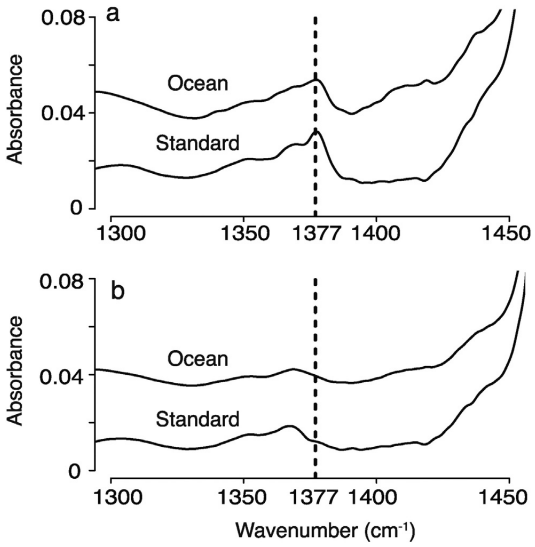

Fig. 2. Portion of FTIR spectra of microplastics collected from the ocean compared to laboratory standards. a) Low-density polyethylene (LDPE) and b) high-density polyethylene (HDPE).

hydroxyl peaks in our spectra had the broad peak shape and location of intermolecular hydrogen bonded O—H bonds (Socrates, 2004; Pavia et al., 2008). When carbon double bonds are non-conjugated in a hydrocarbon, they are often seen from 1620 to 1680 cm^{-1}, and at lower frequencies, around 1600 cm^{-1} if conjugated; however symmetrically substituted bonds are often IR inactive (Socrates, 2004; Pavia et al., 2008). Carbonyl bonds have a strong IR signal and appear in a wide range of wavelengths, even as wide as 1550–1850 cm^{-1} (Socrates, 2004), and so the frequency of a ketone, 1715 cm^{-1}, is often used as the central reference for the range of these values (Pavia et al., 2008).

Three additional areas of change in the plastics' spectra, 1000–1200 cm^{-1}, 1200–1280 cm^{-1}, and 1540 cm^{-1}, were located empirically. The peak at 1540 cm^{-1} was very close to the 1640 cm^{-1} peak and the commonly cited peak for changes in carbonyl bonds (1715 cm^{-1}) (Lacoste and Carlsson, 1992) also often overlapped with the peak centered at 1640 cm^{-1}. The IR signal for double bonds is weaker than that for carbonyl bonds, the bonds are in overlapping ranges, and symmetrically substituted double bonds are inactive. Due to all of these factors, the entire range of 1550–1810 cm^{-1} was referred to as the "carbonyl groups." All carbonyl groups are indicative of oxidized carbon in the plastic hydrocarbon chain, and were grouped together throughout the manuscript. This manuscript is less concerned with which specific carbonyl group is present, but rather with whether plastic has oxidized as it has weathered, and the presence of carbonyls show that oxygen has bonded with the hydrocarbon chain.

The empirically located region at 1000–1200 cm^{-1} is the spectral range of carbon-oxygen bonds and 1200–1280 cm^{-1} is the range of carbon-nitrogen bond stretching in secondary amines (El-Ghaffar et al., 1998; Pavia et al., 2008). Although pure PE and PP do not have any nitrogen in their structure, nitrogen is the main component in air and is present in seawater, and can be found in plastic additives; C—N bonds have been measured on plastics via X-ray photoelectron spectroscopy (Stark and Matuana, 2004). However, these results were not considered further because C—N bonds are unlikely to be seen in large quantities in plastics, and because their peak was weak in our spectra and changed little over time. The commonly cited peak for changes in vinyl groups (centered around 909 cm^{-1}) (Tidjani, 2000) was also too weak in our spectra to be read accurately.

Indices of hydroxyl, carbon-oxygen bonds, and carbonyl group bonds were calculated as the ratio of the maximum absorbance value for the bond peak relative to the value of a reference peak. Several reference peaks have been used previously, including 974 cm^{-1} and 2720 cm^{-1} for PP (Livanova and Zaikov, 1992; Rabello and White, 1997; Rajakumar et al., 2009) and 1465 cm^{-1} and 2020 cm^{-1} for PE (Albertsson et al., 1987; Roy et al., 2011). We selected 2910 cm^{-1} for PE and 2920 cm^{-1} for PP because these peaks, both also characteristic of plastic type, are thought to change little with weathering, as corroborated in our study (Socrates, 2004).

Bond indices were therefore calculated as the ratio of the maximum peak absorbance (numerator) to the value of a reference peak (denominator) as follows (Table 1): hydroxyl (LDPE/HDPE 3300–3400 cm^{-1}/2908–2920 cm^{-1}; PP 3300–3400 cm^{-1}/2885–2940 cm^{-1}), carbonyl groups (LDPE/HDPE 1550–1810 cm^{-1}/2908–2920 cm^{-1}; PP 1550–1810 cm^{-1}/2885–2940 cm^{-1}), and carbon-oxygen (LDPE/HDPE 1000–1200 cm^{-1}/2908–2920 cm^{-1}; PP 1000–1200 cm^{-1}/2885–2940 cm^{-1}).

Before calculating indices, baselines were corrected using Essential FTIR/eFTIR software (http://www.essentialftir.com). All spectra were corrected using eFTIR's Advanced ATR (Attenuated Total Reflectance) Correction that used the Refractive Index (RI) of each plastic type, thickness of each particle, and the Angle of Incidence to correct for dispersion and depth of penetration. The parameters used were: RI: 1.57 for PS, 1.5 for PE, 1.49 for PP, 1.65 for PVC, and 1.5 for PET (Samuels, 1981; Markelz et al., 2000; Ma et al., 2003; Rodriguez-Gonzalez et al., 2003; Piesiewicz et al., 2007); thicknesses: 0.2 cm for PS, 0.2 cm for PE, 0.3 cm for PP, 0.5 cm for PVC, and 0.2 cm for PET; angle of incidence: 42°. The samples were then corrected by normalizing to a minimum of zero and

Table 1
Wavenumbers used to measure weathering in FTIR spectroscopy.
The numerators of the bond indices are the same for PE and PP, but the reference peaks/denominators differ. The peaks used were centered in the ranges given below, with some variability among samples.

	Hydroxyl	Carbonyl groups	Carbon-oxygen
PE numerator	3300–3400[a]	1550–1810[b]	1000–1200[a]
PE denominator	2908–2920[c]	2908–2920[c]	2908–2920[c]
PP numerator	3300–3400[a]	1550–1810[b]	1000–1200[a]
PP denominator	2885–2940[c]	2885–2940[c]	2885–2940[c]

[a] Pavia et al. (2008).
[b] Corrales et al. (2002).
[c] Socrates (2004).

the maximum absorption value of each spectrum (Workman and Springsteen, 1998).

After ATR correction and normalization of the baseline, spectra were excluded that were too low, in order to remove any samples of extremely low signal-to-noise ratio. Samples were also removed that had very jagged or blocky spectral baselines, that did not have flat baselines even after normalization, or that did not have clear definition between the hydroxyl peak and the C—H reference peak at 2910 cm^{-1}. The precision of the plastic placement on the ATR crystal, the humidity of the FTIR analysis room, and the operator of the instrument could all add variability to the spectral readings.

2.4. Brittleness-crystallinity

Crystallinity was calculated by the method used in Zerbi et al. (1989) and Stark and Matuana (2004). Doublet peaks at 730 and 720 cm^{-1} correspond to polyethylene crystalline content (730 cm^{-1}) and amorphous content (720 cm^{-1}) (Zerbi et al., 1989; Stark and Matuana, 2004); 841 cm^{-1} corresponds to polypropylene crystalline content and 1170 cm^{-1} corresponds to polypropylene amorphous content (Tadokoro et al., 1965; Livanova and Zaikov, 1992).

The percentage crystalline content was calculated from:

$$X = 100 - \frac{(1 - I_c/I_a)/1.233}{1 + I_c/I_a}(100)$$

where I_c is the band at 730 cm^{-1} or 841 cm^{-1} and I_a is the band at 720 cm^{-1} or 1170 cm^{-1} and 1.233 relates to the theoretical intensity ratio for I_c/I_a at setting angle 42° (Avitabile et al., 1975; Abbate et al., 1979; Zerbi et al., 1989; Stark and Matuana, 2004).

2.5. Temperature

Elevated temperatures can accelerate aging of plastics (Lacoste and Carlsson, 1992; Stark and Matuana, 2004), so the temperature of the experimental conditions was recorded as follows. Sunlight samples were assumed to weather at the ambient air temperature of La Jolla, CA, obtained from NOAA's National Data Buoy Center Water Level Observation Network (http://www.ndbc.noaa.gov/). Air temperature was measured at Station LJAC1 (9410230) on the Scripps Pier at 32.867° N, 117.257° W at 16.46 m above sea level. NOAA measurements were recorded every 6 min, but here data were averaged every 8 h. For the seawater/darkness treatment, which used running seawater from the Scripps Pier, the seawater temperature was assumed to be the same as the seawater temperature recorded at NOAA Station LJAC1, at a depth of 3.44 m below sea level, also recorded every 6 min and averaged every 8 h.

To test for a difference in temperature between the seawater/sunlight tanks and the NOAA pier readings, in April 2014, HOBO Water Temp Pro v2 data loggers were placed in the seawater/sunlight tanks, recording temperature every 60 min. A HOBO logger was placed in both of the seawater/sunlight treatment tanks, and temperature recordings averaged every 8 h.

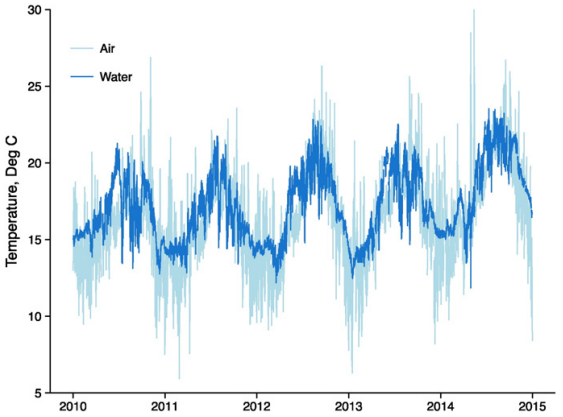

Fig. 3. Temperature. Ambient air temperature from NOAA's National Data Buoy Center's Station LJAC1 on the Scripps Pier (light blue) and ambient seawater temperature from Station LJAC1 (dark blue).

3. Results

3.1. Temperature

Air temperatures at the Scripps Pier varied between 5.9 and 30.4 °C and seawater temperatures near the Scripps Pier varied between 14.6 and 18.3 °C over the course of the plastics weathering experiment, with clear seasonal variation and a slight upward trend (Fig. 3). Data loggers placed in the pellet weathering tanks showed that the experimental tank temperatures averaged 2.7 °C greater than pier seawater, but followed the seasonal trends closely.

3.2. Experimental weathering

There were clear changes in chemical bond structure with weathering (Fig. 4), as evidenced by the difference in height between

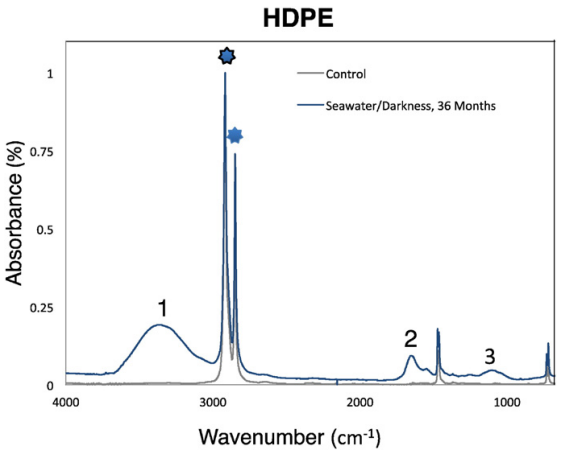

Fig. 4. FTIR spectrogram. Unweathered HDPE at T_0 (gray) and weathered HDPE at 36 months from the seawater/darkness treatment (blue). The changes in bond height at 3350 cm^{-1} (hydroxyl), 1640 cm^{-1} (carbonyl groups), and 1070 cm^{-1} (carbon-oxygen) are indicated by the numerals 1–3, respectively. The blue symbols near 2910 cm^{-1} and 2848 cm^{-1} indicates diagnostic PE doublet peaks, with the black outlined symbol at 2910 cm^{-1} also indicating the reference peak for PE weathering.

the unweathered HDPE (T_0) (gray line), and the HDPE from the seawater/darkness treatment after 36 months (blue line).

For the weathering experiment, we first describe results from the seawater/sunlight treatment, as this best simulates the conditions experienced by particles suspended in seawater in open ocean conditions. We then describe the effects of exposure to seawater/darkness and dry/sunlight for comparison.

Fig. 5 illustrates the seawater/sunlight treatment (pink) in relation to the control treatment of dry/darkness intended to induce the least amount of environmentally-induced weathering (gray; cf. Hidalgo-Ruz et al., 2012). For all three bonds, across all three plastic types, the control barely changed between 0 and 36 months. In contrast, exposure to seawater/sunlight resulted in time-dependent changes in hydroxyl bonds (Fig. 5a–c). For PE, there was a general increase in this bond index to 13 months, then a decrease at 18 months that lasted until 30 months, where it began to increase again. For PP, the same pattern was evident, but with a transient dip at 9 months, and no increase from 30 to 36 months.

Carbonyl groups (Fig. 5d–f) and carbon-oxygen bonds (Fig. 5g–i) show similar temporal patterns to the changes in hydroxyl groups for all three plastic types, with an increase from 0 to 13 months, a decrease between 13 and 30 months, and for PE, another increase from 30 to 36 months. LDPE had the steepest decrease from 13 to 30 months. The magnitude of the change in all PP bonds was substantially larger than the changes in these bonds for either LDPE or HDPE.

Turning to the other weathering treatments, Fig. 5 illustrates that for PE, there was a significant difference between the seawater/sunlight and dry/sunlight treatment at multiple time points ($p < 0.05$, based on non-overlapping confidence limits). There was a significant difference between seawater/sunlight and dry/sunlight treatments for LDPE at 13 months for hydroxyl, 9 and 30 months for carbonyl groups, and 18 months onward for carbon-oxygen. For HDPE, there was only a significant difference at 5 and 36 months for carbon-oxygen. In contrast, for PP, there were significant differences between the seawater/sunlight and dry/sunlight treatments at most time points for hydroxyl and carbonyl groups, though none for carbon-oxygen. Comparing seawater/sunlight and seawater/darkness treatments for PE, there was no significant difference between treatments until 36 months; at T_{36} for many of the bonds one of the two replicates of seawater/darkness had the highest values, though the average of the two replicates was not significantly higher than seawater/sunlight. This contrast also holds for T_{30} for PP hydroxyl. For PP hydroxyl bonds and carbonyl group bonds, the seawater/darkness values were significantly higher at 36 months than the seawater/sunlight values ($p < 0.05$).

Despite the lack of consistent differences between seawater/sunlight and the other treatments, the shapes of the weathering curves of the other two treatments appear somewhat different than seawater/sunlight. Dry/sunlight treatments show a quasi-linear change with time for all LDPE bonds. Seawater/darkness treatments show a much steeper increase from 30 to 36 months across all treatments. For LDPE carbon-oxygen bonds, seawater/darkness does not show the same initial increase at 9 months as seawater/sunlight; but after 13 months the values closely mirror seawater/sunlight until the steeper increase from 30 to 36 months. For HDPE and PP carbon-oxygen, the three treatments show somewhat different temporal progressions.

3.3. Oceanic particles

Fig. 6 compares experimental HDPE particles exposed to sunlight/seawater, and the corresponding control treatment, with oceanic

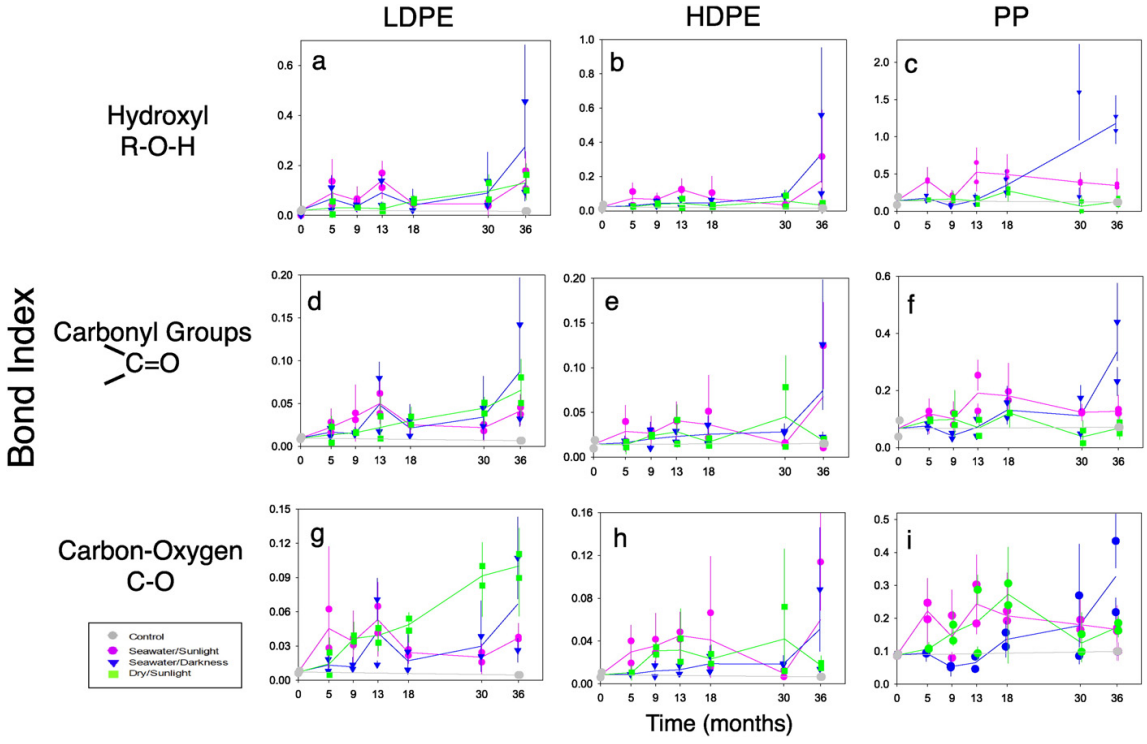

Fig. 5. Experimentally weathered LDPE, HDPE, and PP. FTIR results from experimentally weathered (a, d, g) LDPE, (b, e, h) HDPE, and (c, f, i) PP, for (top row) hydroxyl bonds, (middle row) carbonyl groups, and (bottom row) carbon-oxygen bonds. Seawater/sunlight experimental treatment (pink); dry/sunlight (green); seawater/darkness (blue); control of dry/darkness (gray). The two dots at each treatment represent means of the two separate tanks. Error bars indicate 95% confidence intervals.

HDPE particles from the North Pacific Subtropical Gyre (NPSG, dark gray histograms), transition region (TR, light gray histograms), and the California Current (CC, white histograms). Oceanic particles that could only be assigned to PE (but not to high or low density polyethylene) are compared to experimental results from both LDPE and HDPE in Supplemental Figs. 1 and 2 (discussed below).

Nearly all HDPE particles from all three oceanic regions are within the range of experimental determinations. Values from the three regions typically overlap both the 0–9 month and 18–36 experimental determinations. There is no significant difference among oceanic regions for hydroxyl bonds or carbon-oxygen bonds ($p > 0.05$); for carbonyl groups, the NPSG (dark gray, Fig. 6) and CC (white, Fig. 6) samples differ ($p < 0.05$) but neither is significantly different from the transition region.

For LDPE (Fig. 7), the majority of the oceanic values for all three bonds are within the range of the experimental values, although many exceed the range measured in the laboratory. Thirty percent of the values from the NPSG (dark gray, Fig. 7) are very low, corresponding to either the 0–9 month or 18–30 month experimental values for hydroxyl, with the next 28% corresponding with 30–36 months. For carbonyl, over 50% of the oceanic values correspond with 0–9 or 18–30 month values. For carbon-oxygen, 24% of the values are low, corresponding with 18–30 months. Values from the more nearshore California Current samples (white, Fig. 7) are variable, with a low mode for all three bonds, although sample sizes were small. Values for the transition region samples exceed most of the experimental values for hydroxyl and carbon-oxygen. For hydroxyl and carbon-oxygen bonds, there is a significant difference between the California Current and the transition region samples, and the transition region and the NPSG ($p < 0.05$, Kruskal-Wallis with multiple comparisons test). For carbonyl groups, there is no significant difference among the three oceanic regions ($p > 0.05$) and the majority of all values for all three regions are within the range of experimental values.

In Supplemental Fig. 1, some of the highest NPSG values only overlap the high experimental data point and 95% confidence interval for 36 months. Values from the three regions typically overlap both the 0–9 month and 18–36 experimental determinations. There is no significant difference among all three oceanic regions for any of the three bonds. In Supplemental Fig. 2, we compare the same undifferentiated oceanic PE plastic as Supp. Fig. 1 with experimentally weathered LDPE. The majority of the oceanic values for all three bonds are within the range of the experimental values, although many exceed the range measured in the laboratory. Most of the NPSG samples (dark gray) are low, overlapping with 0–9 months or 18–30 month samples, with the transition region samples being slightly higher. There is no significant difference among all three oceanic regions for any of the three bonds.

Fig. 8 compares experimental PP particles exposed to seawater/sunlight and the corresponding control treatment with ocean-collected PP particles. There is little overlap between the experimental values and the oceanic values, suggesting the bonds used here are not useful for quantifying the exposure time of PP plastic. There is more overlap between experimental and oceanic carbonyl group values than the other two bonds. None of the oceanic regions differ significantly from each other ($p > 0.05$).

3.4. Crystallinity

In both PE and PP, there were only slight differences in crystallinity over time, and a large range of values at every time point except the control. Crystallinity, as measured in Zerbi et al. (1989) and Stark and Matuana (2004), was not found to be a useful metric of aging in the present experiment, and the results are not discussed further here.

3.5. Qualitative observations of yellowness, opacity, and brittleness

There was clear visual evidence of an increase in opacity and yellowness in all experimental samples as time increased. When comparing all six types of consumer plastic tested in this experiment, the plastics that yellowed most were polystyrene (PS) and polyvinyl chloride (PVC). For LDPE, HDPE, and PP, by 36 months the sunlight treatment of both PP and LDPE were turning yellow, although the larger change in all three of these plastic types was in opacity and brittleness. A slight change in opacity could be seen in all of these plastics by 9 months, with clear, translucent PP and white-tinged, glossy HDPE turning fully opaque and dull in the sunlight treatment by 30 months.

Qualitatively, increased brittleness was detected as the experiment progressed. Pellets became more brittle with duration of environmental exposure, with PP becoming the most brittle of the three main plastics examined. By 9 months, HDPE and PP pellets (dry/sunlight treatment) would splinter and split into large pieces under the pressure of the FTIR stabilizing arm, while LDPE was still malleable. By 18 months, the dry/sunlight LDPE samples would flatten and break under the pressure. By 30 months, LDPE seawater/darkness samples were still malleable, but the seawater/sunlight samples would flatten under the pressure of the FTIR stabilizing arm and never regain their shape. By 30 months PP and HDPE dry/sunlight samples would often crumble into powder.

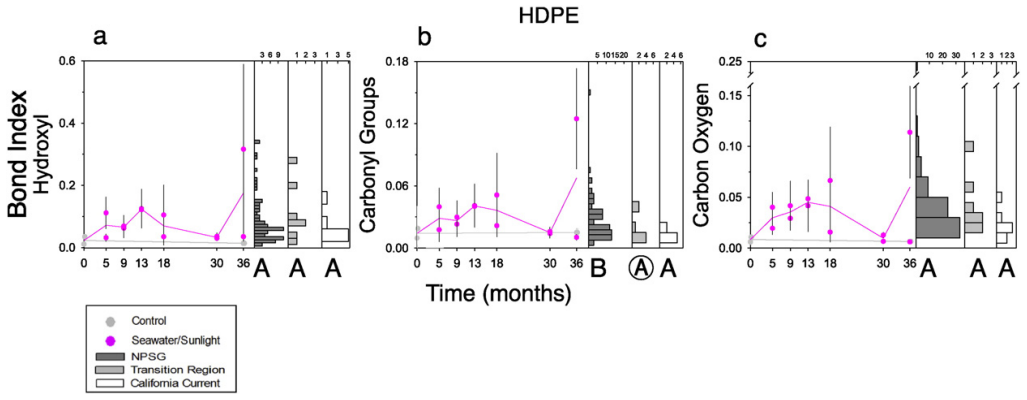

Fig. 6. Experimentally weathered HDPE compared to oceanic HDPE. FTIR results from experimentally weathered HDPE (pink lines) compared to oceanic HDPE particles (histograms), for (a) hydroxyl bonds, (b) carbonyl groups, and (c) carbon-oxygen bonds. Seawater/sunlight experimental treatment (pink line); control of dry/darkness (gray line). The two dots at each treatment represent means of the two separate tanks. Error bars indicate 95% confidence intervals. Histograms are SEAPLEX samples: North Pacific Subtropical Gyre (dark gray), transition region (light gray), California Current (white). The capital letters indicate regions that differ ($p < 0.05$) in a multiple comparisons test. A and B differ, Ⓐ differs from neither.

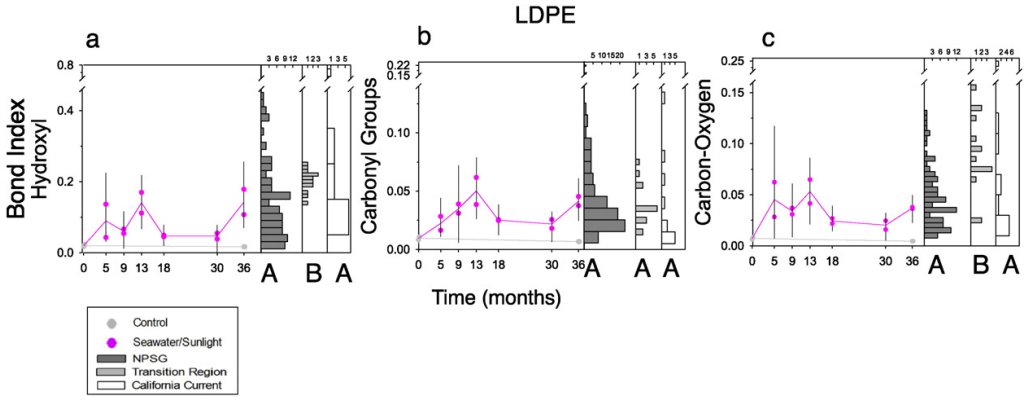

Fig. 7. Experimentally weathered LDPE compared to oceanic LDPE. FTIR results from experimentally weathered LDPE (pink lines) compared to oceanic LDPE particles (histograms), for (a) hydroxyl bonds, (b) carbonyl groups, and (c) carbon-oxygen bonds. Seawater/sunlight experimental treatment (pink line); control of dry/darkness (gray line). The two dots at each treatment represent means of the two separate tanks. Error bars indicate 95% confidence intervals. Histograms are SEAPLEX samples: North Pacific Subtropical Gyre (dark gray), transition region (light gray), California Current (white). The capital letters indicate regions that differ ($p < 0.05$) in a multiple comparisons test. A and B differ, Ⓐ differs from neither.

At 36 months, both PP and LDPE sunlight/seawater samples broke into small pieces as well.

4. Discussion

FTIR is a useful method to differentiate among the most common types of buoyant plastics that are found at the sea surface. We distinguished polypropylene (PP) from polyethylene (PE) in 100% of the ocean-collected particles analyzed. We could differentiate low density polyethylene (LDPE) from high density polyethylene (HDPE) in 70% of the particles. Some of the 30% that could not be distinguished may have been a manufactured PE blend or LLDPE (linear low density polyethylene), which is a rare plastic that we did not test.

Numerous other studies have utilized FTIR spectroscopy to identify marine debris in sediments (Thompson et al., 2004; Reddy et al., 2006; Frias et al., 2010) as well as to identify ingested plastic (Eriksson and Burton, 2003), but the present study appears to be one of the first to identify suspended sea surface marine debris particles with FTIR (Rios et al., 2007). That small fragments whose original purpose and provenance can no longer be identified can nevertheless be sorted to plastic type demonstrates that FTIR is useful for marine debris research. It is more accurate than the buoyancy method often used (Hidalgo-Ruz et al., 2012).

Ioakeimidis et al. (2016) also used FTIR spectroscopy to determine the exposure time of plastic marine debris, though they looked at PET plastic bottles. They also observed plastic change its chemical bond structure with weathering, measuring bonds that had never been documented in PET before. They highlight the need for a laboratory weathering study with which to properly compare their environmental results, which is the aim of this present study.

The bond indices presented here (hydroxyl, carbonyl groups, carbon-oxygen) may be most useful in future work quantifying the exposure time of PE, especially HDPE, from the field, due to the overlap in values in experimental and oceanic PE values. The bonds measured here for experimental weathering changes in PP do not apply well to oceanic PP samples. This may be because the experimental weathering was performed on pure pre-production PP, and the oceanic PP, with colorants and additives, may have reacted differently to environmental exposure.

It would be advisable to carry out weathering experiments for a longer duration than the 36 months considered here, to determine

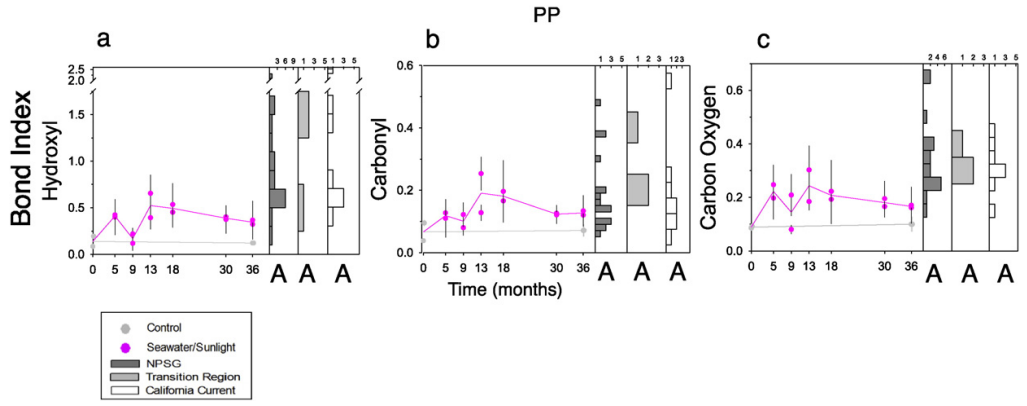

Fig. 8. Experimentally weathered PP compared to oceanic PP. FTIR results from experimentally weathered PP (pink lines) compared to oceanic PP particles (histograms), for (a) hydroxyl bonds, (b) carbonyl groups, and (c) carbon-oxygen bonds. Seawater/sunlight experimental treatment (pink line); control of dry/darkness (gray line). The two dots at each treatment represent means of the two separate tanks. Error bars indicate 95% confidence intervals. Histograms are SEAPLEX samples: North Pacific Subtropical Gyre (dark gray), transition region (light gray), California Current (white). The capital letters indicate regions that differ ($p < 0.05$) in a multiple comparisons test. A and B differ, Ⓐ differs from neither.

whether the observed nonlinear aging patterns continue their upward trajectory after 36 months or dip again. It would also be advisable because floating particles may circulate in gyres indefinitely (Maximenko et al., 2012) and chemical bonds may therefore change substantially in comparison with what we have observed. The increasing PE bond measures from 30 to 36 months and the oceanic samples that are higher than any experimentally recorded values also suggest that an experiment of longer duration than 36 months could be useful. The timeline of 36 months may have been appropriate for comparison for HDPE, as evidenced by the vast majority of the oceanic and experimental particles overlapping, but for LDPE a longer duration experiment may be useful.

The hydroxyl peak was the most readily identified on the spectrograms, followed by the carbon-oxygen peak. The packet of carbonyl groups was less distinctive. Overall, hydroxyl was the most useful index because of ease of identification on spectrograms and the overlap in magnitude of the experimental and oceanic plastics. Carbonyl groups had the next greatest degree of overlap in naturally and experimentally weathered particles.

Although Carlsson et al. (1985) and Lacoste and Carlsson (1992) state that oxidized plastic polymers are always unstable at room temperature in the dark, and should be stored at −30 °C to limit continued slow oxidation, they base this recommendation on Carlsson et al.'s aging experiment with PP exposed to gamma irradiation. In contrast, our experiment, with natural radiance including UV wavelengths, exhibited stable baselines in the controls.

4.1. Nonlinearity of results

Almost all the experimental samples returned to near-T_0 levels of bond index values at some time during the experiment, which introduces some ambiguity in attempting to quantify the exposure time of naturally weathering plastics. HDPE showed a decline to near-T_0 levels at 30 months and LDPE from 18 to 30 months. This nonlinearity could be due to many factors, but one possibility is that the observed "reverse weathering" may actually have been due to the brittleness of the plastic, thus exposing newer, less weathered interior plastic over time. This brittleness hypothesis is discussed below in detail. However, we are still left with nonlinear experimental results to compare to oceanic samples, and it is highly unlikely that the open ocean samples are of new plastic close to weathering duration of 0. Most are likely to be older samples that have weathered for 12 months or more in the ocean environment.

It is also difficult to estimate the apparent age of the oceanic plastics because a piece of plastic may have been manufactured decades earlier but been protected from weathering until it entered the ocean, or it could have aged for years in direct sunlight on a beach before entering the California Current. FTIR thus can only give a rough approximation of exposure time, not true age. However, it still is a useful method for comparison between experimental and naturally weathered particles.

Due to the likely continental source regions of most plastic particles and their different residence times in different ocean circulation features, the North Pacific Subtropical Gyre, transition region, and California Current would be expected to contain suspended plastics of different exposure times. Models of gyre circulation indicate that particles spend different amounts of time in the three provinces analyzed here (Kubota, 1994; Maximenko et al., 2012). Most of the plastic in the ocean is thought to enter from the coasts and be transported into the gyres, although there is likely some lesser amount of direct plastic disposal from ships into the gyres (Kubota, 1994, Ocean Conservancy, 2010), particularly in the years before 1989, when the International Marine Organization's MARPOL Annex V prohibited all plastic disposal at sea by all classes of ships. If the primary source of plastics in this region were continental sources along the west coast of North America into the California Current, followed by transport of particles southward and westward into the transition region, and finally into the NPSG, the exposure times of particles would be expected, on average, to follow this progression. Our oceanic LDPE samples agree with this inference, where there is a significant difference between NPSG and California Current and NPSG and transition region samples for hydroxyl and carbon-oxygen. That the California Current and NPSG samples do not differ is consistent with the nonlinear experimental results. If the CC samples were exposed for less time (0–13 months), the transition region samples intermediate (around 13 months), and NPSG samples exposed for a longer duration (18–36 months), then the California Current and NPSG bond indices should have similar medians and the transition region should have a higher one. Often with the NPSG plastic samples, some qualitative characteristics of brittleness, opacity, or presence of a biofilm helped reinforce this inference of progressive exposure time from the coast to the open ocean. For HDPE, only the CC and NPSG samples significantly varied for carbonyl, and none of the other bonds varied for the oceanic regions.

We expect, according to ocean circulation models, that the majority of NPSG samples would be at least 5 years old, and not younger than 12 months (Kubota, 1994; Maximenko et al., 2012). It takes one year for modeled debris to begin converging into the NPSG (Dotson et al., 1977; Kubota et al., 2005; Maximenko et al., 2012), and the majority of the modeled debris is not only still there, but more concentrated, five to ten years later (Kubota, 1994; Maximenko et al., 2012). The majority of our NPSG PE values are consistent with the experimental values of 13 months or more, with most being consistent with 30 months or more. Results from PP did not permit age approximation.

It is possible that the PE and PP in the ocean are themselves different "ages". Such differences could arise due to differences in input amounts and locations, slight differences in buoyancy (0.89–0.91 g/cm^3 for PP, 0.94–0.965 g/cm^3 for HDPE) (Freund Container & Supply, 2010) and the way in which they weather in the ocean. The SEAPLEX samples from the California Current were comprised of 49% PP particles, but that decreased to only 12% in the NPSG; in the NPSG 86% of the particles tested were PE. This contrast shows that there can be regional differences in distributions of plastic types in the ocean. However, it is also possible that PP samples weather and degrade to pieces smaller than 333 μm, and are thus present in the NPSG but were missed by nets used in this study.

These oceanic distribution numbers also treat PE as one plastic. LDPE and HDPE are used for different consumer products and have vastly differently recycling rates (74% for HDPE versus 2% for LDPE in California in 2015) (CalRecycle, 2016) and our experimental results indicate they weather differently under different conditions. It is essential to be able to spectrally distinguish LDPE from HDPE, as we were able to do in 70% of our oceanic samples, in order to better distinguish inputs of marine debris, how debris is traveling in the ocean, and how each of the most common plastics, PP, LDPE, and HDPE, are degrading in the water column.

4.2. Yellowness, opacity, and brittleness

The nonlinearity of bond measures could be due to many factors, but one possibility is that it demonstrates the complexity in measuring the exposure time of brittle, weathered plastic: the more brittle plastic gets, the more likely it is that it will break and expose the newer, less weathered plastic at its interior.

As discussed, the pellets became very brittle around 9 months, and often split open (PP and HDPE dry/sunlight samples by 9 months, all three plastics dry/sunlight samples by 18 months). Thus what may appear like plastic "reverse weathering" as a bond index decreases may have actually been a result of sampling less exposed plastic in the interior of the particles. Because plastic weathers from the outside, a split pellet would reveal less environmentally exposed plastic on the particle interior. Similarly, pellets that crumbled into powder (ex. HDPE and PP dry/sunlight by 30 months) would have less exposed plastic on the inside that was measured when the powder was sampled. This could

explain the decrease from 18 to 30 months in PP and HDPE and low value at 30 months for LDPE. The subsequent increase by 36 months could occur as the plastic weathered so thoroughly that the effect of a split pellet or powdered pellet did not affect analytical results. This brittleness hypothesis may also explain why so many oceanic samples are higher than experimental samples. If those samples were taken from larger pieces of plastic, they would have less tendency to crumble, and thus may be giving a more accurate measure of changes in bond structures. In contrast, the small nurdles used in this experiment may have been small enough that their cores always became brittle before reaching high index values.

Jabarin and Lofgren (1994) naturally weathered sheets of HDPE in sunlight. They observed increased embrittlement, decreased elongation to break (the amount the sheets could be stretched before breakage or crack formation), increased crystallinity, and decreased molecular weight due to environmental degradation. Although elongation to break can only be measured on long pieces like the plastic sheets they measured, and we did not measure molecular weight, we also saw increased brittleness and loss of ductility, and our results of the effects of natural sunlight on PE agree with their findings. Although our crystallinity results were inconclusive, we observed an increase in brittleness, and brittleness has been associated with an increase in crystallinity (Jabarin and Lofgren, 1994).

Stark and Matuana (2004) exposed plastic samples to xenon light and water for 12 min of every 120. They detected near-immediate surface oxidation of their samples and increased oxidation with time. There was an increase in the ratio of oxidized to unoxidized carbons with continued weathering, and an increase in the elemental ratio of oxygen to carbon. Stark and Matuana (2004) noted that the increase in oxidized: unoxidized carbon appears to be mainly from an increase in hydroxyls, which would explain our short-term increase in hydroxyls as well since hydroxyls form in response to surface oxidation of the plastics. This surface oxidation would also explain the formation of C—O bonds (cf. Stark and Matuana, 2004). Stark and Matuana (2004) stated that oxidative degradation is the main limiting factor on the "active life of synthetic polymers" and that those oxidative degradation reactions are accelerated by UV radiation, which agrees with our carbon-oxygen bonds showing higher values for the two natural sunlight treatments for almost all time points and all three plastics.

Polypropylene has been observed to become brittle on beaches before ever entering the ocean, and its weathering is known to slow once in seawater (Andrady, 2011). The more pronounced temporal changes that we detected in PP relative to the other two plastic types can perhaps be attributed to such a reduction in brittleness in an aqueous medium.

5. Conclusions

We found FTIR to be a useful method to differentiate among the most common buoyant marine microplastic particle types (especially PP, LDPE, and HDPE) that are found suspended in the upper ocean.

The experimental weathering was more complex than predicted; the chemical bonds did not change linearly with time, and there was variability in weathering between the combinations of plastic, weathering experiment, and bond type measured. Due to the nonlinear changes in bond indices with experimental weathering, the indices presented here are of potential use for quantifying the exposure time of plastics only over a relatively limited time period, generally for differentiating younger (0–18 months) from older (>18–30 months) particles. These experimental results are based on pure pre-production plastic pellets, and their applicability to more complex manufactured plastic types requires verification. Changes in hydroxyl and carbon-oxygen bonds are most readily diagnosed by FTIR, followed by carbonyl bonds.

Application of the chronology of changes in experimentally weathered particles to microplastic collected in the open ocean suggests that the PE particles we sampled in the California Current and transition region may have generally weathered for under 18 months, in contrast to the particles from the North Pacific Subtropical Gyre that generally had inferred exposure times longer than 18 months. The indices tested here proved more applicable for comparing oceanic and experimental values of PE than PP, and were the most useful for HDPE. These findings are consistent with oceanic circulation models suggesting a long residence time of suspended micro-plastics in the open ocean.

Acknowledgements

We thank Pacific Plastics Injection Molding, Damar Plastics, P. Dinger, and C. Rochman for their donation of preproduction plastic pellets. G. Arrhenius, M.J. Sailor, J. Lee, N. Chan, and A. Potocny made the FTIR work possible. We thank M.J. Sailor, L. Aluwihare, and M. Landry for comments on the manuscript. We thank NOAA NDBC for temperature data. We are grateful to K.E. Armaiz for assistance in the laboratory, P. Zerofski for help with experimental setup, J. Ellen for help with Python, E. Jacobson and J. Carriere-Garwood for help with R, and the numerous volunteers who helped JAB clean tanks. Funding for the SEAPLEX cruise was provided by University of California Ship Funds, Project Kaisei/Ocean Voyages Institute, AWIS-San Diego, and NSF IGERT Grant No. 0333444. MCG was supported by NSF GK-12 Grant No. 0841407 and donations from Jim & Kris McMillan, Jeffrey & Marcy Krinsk, Lyn & Norman Lear, Ellis Wyer, and an anonymous donor, and JAB was supported by donations from the Furlotti Family. This work was also funded by a contribution from the California Current Ecosystem LTER site, supported by NSF Award No. 1026607.

Appendix A. Supplementary data

Supplementary data to this article can be found online at http://dx.doi.org/10.1016/j.marpolbul.2016.06.048.

References

Abbate, S., Gussoni, M., Zerbi, G., 1979. Infrared and Raman intensities of polyethylene and perdeuteropolyethylene: factor group splittings. J. Chem. Phys. 70, 3577–3585.

Albertsson, A.-C., Andersson, S.O., Karlsson, S., 1987. The mechanism of biodegradation of polyethylene. Polym. Degrad. Stab. 18, 73–87.

American Chemistry Council, 2010. Resin identification codes. http://www.americanchemistry.com/s_plastics/doc.asp?CID=1102&DID=4644.

Andrady, A.L., 1990. Weathering of polyethylene (LDPE) and enhanced photodegradable polyethylene in the marine environment. J. Appl. Polym. Sci. 39, 363–370.

Andrady, A.L., 2003. Common plastics materials. In: Andrady, A.L. (Ed.), Plastics and the Environment. John Wiley & Sons, Hoboken, NJ, pp. 77–121.

Andrady, A.L., 2011. Microplastics in the marine environment. Mar. Pollut. Bull. 62, 1596–1605.

Andrady, A., Pegram, J., Tropsha, Y., 1993. Changes in carbonyl index and average molecular weight on embrittlement of enhanced-photodegradable polyethylenes. Journal of Environmental Polymer Degradation 1, 171–179.

Avitabile, G., Napolitano, R., Pirozzi, B., Rouse, K.D., Thomas, M.W., Willis, B.T.M., 1975. Low temperature crystal structure of polyethylene: results from a neutron diffraction study and from potential energy calculations. Journal of Polymer Science: Polymer Letters Edition 13, 351–355.

Brown, D., Cheng, L., 1981. New net for sampling the ocean surface. Mar. Ecol. Prog. Ser. 5, 224–227.

Browne, M.A., Dissanayake, A., Galloway, T.S., Lowe, D.M., Thompson, R.C., 2008. Ingested microscopic plastic translocates to the circulatory system of the mussel, *Mytilus edulis* (L.). Environ. Sci. Technol. 42, 5026–5031.

CalRecycle, 2016. In: C. D. o. R. R. a. R. (CalRecycle) (Ed.), Biannual Report of Beverage Container Sales, Returns, Redemption, and Recycling Rates. California Environmental Protection Agency (http://www.calrecycle.ca.gov/bevcontainer/Notices/2016/Biannual.pdf).

Carlsson, D.J., Dobbin, C.J.R., Jensen, J.P.T., Wiles, D.M., 1985. Polypropylene degradation by g-irradiation in air. ACS Symposium Series 280.

Carpenter, E.J., Smith, K., 1972. Plastics on the Sargasso Sea surface. Science 175, 1240–1241.

Cole, M., Lindeque, P., Fileman, E., Halsband, C., Goodhead, R., Moger, J., Galloway, T.S., 2013. Microplastic ingestion by zooplankton. Environ. Sci. Technol. 47, 6646–6655.

Corrales, T., Catalina, F., Peinado, C., Allen, N., Fontan, E., 2002. Photooxidative and thermal degradation of polyethylenes: interrelationship by chemiluminescence, thermal gravimetric analysis and FTIR data. J. Photochem. Photobiol. A Chem. 147, 213–224.

Davison, P., Asch, R.G., 2011. Plastic ingestion by mesopelagic fishes in the North Pacific Subtropical Gyre. Mar. Ecol. Prog. Ser. 432, 173–180.

Dotson, A., Magaard, L., Niemeyer, G., Wyrtki, K., 1977. A Simulation of the Movements of Fields of Drifting Buoys in the North Pacific Ocean. Hawaii Institute of Geophysics, University of Hawaii.
El-Ghaffar, M.A., Youssef, E., Darwish, W., Helaly, F., 1998. A novel series of corrosion inhibitive polymers for steel protection. Journal of Elastomers and Plastics 30, 68–94.
EPA. 2014. Municipal Solid Waste Generation, Recycling, and Disposal in the United States: Tables and Figures for 2012. In U. S. E. P. Agency, editor (Washington D.C. USA).
Eriksen, M., Lebreton, L.C., Carson, H.S., Thiel, M., Moore, C.J., Borerro, J.C., Galgani, F., Ryan, P.G., Reisser, J., 2014. Plastic pollution in the world's oceans: More than 5 trillion plastic pieces weighing over 250,000 tons afloat at sea. PLoS One 9, e111913.
Eriksson, C., Burton, H., 2003. Origins and biological accumulation of small plastic particles in fur seals from Macquarie Island. AMBIO: A Journal of the Human Environment 32, 380–384.
Forrest, M., Davies, Y., Davies, J., 2007. The Rapra Collection of Infrared Spectra of Rubbers, Plastics and Thermoplastic Elastomers. Smithers Rapra Publishing.
Freund Container & Supply, 2010. Plastic Properties. Guide to Plastics.
Frias, J.P.G.L., Sobral, P., Ferreira, A.M., 2010. Organic pollutants in microplastics from two beaches of the Portuguese coast. Mar. Pollut. Bull. 60, 1988–1992.
Goldstein, M.C., Goodwin, D.S., 2013. Gooseneck barnacles (*Lepas* spp.) ingest microplastic debris in the North Pacific Subtropical Gyre. Peer J. 1, e184.
Goldstein, M.C., Titmus, A.J., Ford, M., 2013. Scales of spatial heterogeneity of plastic marine debris in the northeast Pacific ocean. PLoS One 8, e80020.
Gulmine, J., Janissek, P., Heise, H., Akcelrud, L., 2002. Polyethylene characterization by FTIR. Polym. Test. 21, 557–563.
Hidalgo-Ruz, V., Gutow, L., Thompson, R.C., Thiel, M., 2012. Microplastics in the marine environment: a review of the methods used for identification and quantification. Environ. Sci. Technol. 46, 3060–3075.
International, A., 2011. ASTM Standard C702/C702M-11. Practice for Reducing Samples of Aggregate to Testing Size (West Conshohocken, PA).
Ioakeimidis, C., Fotopoulou, K., Karapanagioti, H., Geraga, M., Zeri, C., Papathanassiou, E., Galgani, F., Papatheodorou, G., 2016. The degradation potential of PET bottles in the marine environment: an ATR-FTIR based approach. Sci. Report. 6.
Jabarin, S.A., Lofgren, E.A., 1994. Photooxidative effects on properties and structure of high-density polyethylene. J. Appl. Polym. Sci. 53, 411–423.
Jambeck, J.R., Geyer, R., Wilcox, C., Siegler, T.R., Perryman, M., Andrady, A., Narayan, R., Law, K.L., 2015. Plastic waste inputs from land into the ocean. Science 347, 768–771.
Kubota, M., 1994. A mechanism for the accumulation of floating marine debris north of Hawaii. J. Phys. Oceanogr. 24, 1059–1064.
Kubota, M., Takayama, K., Namimoto, D., 2005. Pleading for the use of biodegradable polymers in favor of marine environments and to avoid an asbestos-like problem for the future. Appl. Microbiol. Biotechnol. 67, 469–476.
La Mantia, F.P., Morreale, M., 2008. Accelerated weathering of polypropylene/wood flour composites. Polym. Degrad. Stab. 93, 1252–1258.
Lacoste, J., Carlsson, D., 1992. Gamma-, photo-, and thermally-initiated oxidation of linear low density polyethylene: a quantitative comparison of oxidation products. J. Polym. Sci. A Polym. Chem. 30, 493–500.
Livanova, N., Zaikov, G., 1992. A scale effect in the durability of oriented narrow polypropylene films during oxidation under load. Fracture model of stressed polypropylene films. Polym. Degrad. Stab. 36, 253–259.
Lobo, H., Bonilla, J.V., 2003. Handbook of Plastics Analysis. Crc Press.
Lynn, R.J., Simpson, J.J., 1987. The California Current System: the seasonal variability of its physical characteristics. Journal of Geophysical Research: Oceans (1978–2012) 92, 12947–12966.
Ma, X., Lu, J.Q., Brock, R.S., Jacobs, K.M., Yang, P., Hu, X.-H., 2003. Determination of complex refractive index of polystyrene microspheres from 370 to 1610 nm. Phys. Med. Biol. 48, 4165.
Markelz, A., Roitberg, A., Heilweil, E., 2000. Pulsed terahertz spectroscopy of DNA, bovine serum albumin and collagen between 0.1 and 2.0 THz. Chem. Phys. Lett. 320, 42–48.
Maximenko, N., Hafner, J., Niiler, P., 2012. Pathways of marine debris derived from trajectories of Lagrangian drifters. Mar. Pollut. Bull. 65, 51–62.
Murray, F., Cowie, P.R., 2011. Plastic contamination in the decapod crustacean *Nephrops norvegicus* (Linnaeus, 1758). Mar. Pollut. Bull. 62, 1207–1217.
Niiler, P.P., Reynolds, R.W., 1984. The three-dimensional circulation near the eastern North Pacific Subtropical Front. J. Phys. Oceanogr. 14, 217–230.
Ocean Conservancy, 2010. Trash Travels. International Coastal Cleanup 25th Anniversary Report.
Ogata, Y., Takada, H., Mizukawa, K., Hirai, H., Iwasa, S., Endo, S., Mato, Y., Saha, M., Okuda, K., Nakashima, A., Murakami, M., Zurcher, N., Booyatumanondo, R., Zakaria, M.P., Dung, L.Q., Gordon, M., Miguez, C., Suzuki, S., Moore, C., Karapanagioti, H.K., Weerts, S., McClurg, T., Burres, E., Smith, W., Velkenburg, M.V., Lang, J.S., Lang, R.C., Laursen, D., Danner, B., Stewardson, N., Thompson, R.C., 2009. International Pellet Watch: global monitoring of persistent organic pollutants (POPs) in coastal waters. 1. Initial phase data on PCBs, DDTs, and HCHs. Mar. Pollut. Bull. 58, 1437–1446.
Pavia, D., Lampman, G., Kriz, G., Vyvyan, J., 2008. Introduction to Spectroscopy. Cengage Learning.
Pegram, J.E., Andrady, A.L., 1989. Outdoor weathering of selected polymeric materials under marine exposure conditions. Polym. Degrad. Stab. 26, 333–345.
Piesiewicz, R., Jansen, C., Wietzke, S., Mittleman, D., Koch, M., Kürner, T., 2007. Properties of building and plastic materials in the THz range. International Journal of Infrared and Millimeter Waves 28, 363–371.
Rabello, M., White, J., 1997. The role of physical structure and morphology in the photodegradation behaviour of polypropylene. Polym. Degrad. Stab. 56, 55–73.
Rajakumar, K., Sarasvathy, V., Chelvan, A.T., Chitra, R., Vijayakumar, C., 2009. Natural weathering studies of polypropylene. J. Polym. Environ. 17, 191–202.
Reddy, M.S., Shaik, B., Adimurthy, S., Ramachandraiah, G., 2006. Description of the small plastics fragments in marine sediments along the Alang-Sosiya ship-breaking yard, India. Estuar. Coast. Shelf Sci. 68, 656–660.
Rios, L.M., Moore, C., Jones, P.R., 2007. Persistent organic pollutants carried by synthetic polymers in the ocean environment. Mar. Pollut. Bull. 54, 1230–1237.
Rochman, C.M., Hoh, E., Kurobe, T., Teh, S.J., 2013. Ingested plastic transfers hazardous chemicals to fish and induces hepatic stress. Sci. Report. 3.
Roden, G.I., 1980. On the subtropical frontal zone north of Hawaii during winter. J. Phys. Oceanogr. 10, 342–362.
Rodriguez-Gonzalez, F.J., Ramsay, B.A., Favis, B.D., 2003. High performance LDPE/thermoplastic starch blends: a sustainable alternative to pure polyethylene. Polymer 44, 1517–1526.
Roy, P., Surekha, P., Rajagopal, C., 2011. Surface oxidation of low-density polyethylene films to improve their susceptibility toward environmental degradation. J. Appl. Polym. Sci. 122, 2765–2773.
Samuels, R.J., 1981. Application of refractive index measurements to polymer analysis. J. Appl. Polym. Sci. 26, 1383–1412.
Siegel, S., Castellan, N.J.J., 1988. Non Parametric Statistics for the Behavioural Sciences. MacGraw Hill International, New York.
Socrates, G., 2004. Infrared and Raman Characteristic Group Frequencies: Tables and Charts. third ed. John Wiley & Sons, Ltd., Chichester, England.
Stark, N.M., Matuana, L.M., 2004. Surface chemistry changes of weathered HDPE/wood-flour composites studied by XPS and FTIR spectroscopy. Polym. Degrad. Stab. 86, 1–9.
Tadokoro, H., Kobayashi, M., Ukita, M., Yasufuku, K., Murahashi, S., Torii, T., 1965. Normal vibrations of the polymer molecules of helical conformation. V. Isotactic polypropylene and its deuteroderivatives. J. Chem. Phys. 42, 1432–1449.
Thompson, R.C., Olsen, Y., Mitchell, R.P., Davis, A., Rowland, S.J., John, A.W., McGonigle, D., Russell, A.E., 2004. Lost at sea: where is all the plastic? Science 304, 838.
Tidjani, A., 2000. Comparison of formation of oxidation products during photo-oxidation of linear low density polyethylene under different natural and accelerated weathering conditions. Polym. Degrad. Stab. 68, 465–469.
Wong, C., Green, D.R., Cretney, W.J., 1974. Quantitative tar and plastic waste distributions in the Pacific Ocean. Nature 247, 30–32.
Workman Jr., J., Springsteen, A., 1998. Applied Spectroscopy: A Compact Reference for Practitioners. Academic Press.
Wright, S.L., Thompson, R.C., Galloway, T.S., 2013. The physical impacts of microplastics on marine organisms: a review. Environ. Pollut. 178, 483–492.
Zerbi, G., Gallino, G., Del Fanti, N., Baini, L., 1989. Structural depth profiling in polyethylene films by multiple internal reflection infra-red spectroscopy. Polymer 30, 2324–2327.

Chapter 2, in full, is a reprint of the material as it appears in Marine Pollution Bulletin, 2016. Brandon, Jennifer; Goldstein, Miriam; Ohman, Mark D., 2016. The dissertation author was the primary investigator and author of this paper.

HDPE with Oceanic Other PE

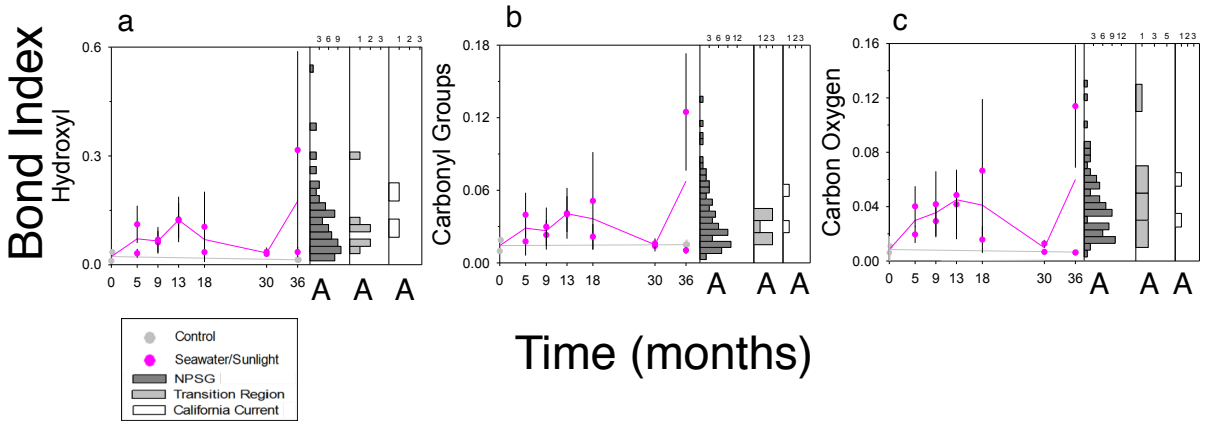

Supplemental Figure 1: **Experimentally weathered HDPE compared to oceanic other/combined PE.** FTIR results from experimentally weathered HDPE (pink lines) compared to oceanic other/combined PE particles (histograms), for (a) hydroxyl bonds, (b) carbonyl groups, and (c) carbon-oxygen bonds. Seawater/sunlight experimental treatment (pink line); control of dry/darkness (gray line). The two dots at each treatment represent means of the two separate tanks. Error bars indicate 95% confidence intervals. Histograms are SEAPLEX samples: North Pacific Subtropical Gyre (dark gray), transition region (light gray), California Current (white). The capital letters indicate regions that differ ($p<0.05$) in a multiple comparisons test. A and B differ, Ⓐ differs from neither.

Supplemental Figure 1

LDPE with Oceanic Other PE

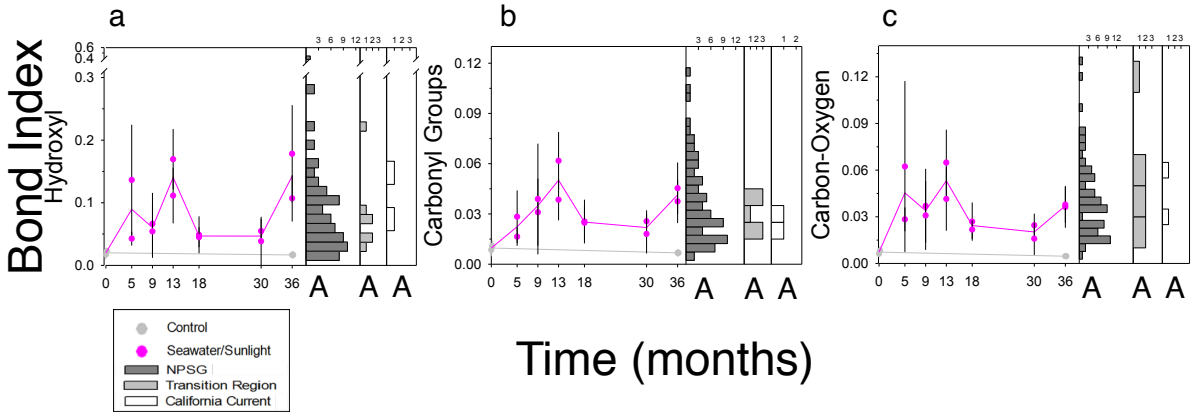

Supplemental Figure 2: **Experimentally weathered LDPE compared to oceanic other/combined PE.** FTIR results from experimentally weathered LDPE (pink lines) compared to oceanic other/combined PE particles (histograms), for (a) hydroxyl bonds, (b) carbonyl groups, and (c) carbon-oxygen bonds. Seawater/sunlight experimental treatment (pink line); control of dry/darkness (gray line). The two dots at each treatment represent means of the two separate tanks. Error bars indicate 95% confidence intervals. Histograms are SEAPLEX samples: North Pacific Subtropical Gyre (dark gray), transition region (light gray), California Current (white). The capital letters indicate regions that differ ($p<0.05$) in a multiple comparisons test. A and B differ, Ⓐ differs from neither.

Supplemental Figure 2

CHAPTER 3: Patterns of suspended microplastic debris in the California Current and North Pacific Subtropical Gyre, imaged by epifluorescence microscopy

Jennifer A. Brandon, Alexandra Freibott

ABSTRACT:

Microplastic debris (< 5 mm) has been a concern in plastic research for some time, but the smallest microplastics (< 333 μm) have been largely ignored because almost all plastic collections have been made with nets (typically > 333 μm). The smallest particles have the potential to be the most abundant size class of plastic in the ocean because plastics break down into successively smaller pieces as they weather. There are currently no abundance estimates of plastic debris < 333 μm, which we term nanoplastics. Using metal buckets to sample all sizes of particles, we collected surface seawater on three research cruises, two in the California Current and one traversing the North Pacific Subtropical Gyre. We imaged plastic nanoparticles on polycarbonate filters using epifluorescence microscopy in four different excitation/emission wavelength combinations. Epifluorescence microscopy permitted us to distinguish plastic short fibers, long fibers, and fragments from naturally occurring phytoplankton and other suspended particles. Nanoplastics were the most abundant in extremely nearshore waters, but once in coastal waters, nanoplastics were distributed relatively consistently across the California Current, North Pacific Subtropical Gyre, and the transitional region in between. Nanoplastic particles varied in concentration from 2,018-41,578 particles L^{-1} and were 5-7 orders of magnitude higher than published densities of microplastics. The ratio of picoplankton: plastic by abundance was estimated at 49:1 in the North Pacific Subtropical Gyre compared to 295:1 in the California Current, indicating that nanoplastic particles play a larger role in the oligotrophic open ocean where plankton densities are lower.

Keywords: Microplastics, Nanoplastics, Marine Debris, Epifluorescence Microscopy, North Pacific Subtropical Gyre, California Current

INTRODUCTION:

Plastics in the Ocean

Marine debris is a worldwide ocean pollution problem. Plastics have been found in virtually all aquatic environments sampled to date. Starting in the 1970s, only a few decades after the surge in popularity of plastic products, scientists began finding plastics in the open ocean, specifically in the subtropical gyres (Venrick et al. 1973, Colton et al. 1974, Wong et al. 1974). Plastic microdebris (generally defined as debris smaller than 5 mm; Arthur et al. 2009) has been found in open ocean gyres (Goldstein et al. 2012), coastal waters (Gilfillan et al. 2009), shorelines (Browne et al. 2011), the deep sea (Van Cauwenberghe et al. 2013), rivers (Lechner et al. 2014), and in the Great Lakes (Eriksen et al. 2013), with the highest abundances in the centers of subtropical gyres (Goldstein et al. 2013).

The high densities of plastics in subtropical gyres are due to entrainment of drifting, positively buoyant plastics into gyres by large-scale ocean circulation (Meehl 1982). Plastics accumulate in these oceanic convergence zones where plastics from the edges of ocean basins aggregate and then circulate, potentially indefinitely (Maximenko et al. 2012).

It is important to understand how much microplastic is accumulating in the nearshore environment because it has been shown that coastal regions near areas of high human density have higher densities of plastics. Browne et al. (2011) found that areas of high population density have significantly more plastic debris in nearby marine sediments. As coastal populations grow and clothes are increasingly manufactured from synthetic

substances in the future, these effluent-derived fibers and other sources of plastic debris will likely become a growing nearshore problem (Browne et al. 2011). A single synthetic fleece jacket can release an average of 1,174 mg of microfibers per washing (Hartline et al. 2016), or an average of 300 microfibers L^{-1} of effluent (Browne et al. 2011). Eriksen et al. (2013) collected an average of 43,000 microplastic particles km^{-2} in the Great Lakes, but the sampling station directly downstream of Cleveland, OH and Erie, PA had 466,000 particles km^{-2}, more than all other stations combined. Although there have been few studies of the consequences of nearshore marine debris, both Browne et al. (2011) and Ogata et al. (2009) emphasize that populated coastal regions could be disproportionately impacted. It is estimated that roughly 60-80% of plastic that ends up in the ocean comes from land-based sources, rather than originating from ships (Ocean Conservancy 2010).

The present study sampled nano- and microplastic debris in the North Pacific Subtropical Gyre (NPSG) because of its large area (Karl 1999), the way its circulation causes large amounts of plastic to aggregate (Maximenko et al. 2012), and the substantial amount of marine debris chronicled there (Moore et al. 2001, Goldstein et al. 2012). We also examined the spatial distribution and size composition of nearshore suspended marine plastics, due to the previously recorded introduction of plastics nearshore (Browne et al. 2011). Our objectives were to determine nanoplastic concentrations for all areas sampled, to compare plastic loading between nearshore and open ocean regions, and to assess whether nanoplastics follow similar distribution patterns as larger plastic debris.

Microdebris

The appearance and effects of macrodebris (> 5 mm) are obvious, with macrodebris causing animal entanglements (Henderson 2001), ingestion (Derraik 2002), entanglement

and damage to coral and other benthic fauna (Donohue et al. 2001, Schlining et al. 2013), and becoming a rafting substrate, including for invasive species (Goldstein et al. 2014). However, the numerical majority of previously analyzed marine debris is microdebris, or plastic smaller than < 5 mm (Hidalgo-Ruz et al. 2012, Goldstein et al. 2013). Goldstein et al. (2013) sampled a combined 32,090 pieces of marine debris, and found that over 90% were smaller than 1 cm^2 in surface area. Hidalgo-Ruz et al.'s (2012) review compared the size range of plastics previously sampled in sediments, the sea surface, and the water column, and in almost every study the numerical majority of particles was smaller than 5 mm.

Even these studies have greatly undersampled plastics smaller than 333 μm (hereafter called nanoplastics), however, due to the methods employed to sample marine debris. Van Sebille et al. (2015)'s review enumerated 11,854 surface plastic tows conducted from 1971-2013 globally, with the mesh size of nets ranging from 150 μm to 3000 μm, but over 90% of the tows used 333 or 335 μm mesh. When sampling with 80 μm mesh instead of 450 μm mesh in the Northeast Atlantic, Lozano and Mouat (2009) collected up to 100,000 times more plastic. It is likely that plastic < 333 μm is far more numerous than the previously sampled microparticles because plastic continues to physically degrade into progressively smaller pieces over time (Gilfillan et al. 2009) and models suggest that smaller plastic particles degrade and fragment into smaller pieces faster than larger pieces (Gerritse 2015, GESAMP 2016).

Nano- and microdebris can be even more deleterious to marine organisms than macrodebris (> 5 mm) because small particles and fibers can be ingested by many suspension-feeding animals (Thompson et al. 2004, Goldstein and Goodwin 2013, Wright et al. 2013). If plastics are ingested by animals like zooplankton, they have the potential to bio-

accumulate in the food web into larger organisms, along with adsorbed persistent organic pollutants and the harmful chemical additives they contain (Ogata et al. 2009, Rochman et al. 2013b, Jang et al. 2016). Microplastics and nanoplastics, due to their size, are also much harder to clean up, quantify, and sample than macrodebris, making new methods of analyzing their abundance and distribution important to understand the full extent of the oceanic plastic problem.

Analytical techniques

Most studies that have examined nano- and microplastic debris have identified particles visually, either by eye or by microscope (Hidalgo-Ruz et al. 2012). Several problems have developed with visual identification. Many microplastics, especially in sediment, are covered in a biofilm and resemble biotic material, and can thus be underestimated (Browne et al. 2011). In contrast, synthetic clothing fibers and particles of bright colors are more noticeable and can be oversampled compared to other, less brightly-colored samples that resemble biota (Browne et al. 2011, Hidalgo-Ruz et al. 2012). Seventy percent of particles that visually resembled microplastics failed confirmation as plastics by FTIR (Fourier Transform Infrared) spectroscopy (Hidalgo-Ruz et al. 2012). Thus, there is a need for alternative means to positively and rapidly distinguish small plastic particles.

Isolating, identifying, and quantifying nanoplastic and microplastic particles in the ocean is difficult, due to their small size and irregularity. Here we adopted modified epifluorescence microscopy to quantify naturally-occurring oceanic plastic in seawater.

This is not the first study to document the autofluorescence of plastic. When high-density polyethylene (HDPE) is excited at 249 nm, it has two broad fluorescence peaks at 354 and 410 nm. When it is excited at 337 nm, there are the same two peaks, but the 410

peak is broader and less well-defined (Ahmad 1983). Low-density polyethylene (LDPE) will fluoresce at 639 nm when excited at 337 nm (Badr et al. 1999). Polystyrene will have a broad fluorescent band from 330-520 nm when excited at 254 nm, with indistinct maxima at 353, 370, 430, 450 nm (Nurmukhametov et al. 2006). Modern recycling also often utilizes the autofluorescence of plastics, separating items of similar chemical makeup such as LDPE and HDPE, and even using fluorescence to isolate certain contaminants in plastic (Langhals et al. 2015).

Epifluorescence microscopy is a common technique to quantify bacteria, cells, phytoplankton, and microzooplankton (Caron 1983, Taylor et al. 2012, Pasulka et al. 2013). However, this appears to be the first investigation to utilize epifluorescence microscopy as a method to identify and quantify nanoplastics suspended in seawater. By taking advantage of plastic autofluorescence, and decreasing the noise of autofluorescent biota on our slides, we were able to quantify previously undersampled nanoplastics and estimate nanoplastic concentrations for the Northeast Pacific.

MATERIALS AND METHODS:

Sampling at Sea

This study aimed to identify the smallest nanoplastics, so metal buckets were used to collect whole surface seawater samples on three research cruises. On the R/V *Falkor* (21-30 October 2013), 20 L buckets were lowered off a crane at 11.8 m off the port side of the ship travelling at 5 knots on a transect from Seattle to Honolulu (Fig. 3.2a). The total distance spanned was 4,055 km. On the SKrillEx I cruise (26-31 July 2014), 20 L metal buckets were lowered off the R/V *New Horizon* starboard J-frame at full-extension (2.29 m) while

the boat was stopped (Fig. 3.2b, red). On SKrillEx II (11-17 June 2015), 20 L metal buckets were lowered off the aft A-frame of the R/V *Sproul* at full-extension (2.13 m) while the boat was stopped (Fig. 3.2b, green). All buckets sampled the top 1-2 m of water.

Up to 5.3 L of water from surface bucket tows was vacuum-filtered through vinyl tubing onto 5.0 μm transparent polycarbonate filters on the R/V *Falkor*. Up to 5.0 L of water from surface bucket tows was vacuum filtered on transects across 9 Mile Bank off of San Diego on SKrillEx I and SKrillEx II. For SKrillEx I and SKrillEx II, the vinyl tubing was replaced with blown-glass tubing so that the ocean water never came in contact with any plastic lab equipment before encountering the filter. For all three cruises, the filters were wrapped in aluminum foil and frozen at -80°C (R/V *Falkor)* or -20°C (SKrillEx I and SKrillEx II) onboard before being transferred to -80°C onshore until analysis.

Identifying Water Masses

To determine which stations on the R/V *Falkor* expedition were in the California Current, the North Pacific Subtropical Gyre, and transition region in between, we compared shipboard measurements taken on the R/V *Falkor* with satellite data (Fig. 3.1a-c) from the same time period and with published temperature and salinity ranges for each province. The California Current was defined as having a surface temperature < 19°C and surface salinity < 33.5 (Lynn and Simpson 1987), the North Pacific Subtropical Gyre (NPSG) surface temperatures > 22°C and salinity > 34.8 (Roden 1980, Niiler and Reynolds 1984), and the transition region as surface temperature 19-22°C and surface salinity 33.5-34.8 (Roden 1980, Lynn and Simpson 1987). Because only surface data were used, these water masses should be viewed as approximations rather than absolute oceanographic definitions (Goldstein et al. 2013, Brandon et al. 2016). Using these criteria values, *Falkor* stations 1.1-3.1 were in the

California Current, stations 3.2-5.1 in the transition region, and stations 5.2-8.2 in the North Pacific Subtropical Gyre (Fig. 3.2a).

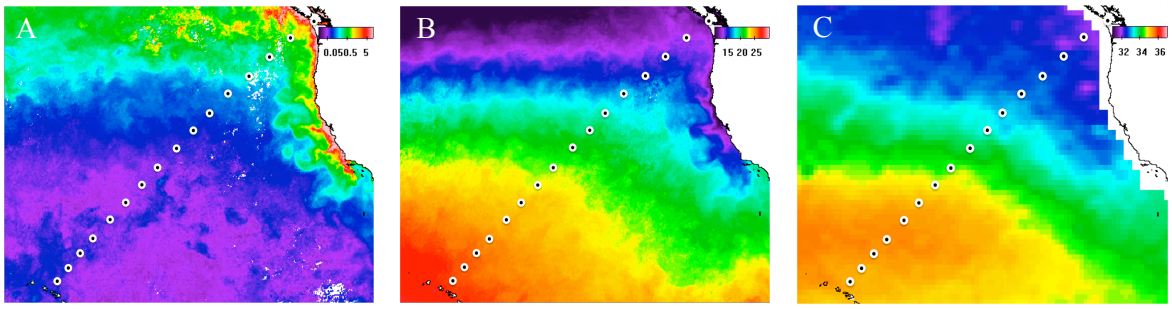

Figure 3.1: Satellite measurements on the R/V *Falkor* expedition. October 2013: A) Chl *a*, B) sea surface temperature (°C), C) sea surface salinity. Points indicate sampling stations. Satellite maps courtesy of Mati Kahru, SIO.

Chl *a* samples were taken for all shipboard stations on all three cruises from 250 mL aliquots from surface bucket samples and filtered through glass fiber filters. *Falkor* filters were frozen at -80°C at sea and then extracted in 90% acetone and analyzed on a Turner Designs 10AU fluorometer before and after acidification ashore; SKrillEx I and II filters were extracted in acetone and their fluorescence measured at sea. The coefficient of determination (R^2) between the satellite (Fig. 3.1a) and shipboard measurements was 0.66. For salinity and temperature, R/V *Falkor* could only measure these variables outside of U.S. waters, starting at Station 2.2. However, the R^2 between the satellite (Fig. 3.1b,c) and available shipboard measurements was 0.99 for temperature and 0.98 for salinity, respectively, so the missing stations are well represented by the satellite data.

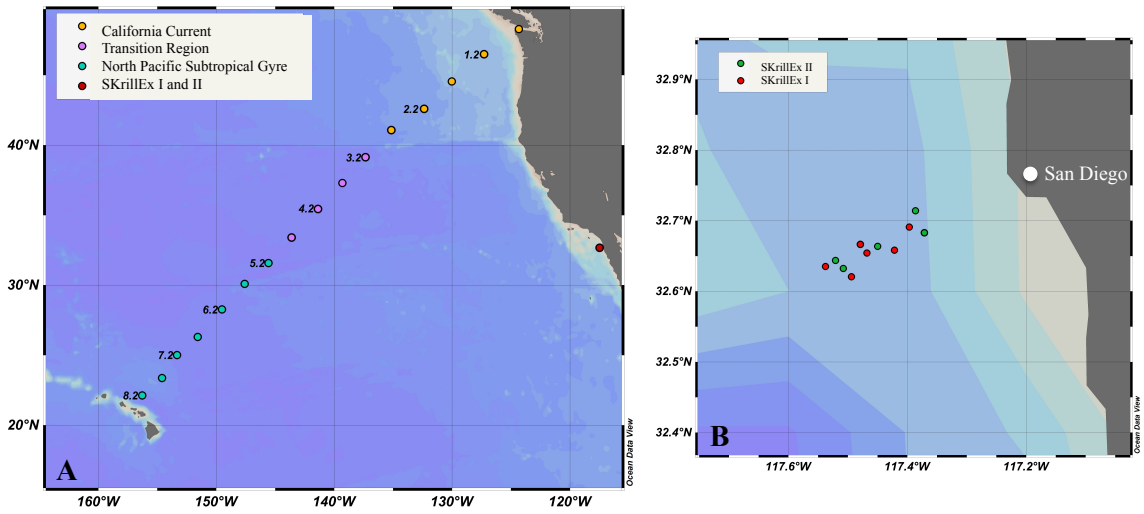

Figure 3.2: Microplastic sampling locations. A) R/V *Falkor*, Fall 2013. Orange symbols: California Current; purple: transition region; green: North Pacific Subtropical Gyre; red: SKrillEx I and II. B) SKrillEx I and SKrillEx II. Red: SKrillEx I, July 2014; green: SKrillEx II, June 2015. One location from SKrillEx I was sampled again on SKrillEx II.

Epifluorescence Microscopy

Slide Preparation and Analysis

Once back on land, the frozen transparent polycarbonate (PC) filters were allowed to come to room temperature, unwrapped from the aluminum foil wrapper, then placed on a glass vacuum filtering device, with a 20 µm nylon support filter to promote even sample distribution. A small volume of Milli-Q water was added to promote a good seal to the support filter and sample filter (Freibott et al. 2014). After seawater sample filtration, residual microplastics adhering to the aluminum foil were rinsed onto the sample filter with Milli-Q water. The 47 mm PC filter was then separated from the backing filter with forceps, mounted on a 50 mm glass slide with immersion oil, which had a refractive index matching the PC filter, and two cover slips, 24 x 50mm, No. 2 thickness, applied to the slide.

Traditional epifluorescence techniques add fluorochromes such as DAPI to stain DNA and proflavin to stain proteins (Caron 1983, Kemp et al. 1993, Taylor et al. 2012). However, none of those fluorochromes were used here, since living organisms were not the

targets of the study. Slides were digitally imaged using a Zeiss Axiovert 200M inverted compound microscope, equipped for epifluorescence microscopy and driven by Zeiss Axiovision software. The stage, filter set, and focus drive were motorized to allow for automated image acquisition. Digital images were acquired with a Zeiss AxioCam HRc color CCD digital camera. Exposure times for each image were automatically determined by the software in order to avoid over exposure. Samples were viewed at 200x magnification (Taylor et al. 2012). Forty random positions were imaged for each slide, with each position consisting of a transmitted light image and three reflected fluorescent channels. The channels included a blue excitation/green long-pass emission filter set normally used to identify protein dyed with the fluorochrome proflavin (excitation wavelengths: 450–490 nm; emission: > 515 nm); a blue excitation/red emission filter set normally used for chlorophyll *a* (excitation: 465–495 nm; emission: 635–685 nm); and a UV excitation/blue emission filter set normally used for DNA stained with DAPI (excitation: 340–380 nm; emission: 435–485 nm)(Fig. 3.3; Pasulka et al. 2013). The separate images from each channel were combined to form one composite 24-bit Red-Green-Blue (RGB) image for each position.

The resulting images were processed and analyzed with ImagePro, using modified methods from Taylor et al. (2012), to semi-automate the analysis of particles larger than 5 μm in length. Using a VBA script within ImagePro, a series of pre-processing steps was performed, including extraction of an 8-bit gray scale image from the original 24-bit RGB image, use of a fast Fourier transform to remove background noise, and application of a Laplace filter to improve the definition of the particle edge and minimize the halo effect common in epifluorescence images. Images that were out of focus or of poor quality were discarded. Particles were manually outlined and the outlines were reapplied to the original

24-bit RGB image.

The images showed some autofluorescence, including that attributable to chlorophyll *a*. By leaving slides at room temperature for 24 hours or more, the autofluorescence of Chl *a* was dampened, but the autofluorescence of plastic was not affected. Thus, most fluorescent particles on the images were microplastics, bacteria, or TEP (transparent exopolymer particles; Samo et al. 2008).

Enumeration of Plastic and Fiber Particles

A decision tree was created to determine whether an object should be counted as plastic (Fig. 3.3). Particles were counted if they looked like plastic on the transmitted light image and fluoresced under the reflected light. Plastics, in general, looked like long, skinny fibers or flat fragments that had sharp, non-gelatinous edges, fluoresced uniformly, and did not have inner striations, coloration patterns, or areas suggestive of diatom chains, nuclei, etc. If the particles were invisible on the transmitted light image but fluorescent, they were determined to be TEP and not counted (Fig. 3.3, Fig. 3.4c; Samo et al. 2008). If they looked like plastic on the transmitted light image, but were not fluorescent, they were still counted, because not all plastics fluoresce (Table 3.1). We did not enumerate fiber-like objects that showed regular in-and-out indentations along their long axis, in the way that *Pseudo-nitzchia* and other long diatom chains do. Similarly, long skinny particles with an enlarged center or a circle in the center were also assumed to be diatoms and were not counted. When in doubt, particles were not counted as plastic, so the estimates in this paper are most likely underestimates of total plastic abundance.

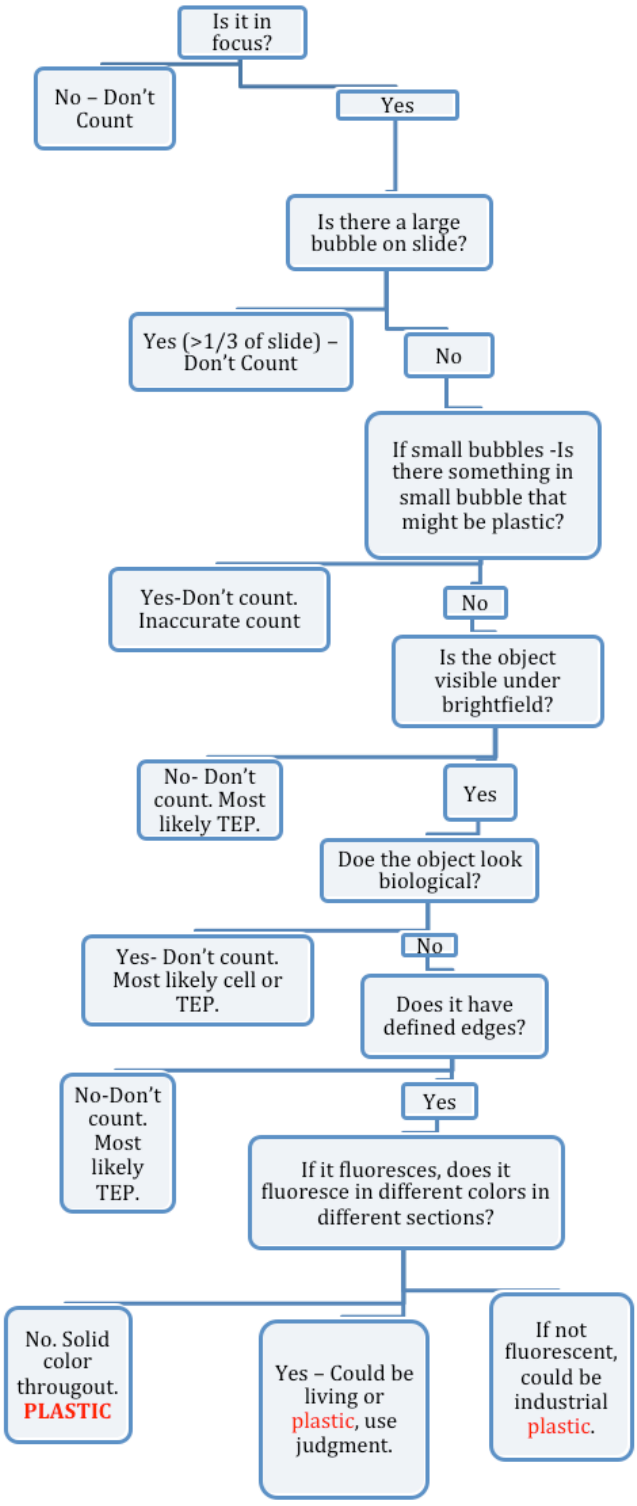

Figure 3.3: Flow chart for enumerating plastic microdebris on slides.

Particles were categorized as short fibers, fragments, or partial long fibers (Fig. 3.3).

Long fibers were fibers that could not fit in a single image on the slide, introducing the possibility of counting parts of the same long fiber twice in separate image fields selected randomly. The presence of long fibers was therefore not recorded with automated image processing, and instead enumerated in separate visual transects manually at the microscope. Their lengths, widths, and colors were also recorded. The lengths (as maximum feret length), widths (minimum feret length), areas, and fluorescence were recorded for every small fiber and fragment piece recognized in the slide images by ImagePro.

For visual transects of long fibers, slides were examined at 100x magnification. Every long fiber encountered down the center transect of the slide was enumerated, and the microscope stage was moved to manually measure its length and width. Then the stage was returned to center to continue the visual transect. Lengths and widths were recorded on a calibrated ocular micrometer. Width was manually measured at the widest point in the fiber. Some of the fibers were not a consistent width, so the calculated surface areas are an overestimate. Any fiber under 200 μm in length was not counted visually, in order to avoid double-counting fibers in the short fibers category from the processed images. However, there is likely a small amount of overlap between short and long fibers, because a few short fibers reached lengths up to 300 μm.

Long fibers were observed under four channels of fluorescence: the three channels used previously, as well as a channel available on the manual microscope: a green excitation/yellow-orange emission filter set, usually used for detecting phycoerythrin (excitation: 536–556 nm; emission: 550–610 nm; Pasulka et al. 2013). The intensity of perceived fluorescence was recorded on a qualitative scale for each fiber in each channel because the plastics were being observed by the human eye.

Determination of Plastic Fluorescence

Standard plastic and non-plastic reference materials were tested to determine fluorescence responses in the four excitation channels (Table 3.1). The six most common consumer plastics of various ages (Brandon et al. 2016) were tested, as well as additional industrial plastics. The non-plastic materials tested, such as cotton and wool, could be present in natural seawater but are more likely to be airborne contaminants from clothing worn while processing the samples. Standards were measured under both sampling methods – visually under the microscope, where the strength of fluorescence for each of the standards was recorded qualitatively (right side of Table 3.1), and in images from the microscope, where only presence/absence was recorded (left side of Table 3.1). This table compares the visual method of surveying slides through an eyepiece, where the sensitivity to fluorescence is that of the human eye, with the camera survey image method, where the sensitivity is much higher than the human eye. The camera images are post-processed and artificially colored in ImagePro software, and the fluorescence intensity can be manipulated in that process. The plastics in this standards table were compared to the plastics in our filtered seawater samples.

Contamination

To test for the possibility of airborne nano- and microplastic contamination during our collection and filtration process, we conducted control sample preparation on a separate cruise in January 2017, on the R/V *Sproul*, the same ship used for SKrillEx II, in a similar location as SKrillEx I and II and utilizing the same sampling protocol. We filtered two samples of surface seawater for microplastics and two samples of control, ultra-filtered Milli-Q water processed with the same protocol as all other samples.

RESULTS:

Epifluorescence Microscopy

Enumeration of Plastic and Fiber Particles

We found that almost no natural or biological particles autofluoresced under green excitation/yellow emission. Thus, any autofluorescence we observed in this channel was most likely a signature of plastic particles. Under blue excitation/green emission, some cellular material can autofluoresce (Scordato et al. 2016). When we saw non-specific cellular biological material fluorescing, it was organic material or biofilm on plastic. When something was solidly bright green, it was most likely plastic (Fig. 3.3, Fig. 3.4) or bacteria that were then ignored. There was considerable autofluorescence in the blue excitation/red emission channel, because even after leaving slides at room temperature, some organic material maintained Chl *a* autofluorescence. In that channel, we observed the most overlap between plastic and biological particles. When observing long fibers in visual transects, perceived red fluorescence was most likely underestimated, because in low light conditions, the human eye's visual acuity and contrast discrimination for red light greatly decreases compared to blue light (Shlaer et al. 1942, Rose 1948).

Figure 3.4 and Table 3.1 reveal that nearly all plastic types autofluoresce under these microscopy conditions, although different consumer plastics autofluoresce at different intensities (right side of Table 3.1). There are a few exceptions. Polyester did not fluoresce, and fluorescence of nylon was barely detectable in visual examination. These two are not among the six most common consumer plastics, but are often used for rope, nets, and fabrics. Wool also did not fluoresce at any wavelength tested.

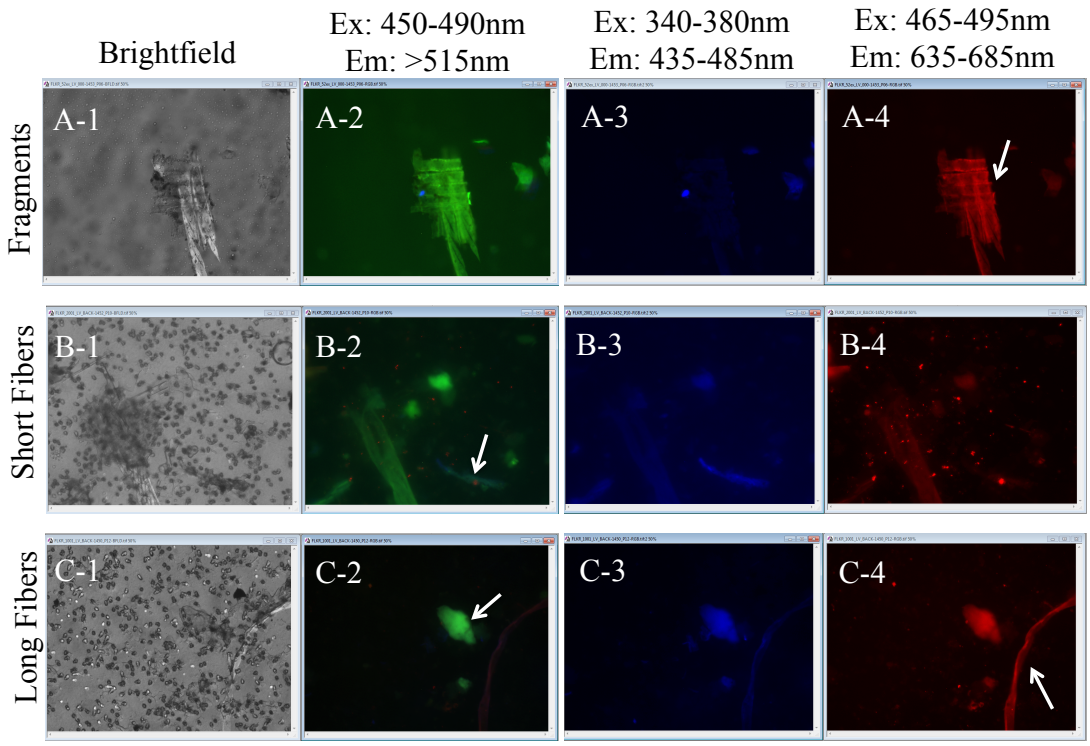

Figure 3.4: Brightfield and epifluorescence image. A) Plastic fragment, B) Thick and thin short plastic fibers, C) Long fiber and TEP. Column 1) brightfield; Column 2) Excitation 450-490nm, Emission > 515nm; Column 3) Excitation 340-380nm, Emission 435-485nm; Column 4) Excitation 465-495nm, Emission 635-685nm.

Figure 3.4a shows a fragment that was visible in transmitted light (A-1) and fluoresced strongly in the blue excitation/green emission channel (A-2) and blue excitation/red emission channel (A-4), but weakly in the UV excitation/blue emission channel (A-3). Because of this fluorescence signature, it is almost certainly a different type of plastic than the skinny short fiber shown in the bottom right of Fig. 3.4b, which fluoresced strongly in the blue excitation/green emission channel (B-2) and the UV excitation/blue emission channel (B-3) but was not detectable in the blue excitation/red emission channel (B-4). It is possible the plastic in 4a is polystyrene, based on its strong fluorescence in A-2 and A-4, and that the plastic in 4b is polypropylene or polyethylene

terephthalate, based on its strength in B-2 and B-3 (Table 3.1). However, such diagnostic determinations of plastic type were uncertain and beyond the scope of this paper.

Figure 3.4c illustrates a long fiber that would have been noted but not measured in these images, since it was not fully captured in the image. That image also shows, in the middle right part of the image, a bright piece of TEP that was almost invisible in the transmitted light image (C-1) but brightly fluorescent in all three channels (C-2, C-3, C-4). It also had indistinct borders. This particle would not have been counted as plastic due to these TEP-like characteristics.

Contamination

In Figure 3.5, we compare nearshore surface seawater with Milli-Q water to assess possible contamination during collection and filtration. Although the Milli-Q sample did include some microplastics (Fig. 3.5, blue bars), the numerical density of particles recorded from Milli-Q water was markedly lower than the density of all particle types recorded from surface seawater ($p < 0.05$, Wilcoxon Signed Rank Test). This indicates that the vast majority of microplastic materials recorded from the seawater samples are actually from the seawater sample and not from airborne or clothing contamination during processing.

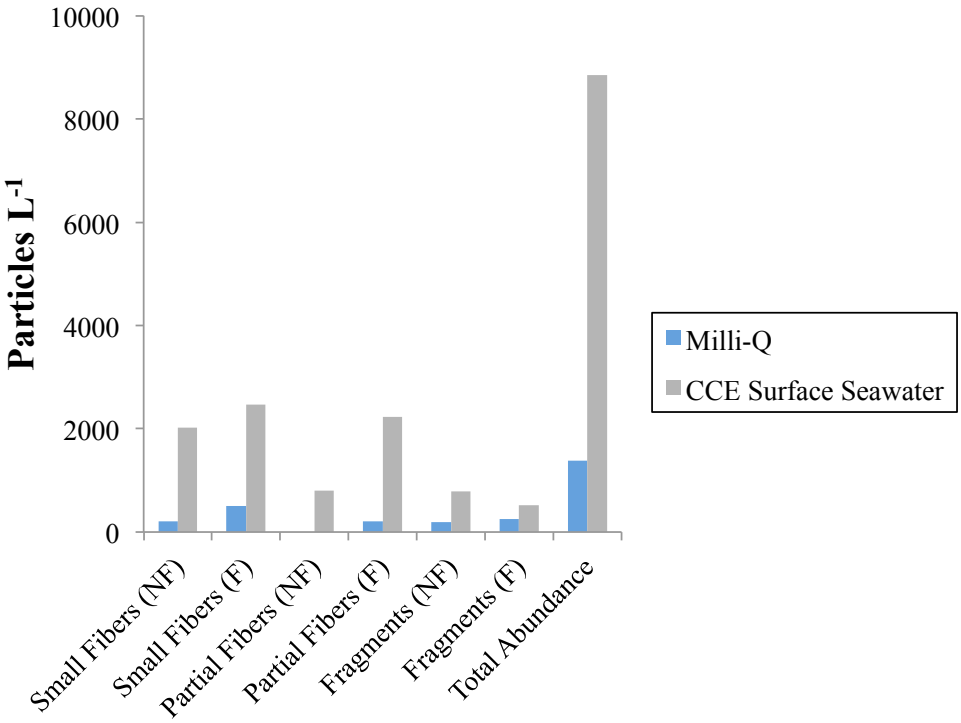

Figure 3.5: Control for environmental contamination. Grey: Concentration (particles L^{-1}), of nanoplastics in California Current Ecosystem (CCE) surface seawater. Green: concentration (particles L^{-1}), of nanoplastics in control sample of Milli-Q water. Samples taken on R/V *Sproul* in January 2017. Difference between seawater and control $p < 0.05$, Wilcoxon Signed Rank Test.

Plastic Concentration and Distribution Patterns

Figure 3.6 compares the mean nanoplastic particle concentrations across the three regions sampled in the *Falkor* transect (CCE, TR, NPSG) with the more nearshore SKrillEx I and SKrillEx II (averaged together, labeled Nearshore). There was significant heterogeneity among regions ($p < 0.001$, Kruskal-Wallis). SKrillEx I and II differ from all other regions ($p < 0.05$, Dunn's post-hoc test with Benjamini-Hochberg adjustment).

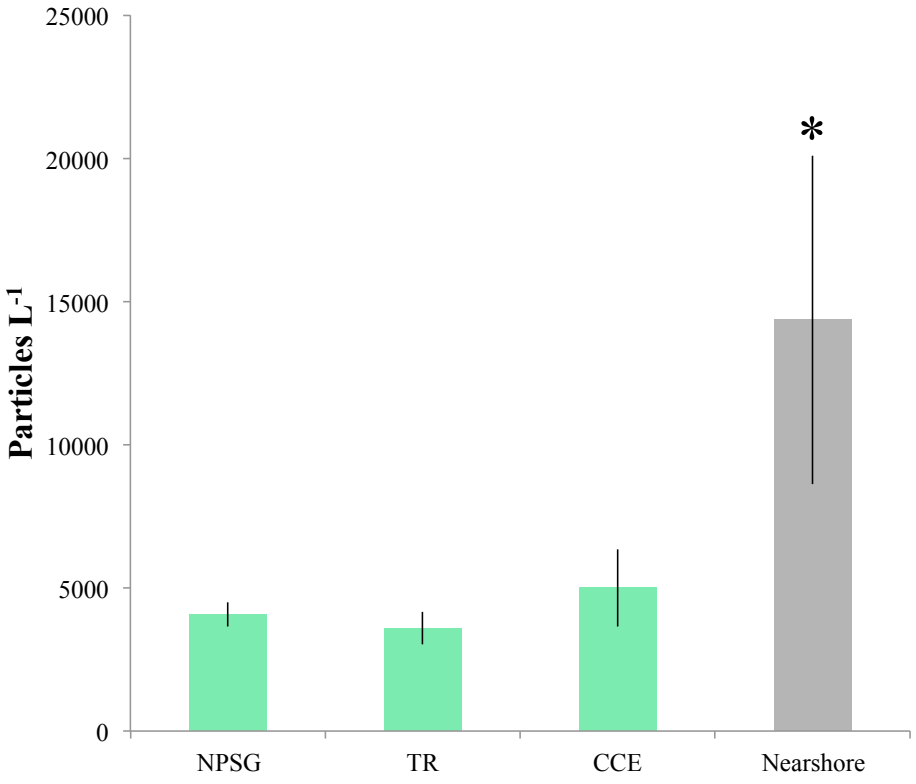

Figure 3.6: Mean concentrations (particles L^{-1}) from each sampling region. Mean concentration=concentration of small fibers and fragments by digital image surveys, long fibers by visual counts (mean ±95% C.I.). Green=*Falkor*, Grey=SKrillEx I and SKrillEx II, averaged together. Significant difference between regions ($p < 0.001$, K-W). * = SKrillEx I and II are significantly different than all other regions ($p < 0.05$, Dunn's post-hoc test with Benjamini-Hochberg adjustment).

Figure 3.7 combines all three plastic categories – small fibers, long fibers, and fragments - into the total filtered plastic concentration measured at each station. In Figure 3.7a, Station 1-1 on the right is nearshore in the northern California Current and Station 8-2 on the left is near Honolulu. We detected no significant spatial heterogeneity in plastic concentration across the *Falkor* transect among the three regions: North Pacific Subtropical Gyre (NPSG), California Current ecosystem (CCE), and the transition region (TR) ($p > 0.05$, Kruskal-Wallis). The nearshore samples from SKrillEx I (Fig. 3.7b) and SKrillEx II (Fig. 3.7c) were collected in a much smaller spatial sampling domain than the *Falkor* stations. On

this scale of sample separation (approx. 15 km), there was again no significant spatial heterogeneity ($p > 0.05$, Kruskal-Wallis, probably due to small sample sizes), although two samples on SKrillEx II appeared to have elevated concentrations.

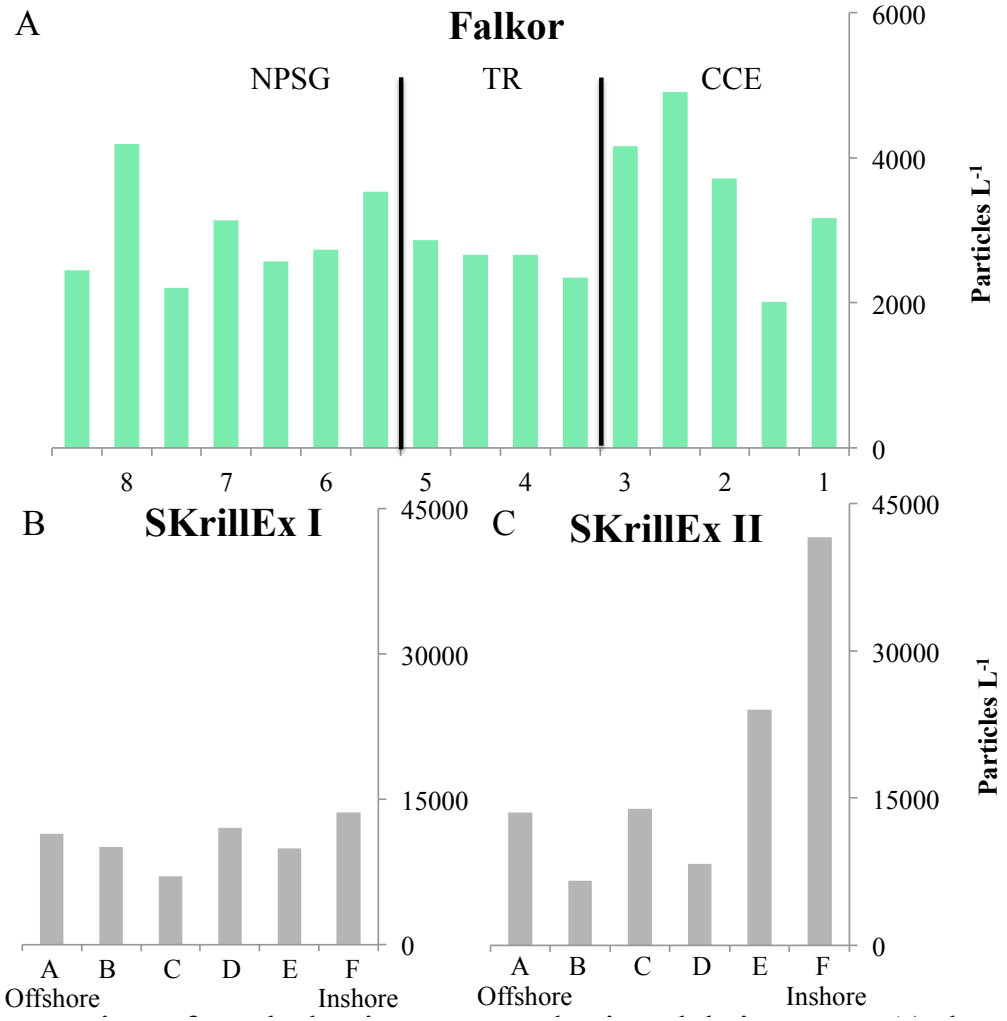

Figure 3.7: Concentration of total plastic nano- and microdebris across A) three regions in the NE Pacific, and B) SKrillEx I and C) SKrillEx II off San Diego, California. Concentration (particles L^{-1}). Total concentration = concentration of small fibers and fragments by digital image surveys, long fibers by visual counts. NPSG: North Pacific Subtropical Gyre, TR: transition region, CCE: California Current Ecosystem. No significant spatial heterogeneity in concentrations within any one cruise ($p > 0.05$, K-W).

Falkor

The concentration of nanoplastics sampled on the R/V *Falkor* cruise (Fig. 3.8) ranged from 100s-1,000s L^{-1} for short fibers and fragments (Fig. 3.8a, b), but much lower concentrations of long fibers were detected ($p < 0.0001$, Kruskal-Wallis, Fig. 3.8c). Dark blue bars above the x-axis in Fig. 3.8 indicate fluorescent plastics and the light blue bars below the x-axis indicate non-fluorescent plastics. There were always more fluorescent plastics than non-fluorescent plastics, however, the ratios of fluorescent: non-fluorescent plastic were much smaller for the long fibers than for the other two plastic types. When partitioning the sampling stations into regions based on environmental variables (Fig. 3.1), there was no regional heterogeneity for any of the three particle categories ($p > 0.05$, fluorescent and non-fluorescent particles combined, Kruskal-Wallis).

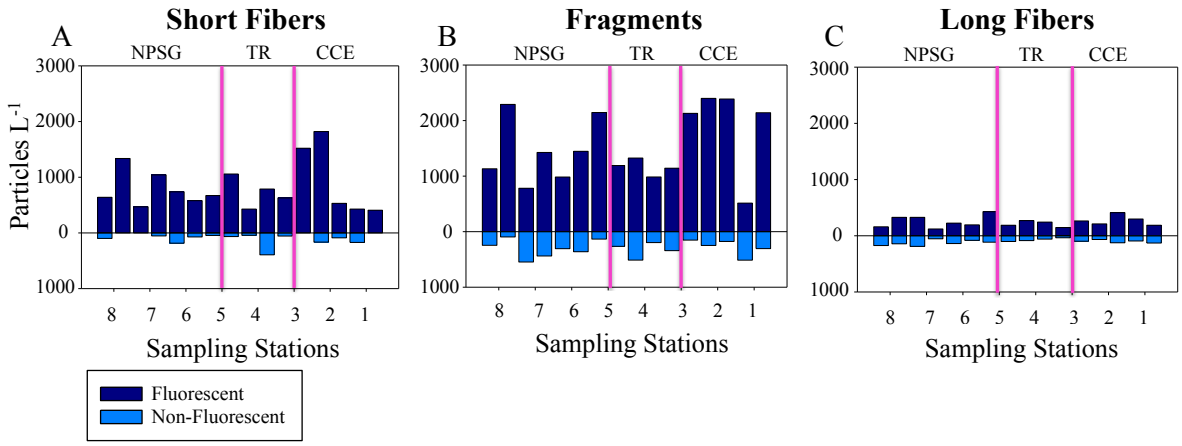

Figure 3.8: Concentrations (particles L^{-1}), R/V *Falkor*. A) Short fibers, B) Fragments, C) Long Fibers in three regions: NPSG: North Pacific Subtropical Gyre, TR: transition region, CCE: California Current Ecosystem. Fluorescent particles (upward bars), non-fluorescent particles (downward bards) combined - no spatial heterogeneity between regions ($p > 0.05$, Kruskal-Wallis).

SKrillEx I and II

In Fig. 3.9, the fluorescent short fibers from the nearshore SKrillEx I and SKrillEx II samples showed mean concentrations of 1,709 particles L^{-1} for SKrillEx I and 1,606 particles L^{-1} for SKrillEx II, and fluorescent fragments had concentrations of 916 particles

L^{-1} for SKrillEx I and 563 particles L^{-1} for SKrillEx II. The fluorescent long fibers of SKrillEx I were 3.5-6.5 times more abundant than the mean concentration of the short fibers and fragments at 6,028 particles L^{-1}. Similarly, the fluorescent long fibers of SKrillEx II were almost 8 times more abundant than the mean concentration of short fibers at 12,710 particles L^{-1}. Long fibers had high fluorescent: non-fluorescent ratios on both cruises, but there were similar values of fluorescent and non-fluorescent fragments, with a few stations even having higher non-fluorescent concentrations. No significant spatial heterogeneity was found among any of the stations for any plastic type ($p > 0.05$, fluorescent and non-fluorescent plastic combined, Kruskal-Wallis).

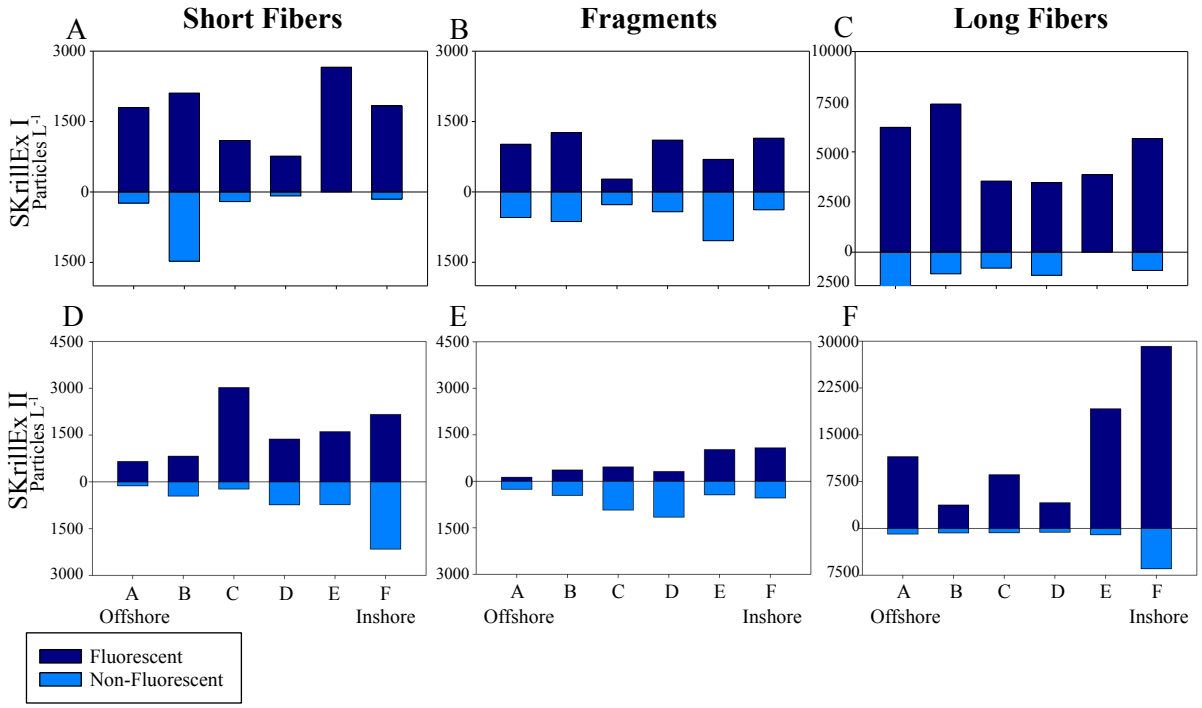

Figure 3.9: Concentrations (particles L^{-1}), SKrillEx I and SKrillEx II. A), D) Short fibers; B), E) Fragments; C), F) Long Fibers. No spatial heterogeneity in concentrations ($p > 0.05$, Kruskal-Wallis).

Plastic Dimensions

Falkor

Figure 3.10 illustrates the dimensions, as both surface area and length (feret length), of particles from the *Falkor* expedition. Almost every fragment and short fiber was smaller than 333 μm, and would have been missed by previous studies using larger mesh nets. The long fibers were much longer than 333 μm, but were so skinny that they could have easily slipped through a 333 μm mesh. The minimum lengths (i.e., the longest sides of particles) of fragments and short fibers were between 14-50 μm for all stations. Since the particles were sampled on filters with 5 μm pores, almost the entire range of particles down to the limiting pore size was measured. For long fibers, both area and length showed significant differences among regions ($p < 0.01$, Kruskal-Wallis). The transition region differed significantly from the CCE and NPSG in both area and length of long fibers, with shorter fibers in the transition region ($p < 0.0001$, Dunn's post-hoc test with Benjamini-Hochberg adjustment).

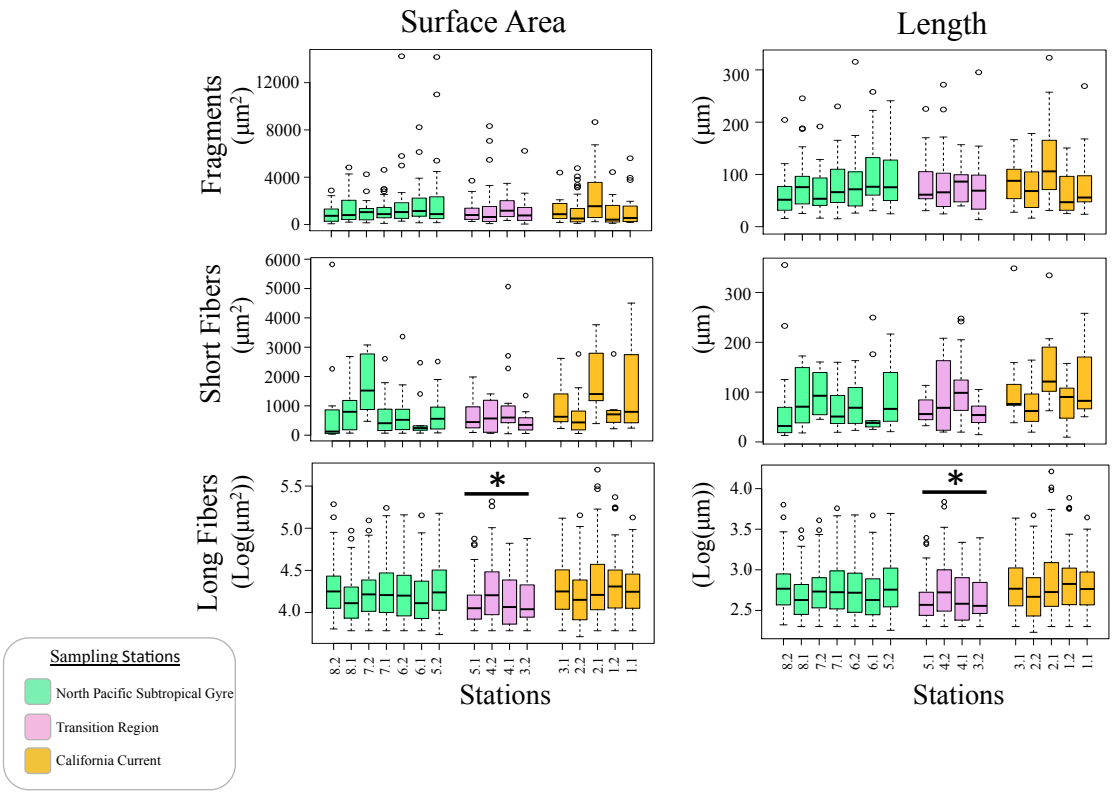

Figure 3.10: Linear and areal dimensions of plastic nano- and microplastics from the R/V *Falkor*. Green = NPSG, Pink= Transition Region, Yellow = California Current. Black line and asterisk indicate region significantly different from other two regions ($p < 0.01$, Kruskal-Wallis; $p < 0.001$, Dunn's post-hoc test with Benjamini-Hochberg adjustment).

SKrillEx I and II

On SKrillEx I, every fragment and short fiber length measured was smaller than 333 µm, so they would have been missed by previous studies using larger mesh nets (Fig. 3.11). Again, the minimum lengths approached the limiting size of 5 µm pores on the filters. The six stations differed significantly in regards to fragment length ($p < 0.05$, Kruskal-Wallis), short fiber area ($p < 0.01$, Kruskal-Wallis), and short fiber length ($p < 0.05$, Kruskal-Wallis). Station D was significantly different from all other stations except Station F for short fiber area ($p < 0.05$, Dunn's post-hoc test with Benjamini-Hochberg adjustment).

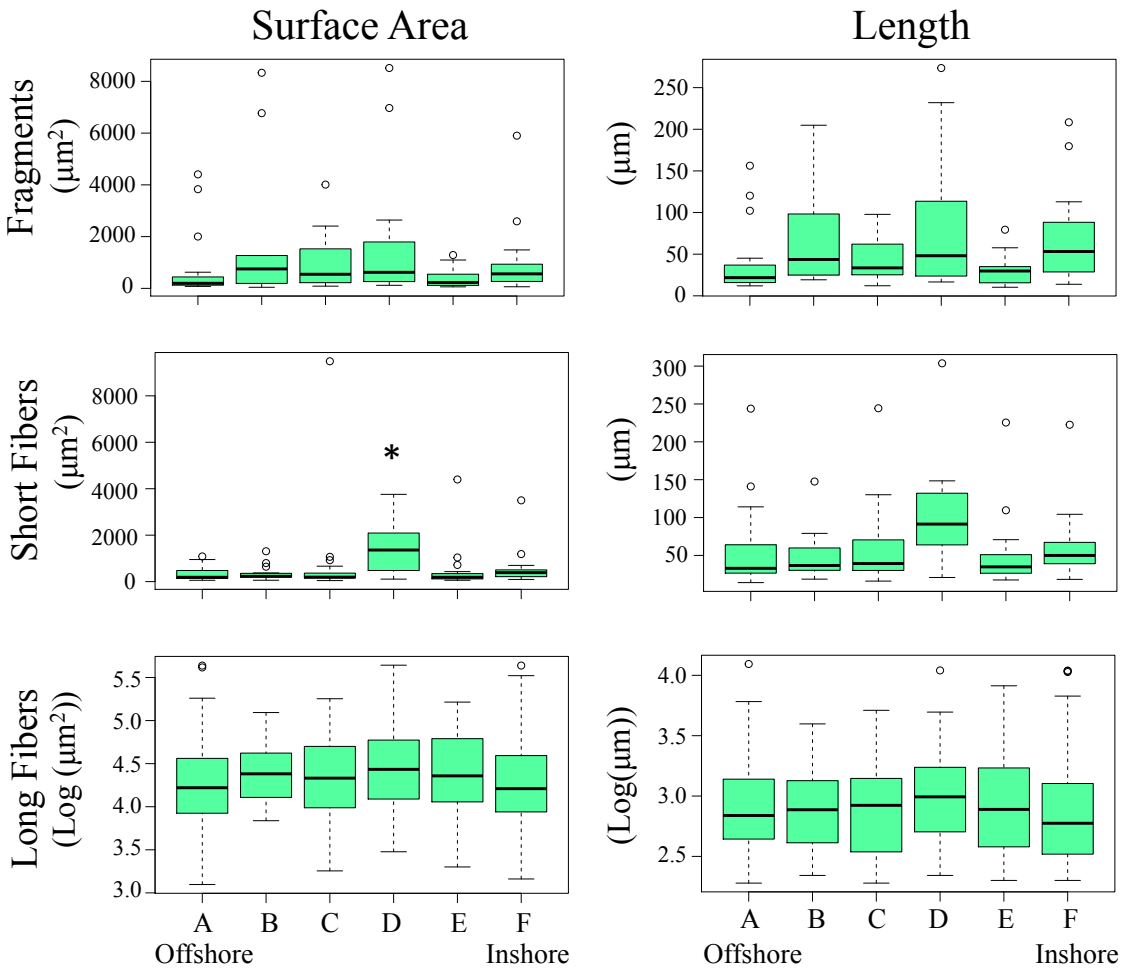

Figure 3.11: SKrillEx I plastic dimensions. Asterisk indicates when station significantly different than most others by Dunn's post-hoc test with Benjamini-Hochberg adjustment. Station A is the most offshore, Station F the most inshore.

With minimum lengths of 10-21 µm for fragments and short fibers, the whole range of particles down to the limiting size of 5 µm pores was sampled for SKrillEx II (Fig. 3.12). There was significant spatial heterogeneity among the six stations for fragment length ($p < 0.05$, Kruskal-Wallis) and long fiber area and length ($p < 0.01$, Kruskal-Wallis). For long fiber area, Station B was significantly different from every other station ($p < 0.001$, Dunn's post-hoc test with Benjamini-Hochberg adjustment). For long fiber length, Station B was only significantly different from Station C and Station F ($p < 0.01$, Dunn's post-hoc test with Benjamini-Hochberg adjustment).

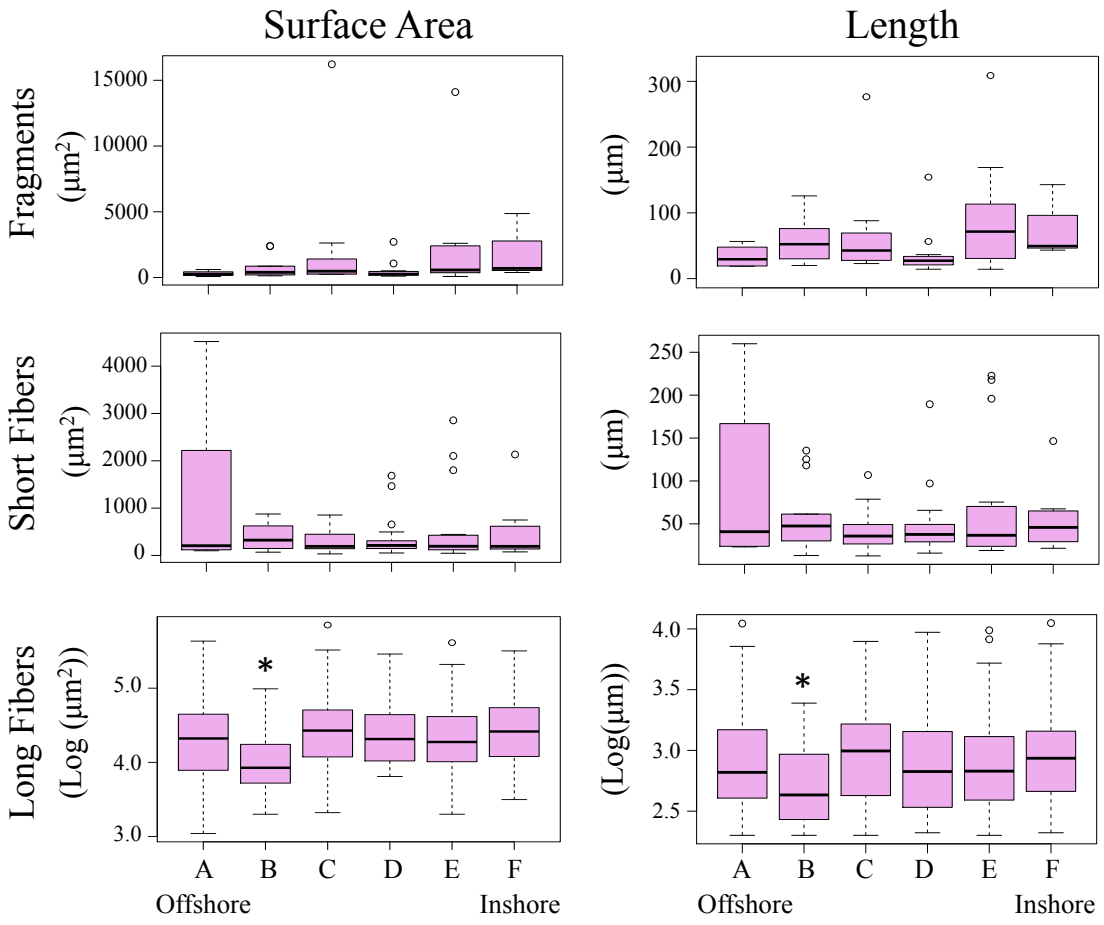

Figure 3.12: SKrillEx II plastic dimensions. Asterisk indicates when station significantly different than most others by Dunn's post-hoc test with Benjamini-Hochberg adjustment. Station A is the most offshore, Station F the most inshore.

Nanoplastics vs. Microplastics

In order to compare the concentration of nanoplastic particles that we sampled with microplastic and larger particles sampled in previous studies, in Figures 3.13 and 3.14 we combine our results with published results of Goldstein et al. (2013). Goldstein et al. (2013)'s results chronicle plastics from two cruises (SEAPLEX and EX1006) through the California Current to the North Pacific Subtropical Gyre, both using a 333 µm mesh neuston net for sampling. With respect to particle surface area (Fig. 3.13a), Goldstein et al. (2013) detected no particles with areas smaller than 0.01 mm^2 (range: 0.01 – 565 mm^2), while in the

three cruises from the present study, we measured particles ranging in individual surface area from $3x10^{-5}$ -0.71 mm^2. Considering particle length, Goldstein et al. (2013) measured plastic particles from 0.34-65.7 mm, and our range was 0.01-16.27 mm (including our long fibers). However, the most pronounced difference between studies was not in the size range of the particles, but in their concentrations. The small nanoplastics from this study were five orders of magnitude more abundant in numerical concentration than the larger microplastics from Goldstein et al. (2013). However, when expressed as the areal concentration (i.e. log μm^2 of plastic m^{-3} water), we found that the larger microplastic collected by neuston net (Goldstein et al. 2013) had significantly different concentrations than the nanoplastics collected in this study ($p < 0.0001$, Kruskal-Wallis; Figure 3.14). SEAPLEX's areal concentration was significantly higher than all other studies, and EX1006 was significantly different than *Falkor*, but not the nearshore cruises ($p < 0.05$, Dunn's post-hoc test with Benjamini-Hochberg adjustment). The nearshore cruises and Falkor are also not significantly different, as expected ($p < 0.05$, Dunn's post-hoc test with Benjamini-Hochberg adjustment).

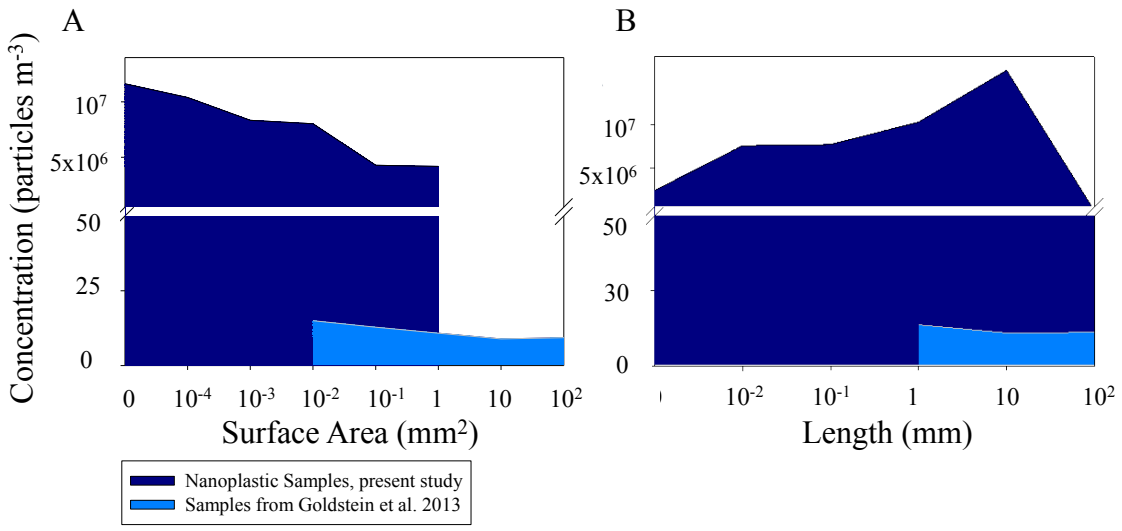

Figure 3.13: Frequency distributions of particles by A) surface area and B) length. Nanoplastics from the present study (dark blue) compared with net-collected microplastics from Goldstein et al. 2013 (light blue). Note break in the y-axis. X-axis values indicate lower boundaries of frequency distributions.

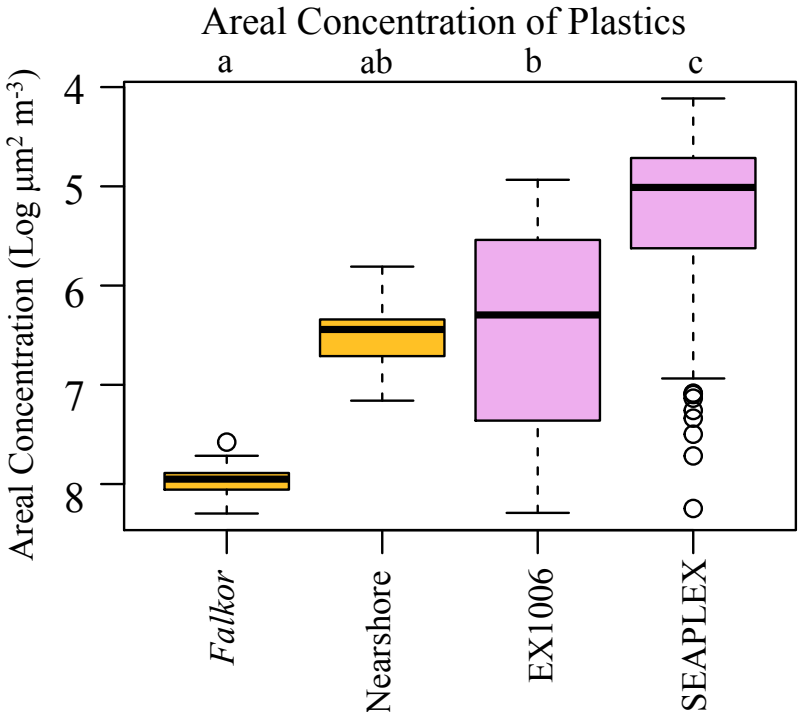

Figure 3.14: Areal concentration of plastics. Box and Whisker plot, circles are outliers beyond 3/2 outer quartile. Yellow= results from present study. Nearshore = SKrillEx I and II combined. Pink= results from Goldstein et al. 2013. Falkor (a) and EX1006 (b) do not differ significantly from nearshore samples (ab), although they do differ from each other. SEAPLEX concentrations (c) differ significantly from all other cruises ($p < 0.05$, Dunn's post-hoc test with Benjamini-Hochberg adjustment).

Plastic: Plankton Ratio

We estimated the ratio of plankton: plastic in the regions we sampled (Table 3.2). We used previously published concentrations of planktonic organisms from these same regions (CCE-LTER , Pasulka et al. 2013). Although these are based on mean values from studies in different years with different sampling locations, the results of Table 3.2 showed that, in general, the concentration of nano- and microplankton dwarfed the concentration of plastic, with a ratio of combined heterotrophs and autotrophs (> 5.0 μm) to nanoplastic in the CCE of $3.0x10^{2}$:1 (abundance L^{-1}:abundance L^{-1}). The corresponding mean ratio in the NPSG was almost an order of magnitude lower: $4.9x10^{1}$:1.

Although there was little spatial heterogeneity in nanoplastic concentrations across our large scale spatial transect of open ocean water, the plankton: plastic ratio did differ by region, reflecting the difference in plankton communities in the sampled areas.

DISCUSSION:

Epifluorescent microscopy successfully identified nanoplastic particles in natural seawater samples. We observed almost no biotic autofluorescence in the green excitation/yellow emission channel and very little under UV excitation/blue emission. We detected minimal biotic autofluorescence under blue excitation/green emission, with considerable residual autofluorescence under blue excitation/red emission. These channels required careful judgment in order to distinguish biotic, TEP, and plastic particles, but by utilizing transmitted light images, the shapes and edges of objects, and color patterns across an object, we were able to separate biotic from plastic materials. When examining slides via visual transects, we underestimated fluorescence under blue excitation/red emission because

the human eye is not as adept at detecting red light contrast under low light conditions (Shlaer et al. 1942, Rose 1948). Thus, comparing fluorescent: non-fluorescent ratios between long fibers observed visually, and short fibers and fragments observed in the processed images, is imperfect. However, the ultimate goal of this method was to be able to use autofluorescence to differentiate plastics from non-plastic particles, not to differentiate plastic types from one another. This epifluorescence microscopy protocol was successful in this goal and for obtaining a bulk measurement of plastics < 333 μm.

It was challenging to differentiate some plastic fragments from transparent exopolymer particles (TEP). The production of TEP has been attributed to phytoplankton, notably diatoms, which are abundant in the CCE and coastal regions sampled in these cruises. TEP is chemically complex, with a wide range of sizes and morphologies, and may be created and modified by a myriad of biological, chemical, and physical interactions, including colonization by bacteria (Alldredge et al. 1993, Verdugo et al. 2004, Azam and Malfatti 2007, Samo et al. 2008). TEP is completely transparent under transmitted light illumination, but can be made visible by staining with Alcian Blue and SYBR gold; where transparent particles land on the filter they prevent Alcian Blue from quenching SYBR Gold induced fluorescence and appear yellow-green (Samo et al. 2008).

We first attempted to stain test slides with 1% Alcian Blue in 3% glacial acetic acid, according to the methods of Alldredge et al. (1993) and Samo et al. (2008), but we did not add SYBR Gold like Samo et al. (2008). Although TEP particles that were previously transparent in visible light were dyed blue by the Alcian Blue, and entire plastic pieces were not blue, the plastic did exhibit some blue coloration in crevices. More troublesome was that with the addition of Alcian Blue, the plastic did not fluoresce normally and the blue

excitation/green emission channel showed very high background fluorescence. Samo et al. (2008) did not see such responses, perhaps attributable to their addition of SYBR gold. Based on these issues, we did not add Alcian Blue to our sample slides and instead differentiated TEP from plastic fragments by the transmitted light transparency and the hardness or sharpness of particle edges (Fig. 3.3, Fig. 3.4).

Airborne contamination of microfibers and microplastics has become a recent concern in marine debris research (Davison and Asch 2011, Foekema et al. 2013). Some studies (e.g., Foekema et al. 2013) choose to disregard all fiber counts, since they consider some fibers to be contamination, but we did not take that extreme measure. We do not believe that the color, length, or distribution of the fibers can be used to determine which fibers were contamination; however, we did record the color of each fiber on the visual transect. We discarded one extremely long fiber that had a clear sheath around it and had the same fluorescent pattern as a human hair (Table 3.1). Compared to Milli-Q filtered controls, most of the plastics in our samples were from seawater, not contamination. Although there were still plastics in the Milli-Q control samples, these may come from either airborne contamination or from the Milli-Q water itself, since the extreme filtration system used to make Milli-Q water is made of plastic. To confidently determine the exact contribution of contamination in future plastics studies, a more suitable control may be to find laboratory-grade ultra-filtered water that has been filtered through glass or carbon filters.

We recorded nano- and microplastic concentrations in the range of 100s-10,000s particles L^{-1}, with a mean concentration of all particles sampled on all cruises of 8,277 particles L^{-1} (8.3×10^6 particles m^{-3}). Goldstein et al. (2012) used a 333 μm mesh net and found a maximum concentration of micro-debris at the center of the North Pacific

Subtropical Gyre of 10 particles m^{-3}. Law et al. (2010) used a 335 μm mesh net and found a maximum abundance of micro-debris at the center of the North Atlantic Subtropical Gyre of 0.4 particles m^{-3}. Our particle concentrations averaged approximately 6 orders of magnitude higher than these previous studies, pointing to the previously undetected significance of nanoplastics in marine debris.

We saw spatial heterogeneity in nanoplastic concentration, with the very nearshore coastal samples having the highest plastic concentrations compared to the open ocean samples. These extremely high values of coastal plastics, and the difference between them and open ocean samples, do agree with published patterns of microplastic concentration that have recorded a similar spike in plastic concentration at extremely nearshore stations, near areas of high population, then a decrease as sampling moves offshore (Barnes et al. 2009, Law et al. 2010, Goldstein et al. 2012, Van Sebille et al. 2015). The difference in plastic densities between SKrillEx I and SKrillEx II was most likely due to annual differences in rainfall and riverine input to these nearshore waters. The sources of many microfibers are coastal watersheds and wastewater outflows (Zubris and Richards 2005, Browne et al. 2011). So if there is a difference in the outflow between years, there will also be a difference in plastic concentrations at these nearshore locations.

Many experimental sampling studies of macro- and microdebris (Law et al. 2010, Goldstein et al. 2012, Law et al. 2014, Van Sebille et al. 2015), as well as model studies of debris trajectories (Maximenko et al. 2012, Eriksen et al. 2014), agree that the highest concentrations of open ocean marine debris occur in convergence zones of subtropical gyres. However, we did not detect a significant increase in plastic concentration in the NPSG. Our open ocean samples are not significantly different across regions. There are many possible

sinks of nanoplastics that could account for this; small nanoplastics presumably break down into plastics smaller than 5.0 μm, and would not have been counted on the filters used in this study. Plastics are eventually biofouled and sink out of surface water, or are ingested and thus also removed from surface water. All of these sinks would happen more in the NPSG as plastic accumulates there. So even though plastic accumulates in the gyre, and larger plastic is continually breaking down into smaller plastic in that accumulation zone, our data imply that nanoplastic-sized plastic is being removed from the system at the same rate it is being supplied. In contrast, in the nearshore zone, nanoplastics, especially long fibers, have a higher input than loss term. All of these inputs and losses require further research to be better parameterized.

Large fiber areas and lengths were significantly smaller in the transition region than in the California Current and the North Pacific Subtropical Gyre. The difference in fiber lengths suggests that microfibers mainly originated from the coast, especially in wastewater (Zubris and Richards 2005, Browne et al. 2011). Such microfibers would be longer when newer, hence the long fibers in the CCE, and would then accumulate in the NPSG. The shorter fibers in the transition region may be due to the fact that longer fibers travel to the NPSG faster, but shorter fibers may have a longer travel time.

Another surprising result was the fluorescent: non-fluorescent plastic ratio (Fig. 3.8). The expectation from Table 3.1 was that non-fluorescent particles would be much rarer than fluorescent particles. However, the ratios are much smaller than expected for multiple plastic types. The similarities in numbers of fluorescent and non-fluorescent particles may be attributable to the uses of non-fluorescent fibers: polyester and nylon are often used for

fishing nets, ropes, lines, and monofilament, while fishing nets used to be commonly made of non-fluorescent wool.

The concentrations recorded here were between 5 and 7 orders of magnitude higher than previously recorded microplastic concentrations. Plankton: plastic ratios showed that, in general, the abundance of nano- and microplankton dwarfed the density of plastic, but with a marked regional difference: the ratio of combined heterotrophs and autotrophs to nanoplastic in the NPSG (49:1) was 6 times less than the ratio in the CCE (295:1). It is of note that these CCE values are for the southern CCE region, not the northern CCE region where the *Falkor* sampled; although there are published studies of microplankton biomass for the northern CCE region, and abundance values for plankton subcategories such as bacteria or heterotrophs, comparable, comprehensive microplankton abundance values do not appear to be available for this region. It is also of note that these ratios only sample plankton > 5.0μm, the same size range as the nanoplastic sampled here. Though some planktonic consumers only consume microplankton > 5.0 μm, some filter feeders at highest risk of consuming nanoplastics also consume smaller nano- and picoplankton. Abundance numbers that included picoeukaryotes, *Prochlorococcus*, and *Synechococcus* were calculated for the NPSG and CCE, and although the plankton: plastic ratios increased dramatically in both regions, the difference between the two regions' ratios remained relatively the same.

Although there was little spatial heterogeneity in nanoplastic concentrations across our open ocean spatial transect, the plankton: plastic ratio did differ by region, reflecting the difference in plankton communities in the sampled areas. The potential effects of nanoplastic debris would be greater in the oligotrophic gyre, where there was lower mean plankton abundance, than in the productive CCE. This subtle difference has significant implications

for understanding plastic flow in the food web. It implies that suspension-feeding consumers in the gyre are much more likely to interact with nano- and microplastic particles while feeding on their native microplankton prey than similar consumers in more productive regions of the ocean. Goldstein et al. (2013) found a similar spatial trend in plankton: plastic ratios from the NPSG to the CCE for the larger microdebris, underscoring that this is a consistent pattern governing the influence of plastic on pelagic food webs.

Goldstein et al. (2013) sampled almost no particles smaller than 0.333 mm x 0.333 mm (0.11 mm^2), as expected from the net mesh size. This directly points to limitations imposed by the sampling methodology. On the other hand, the three cruises from this study had many particles much smaller than 0.11 mm^2, down to 3 x 10^{-5} mm^2, and these much more abundant particles would have been entirely missed by a 333 μm net. Our results show that the majority of plastic concentrations occur at sizes smaller than 333 μm and 0.11 mm^2. However, when comparing areal concentrations (μm^2 of plastic m^{-3} of water), the larger plastics collected by neuston net are so much larger that they still dominate available surface area. Therefore, even though the nanoplastics measured here were more numerically abundant by 5-7 orders of magnitude, they did not comprise most of the plastic surface area in the water. Organisms that colonize surface substrates in the ocean are more likely to find surface area available in the form of micro- and macroplastics rather than nanoplastics, even though nanoplastics are more numerically abundant.

CONCLUSIONS:

This study may be the first to estimate the abundance of the smallest nanoplastics that have been consistently undersampled in marine debris studies, by employing sample

collection and analysis methods that maximized the identification of nano- and microplastic particles in seawater. We used a novel application of epifluorescence microscopy to visualize and enumerate nano- and microplastics in seawater. We were able to quantify nano- and microplastic concentrations that were 5- 7 orders of magnitude higher than previously published estimates, showing that previous net-based sampling greatly underestimated the presence of the smallest plastic in the ocean. This points to the different role that nanoplastics specifically may have on the ocean ecosystems compared to larger debris. While larger plastics may impact the food web at higher trophic levels by interacting directly with large animals, nanoplastic may have direct impacts on the lower levels of the food web because these particles are similar in size to plankton prey items of suspension-feeding consumers. This method allowed us to distinguish plastic from non-plastic particles and fluorescent from non-fluorescent plastic, but not to identify specific plastic types. Isolating plastic-specific autofluorescent patterns under specific emission wavelengths may permit such differentiation in future work.

We found the highest abundances of nanoplastic in the extreme nearshore environment, but contrary to previous studies addressing microplastic debris, we found no accumulation of nanoplastics in the North Pacific Subtropical Gyre. However, nanoplastic will have differential effects on the plankton communities and food webs in eutrophic and oligotrophic ocean regions due to the differences in plankton: plastic ratios determined here.

ACKNOWLEDGEMENTS: The research on R/V *Falkor* was supported by ship time from the Schmidt Ocean Institute. We express thanks to CCE-LTER for funding SKrillEx I and UC Ship Funds for funding SKrillEx II. We thank the entire M.R. Landry lab for their

patience and assistance with the epifluorescence microscope and software. We especially thank A.G. Taylor for his help at the beginning of this work. We thank M. Kahru for the satellite images. Dr. L. Aluhiware provided chemistry advice and guidance. E. Jacobsen and K. Blincow helped with analysis in R. We thank M.D. Ohman for guidance, extended discussions, and assistance throughout this study.

Chapter 3, in part is currently being prepared for submission for publication of the material. Brandon, Jennifer; Freibott, Alexandra. The dissertation author was the primary investigator and author of this material.

Table 3.1: Fluorescence signature of reference materials.

Standards of plastics and non-plastics examined under four channels of fluorescence. Plastics: HDPE (high-density polyethylene, LDPE (low-density polyethylene), PS (polystyrene), PP (polypropylene), PET (polyethylene terephthalate), PVC (poly-vinyl chloride). Reference material examined with both methods: images, post-processed with ImagePro, for presence/absence of fluorescence, and visually for strength of fluorescence.

Excitation Wavelength	340-380 nm	450-490 nm	465-495 nm	536-556 nm	340-380 nm	450-490 nm	465-495 nm	536-556 nm
Emission Wavelength	**435-485 nm**	**>515 nm**	**635-685 nm**	**550-610 nm**	**435-485 nm**	**>515 nm**	**635-685 nm**	**550-610 nm**
	Images Post-Processed				**Visually Through Microscope**			
SAMPLE								
Standard Consumer Plastics								
PE microscheres	X	X	X	X	X (+)	X (+++)		X (+)
HDPE (0 yrs)	X	X	X		X (+)	X (+)		
HDPE (3 yrs)	X	X	X	X	X (++)	X (++++)		X (++++)
HDPE (6 yrs)	X	X	X		X (++)	X (+++)		
LDPE (0 yrs)	X	X	X	X	X (++)	X (+++)		
LDPE (3 yrs)	X	X	X	X	X (++)	X (+++)		X (++)
LDPE (6 yrs)	X	X	X	X	X (+++++)	X (++++++)		X (++++)
PS (0 yrs)	X	X	X	X	X (+++++)	X (++++)		X (+)
PS (3 yrs)	X	X	X	X	X (+++++)	X (++++)	X (++++)	X (++++)
PS (6 yrs)	X	X	X	X	X (+++++)	X (++++++)	X (++++)	X (++++)
PP (0 yrs)	X	X	X	X	X (+++)	X (+++)		X (++)
PP (3 yrs)	X	X	X	X	X (+++)	X (++++)		X (++)
PP (6 yrs)	X	X	X	X	X (+++++)	X (++++)		X (+++)
PET (0 yrs)	X	X	X	X	X (+++++)	X (++++)		X (++)
PET (3 yrs)	X	X	X	X	X (++)	X (++)		X (+)
PET (6 yrs)	X	X	X	X	X (+++++)	X (+++)		X (+)
PVC (0 yrs)	X	X	X	X	X (+++)	X (+++)	X (+)	X (++)
PVC (3 yrs)	X	X	X	X	X (+++)	X (++++)		X (++)
PVC (6 yrs)	X	X		X	X (++)	X (+++)		X (++)
Assorted Plastics								
ACRYLIC	X	X	X	X	X (+++)	X (++++)		X (+)
ELASTIC	X	X	X	X	X (++++)	X (++++++)	X (++++)	X (++++++)
NYLON	X	X	X	X	X (+)	X (++)		
POLYESTER								
RUBBER TUBING	X	X		X	X (+++)	X (+++)		X (+)
STYROFOAM	X	X	X		X (+++++)	X (+++)		
VINYL	X	X			X (+++)	X(++++)		X (+)
MONOFILAMENT LINE	X	X		X	X (+++)	X (++++)		X (+)
Non-Plastics								
COTTON	X	X	X	X	X (+++++)	X (+++)		
HUMAN HAIR	X	X	X	X	X (+++)	X (++++)		X (+)
SILK	X	X	X	X	X (++++++)	X (+++)		X (+++)
WOOL								
RAYON	X	X	X	X	X (+++)	X (++++)		X (++++)

Key
X=Fluorescent
v.low=++
low=++
medium=+++
high=++++
v.high=+++++

Table 3.2: Plankton: Plastic Ratios

Plankton: Plastic Ratios in the Southern California Current Ecosystem (SCCE) and the North Pacific Subtropical Gyre (NPSG), for particles > 5 μm.

Organism	Plankton Abundance (L^{-1})	Plastic Abundance (L^{-1})	Plankton: Plastic Ratio
SCCE			
Microplankton (> 5 μm)[a]	$1.5x10^6$	$5x10^3$	295:1
NPSG			
Microplankton (> 5 μm)[b]	$1.8x10^5$	$4x10^3$	49:1

[a]CCE DATAZOO, averaged cell abundance from multiple cruises. > 5.0 μm. Top 5m of water sampled.

[b]Station ALOHA, averaged cell abundance from multiple cruises. > 5.0 μm. Top 5m of water sampled.

REFERENCES:

Abu-Hilal, A. H., and T. H. Al-Najjar. 2009. Plastic pellets on the beaches of the northern Gulf of Aqaba, Red Sea. Aquatic Ecosystem Health & Management **12**:461-470.

Ahmad, S. R. 1983. UV laser induced fluorescence in high-density polyethylene. Journal of Physics D: Applied Physics **16**:L137.

Alldredge, A., and L. Madin. 1982. Pelagic tunicates: unique herbivores in the marine plankton. Bioscience **32**:655-663.

Alldredge, A. L., U. Passow, and B. E. Logan. 1993. The abundance and significance of a class of large, transparent organic particles in the ocean. Deep Sea Research Part I: Oceanographic Research Papers **40**:1131-1140.

Andrady, A. L. 2011. Microplastics in the marine environment. Marine Pollution Bulletin **62**:1596-1605.

Arthur, C., Baker, J., and Bamford, H. (Eds.). 2009. Proceedings of the International Research Workshop on the Occurrence, Effects, and Fate of Microplastic Marine Debris, September 9-11, 2008, University of Washington Tacoma, Tacoma, WA, USA. U.S. Dept. of Commerce, National Oceanic and Atmospheric Administration, National Ocean Service, Office of Response & Restoration, Silver Spring, Md.

Azam, F., and F. Malfatti. 2007. Microbial structuring of marine ecosystems. Nature Reviews Microbiology **5**:782-791.

Backhurst, M. K., and R. G. Cole. 2000. Subtidal benthic marine litter at Kawau Island, north-eastern New Zealand. Journal of Environmental Management **60**:227-237.

Badr, Y., Z. Ali, and R. Khafagy. 1999. UV laser induced fluorescence of unirradiated and irradiated low density polyethylene. Journal of Photochemistry and Photobiology A: Chemistry **124**:35-40.

Barnes, D. K., F. Galgani, R. C. Thompson, and M. Barlaz. 2009. Accumulation and fragmentation of plastic debris in global environments. Philosophical Transactions of the Royal Society B: Biological Sciences **364**:1985-1998.

Besseling, E., A. Wegner, E. M. Foekema, M. J. Van Den Heuvel-Greve, and A. A. Koelmans. 2012. Effects of microplastic on fitness and PCB bioaccumulation by the lugworm *Arenicola marina* (L.). Environmental science & technology **47**:593-600.

Bone, Q. 1998. The biology of pelagic tunicates. Oxford University Press, Oxford.

Brandon, J., M. Goldstein, and M. D. Ohman. 2016. Long-term aging and degradation of microplastic particles: Comparing *in situ* oceanic and experimental weathering patterns. Marine Pollution Bulletin.

Browne, M. A., P. Crump, S. J. Niven, E. Teuten, A. Tonkin, T. Galloway, and R. Thompson. 2011. Accumulation of microplastic on shorelines worldwide: sources and sinks. Environmental science & technology **45**:9175-9179.

Browne, M. A., A. Dissanayake, T. S. Galloway, D. M. Lowe, and R. C. Thompson. 2008. Ingested microscopic plastic translocates to the circulatory system of the mussel, Mytilus edulis (L.). Environmental science & technology **42**:5026-5031.

Browne, M. A., T. S. Galloway, and R. C. Thompson. 2010. Spatial patterns of plastic debris along estuarine shorelines. Environmental science & technology **44**:3404-3409.

Browne, Mark A., Stewart J. Niven, Tamara S. Galloway, Steve J. Rowland, and Richard C. Thompson. 2013. Microplastic moves pollutants and additives to worms, reducing functions linked to health and biodiversity. Current Biology **23**:2388-2392.

Bruland, K., and M. Silver. 1981. Sinking rates of fecal pellets from gelatinous zooplankton (salps, pteropods, doliolids). Marine Biology **63**:295-300.

Carlton, J. T., J. W. Chapman, J. B. Geller, J. A. Miller, D. A. Carlton, M. I. McCuller, N. C. Treneman, B. P. Steves, and G. M. Ruiz. 2017. Tsunami-driven rafting: Transoceanic species dispersal and implications for marine biogeography. Science **357**:1402-1406.

Caron, D. A. 1983. Technique for enumeration of heterotrophic and phototrophic nanoplankton, using epifluorescence microscopy, and comparison with other procedures. Applied and Environmental Microbiology **46**:491-498.

Carpenter, E. J., and K. Smith. 1972. Plastics on the Sargasso Sea surface. Science **175**:1240-1241.

CCE-LTER. LTER Process Cruises. California Current Ecosystem Long Term Ecological Research.

Chan, W. Y., and J. Witting. 2012. The impact of microplastics on salp feeding in the tropical Pacific. Australian National University Undergraduate Research Journal **4**.

Cole, M., P. Lindeque, E. Fileman, C. Halsband, R. Goodhead, J. Moger, and T. S. Galloway. 2013. Microplastic ingestion by zooplankton. Environmental science & technology **47**:6646-6655.

Colton, J. B., F. D. Knapp, and B. R. Burns. 1974. Plastic particles in surface waters of the northwestern Atlantic. Science **185**:491-497.

Connection, Population. 2003. World Population: A Graphic Simulation of the History of Human Population Growth. PBS NOVA, http://www.pbs.org/wgbh/nova/earth/global-population-growth.html.

Conservancy, Ocean. 2010. Trash Travels. International Coastal Cleanup 25th Anniversary report.

Council, American Chemistry. 2014a. History of Polymers & Plastics for Teachers. http://www.americanchemistry.com/hops/intro_to_plastics/teachers.html.

Council, American Chemistry. 2014b. Life Cycle of a Plastic Product. http://www.americanchemistry.com/s_plastics/doc.asp?CID=1571&DID=5972.

Council, American Chemistry. 2014c. Resin Identification Codes. http://plastics.americanchemistry.com/Plastic-Resin-Codes-PDF.

Cózar, A., F. Echevarría, J. I. González-Gordillo, X. Irigoien, B. Úbeda, S. Hernández-León, Á. T. Palma, S. Navarro, J. García-de-Lomas, and A. Ruiz. 2014. Plastic debris in the open ocean. Proceedings of the National Academy of Sciences **111**:10239-10244.

Davison, P., and R. G. Asch. 2011. Plastic ingestion by mesopelagic fishes in the North Pacific Subtropical Gyre. Marine Ecology Progress Series **432**:173-180.

Defossez, J.-M., and A. Hawkins. 1997. Selective feeding in shellfish: size-dependent rejection of large particles within pseudofaeces from *Mytilus edulis*, *Ruditapes philippinarum* and *Tapes decussatus*. Marine Biology **129**:139-147.

Derraik, J. G. B. 2002. The pollution of the marine environment by plastic debris: a review. Marine Pollution Bulletin **44**:842-852.

Donohue, M. J., R. C. Boland, C. M. Sramek, and G. A. Antonelis. 2001. Derelict fishing gear in the northwestern Hawaiian Islands: Diving surveys and debris removal in 1999 confirm threat to coral reef ecosystems. Marine Pollution Bulletin **42**:1301-1312.

Dotmar. 2014. Density of Plastics. http://www.dotmar.com.au/density.html.

Dupont. 2014a. Dupont Heritage Timeline: 1939 Nylon. History, http://www2.dupont.com/Phoenix_Heritage/en_US/1939_c_detail.html.

Dupont. 2014b. Dupont Heritage Timeline: 1941 Orlon. History, http://www2.dupont.com/Phoenix_Heritage/en_US/1941_detail.html.

EPA. 2016. Advancing Sustainable Materials Management: 2014 Fact Sheet. Advancing Sustainable Materials Management. U.S. Environmental Protection Agency.

Eriksen, M., L. C. Lebreton, H. S. Carson, M. Thiel, C. J. Moore, J. C. Borerro, F. Galgani, P. G. Ryan, and J. Reisser. 2014. Plastic pollution in the world's oceans: More than 5 trillion plastic pieces weighing over 250,000 tons afloat at sea. PloS one **9**:e111913.

Eriksen, M., S. Mason, S. Wilson, C. Box, A. Zellers, W. Edwards, H. Farley, and S. Amato. 2013. Microplastic pollution in the surface waters of the Laurentian Great Lakes. Marine Pollution Bulletin **77**:177-182.

Foekema, E. M., C. De Gruijter, M. T. Mergia, J. A. van Franeker, A. J. Murk, and A. A. Koelmans. 2013. Plastic in North sea fish. Environmental science & technology **47**:8818-8824.

Freibott, A., L. Linacre, and M. R. Landry. 2014. A slide preparation technique for light microscopy analysis of ciliates preserved in acid Lugol's fixative. Limnology and Oceanography: Methods **12**:54-62.

Fry, D. M., S. I. Fefer, and L. Sileo. 1987. Ingestion of plastic debris by Laysan albatrosses and wedge-tailed shearwaters in the Hawaiian Islands. Marine Pollution Bulletin **18**:339-343.

Gerritse, L. J., and D.Vethaak. 2015. CLEANSEA Special Newsletter. CLEANSEA.

GESAMP. 2015. Sources, fate and effects of microplastics in the marine environment: a global assessment. IMO/FAO/UNESCO-IOC/UNIDO/WMO/IAEA/UN/ UNEP/UNDP Joint Group of Experts on the Scientific Aspects of Marine Environmental Protection.

GESAMP. 2016. Sources, fates, and effects of microplastics in the marine environment: part two of a global assessment. IMO/FAO/UNESCO-IOC/UNIDO/WMO/IAEA/UN/ UNEP/UNDP Joint Group of Experts on the Scientific Aspects of Marine Environmental Protection.

Gilfillan, L. R., M. D. Ohman, M. J. Doyle, and W. Watson. 2009. Occurrence of plastic micro-debris in the southern California Current system. California Cooperative Oceanic Fisheries Investigations Reports **50**:123-133.

Goldstein, M. C., H. S. Carson, and M. Eriksen. 2014. Relationship of diversity and habitat area in North Pacific plastic-associated rafting communities. Marine Biology **161**:1441-1453.

Goldstein, M. C., and D. S. Goodwin. 2013. Gooseneck barnacles (Lepas spp.) ingest microplastic debris in the North Pacific Subtropical Gyre. PeerJ **1**:e184.

Goldstein, M. C., M. Rosenberg, and L. Cheng. 2012. Increased oceanic microplastic debris enhances oviposition in an endemic pelagic insect. Biology Letters **8**:817-820.

Goldstein, M. C., A. J. Titmus, and M. Ford. 2013. Scales of spatial heterogeneity of plastic marine debris in the northeast Pacific ocean. PloS one **8**:e80020.

Graham, E. R., and J. T. Thompson. 2009. Deposit- and suspension-feeding sea cucumbers (Echinodermata) ingest plastic fragments. Journal of Experimental Marine Biology and Ecology **368**:22-29.

Gregory, M. R. 2009. Environmental implications of plastic debris in marine settings—entanglement, ingestion, smothering, hangers-on, hitch-hiking and alien invasions. Philosophical Transactions of the Royal Society B: Biological Sciences **364**:2013-2025.

Harbison, G., and V. McAlister. 1979. The filter‐feeding rates and particle retention efficiencies of three species of *Cyclosalpa* (Tunicata, Thaliacea). Limnology and Oceanography **24**:875-892.

Hart, M. W. 1991. Particle captures and the method of suspension feeding by echinoderm larvae. The Biological Bulletin **180**:12-27.

Hartline, N. L., N. J. Bruce, S. N. Karba, E. O. Ruff, S. U. Sonar, and P. A. Holden. 2016. Microfiber masses recovered from conventional machine washing of new or aged garments. Environmental science & technology **50**:11532-11538.

Henderson, J. R. 2001. A pre- and post-MARPOL Annex V summary of Hawaiian monk seal entanglements and marine debris accumulation in the Northwestern Hawaiian Islands, 1982–1998. Marine Pollution Bulletin **42**:584-589.

Hendy, I. L., L. Dunn, A. Schimmelmann, and D. Pak. 2013. Resolving varve and radiocarbon chronology differences during the last 2000 years in the Santa Barbara Basin sedimentary record, California. Quaternary International **310**:155-168.

Hidalgo-Ruz, V., L. Gutow, R. C. Thompson, and M. Thiel. 2012. Microplastics in the marine environment: a review of the methods used for identification and quantification. Environmental science & technology **46**:3060-3075.

Hoffman, D. L. 1989. Settlement and recruitment patterns of a pedunculate barnacle, *Pollicipes polymerus* (Sowerby), off La Jolla, California. Journal of Experimental Marine Biology and Ecology **125**:83-98.

Jambeck, J. R., R. Geyer, C. Wilcox, T. R. Siegler, M. Perryman, A. Andrady, R. Narayan, and K. L. Law. 2015. Plastic waste inputs from land into the ocean. Science **347**:768-771.

Jang, M., W. J. Shim, G. M. Han, M. Rani, Y. K. Song, and S. H. Hong. 2016. Styrofoam debris as a source of hazardous additives for marine organisms. Environmental science & technology **50**:4951-4960.

Kaiser, D., N. Kowalski, S. Oberbeckmann, and J. J. Waniek. 2017. Proving a paradigm: biofilms enhance microplastic deposition. *in* ASLO 2017: Mountains to the Sea, Honolulu, HI.

Karl, D. M. 1999. A sea of change: biogeochemical variability in the North Pacific Subtropical Gyre. Ecosystems **2**:181-214.

Katija, K., C. A. Choy, R. E. Sherlock, A. D. Sherman, and B. H. Robison. 2017. From the surface to the seafloor: How giant larvaceans transport microplastics into the deep sea. Science Advances **3**:e1700715.

Kemp, P. F., J. J. Cole, B. F. Sherr, and E. B. Sherr. 1993. Handbook of methods in aquatic microbial ecology. CRC press.

Koelmans, A. A., E. Besseling, and W. J. Shim. 2015. Nanoplastics in the aquatic environment. Critical review. Pages 325-340 Marine anthropogenic litter. Springer.

Langhals, H., D. Zgela, and T. Schlücker. 2015. Improved High Performance Recycling of Polymers by Means of Bi-Exponential Analysis of Their Fluorescence Lifetimes. Green and Sustainable Chemistry **5**:92.

Law, K. L., S. Morét-Ferguson, N. A. Maximenko, G. Proskurowski, E. E. Peacock, J. Hafner, and C. M. Reddy. 2010. Plastic accumulation in the North Atlantic subtropical gyre. Science **329**:1185-1188.

Law, K. L., S. E. Morét-Ferguson, D. S. Goodwin, E. R. Zettler, E. DeForce, T. Kukulka, and G. Proskurowski. 2014. Distribution of surface plastic debris in the eastern Pacific Ocean from an 11-Year data set. Environmental science & technology **48**:4732-4738.

Lechner, A., H. Keckeis, F. Lumesberger-Loisl, B. Zens, R. Krusch, M. Tritthart, M. Glas, and E. Schludermann. 2014. The Danube so colourful: A potpourri of plastic litter outnumbers fish larvae in Europe's second largest river. Environmental Pollution **188**:177-181.

Lozano, R., and J. Mouat. 2009. Marine litter in the northeast Atlantic region: Assessment and priorities for response. KIMO International. 9781906840266

Lynn, R. J., and J. J. Simpson. 1987. The California Current System: The seasonal variability of its physical characteristics. Journal of Geophysical Research: Oceans (1978–2012) **92**:12947-12966.

Masterson, K. 2009. The history of plastic: From billiards to bibs. Plastic Peril? NPR, http://www.npr.org/templates/story/story.php?storyId=114331762.

Mattsson, K., E. V. Johnson, A. Malmendal, S. Linse, L.-A. Hansson, and T. Cedervall. 2017. Brain damage and behavioural disorders in fish induced by plastic nanoparticles delivered through the food chain. Scientific Reports **7(1)**: 11452.

Maximenko, N., J. Hafner, and P. Niiler. 2012. Pathways of marine debris derived from trajectories of Lagrangian drifters. Marine Pollution Bulletin **65**:51-62.

Meehl, G. A. 1982. Characteristics of surface current flow inferred from a global ocean current data set. Journal of Physical Oceanography **12**:538-555.

Moody, S. 2010. Washed Up: The curious journeys of flotsam and jetsam. Sasquatch Books.

Moore, C. J., S. L. Moore, M. K. Leecaster, and S. B. Weisberg. 2001. A comparison of plastic and plankton in the North Pacific Central Gyre. Marine Pollution Bulletin **42**:1297-1300.

Murray, F., and P. R. Cowie. 2011. Plastic contamination in the decapod crustacean *Nephrops norvegicus* (Linnaeus, 1758). Marine Pollution Bulletin **62**:1207-1217.

Niiler, P. P., and R. W. Reynolds. 1984. The three-dimensional circulation near the eastern North Pacific Subtropical Front. Journal of Physical Oceanography **14**:217-230.

Nurmukhametov, R., L. Volkova, and S. Kabanov. 2006. Fluorescence and absorption of polystyrene exposed to UV laser radiation. Journal of Applied Spectroscopy **73**:55-60.

Ogata, Y., H. Takada, K. Mizukawa, H. Hirai, S. Iwasa, S. Endo, Y. Mato, M. Saha, K. Okuda, A. Nakashima, M. Murakami, N. Zurcher, R. Booyatumanondo, M. P. Zakaria, L. Q. Dung, M. Gordon, C. Miguez, S. Suzuki, C. Moore, H. K. Karapanagioti, S. Weerts, T. McClurg, E. Burres, W. Smith, M. V. Velkenburg, J. S. Lang, R. C. Lang, D. Laursen, B. Danner, N. Stewardson, and R. C. Thompson. 2009. International Pellet Watch: Global monitoring of persistent organic pollutants (POPs) in coastal waters. 1. Initial phase data on PCBs, DDTs, and HCHs. Marine Pollution Bulletin **58**:1437-1446.

Pasulka, A. L., M. R. Landry, D. A. Taniguchi, A. G. Taylor, and M. J. Church. 2013. Temporal dynamics of phytoplankton and heterotrophic protists at station ALOHA. Deep Sea Research Part II: Topical Studies in Oceanography **93**:44-57.

PlasticsEurope. 2012. Plastics- The Facts 2012: An analysis of European plastics production, demand and waste data for 2011. http://www.plasticseurope.org/.

Rochman, C. M., E. Hoh, T. Kurobe, and S. J. Teh. 2013. Ingested plastic transfers hazardous chemicals to fish and induces hepatic stress. Scientific Reports **3**:3263.

Roden, G. I. 1980. On the subtropical frontal zone north of Hawaii during winter. Journal of Physical Oceanography **10**:342-362.

Rose, A. 1948. The sensitivity performance of the human eye on an absolute scale. JOSA **38**:196-208.

Ryan, P. G., C. J. Moore, J. A. van Franeker, and C. L. Moloney. 2009. Monitoring the abundance of plastic debris in the marine environment. Philosophical Transactions of the Royal Society of London B: Biological Sciences **364**:1999-2012.

Samo, T. J., F. Malfatti, and F. Azam. 2008. A new class of transparent organic particles in seawater visualized by a novel fluorescence approach. Aquatic Microbial Ecology **53**:307-321.

Schimmelmann, A., I. L. Hendy, L. Dunn, D. K. Pak, and C. B. Lange. 2013. Revised~ 2000-year chronostratigraphy of partially varved marine sediment in Santa Barbara Basin, California. GFF **135**:258-264.

Schlining, K., S. von Thun, L. Kuhnz, B. Schlining, L. Lundsten, N. J. Stout, L. Chaney, and J. Connor. 2013. Debris in the deep: Using a 22-year video annotation database to survey marine litter in Monterey Canyon, central California, USA. Deep Sea Research Part I: Oceanographic Research Papers **79**:96-105.

Scordato, A., S. Schwartz, J. D. Griffin, N. S. Claxton, M. J. Parry-Hill, T. J. Fellers, K. M. Vogt, I. D. Johnson, S. H. Neaves, O. Alvarado, J. Parsons, Lionel , M. A. Sodders, R. L. Ludlow, and M. W. Davidson. 2016. Blue Excitation: B-1A (Longpass Emission). MicroscopyU: The source for microscopy education. Nikon Instruments, Inc.

Shlaer, S., E. L. Smith, and A. M. Chase. 1942. Visual acuity and illumination in different spectral regions. The Journal of general physiology **25**:553-569.

Smith, K., A. Sherman, C. Huffard, P. McGill, R. Henthorn, S. Von Thun, H. Ruhl, M. Kahru, and M. Ohman. 2014. Large salp bloom export from the upper ocean and benthic community response in the abyssal northeast Pacific: Day to week resolution. Limnology and Oceanography **59**:745-757.

Stefatos, A., M. Charalampakis, G. Papatheodorou, and G. Ferentinos. 1999. Marine debris on the seafloor of the Mediterranean Sea: Examples from two enclosed gulfs in western Greece. Marine Pollution Bulletin **38**:389-393.

Supply, Freund Container 2010. Plastic Properties. Guide to Plastics. http://www.freundcontainer.com/guide-to-plastics/a/72/

Taylor, A. G., R. Goericke, M. R. Landry, K. E. Selph, D. A. Wick, and M. J. Roadman. 2012. Sharp gradients in phytoplankton community structure across a frontal zone in the California Current Ecosystem. Journal of Plankton Research **34**:778-789.

Thiel, M., and L. Gutow. 2005. The ecology of rafting in the marine environment. II. The rafting organisms and community. Oceanography and Marine Biology: an annual review **43**:279-418.

Thompson, R. C., Y. Olsen, R. P. Mitchell, A. Davis, S. J. Rowland, A. W. John, D. McGonigle, and A. E. Russell. 2004. Lost at sea: where is all the plastic? Science **304**:838-838.

USEPA. 1992. Plastic pellets in the aquatic environment: Sources, and recommendations. Washington, DC.

Van Cauwenberghe, L., A. Vanreusel, J. Mees, and C. R. Janssen. 2013. Microplastic pollution in deep-sea sediments. Environmental Pollution **182**:495-499.

Van Sebille, E., C. Wilcox, L. Lebreton, N. Maximenko, B. D. Hardesty, J. A. Van Franeker, M. Eriksen, D. Siegel, F. Galgani, and K. L. Law. 2015. A global inventory of small floating plastic debris. Environmental Research Letters **10**:124006.

Venrick, E., T. Backman, W. Bartram, C. Platt, M. Thornhill, and R. Yates. 1973. Man-made objects on the surface of the central North Pacific Ocean. Nature **241**:271-271.

Verdugo, P., A. L. Alldredge, F. Azam, D. L. Kirchman, U. Passow, and P. H. Santschi. 2004. The oceanic gel phase: a bridge in the DOM–POM continuum. Marine Chemistry **92**:67-85.

Wilson, D. S. 1973. Food size selection among copepods. Ecology **54**:909-914.

Wong, C., D. R. Green, and W. J. Cretney. 1974. Quantitative tar and plastic waste distributions in the Pacific Ocean. Nature **247**:30-32.

Woodall, L. C., A. Sanchez-Vidal, M. Canals, G. L. Paterson, R. Coppock, V. Sleight, A. Calafat, A. D. Rogers, B. E. Narayanaswamy, and R. C. Thompson. 2014. The deep sea is a major sink for microplastic debris. Royal Society open science **1**:140317.

Wright, S. L., R. C. Thompson, and T. S. Galloway. 2013. The physical impacts of microplastics on marine organisms: a review. Environmental Pollution **178**:483-492.

Zalasiewicz, J., C. N. Waters, J. A. I. do Sul, P. L. Corcoran, A. D. Barnosky, A. Cearreta, M. Edgeworth, A. Gałuszka, C. Jeandel, and R. Leinfelder. 2016. The geological cycle of plastics and their use as a stratigraphic indicator of the Anthropocene. Anthropocene **13**:4-17.

Zalasiewicz, J., C. N. Waters, C. P. Summerhayes, A. P. Wolfe, A. D. Barnosky, A. Cearreta, P. Crutzen, E. Ellis, I. J. Fairchild, and A. Gałuszka. 2017. The Working Group on the Anthropocene: Summary of evidence and interim recommendations. Anthropocene **19**:55-60.

Zubris, K. A. V., and B. K. Richards. 2005. Synthetic fibers as an indicator of land application of sludge. Environmental Pollution **138**:201-211.

CHAPTER 3 APPENDIX: Other analytical methods besides epifluorescence microscopy

SAMPLING METHODS:

The methods to retrieve the seawater samples used here are all the same as included in the main chapter. Along with the polycarbonate filters described in the methods section of the main chapter, more filters were taken on each cruise than were discussed in the main chapter because they were not analyzed with epifluorescence microscopy. A 202 μm stainless steel mesh pre-filter was made after the *Falkor* expedition in an attempt to exclude larger, unwanted microorganisms. Therefore, four filters were used at each sampling location on SKrillEx I and SKrillEx II: one 5.0 μm polycarbonate and one 0.7 μm glass fiber filter (GFF), and one 5.0 μm polycarbonate and one 0.7 μm glass fiber filter following 202 μm pre-filtering of the water. Both GFF and polycarbonate filters are discussed below.

SECTION 1: RAMAN SPECTROSCOPY:

Introduction

Plastics have been identified and analyzed numerous times by Raman spectroscopy (Allen et al. 1999, Sato et al. 2002), even identifying heterogeneities in polymer blends down to 1 μm (Markwort and Kip 1996). Raman spectroscopy has been used to identify marine debris pieces as small as a few mm in diameter (Zettler et al. 2013) and to identify plastic in lobster gut contents (Murray and Cowie 2011). Raman spectroscopy is often recommended as a good way to confirm the identify of small oceanic particles that are being identified as plastics visually (Hidalgo-Ruz et al. 2012). However, almost all studies that have utilized Raman spectroscopy have examined pure, clean, unweathered plastic that has a clear Raman signal, or at relatively large microdebris (> 500 μm).

Raman is generally a non-destructive technique, which, with a high quality instrument, can identify particles as small as 1 μm (Markwort and Kip 1996, Bocklitz et al. 2011). Raman scattering is inelastic, but it is usually much weaker than the Rayleigh scattering of laser light, which is why it must be amplified to give a good signal (Bowley et al. 2012). Raman signals are often easily contaminated; they can be modified by the appearance of a fluorescence background, cosmic spikes originating from high-energy particles hitting the charged-coupled device (CCD), Gaussian noise and cosmic noise (Appendix Fig. 3.1; Bocklitz et al. 2011). All of these effects contribute to a certain wavenumber region of the experimentally recorded Raman spectra, and therefore have to be corrected for in order to analyze the Raman spectra. Beside these corrections it is often necessary to correct for varying sampling geometries and reject highly redundant variables (Bocklitz et al. 2011).

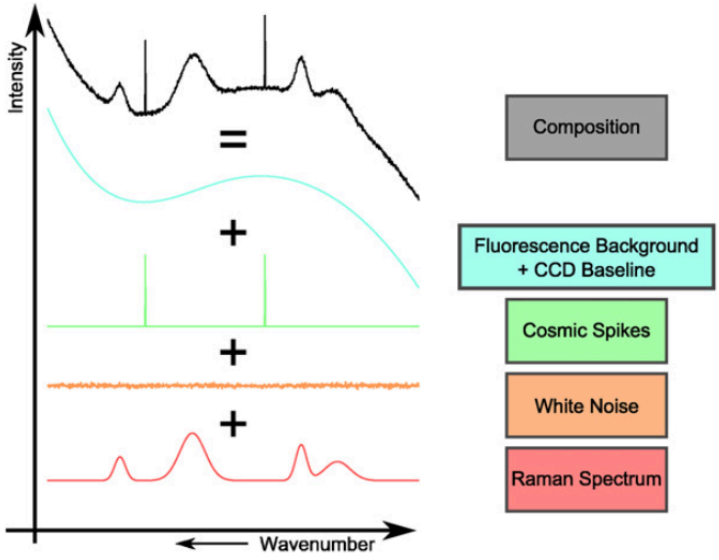

Appendix Figure 3.1: Raman Spectrum Composition. The measured Raman spectrum is suffering from multiple interfering side effects that have to be rejected prior to analyzing the spectrum. Figure reproduced from Bocklitz et al. 2011.

When additives and colorants are added to plastic, it greatly complicates the Raman

signal, by causing fluorescence and interference, leading to un-interpretable spectra (DiraMED). They can also cause the Raman spectra to be of the pigments themselves and not the plastics, leading to an inability to identify plastic to type (Van Cauwenberghe et al. 2013). Dark colored plastics have been known to burn and/or heat up, causing thermal emission curves that disrupt the Raman signal and alter the sample structure (Grasselli and Bulkin 1991, Markwort and Kip 1996). Water and salt can also have their own Raman spectra, adding confusion (Murray and Cowie 2011, Potgieter-Vermaak et al. 2012). Real world ocean plastic samples also have uneven surfaces that can lead to complications getting the particle in focus; especially with transparent samples, regions tens of micrometers from the section in focus can cause readily detectable signal contributions (Everall 2008).

Methods

The Raman spectra of samples were measured with a Renishaw inVia Raman spectrometer equipped with a Renishaw CCD camera and a Leica microscope. The Renishaw system is equipped with a 200 mW CW laser at 785 nm with a 1200 l/mm grating and a 100 mW CW laser at 532 nm with a 1800 l/mm grating, but plastics were only analyzed with 785 nm light, because the near infrared wavelength is known to often overcome the fluorescence interference experienced with Raman analysis of plastic polymers (Grasselli and Bulkin 1991, Allen et al. 1999).

The Raman signals of polymers are very weak (Socrates 2004). Originally the samples were analyzed with the lights on in the laboratory space, and then with lights off and the microscope covered with black fabric, but the signature of the ambient fluorescent light bulbs continually caused contamination in the sample readings (Appendix Fig. 3.2). For good polymer readings, samples must be analyzed in total darkness; after discovering this,

the Renishaw inVia system was fitted with a complete microscope enclosure to prevent stray light from entering the sampling chamber. Light contamination was not an issue after the microscope enclosure was fitted on the microscope.

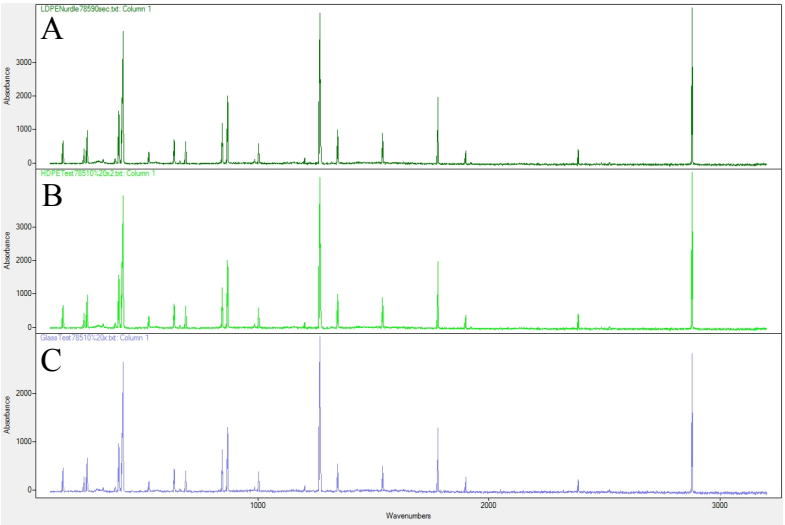

Appendix Figure 3.2: Light Contamination. The three identical spectra are of A) LDPE pre-production plastic pellet, B) HDPE powder, and C) a glass slide, proving that what was actually being measured was an artifact. It was proven to be the Raman signal of the ambient fluorescent light bulbs in the laboratory. These spectra were obtained with all lights on in the laboratory.

All measurements were taken with 785 nm light, at 20x or 50x magnification. The laser was at 10%, to not cause thermal degradation of the sample or thermal emission curves that drown out the polymer signal (Grasselli and Bulkin 1991). The scans were for 10 seconds, sometimes 30 seconds, which allowed for a cleaner reading if there was excessive noise at 10 seconds.

Standards and beach plastic

Before the R/V *Falkor* cruise, samples of virgin polypropylene (PP), high-density polyethylene (HDPE) and low-density polyethylene (LDPE) pellets were crushed and sent to Professor George Rossman in the Division of Geological and Planetary Sciences at the California Institute of Technology for preliminary Raman analysis to test whether the three

plastic types could be identified and differentiated via Raman. Preliminary tests were also conducted on the filters used to determine whether the filters had interfering background fluorescence. Samples were analyzed at CalTech with a 514 nm laser at 10% laser power at 100x magnification for 10 seconds.

On the Renishaw microscope at UCSD, pure preproduction plastics were tested as nurdles, of average size 2 mm diameter, and ground up into shavings of minimum size ~40-50 μm diameter. Then samples of small plastics that were collected on the North Shore of Oahu, (most likely washed ashore from the North Pacific Subtropical Gyre), were shaved down to minimum size ~40-50 μm diameter, and those shavings were tested for plastic type on top of glass slides.

Oceanic samples

Oceanic water was filtered for surface plastic contaminants by the above-mentioned methods on the R/V *Falkor* and on SKrillEx I and SKrillEx II. All oceanic samples were analyzed at 10% laser power to diminish the potential for thermal emission, unless a dark particle burned, in which case a different spot on the particle was re-analyzed at 1% laser power. All samples were analyzed at 50x magnification for 10 seconds, unless there was a significant fluorescent curve or too much noise in the spectra, and then the sample was re-analyzed for 30 seconds.

Results

Standards and beach plastic

The Rossman Lab at CalTech identified that Alumina filters had their own Raman signal and caused interference with the plastic signal (Appendix Fig. 3.3c), but that glass

fiber filters (GFF) and polycarbonate filters had very minimal Raman signals (Appendix Fig. 3.3b and 3.3a).

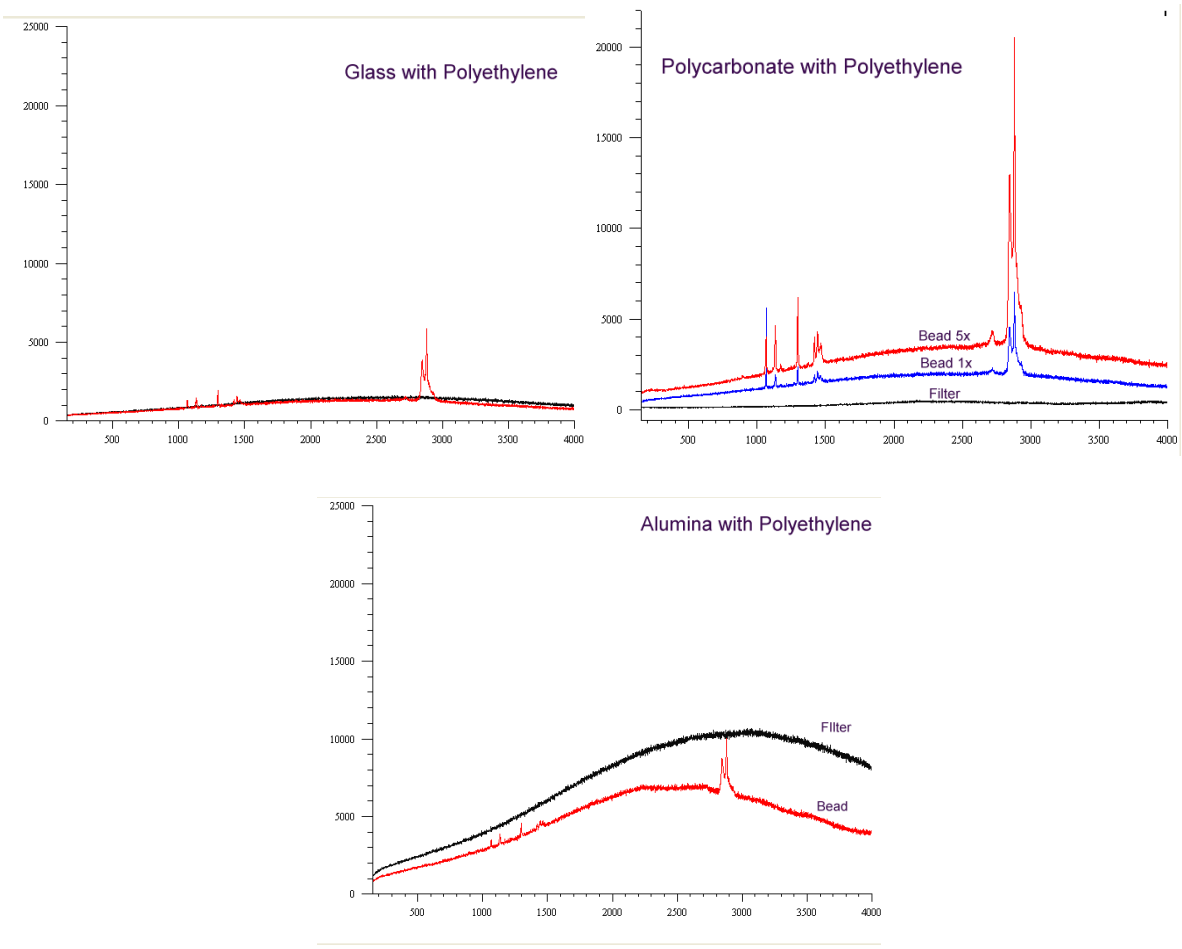

Appendix Figure 3.3: Raman signal of polyethylene on filters. A) Glass fiber filter with polyethylene bead. B) Polycarbonate filter with polyethylene bead. C) Alumina filter with polyethylene. Samples analyzed on 514 nm laser at 10% laser power for 10 seconds at 100x magnification. The black line in each is the laser reading from only the filter, with no plastic; the red line is the reading of a piece of plastic on top of the filter. The blue line in B is at 10% laser power and the red line is at 50% laser power.

The curve in the black filter baseline of Appendix Fig. 3.3c is the Raman signal of Alumina filters. The baseline of the polyethylene spectra (red line) is not flat in Appendix Fig. 3.3c as it is in Appendix Fig. 3.3a or Appendix Fig. 3.3b but also curves, proving that the Alumina filter's signal is interacting with the plastic's signal and causing background interference. The Rossman lab found the same interference results with polypropylene

plastic on GFF, polycarbonate, and Alumina filters. For this reason, all samples on all three cruises were taken on glass fiber filters (GFF) and polycarbonate filters, not Alumina filters.

On the Renishaw spectrometer at UCSD, both nurdles and shavings gave good readings that were compared to the Rossman lab and literature values (Allen et al. 1999, Sato et al. 2002, Zettler et al. 2013) and could be identified down to size ~100 µm diameter (Appendix Fig. 3.4). Using Appendix Fig. 3.5 from Sato et al. (2002) (reproduced here), the subtle differences between HDPE and LDPE standards could be distinguished.

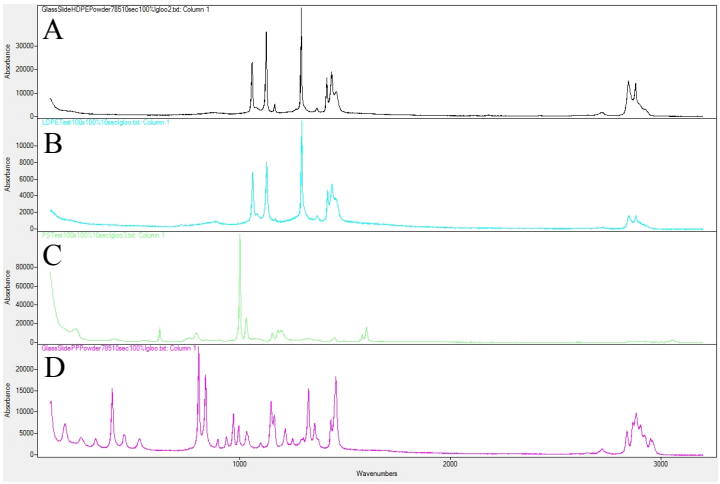

Appendix Figure 3.4: Standards of known plastics analyzed by Raman spectroscopy. A) high density polyethylene B) low density polyethylene C) polystyrene, D) polypropylene. 785 nm laser.

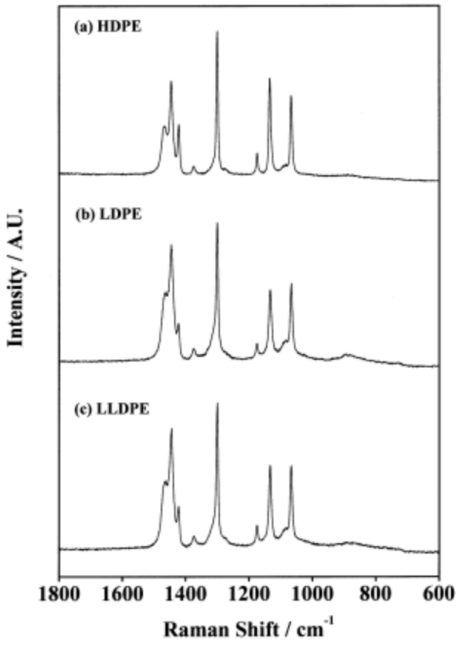

Appendix Figure 3.5: Representative Raman spectra of A) HDPE, B) LDPE, and C) LLDPE. Reproduced from Sato et al. 2002. HDPE – high density polyethylene. LDPE – low density polyethylene. LLDPE – linear low density polyethylene.

The samples from the Oahu beach were also identified to plastic type, and were identified down to ~100 μm diameter. There was blue beach plastic that was identified as polyethylene (PE) until it was too small (< 100 μm diameter); the small pieces did not give clear spectra. Rather they gave a high-sloped curve that had no distinct peaks except at 138 cm^{-1}. They did not show the doublet peak characteristic of PE at 2845 and 2880 cm-1 (Appendix Fig. 3.6c), or they showed the doublet peak at 2845 and 2880 cm^{-1} as the spectrum was being formed, but the doublet was washed out by the height of the peak at 1379 cm^{-1} (Appendix Fig. 3.6a). But once a slightly larger piece was in focus, the doublet peak could clearly be seen as the full PE spectrum formed (Appendix Fig. 3.6b). Thus, the lower size of a particle tested is limited in Raman spectroscopy. For the white beach plastic tested, the characteristic three peaks of polystyrene (PS) at 2700-3000 cm^{-1} were also very low compared to the rest of the peaks formed. This result may be due to a difference in that

piece's individual weathering or colorants that caused the spectrum to not look like a standard PS spectrum.

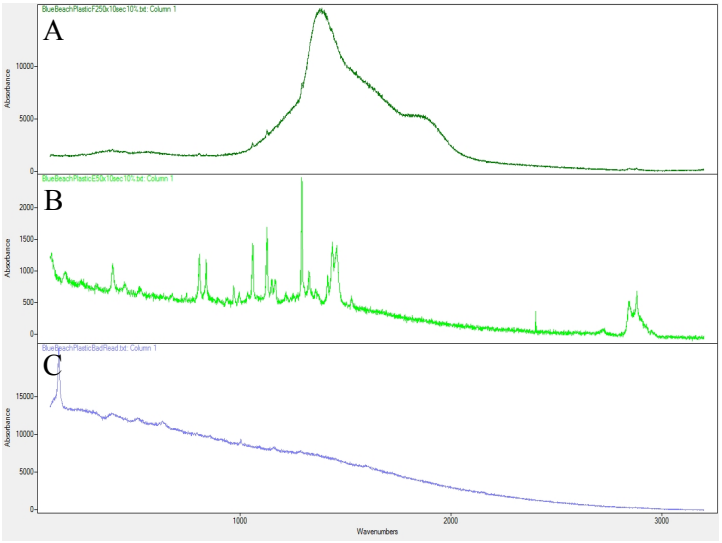

Appendix Figure 3.6: Blue beach plastic. A) A small piece of blue beach plastic that could be identified as PE until the 1379 cm^{-1} peak drowned out the 2845 and 2880 cm^{-1} doublet, B) a clear PE reading, C) a poor reading, with no legible doublet.

Oceanic samples

When analyzing the collected oceanic water samples on filters, multiple difficulties came into play. There were small amounts of salt and biomass all over the filters, as well as a significant amount of rust from the metal buckets used, even though the buckets were replaced often at sea to try to curtail the rust from entering the samples. Especially on the GFF filters from R/V *Falkor*, the rust was quite apparent. There were also black flecks on the samples that may be paint from the buckets. Paint is regularly observed in net and sediment samples from painted frames of nets and boat hulls, so boat and bucket paint chips should be expected (Turner et al. 2008). All of these substances (rust, salt, paint) interfered with Raman, but not with epifluorescence slides under immersion oil.

There were apparent plastic microfragments and microfibers on the filters when visually examining them at 20-50x magnification, but the aim of Raman is to confirm spectrally what we detect visually. The difficulty comes in the clarity of spectra that can be obtained from real world plastic of this size.

It was particularly difficult to obtain spectral readings of fibers, potentially due to their rounded exterior and the way the laser light reflects off of them. The fibers did not have any spectral peaks in the diagnostic region of 2700-3000 cm^{-1}, characteristic of the most common plastics: polypropylene (PP), PS, and PE. Nylon, acrylic, and polyester also have key peaks in that region, where the ocean samples were all flat at the baseline. They all had rising baselines, characteristic of fluorescence interference (Allen et al. 1999, Bocklitz et al. 2011). Dark fibers also produced thermal emission curves, similar in appearance to CCD emission curves (Appendix Fig. 3.1).

Some dark fragments burned under the laser, including a navy blue fragment that burnt under 10% and 1% laser light (Appendix Fig. 3.7a). This fragment had a unique spectrum that may have really been a reading of the burnt spot, not the intact navy blue "plastic" (Appendix Fig. 3.7b). One white, almost crystalline fragment curiously burnt under the laser as well; it burnt first at 100% laser power but also at 10% laser power (Appendix Fig. 3.8). Appendix Fig. 3.8's spectra are impossible to identify to plastic type because the thermal emission curves overpowered the spectra.

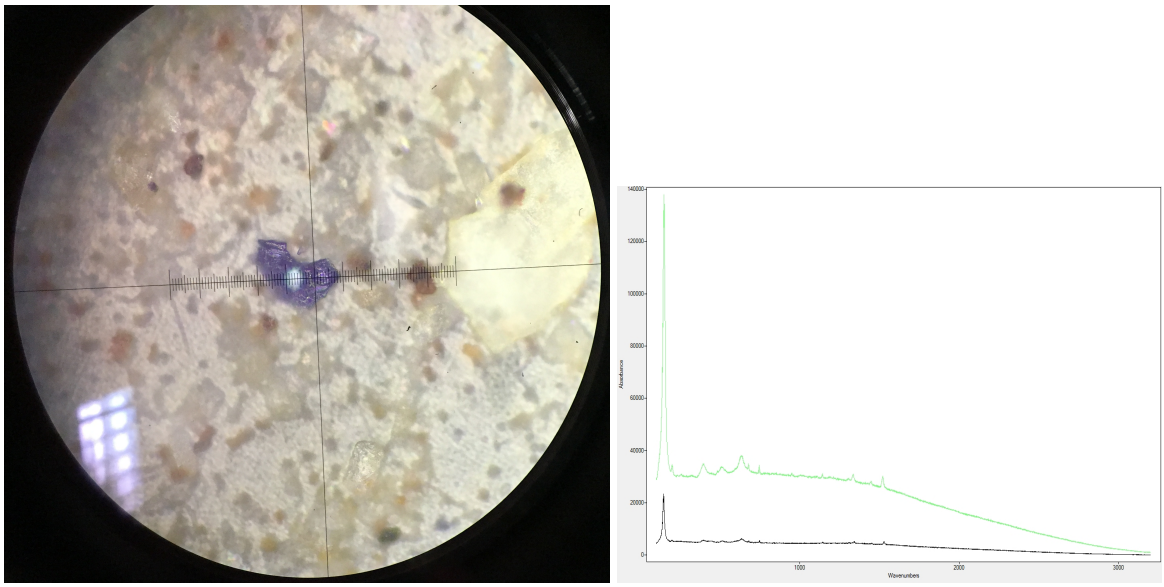

Appendix Figure 3.7: Navy blue fragment from North Pacific Subtropical Gyre, sampled on R/V *Falkor.* A) Photograph of the navy fragment, with the white spot indicating where the laser burnt the piece at 10% laser power; B) Navy fragment spectra. Green line is fragment's reading at 10% laser power, black line is fragment's reading at 1% laser power.

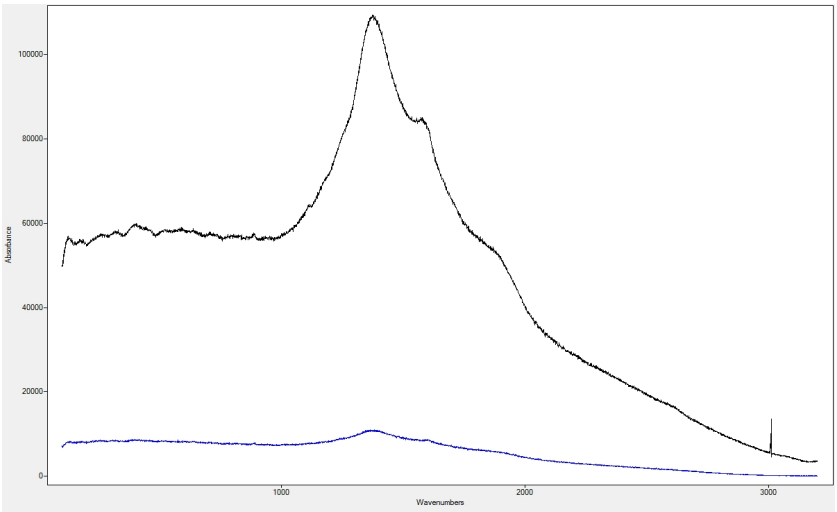

Appendix Figure 3.8: Burnt White Particle Spectra. Black line is particle's reading at 100% laser power for 90 seconds at 50x magnification; blue line is particle's reading at 10% laser power for 30 seconds at 50x magnification.

One particle out of 32 tested in the oceanic samples gave a good enough reading to be identified – it was polyethylene plastic. It was a fragment of opaque white plastic with a relatively smooth surface, measuring 64 x 88 µm (Appendix Fig. 3.9a). Comparing its spectrum to the standards in Appendix Fig. 3.2 and Appendix Fig. 3.3, it was determined to be high density polyethylene (Appendix Fig. 3.9b).

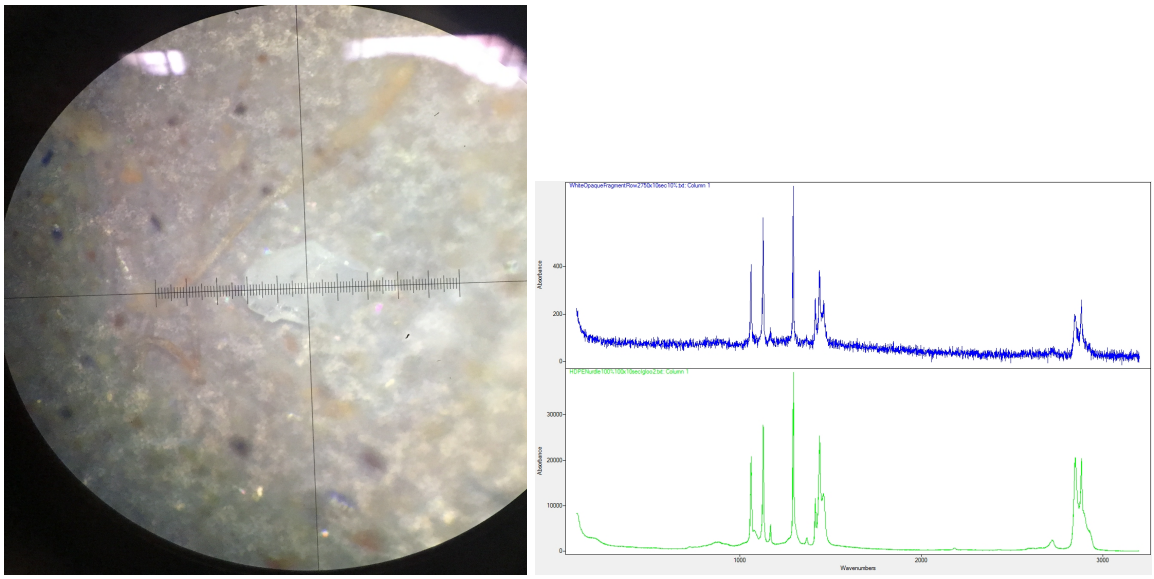

Appendix Figure 3.9: White plastic particle from North Pacific Subtropical Gyre, sampled on R/V *Falkor.* A) photograph of piece at 50x magnification, piece directly under crosshairs of microscope. B) top (blue) is white oceanic plastic's spectrum and bottom (green) is standard spectrum of known HDPE (a preproduction nurdle).

Discussion

Standards and beach plastics

Moderate success was found by modifying traditional Raman spectroscopy techniques to improve the readings of the small plastic standards and beach plastics. For a very fluorescent reading, a longer running time on each spectrum (the "drench and quench" method to reduce fluorescence) moderately cleaned the reading, but would not totally flatten the baseline. If a particle was really plastic, one technique that worked was to watch the spectrum form in real time like in Appendix Fig. 3.4a and Appendix Fig. 3.5b; the diagnostic

spectral region was often quite obvious before some higher peak formed and caused it to be drowned out. Most analysis software, like the post-processing eFTIR, can truncate a scan to just the region of interest. But this does not always make the spectrum as clear as viewing the entire spectral range, because it amplifies the white noise shown in Appendix Fig. 3.1. Post-processing software like eFTIR also allowed me to flatten the baseline or crop the spectra after processing to make the diagnostic peaks clearer. For a peak with a large thermal emission curve, running a sample with less laser power is advised for a long time (the "drench and quench" method), so I ran samples for a relatively long time (30 sec per scan) on low laser power (10%) to attempt to get clear readings.

All of these modifications allowed me to identify known standards and unknown beach plastics to type. The beach plastic was much larger than the plastic in the oceanic samples however, and it was obvious that it was plastic; it could also only be identified to type until the plastic reached a minimum size.

Oceanic samples

Oceanic plastic, mixed in with filtered seawater and biomass, provided more of a real-world test as to the effectiveness of Raman on identifying microplastics as plastic. There was much interference in reading the oceanic samples due to fluorescence, thermal emission, reflectance off the shiny fibers, and burning of particles. The same particle would be read multiple times and not give consistent results, most likely due to an issue with focusing on the particle (Everall 2008), or the laser's thermal emissions causing changes to the particle's morphology and thus the Raman position (Markwort and Kip 1996). One way this can be overcome is to utilize a scanning Raman laser, because a static-beam laser cannot be run nearly as long or at as high of power without causing sample degradation (Markwort and

Kip 1996). Another method is to spin the sample rapidly to allow the heat of the laser to dissipate (Grasselli and Bulkin 1991). Otherwise the heat of the laser, especially when run at long intervals to limit fluorescence, can alter the sample's morphology.

Conclusions

Laser Raman spectroscopy works to identify clean plastics to type, and can identify very small pieces (~100 μm) to plastic polymer. However, when seawater is filtered, with all of the included biomass, rust, salt, and micro-marine debris, and then examined under a microscope and identified by Raman spectroscopy, the ability to accurately quantify how much plastic is present is relatively low. Not all dark plastic and particles can be identified to plastic type, because the laser either cannot read them or burns them, even at 1% laser power. Fibers, the vast numerical majority of assumed plastic particles observed, were very rarely able to give a good reading. Many particles had too much fluorescent interference to be read, including many abundant white crystalline particles that may have been biogenic, or may have been plastic. Raman can identify plastics down to a very small size, but only if they meet certain requirements of surface smoothness, color, width, and sheen. Thus the method can sometimes be useful in identifying microplastics, but as the one out of 32 particle success rate demonstrates, it cannot be used as a quantitative means to count or identify all microplastics. The utility of Raman spectroscopy was too low, even when all methodology was optimized, to properly quantify micro- and nanoplastics in seawater.

SECTION 2: FTIR MICROSCOPY:

Fourier Transform Infrared Spectroscopy (FTIR) has often been used in many microplastic studies to identify fragments to type, including 28 out of 43 studies reviewed in

Hidalgo-Ruz et al. (2012). ATR (Attenuated Total Reflectance) FTIR can be cost prohibitive (Hidalgo-Ruz et al. 2012) but works very well because it can identify irregularly shaped plastic that normal FTIR cannot, and requires no sample preparation – the sample can be read directly on the ATR crystal (Hidalgo-Ruz et al. 2012, Brandon et al. 2016). However, the plastics on the filters in this study were so small that FTIR microscopy, a FTIR machine equipped with a microscope, was needed to find all the plastics. A normal FTIR with no microscopy capacity could not find all particles. Micro-FTIR machines are rare, and adapting a normal FTIR to a micro-FTIR system is prohibitively expensive.

Molecular mapping by FTIR has recently been attempted to detect microplastics by scanning the surface of filters of sediment spiked with 150 μm polyethylene fragments, with a 61% fragment recovery rate of spiked plastic (Harrison et al. 2012, Hidalgo-Ruz et al. 2012), but was not attempted here.

Methods

We contacted the Lawrence Berkeley National Laboratory to use their micro-FTIR; their main concern was that the GFF and polycarbonate filters used for low Raman interference would cause FTIR interference. The filters were analyzed on an ATR-FTIR in the M. Sailor Lab at UCSD to determine if there was filter interference. When the laser interacted with the filter or glass slide first, it could not read anything else (Appendix Fig. 3.10). There is no diagnostic peak of PP or LDPE in Appendix Fig. 3.10b because the ATR crystal only reads the glass slide. When the filter was inverted on the ATR-FTIR apparatus, the laser hit the plastics first, the plastic reading was detected on that same side, and the plastic was identified. An ATR crystal allows the infrared beam and the detector to be on the same side of the particle, so it allows solid particles to be tested without any sample

preparation (PerkinElmer 2005).

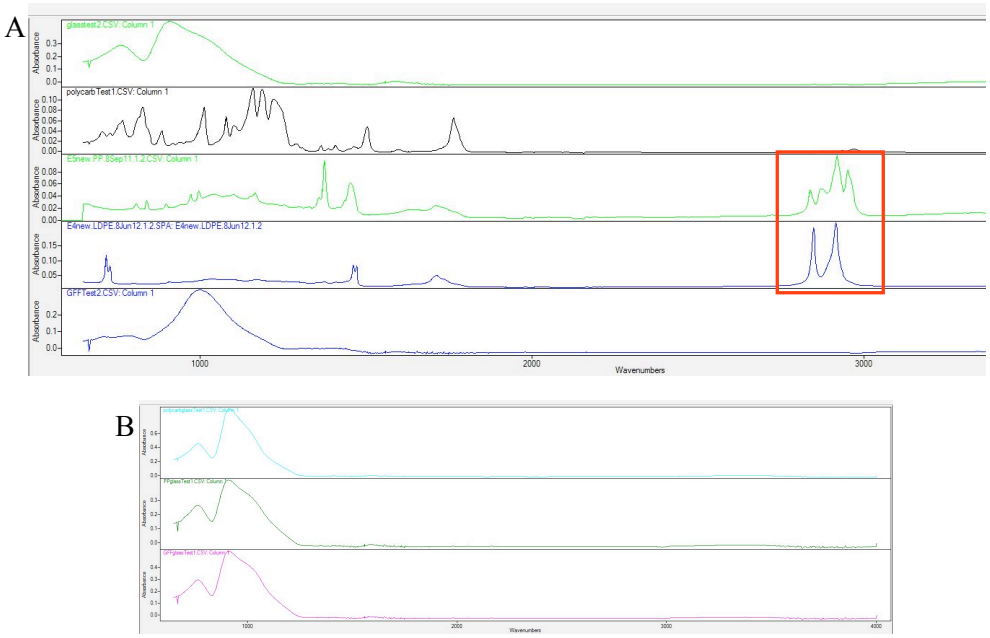

Appendix Figure 3.10: FTIR samples. A) Samples analyzed separately on FTIR-ATR crystal for pure reading – A1) glass slide, A2) polycarbonate filter, A3) Polypropylene, A4) Low density polyethylene, A5) GFF filter. Red rectangle – diagnostic peaks of plastic spectra. B) Readings on glass slide, glass slide in contact with ATR crystal first – B1) polycarbonate filter on glass slide, B2) PP on glass slide, B3) LDPE on glass slide.

There are currently two micro-FTIRs at the Lawrence Berkeley National Laboratory: the focal plane array microscope uses excitation from the bottom and detection from the top, and the synchrotron microscope in transmission mode has excitation from the top and detection from the bottom, both requiring filters that do not cause FTIR interference. Both machines were tested with our GFF and polycarbonate filters, and the filters did not give good readings. An addition of a germanium hemisphere could be added to either microscope for ATR imaging, but it is a destructive technique, due to the fact that the hemisphere has to touch the sample and when lifting off, some microplastics can be lost from the sample. When analyzing nanoplastics, loss of any microscopic particles could greatly affect the results.

Scientists at Lawrence Berkeley National Laboratory attempted to run the samples with the ATR hemisphere, however the 47 mm filters were much larger than anything they normally analyze. The focal plane array microscope has a sample region of 128 x 128 pixels, each pixel being 5 μm (Hans Bechtel, personal communication).

If pursuing FTIR microscopy, different filters should be used, though many are extremely expensive. High resistivity silicon filters work on micro-FTIR, as well as pure gold or silver, which are both IR- invisible. Silver 47 mm, 5 μm filters are ~$20/filter, which is not practical for high volume analysis. Gold membrane filters are very rare, but if in stock, 25 mm gold membrane filters are ~$36/filter. In general, metal substrates should be used for IR reflection measurements, and inorganic crystals for IR transmission measurements.

Another possibility is filter transfer, from polycarbonate filters at sea to sheets of pure gold or silver for the micro-FTIR. Filter-transfer-freeze was originally developed to transfer nanoplankton and other filtered material from a polycarbonate filter to a glass slide for light or fluorescence microscopy (Hewes and Holm-Hansen 1983). The results are best with fresh material, when the filters are still somewhat wet. This method does not have full recovery of filter material to slide, though phytoplankton suspensions transferred more than 90% of the material (Hewes and Holm-Hansen 1983). The method also causes a loss of randomness, which can affect cell/volume or plastics/volume counts. The filter-transfer-freeze technique would transfer all biomass with the nanoplastic, leading to noisy micro-FTIR readings. We did not pursue it for that reason, and because our samples were not fresh, and re-suspending the frozen samples would most likely have led to even lower filter material recovery.

Another technique of filter transfer involves actually dissolving the glass fiber filters

(GFF) used. Acid digestion of GFF filters is a technique regularly used for isotopic analysis (EPA 2012). 47 mm GFF filters can be dissolved in one hour by direct application of hydrofluoric acid; all siliceous deposits, such as diatoms, will be dissolved as well. Normal protocol includes dry-ashing the filter first in a 450°C muffle furnace, but this will destroy some plastics, as it is beyond their melting point (EPA 2012). This is a very dangerous procedure, and requires a good fume hood, great care for safety and proper safety gear, and using only Teflon labware that will not dissolve with HF acid or melt at the temperatures of the experiment (EPA 2012). There is also the potential of sonicating GFF filters in NaCl for a few hours, removing the filter, and then transferring the buoyant supernatant to an IR-optical substrate, although this was never attempted for this study.

Results

Shavings of pure preproduction nurdles of HDPE, LDPE, and PP were sent to Lawrence Berkeley National Laboratory to analyze on GFF and polycarbonate filters with a germanium hemisphere for FTIR-ATR images. Approximately a 700 μm x 700 μm area of filter could be analyzed at one time. However, each image took about 20 minutes to complete, so it would be prohibitively time-consuming to measure an entire filter, much less an entire cruise.

The FTIR with ATR was able to get FTIR spectra readings of all three sample plastics that matched literature values. Then these plastics were tested on both kinds of filters, using the germanium hemisphere ATR crystal. Readings were cleaner with a resolution of 8 cm^{-1} instead of 4 cm^{-1}. Appendix Fig. 3.11 displays the spectra for HDPE or LDPE on a GFF filter, utilizing the ATR hemisphere; the difference between the two plastics is the absence or presence of a tiny peak at 1377 cm^{-1} (Brandon et al. 2016), and the

difference is indiscernible here. The top panel of this figure is the 700 µm x 700 µm area of GFF filter being processed, with crosshairs at exactly the point where the FTIR spectrum (bottom panel) was recorded. This is a clean PE spectrum, very similar to the ones in Appendix Fig. 3.10.

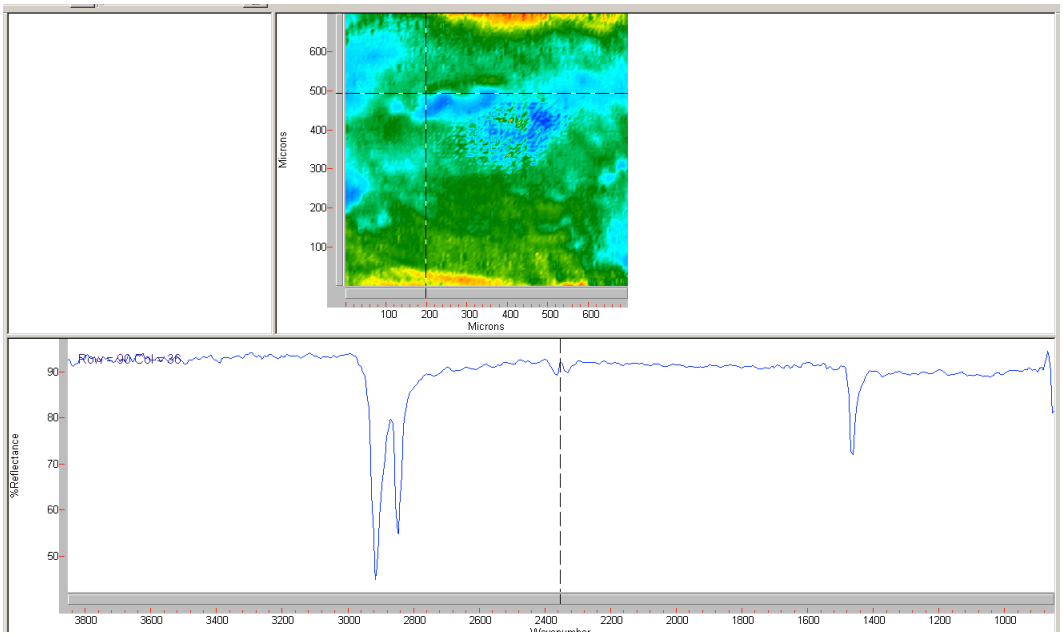

Appendix Figure 3.11: PE on GFF. Hemisphere ATR. Resolutions Pro software. Resolution- 8 wavenumbers. 128 scans.

Appendix Fig. 3.12 demonstrates that PP can also be read on GFF filters. However, Appendix Fig. 3.12a is a partial reading of PP and partial reading of GFF, which is illustrated in the large peak at 1000 cm^{-1} drowning out the diagnostic peaks of PP visible in the clean reading of Appendix Fig. 3.12b. Both images come from the same 700 µm x 700µm area of GFF filter, pictured, with the crosshairs in each image pinpointing where the spectral readings were taken.

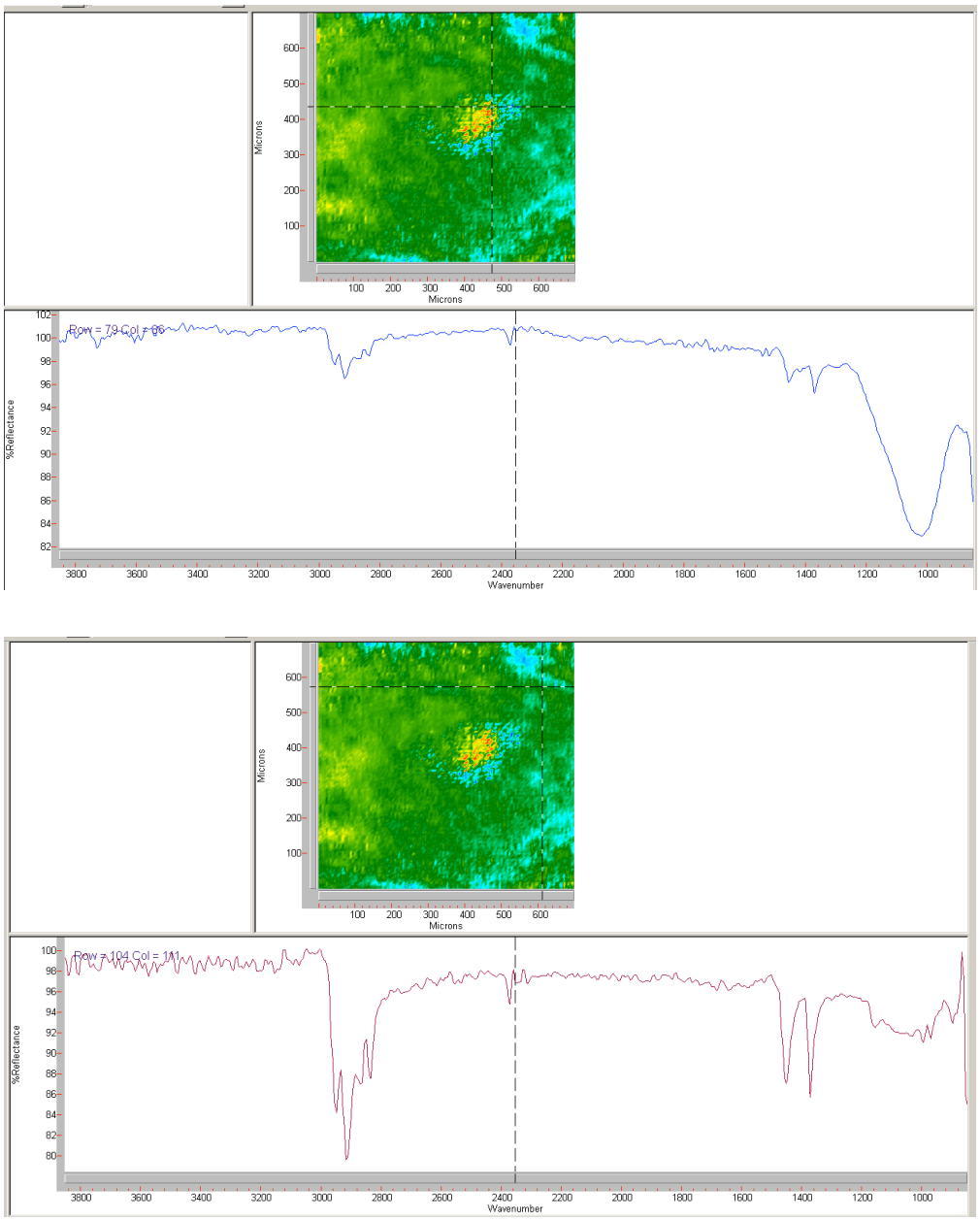

Appendix Figure 3.12: PP on GFF. Hemisphere ATR. Resolutions Pro software. Resolution- 8 wavenumbers. 128 scans. Spectra from same 700 µm x 700 µm sample, crosshairs designate where exact spectral reading occurred. A) Reading of PP (polypropylene) with GFF filter interference, B) Reading of PP with no filter effect.

The plastics also gave clean readings on polycarbonate filters with ATR (Appendix Fig. 3.13). Both images of Appendix Fig. 3.13 are from the same 700 µm x 700 µm area, pictured, with Appendix Fig. 3.13a reading the spectra of a minute piece of HDPE or LDPE

and Appendix Fig. 3.13b reading the spectra of PP. This illustrates that on a diverse sample, different plastics can be detected, even at nanoplastic sizes. However, this sample was just seeded with clean, dry plastic, and no biomass or "real world" seawater samples were ever tried on this method.

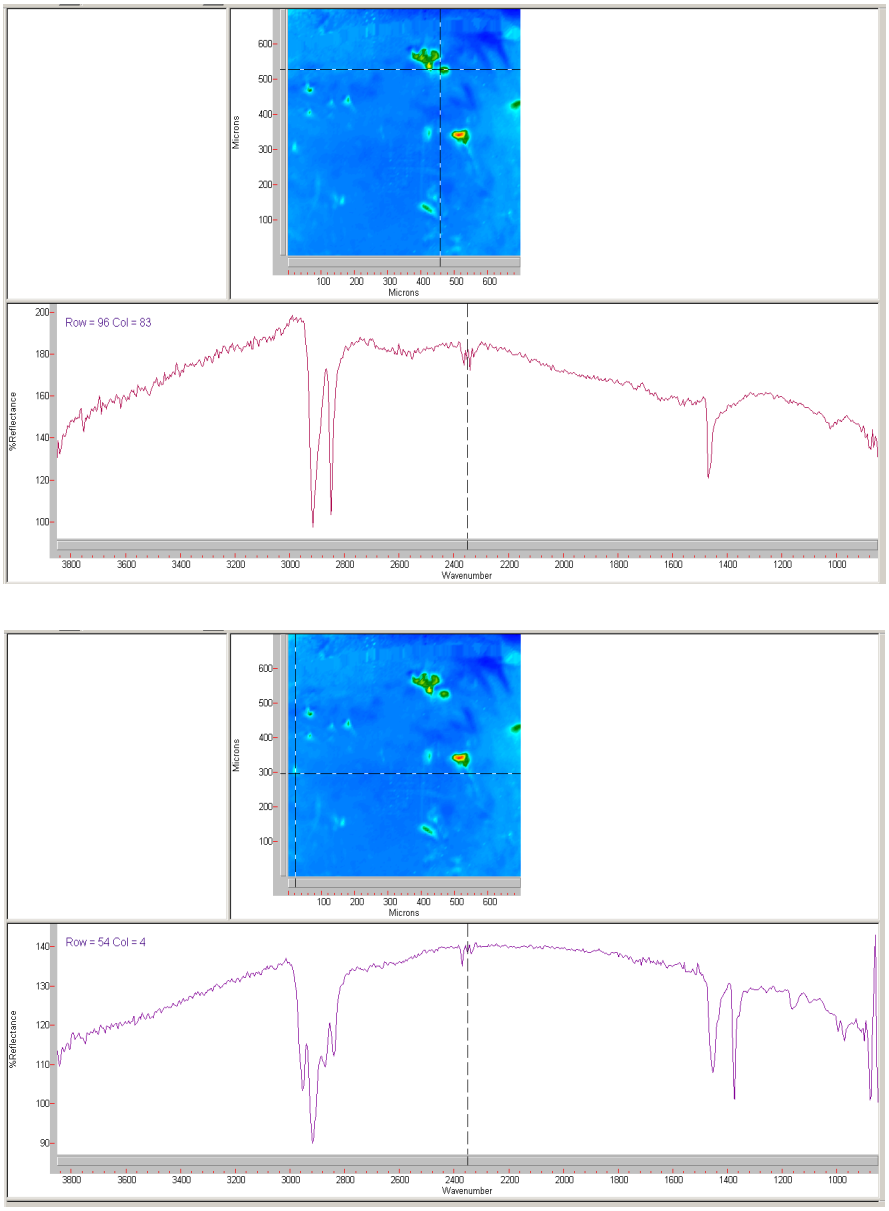

Appendix Figure 3.13: Plastics on polycarbonate filter. Hemisphere ATR. Resolutions Pro software. Resolution- 4 wavenumbers. 128 scans. Spectra from same 700 µm x 700 µm sample, crosshairs designate where exact spectral reading occurred. A) HDPE or LDPE on polycarbonate, B) PP on polycarbonate.

Conclusions

Micro-FTIR and focal plane array FTIR are very promising for microplastic work because they can sample very small particles and identify them to plastic type. FPA can also identify multiple different particles in one reading. However, the rarity of these instruments, the cost of their use, the cost of filters that can be used on these instruments without destructive ATR imaging, and the time it takes to properly get FPA images, all lead us to conclude that this method is not practical for high throughput sampling of large volumes of seawater. However, this method would work and be accurate to plastic type for very small sample volumes of nanoplastics.

SECTION 3: OTHER METHODS:

Many other methods have been suggested or attempted for imaging microplastics and nanoplastics. Electrostatic separation of plastics from sediments was extensively examined by R. C. Thompson and while it proved efficient in separating known plastics spiked into specific sediments, it was not advantageous in the separation of mixtures of polymers from diverse "real world" sediments and organic matter (Hidalgo-Ruz et al. 2012).

Plastics have been imaged for physical degradation with SEM (scanning electron microscopy), but SEM can only image the surface of particles, not diagnose the composition of the plastic (Murray and Cowie 2011, Zettler et al. 2013). SEM-EDX (scanning electron microscopy with energy dispersive X-ray spectroscopy), where EDX is used for detailing the elemental analysis of compounds, was used by Eriksen et al. (2013) to identify what visually looked like microplastics as, in fact, coal fly ash. However, SEM-EDX is not a good option for identifying plastics to type because of the kind of data it produces. It is very poor at

differentiating hydrocarbons, since the EDX spectrum measures the amount of each element present, and hydrocarbons, including plastics, are made up of a majority of hydrogen and carbon atoms. Every kind of plastic would have very high carbon spikes, and similar spikes denoting their similar additives.

A common chemistry technique for reading the IR spectra of powders is making KBr (potassium bromide) pellets. This method is easy and cheap, but answers a different question than attempted in this chapter; it would provide the bulk IR spectrum of the entire sample, not each individual particle. But FTIR spectra are additive, so it would be possible to separate the PE and PP spectra from each other (Mark Reineke, personal communication). This method would require dessicating samples into powder first, so would also require removing them from their at-sea filters.

FUTURE RECOMMENDATIONS:

The metal buckets were part of the problem for Raman, releasing paint chips and rust onto the slides. These were not as much of a problem with epifluorescence microscopy; salt was also not a problem under immersion oil, as it was under Raman microscopy. A glass bucket or filtering device is recommended for future water sampling procedures, to eliminate all rust. And the shed fibers from net sampling would also not be a concern with a glass sampling apparatus.

It is possible that not all microplastic is removed from the aluminum foil wrapper when it is rinsed with Milli-Q water. It also introduces a new source of metallic particles as the filters were not always fully dry when wrapped in aluminum foil at sea. In the future, we recommend mounting the filters immediately onto glass slides with immersion oil so that

there is no loss of microplastics with the aluminum foil, and so there is no addition of rust to the slides.

ACKNOWLEDGEMENTS:

The research on R/V *Falkor* was funded by generous donated ship time from the Schmidt Ocean Institute. Thank you to CCE-LTER for funding SKrillEx I and UC Ship Funds for funding SKrillEx II. Thank you to Dr. George Rossman for the preliminary Raman work. Thank you to Dr. Mike Sailor and Nicole Chan for all the assistance and access to the Raman. Thank you to Dr. Hans Bechtel and Flavia Sannibale for their assistance with the micro-FTIR. Natasha Gallo collected the Oahu beach plastics tested on the Raman. Dr. Lihini Aluhiware and Dr. Farooq Azam provided much-needed chemistry advice and guidance.

Chapter 3, in part is currently being prepared for submission for publication of the material. Brandon, Jennifer; Freibott, Alexandra. The dissertation author was the primary investigator and author of this material.

REFERENCES:

Allen, V., J. H. Kalivas, and R. G. Rodriguez. 1999. Post-consumer plastic identification using Raman spectroscopy. Applied spectroscopy **53**:672-681.

Bocklitz, T., A. Walter, K. Hartmann, P. Rösch, and J. Popp. 2011. How to pre-process Raman spectra for reliable and stable models? Analytica chimica acta **704**:47-56.

Bowley, H. J., D. L. Gerrard, J. D. Louden, G. Turrell, D. J. Gardiner, and P. R. Graves. 2012. Practical Raman Spectroscopy. Springer Science & Business Media.

Brandon, J., M. Goldstein, and M. D. Ohman. 2016. Long-term aging and degradation of microplastic particles: Comparing *in situ* oceanic and experimental weathering patterns. Marine Pollution Bulletin **110(1)**:299-308.

Browne, M. A., P. Crump, S. J. Niven, E. Teuten, A. Tonkin, T. Galloway, and R. Thompson. 2011. Accumulation of microplastic on shorelines woldwide: sources and sinks. Environmental science & technology **45**:9175-9179.

DiraMED. Raman Applications. Research of non-invasive Raman spectroscopy based diagnostic systems and application to medical and narcotic screening, monitoring, and therapeutic treatment of substances *in vivo.* *http://www.diramed.com/raman_applications.html*

EPA, U.S. 2012. Rapid method for acid digestion of glass-fiber and organic/polymeric composition filters and swipes prior to isotopic uranium, plutonium, americium, strontium, and radium analyses for environmental remediation following homeland security events. *in* Office of Air and Radiation, editor. U.S. Environmental Protection Agency, Montgomery, AL.

Eriksen, M., S. Mason, S. Wilson, C. Box, A. Zellers, W. Edwards, H. Farley, and S. Amato. 2013. Microplastic pollution in the surface waters of the Laurentian Great Lakes. Marine Pollution Bulletin **77**:177-182.

Everall, N. 2008. The influence of out-of-focus sample regions on the surface specificity of confocal Raman microscopy. Applied spectroscopy **62**:591-598.

Grasselli, J. G., and B. J. Bulkin. 1991. Analytical Raman Spectroscopy. Wiley.

Harrison, J. P., J. J. Ojeda, and M. E. Romero-González. 2012. The applicability of reflectance micro-Fourier-transform infrared spectroscopy for the detection of synthetic microplastics in marine sediments. Science of the Total Environment **416**:455-463.

Hewes, C. D., and O. Holm-Hansen. 1983. A method for recovering nanoplankton from filters for identification with the microscope: the filter-transfer-freeze (FTF) technique. Limnology and Oceanography **28**:389-394.

Hidalgo-Ruz, V., L. Gutow, R. C. Thompson, and M. Thiel. 2012. Microplastics in the marine environment:A review of the methods used for identification and quantification. Environmental science & technology **46**:3060-3075.

Markwort, L., and B. Kip. 1996. Micro‐Raman imaging of heterogeneous polymer systems: General applications and limitations. Journal of Applied Polymer Science **61**:231-254.

Murray, F., and P. R. Cowie. 2011. Plastic contamination in the decapod crustacean *Nephrops norvegicus* (Linnaeus, 1758). Marine Pollution Bulletin **62**:1207-1217.

PerkinElmer. 2005. FT-IR Spectroscopy Attenuated Total Reflectance (ATR).*in* Perkin Elmer Life and Analytical Sciences, http://www.perkinelmer.com.

Potgieter‐Vermaak, S., B. Horemans, W. Anaf, C. Cardell, and R. V. Grieken. 2012. Degradation potential of airborne particulate matter at the Alhambra monument: a Raman spectroscopic and electron probe X‐ray microanalysis study. Journal of Raman Spectroscopy **43**:1570-1577.

Sato, H., M. Shimoyama, T. Kamiya, T. Amari, S. Šašic, T. Ninomiya, H. W. Siesler, and Y. Ozaki. 2002. Raman spectra of high‐density, low‐density, and linear low‐density polyethylene pellets and prediction of their physical properties by multivariate data analysis. Journal of Applied Polymer Science **86**:443-448.

Socrates, G. 2004. Infrared and Raman characteristic group frequencies: tables and charts. Third Edition. John Wiley & Sons, Ltd., Chichester, England.

Turner, A., S. Fitzer, and G. A. Glegg. 2008. Impacts of boat paint chips on the distribution and availability of copper in an English ria. Environmental Pollution **151**:176-181.

Van Cauwenberghe, L., A. Vanreusel, J. Mees, and C. R. Janssen. 2013. Microplastic pollution in deep-sea sediments. Environmental Pollution **182**:495-499.

Zettler, E. R., T. J. Mincer, and L. A. Amaral-Zettler. 2013. Life in the "plastisphere": microbial communities on plastic marine debris. Environmental science & technology **47**:7137-7146.

CHAPTER 4: Consumption of Microplastics by Salps *in situ*

Jennifer Brandon

ABSTRACT:

Salps were collected in the nearshore Southern California Bight, as well as the California Current out to the North Pacific Subtropical Gyre. They were dissected for gut content analysis by epifluorescence microscopy to analyze the amount of nanoplastics ingested *in situ*. Every salp examined had ingested nanoplastics, regardless of species, life history stage, or oceanic region. Zooids from the aggregate life history phase had higher ingestion rates than solitary zooids. There was no significant difference in ingestion rates among regions. Salps ingested significantly smaller plastic particles than were available in ambient surface seawater.

Keywords: Microplastics, Salps, Epifluorescent Microscopy, California Current, North Pacific Subtropical Gyre

INTRODUCTION:

Nanoplastics

Marine debris is a growing issue of concern, as the abundance estimates of marine debris reach 5 trillion pieces (Eriksen et al. 2014) and a yearly oceanic input of 4.8-12.7 million tons (Jambeck et al. 2015). Although the appearance and effects of macrodebris (> 5 mm) are obvious, with macrodebris causing animal entanglements (Donohue et al. 2001, Henderson 2001, Schlining et al. 2013), ingestion (Derraik 2002), and forming a rafting substrate for invasive species (Goldstein et al. 2014, Carlton et al. 2017), the numerical majority of marine debris is microdebris, or plastic smaller than < 5 mm (Hidalgo-Ruz et al.

2012, Goldstein et al. 2013). Microdebris, and especially the newly considered subcategory of nanodebris (< 333 μm), although numerically abundant, is highly undersampled, due to methods previously employed to sample marine debris (Lozano and Mouat 2009, Van Sebille et al. 2015, Brandon and Freibott 2017).

Nano- and microdebris can be even more deleterious to marine organisms than macrodebris (> 5 mm) because small particles and fibers can be ingested by many suspension-feeding animals (Thompson et al. 2004, Goldstein and Goodwin 2013, Wright et al. 2013). Nanoplastics (0-333 μm) are the size range of particles ingested by many suspension-feeders, including salps, copepods, mussels, clams, appendicularians, and echinoderm larvae (Wilson 1973, Harbison and McAlister 1979, Hart 1991, Defossez and Hawkins 1997, Browne et al. 2008, Katija et al. 2017). If plastics are ingested by animals like zooplankton, they have the potential to bio-accumulate in the food web into larger organisms, along with adsorbed persistent organic pollutants and the harmful chemical additives they contain (Ogata et al. 2009, Rochman et al. 2013b, Jang et al. 2016). Plastics are rarely just a simple hydrocarbon chain; the plastic debris being consumed in the ocean often incorporates bisphenol A (BPA), phthalates, plasticizers, colorants, flame retardants and other compounds that can enter the food web and accumulate in animal tissue (Browne et al. 2013, Rochman et al. 2013b, Jang et al. 2016). Plastics are hydrophobic, and as such can sorb polyaromatic hydrocarbons (PAHs), PCBs, and other persistent, bioaccumulative, and toxic substances (PBTs) from the atmosphere and ocean, which can become bioavailable once consumed (Ogata et al. 2009, Browne et al. 2011, Rochman et al. 2013b). There are unknown food web consequences if the base consumers are ingesting large amounts of synthetic plastic.

Although studies have demonstrated uptake of plastic particles by suspension-feeding organisms in simplified laboratory settings (e.g., doliolids, bivalve larvae (Cole et al. 2013), coral polyps (Hall et al. 2015), mussels (Browne et al. 2008)), results demonstrating ingestion of microplastics by planktonic suspension-feeders *in situ* are sparse (e.g., appendicularians fed microplastics *in situ*, Katija e al. 2017). Suspension-feeders have the potential to be especially affected by micro- and nanoplastic because some species are relatively non-selective feeders and can ingest a significant amount of inorganic material (Moore et al. 2001).

Salps

Salps are pelagic, holoplanktonic tunicates (Govindarajan et al. 2011). Salps display alternation of generations, between a solitary form, which asexually produce hundreds of genetically identical blastozooid aggregates, and an aggregate form, where each aggregate sexually reproduces one oozooid (Madin 1974, Bone 1998). Both forms are pelagic and are of equal importance in the lifecycle (Bone 1998).

Salps are observed mainly in the open ocean, down to 1500 m (Bone 1998). The highest species richness is observed in tropical and temperate waters (Yount 1958, Van Soest 1975, Harbison and Campenot 1979, Bone 1998). Many salps remain in surface waters, but some are known to vertically migrate on a diel cycle (Harbison and Campenot 1979).

In the California Current System, some species, (*Salpa aspera, S. fusiformis, Thalia democratica*, *Ritteriella picteti*, and *Iasis zonaria)* are persistently present, regardless of the ocean temperature and circulation in the region. Other, cool-phase salps (*Salpa maxima, Pegea socia, Cyclosalpa bakeri,* and *C. affinis*) were common in the California Current from

1951 to 1976, but were virtually absent from those waters from 1977 until 2001, when *C. bakeri* and *C. affinis* reappeared (Lavaniegos and Ohman 2003).

Salp swarms

Salps occasionally form large swarms that can develop rapidly. A single swarm of *Thalia democratica* off Southern California in 1950 covered 3500 square miles, with a density of 275 salps/m^3 to a depth of 70 m (Berner 1967, Madin 1974). In 10 years in the California Current, *T. democratica* swarms were reported 22 times (Berner 1967). The swarms, or blooms, of salps are due to a life cycle that is adapted to patchy, unpredictable food sources (Alldredge and Madin 1982). Although they only seem to be able to grow to swarm densities when there are above average phytoplankton stocks, salps may be able to remove all the available phytoplankton and deprive other grazers when they swarm (Alldredge and Madin 1982). Even multiple salp species are rarely seen simultaneously swarming in the California Current (Silver 1975, Silver and Bruland 1981, Alldredge and Madin 1982). The California Current experienced salp swarm years in 2012 (Smith et al. 2014) and again in 2014.

Feeding

Salps are filter-feeders, like other tunicates. They employ a mucus feeding net secreted by the endostyle (Madin 1974). The net is made of regular, rectangular mesh (Bone et al. 2003). Salps both feed and swim using circumferential muscle bands along with inhalant and exhalent muscular valves (Madin 1974). Unlike doliolids, which have separated the motions, salps cannot eat without swimming (Alldredge and Madin 1982). All water passing through the inhalant opening must be filtered through the mucous net and Harbison

and McAlister (1979) argue this may be the cause of the upper limit of the mucous net mesh size – it cannot be so fine that the salp cannot maintain locomotion.

Salps feed at a constant rate regardless of food concentration (Harbison and McAlister 1979, Alldredge and Madin 1982), thus at high concentrations, their nets can clog. Harbison et al. (1986) found that *P. confoederata* clogging never occurred at < 0.5 ppm particle concentration and occurred every time concentrations were > 5.0 ppm. Though it is often assumed that net clogging leads to mortality, Madin and other studies documented a renewal of nets after clogging (Madin 1974, Alldredge and Madin 1982).

Salps are generalist, omnivorous feeders (Silver 1975, Vargas and Madin 2004). The diameter of the esophagus is the apparent upper constraint on particle size (Madin 1974). Madin (1974) witnessed some particles 1 mm or larger deflected from the inhalant valve opening by turbulence. Although many papers have reported that salps cannot graze on particles below 2 μm, Vargas and Madin found that *T. democratica* and *C. affinis* can graze on particles below 1 μm and fecal pellets have been found to contain particles ranging from < 1 μm to approximately 1 mm (Madin 1974, Vargas and Madin 2004). Experiments have shown that salps are able to efficiently (100%) retain particles above 4.6 μm (Harbison and McAlister 1979, Caron et al. 1989). Sutherland et al. (2010)'s model predicts that particles down to 0.05 μm could be caught on filtering nets by direct interception. As individual salps increase in length, the size of the smallest particle obtained with 100% efficiency also increases (Harbison and McAlister 1979, Kremer and Madin 1992).

Fecal pellets

Salp fecal pellets are relatively large and sink up to 2700 meters per day, which is at least an order of magnitude faster than most copepod pellets (Bruland and Silver 1981).

Salps produce large quantities of fecal matter (Silver and Bruland 1981, Alldredge and Madin 1982, Madin 1982), their pellets stay relatively intact as they travel to the deep sea (Small et al. 1979, Bruland and Silver 1981, Caron et al. 1989), and salp swarms lead to large pulses of pellets. All of these factors suggest that salp fecal pellets, especially during a salp swarm, significantly affect the deep sea ecosystem beneath them (Alldredge and Madin 1982), and these fecal pellets have been shown to have a significant role in the deep sea carbon cycle (Stone and Steinberg 2016). If these pellets include microplastics, they could have important ecological effects on the benthos.

Salp tunics

Not until recently did people start considering mechanisms beyond fecal pellets as the method of transfer of salp-derived organic matter to the deep sea. After salps die, their entire tunics can sink to the benthos. Henschke et al. (2013) examined a 30-year trawl and video data series in the Tasman Sea and found that salps fell to the seafloor year round, but that they could pulse to a maximum density of 408 individuals 1000 m^{-2}, with *Thetys vagina* carcasses sometimes making up 48% of the total fauna observed. Salps and pyrosomes exceeded 100 t km^{-1} wet weight in approximately half of the years (Henschke et al. 2013). Smith et al. (2014) observed salp tunics covering 98% of the seafloor in images from June to July 2012, right after a significant swarm in surface waters (Smith et al. 2014). Stone and Steinberg (2016) found that salp fecal pellets contributed, on average, 78% of salp carbon transport, but that respiration at depth by diel vertically migrating salps and sinking salp carcasses contributed the rest of the carbon budget. They also found that different species were higher contributors to the carbon flux than others, with *Thalia democratica* contributing the most carbon flux in their North Atlantic study site.

Salps and Nanoplastics

Salps are generalist feeders that can ingest particles from < 1.0 μm to ~1.0mm, and they primarily reside in surface waters, where they cannot swim without also eating. The most abundant microplastics are nanoplastics, sizes < 333 μm, in concentrations of 5,000-15,000 particles/L in surface waters of the California Current (Brandon and Freibott 2017, chapter 3 above). Salps' consumption of these abundant nanoplastics is likely, but studies that have shown *in situ* ingestion of microplastic by zooplankton are rare (Carpenter and Smith 1972, Desforges 2015). Although many plankton species will consume microplastic when fed it in laboratory studies (Wilson 1973, Frost 1977, Ayukai 1987, Cole et al. 2013), the ecologically significant question lies in whether they are ingesting such particles *in situ*. Furthermore, although the abundance of microplastics are high (Law et al. 2010, Cózar et al. 2014, Eriksen et al. 2014, Law et al. 2014), they are actually 1-3 orders of magnitude smaller than modeled input studies (Cózar et al. 2014, Jambeck et al. 2015). Salps could be a key link in connecting the modeled and measured inputs, because the measured abundance estimates are only for buoyant plastics, and salps' fast-sinking fecal pellets and tunics could be a vector of surface plastic to the deep sea.

This study addresses three questions: are salps ingesting nanoplastics *in situ*? Is ingestion directly proportional to the concentration of ambient nanoplastic available in surface water? And, if consumed, does the size distribution of ingested particles reflect the size distribution of available plastic particles?

MATERIALS AND METHODS:

Field Collection

Since this study aimed to answer how much nanoplastic salps are ingesting *in situ*, salps were analyzed from areas where the nanoplastic abundance in the surface water was already known (Brandon and Freibott 2017, chapter 3 above). In July 2014, SKrillEx I sampled the nearshore California Current over Nine Mile Bank. Bongo tows (plankton net samples) were taken in nightly transects for zooplankton abundance, along with surface bucket tows to analyze the surface nanoplastic concentration via epifluorescence microscopy (Brandon and Freibott 2017). The bongo nets were 202 μm mesh, towed to approximately 200 m depth, with samples then preserved in 5% formaldehyde buffered with sodium tetraborate. SKrillex II occurred in June 2015 and repeated the same bongo measurements in the same area. SEAPLEX zooplankton samples were also analyzed; those samples were taken by manta net, 333 μm mesh, towed for 15 minutes at the surface in August 2009, and then preserved in 5% formaldehyde buffered with sodium tetraborate.

Figure 4.1a shows the open ocean salp samples. When possible, only night samples were examined, because some salps display diel vertical migration (Harbison and Campenot 1979) and so would be more prevalent and be expected to ingest more at night.

Figure 4.1b shows the nearshore Southern California Bight samples that were sampled for salps in this study. Salps were abundant in this region in 2014. All samples from SKrillEx II (2015) were examined for salps, but there were no salps present that year in the bongo samples.

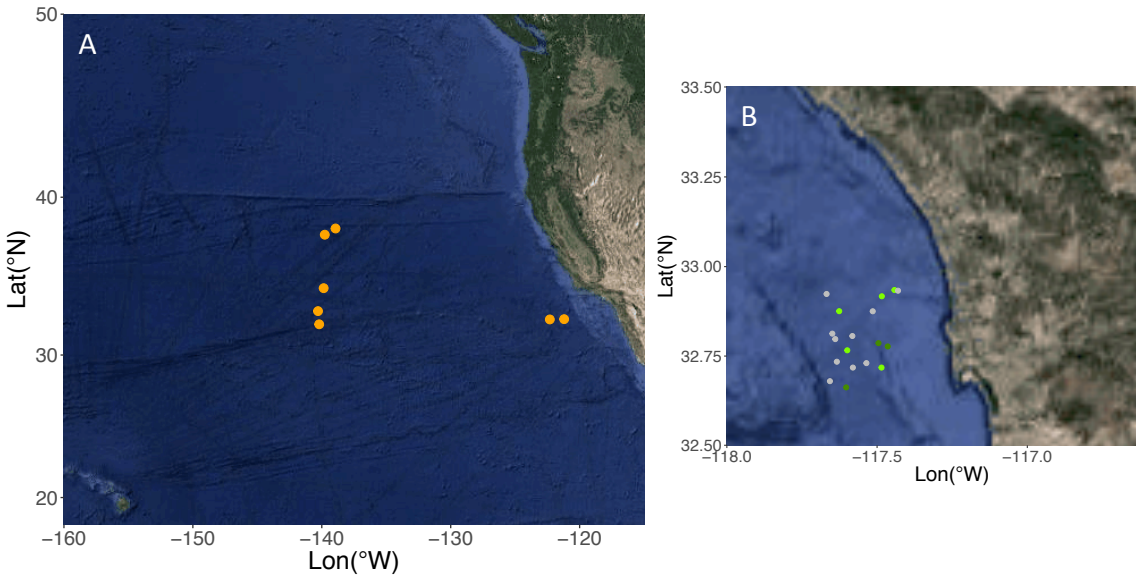

Figure 4.1: Salps sampled for plastic ingestion by epifluorescent microscopy. a) Open ocean samples. Orange=SEAPLEX manta tows (August 2009). b) Nearshore samples. SKrillEx I (July 2014). Bright green=10 salps sampled, Dark green= < 10 salps sampled, Grey=no salps in sample.

Salp Dissections

Salps were removed from preserved samples. Ten salps from each sample were removed, unless there were less then 10 salps present. All other plankton affixed to the outer tunic of the salp were removed and replaced in the sample jar. For SKrillEx I and II, the port side of the bongo tows was examined for salps; for SEAPLEX there was only one sample per tow.

Salps were identified to species, measured for zooid length, and life history phase noted (solitary or aggregate). Species identifications were done by expert opinion by Linsey Sala based on literature characteristics (Fraser 1947, Yount 1954, Van Soest 1974, 1975). The cruise, station number, species, and number of salps removed for analysis from each station are listed in Table 4.1.

The length of the stomach was measured, noted for degree of fullness, and dissected from each salp. It was also noted whether a fecal pellet could be seen forming at the end of the gut. Care was taken to cut above the top of the stomach so that no ingested material was released during dissection. Mucus nets and upper esophagus contents were not examined because any plastics found in these regions may have been consumed during net feeding or entered the salp's oral siphon while in the sample jar and might not reflect *in situ* consumption of nanoplastic.

The dissected salp guts were cut in half and placed in 15.0 mL of Milli-Q water for at least 24 hours to soften and release gut contents. The contents were then filtered onto a Whatman 47mm Nuclepore polycarbonate track-etched membrane filter with 5.0 μm pores using an additional 70 mL of Milli-Q water. The filtering apparatus was all glass, so the filter never came in contact with laboratory plastic, following the slide preparation methods of Brandon and Freibott (2017).

A small volume of Milli-Q water was added to promote a good seal to the sample filter (Freibott et al. 2014). The 47 mm filter was then mounted on a 50 mm glass slide with immersion oil on top, and two cover slips, 24 x 50 mm, No. 2 thickness, applied.

Epifluorescence Microscopy

Slides were analyzed for nanoplastics via epifluorescence microscopy (see Brandon and Freibott, 2017; chapter 3 above). No fluorochromes like DAPI or proflavin were added to the slides for epifluorescence analysis (Caron 1983, Kemp et al. 1993, Taylor et al. 2012), since living organisms were not the targets of the study.

Slides were analyzed at 200x magnification on a visual transect, using a Zeiss Axiovert 200M inverted compound microscope, equipped for epifluorescence microscopy

and driven by Zeiss Axiovision software. The stage, filter set, and focus drive were motorized to allow for slide navigation. The channels included a blue excitation/green long-pass emission filter set normally used to identify protein dyed with the fluorochrome proflavin (excitation wavelengths: 450–490 nm; emission: > 515 nm); a blue excitation/red emission filter set normally used for chlorophyll *a* (excitation: 465–495 nm; emission: 635–685 nm), a UV excitation/blue emission filter set normally used for DNA stained with DAPI (excitation: 340–380 nm; emission: 435–485 nm), and a green excitation/yellow-orange emission filter set, usually used for detecting phycoerythrin (excitation: 536–556 nm; emission: 550–610 nm (Pasulka et al. 2013).

Every plastic particle encountered down the center transect of the slide was enumerated, and the microscope stage was moved to manually measure its length and width. Then the stage was returned to center to continue the visual transect. Lengths and widths were recorded on a calibrated ocular micrometer. Width was manually measured at the widest point in the piece. Some of the pieces were not a consistent width, so the calculated surface areas are an overestimate. The intensity of perceived fluorescence was recorded on a qualitative scale for each particle in each channel because the plastics were being observed by the human eye (Brandon and Freibott 2017).

Brandon and Freibott (2017) determined plastic fluorescence of standard plastic and non-plastic reference materials on this same microscope (Table 3.1; Brandon and Freibott 2017). The six most common consumer plastics of various ages (Brandon et al. 2016) were tested, as well as additional industrial plastics. I also used Figure 3.3 from Brandon and Freibott (2017), a decision tree that outlines whether an object should be counted as plastic. Particles were counted if they looked like plastic on the transmitted light image and

fluoresced under the reflected light. Plastics, in general, looked like long, skinny fibers or flat fragments that had sharp, non-gelatinous edges, fluoresced uniformly, and did not have inner striations, coloration patterns, or areas suggestive of diatom chains, nuclei, etc. If particles were invisible on the transmitted light image but fluorescent, they were determined to be TEP and not counted (Samo et al. 2008). If they appeared like plastic on the transmitted light image, but were not fluorescent, they were still counted, because not all plastics fluoresce (Table 3.1; Brandon and Freibott 2017). Especially due to the presence of fluorescence due to salps' gut walls and ingested biogenic material that could sometimes overlap with the plastic, fluorescence was considered a secondary characteristic of plastic over shape and reflectivity under brightfield illumination. However, epifluoresence was still checked to make sure inner striations or patterns of diatom chains, etc. did not appear. When in doubt, particles were not counted as plastic. The thick gut walls of salps and ingested biogenic material most likely occluded some plastic as well, so the estimates in this paper are most likely underestimates of total plastic ingestion by salps.

Ingestion Rates

To calculate ingestion rate from the microscopy enumerations, counts were divided by gut clearance times from published studies. Gut clearance times in salps are understudied, likely because salps are hard to keep alive in laboratory experiments. The methods of Huskin et al (2003) were used here, who, noting the sparsity of gut clearance data, used the length-dependent turnover time of *Pegea confoederata*, measured by Madin and Cetta (1984), for multiple other species, but checked them against Madin and Kremer's unpublished turnover times for *Salpa fusiformis*. In addition, we used species-specific gut clearance times for *Iasis cyclindrica* and *Salpa fusiformis* from Madin and Cetta (1984) and Huskin et al. (2003) . Gut

clearance times ranged from 2.5-6.25 hours for salps in this study.

Ingestion Rates estimated from Clearance Rates

Ingestion rates (plastic particles individual^{-1} hour^{-1}) were also estimated from the product of salp clearance rates times ambient plastic concentrations. Species-specific clearance rates were mined from the literature (collected in Table 5.1, Bone 1998) for the clearance rate of seawater (in mL individual^{-1} hour^{-1}) for each salp measured. Those calculations are length-specific and specific to life history stage. For ambient nanoplastic particle concentrations, the nearest sampling station from Brandon and Freibott (2017) was aligned to each salp sampling station, to approximate ambient surface seawater nanoplastic abundance at that location.

RESULTS:

Salps

The species identified were: *Cyclosalpa affinis*, *Ritteriella retracta*, and *Salpa aspera* in the nearshore Southern California Bight, *Thalia democratica* and *Salpa fusiformis* from the California Current, *Iasis cylindrica*, *Ihlea punctata*, and *Rittriella retracta* in the transition region, and *Cyclosalpa bakeri*, *Cyclosalpa pinnata*, *Salpa fusiformis*, *Iasis cylindrica*, *Ihlea punctata*, *Salpa maxima*, and *Thalia democratica* in the North Pacific Subtropical Gyre.

Agreement Between Methods

A comparison of the two methods to estimate salp ingestion rates of plastic (i.e., microscopically identified prey divided by gut passage time vs. literature-derived clearance

rates times ambient plastic concentration) showed that assumptions of constant clearance rates greatly overestimated the rate of plastic ingestion (Fig. 4.2).

The highest ingestion rate seen in the epifluorescence microscopy-derived ingestion rates is 160 particles/hour, compared to 45,000 particles/hour from the clearance rate-derived approach. Figure 4.2 also shows little relationship between the methods. There is better fit for salps with low ingestion rates than high rates, and somewhat better for solitary than aggregate life history phases. However, the direct measures of ingestion by microscopy seem to saturate, while clearance-rate projected values suggest a continual increase in ingestion. Overall, there is poor agreement between the methods, hence direct ingestion as recorded by microscopy is used for the rest of the paper.

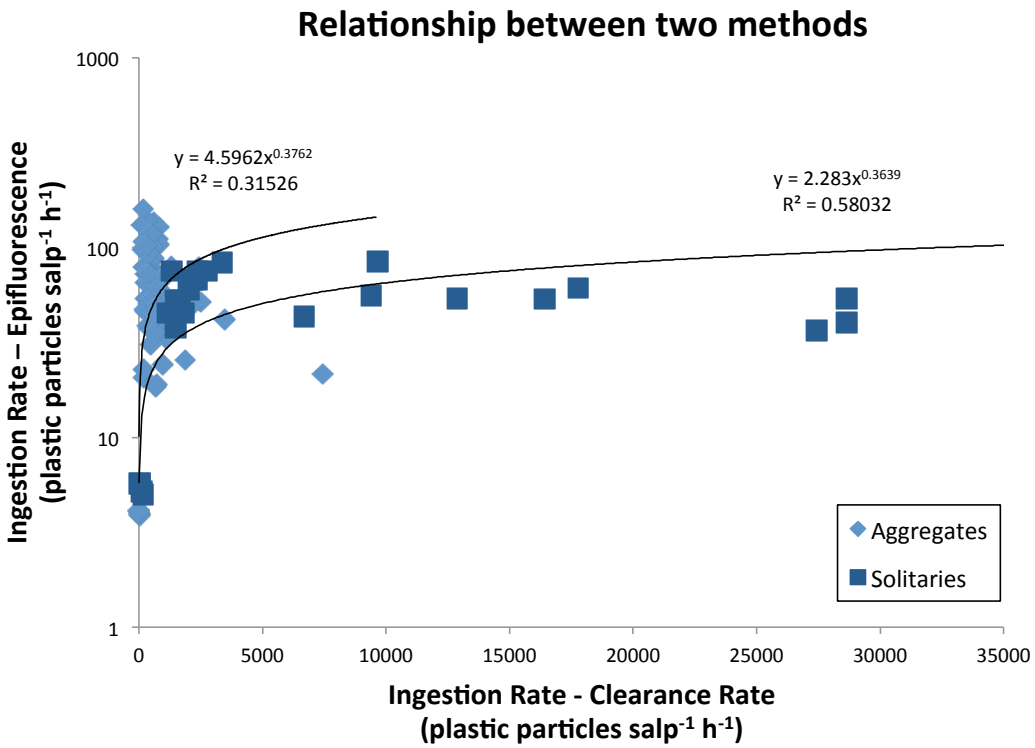

Figure 4.2: Relationship between two methods of calculating salp ingestion rate of plastic particles. Y-axis: Ingestion rate by epifluorescence microscopy of salp gut contents. X-axis: Ingestion rate estimated from published clearance rates.

Epifluorescence Ingestion Rates

Every single salp dissected had plastic in its gut.

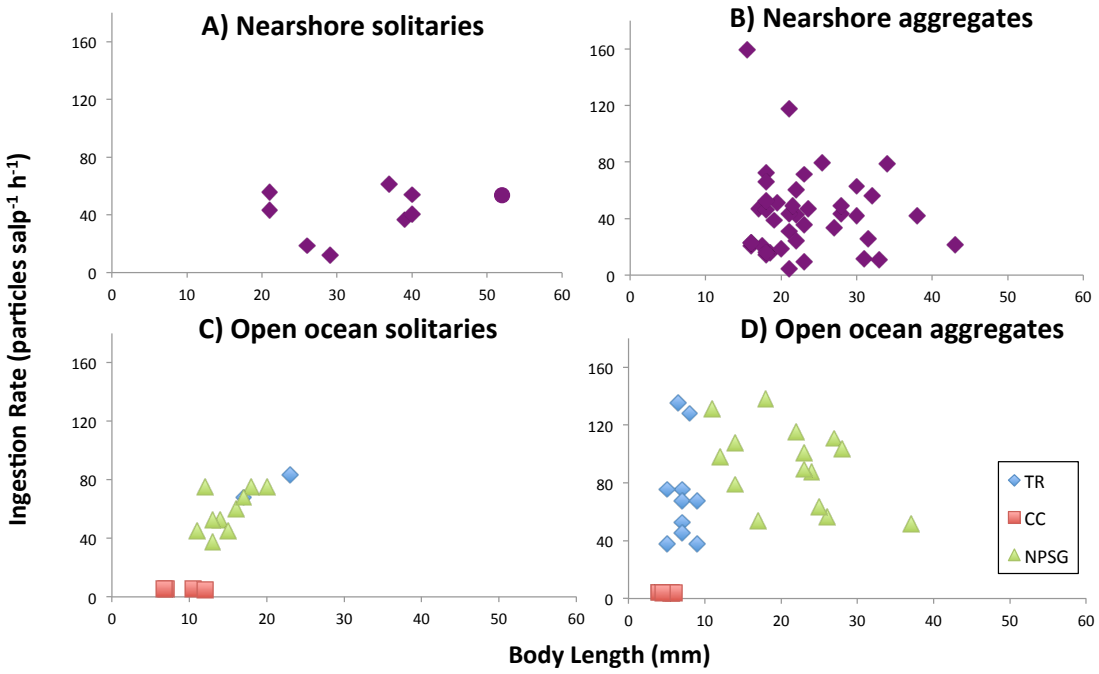

Figure 4.3: Ingestion rate vs. body length, from epifluorescence microscopy of salp gut contents, by life history stage. A) solitaries, B) aggregates, for the nearshore salps. All *Cyclosalpa affinis* except circle = *Salpa aspera*. C) solitaries, D) aggregates, for the three open ocean regions. TR=transition region, CC=California Current, NPSG=North Pacific Subtropical Gyre.

Figures 4.3a and 4.3b illustrate that for nearshore salps, there was no body-length dependent pattern of ingestion of plastic particles. In general, the nearshore salps (all *Cyclosalpa affinis* except for one *Salpa aspera* solitary) were larger than the open ocean salps, with some overlap of the nearshore and NPSG aggregates in body length. The *Salpa aspera* solitary (purple dot, 4.3a) was markedly bigger than the other nearshore solitary *Cyclosalpa affinis* specimens, but with an ingestion rate of 53.7 particles h^{-1}, it did not show the highest ingestion rate of all nearshore salps.

Figures 4.3c and 4.3d illustrate region-specific patterns in ingestion rate for open ocean solitaries and aggregates, respectively. For both solitaries and aggregates, the

California Current salps were the smallest and had the smallest plastic particle ingestion rates. For the solitaries, the NPSG salps' ingestion rates follow an almost linearly length-dependent pattern. There are only two transition region solitaries, but they are both long with high ingestion rates. For Figure 4.3d, the pattern in ingestion rates between the NPSG and transition region salps reverses from Figure 4.3c. The transition region salps are smaller, and the NPSG aggregate salps are larger. There is no detectable relationship between body length and ingestion rate for salps from either region.

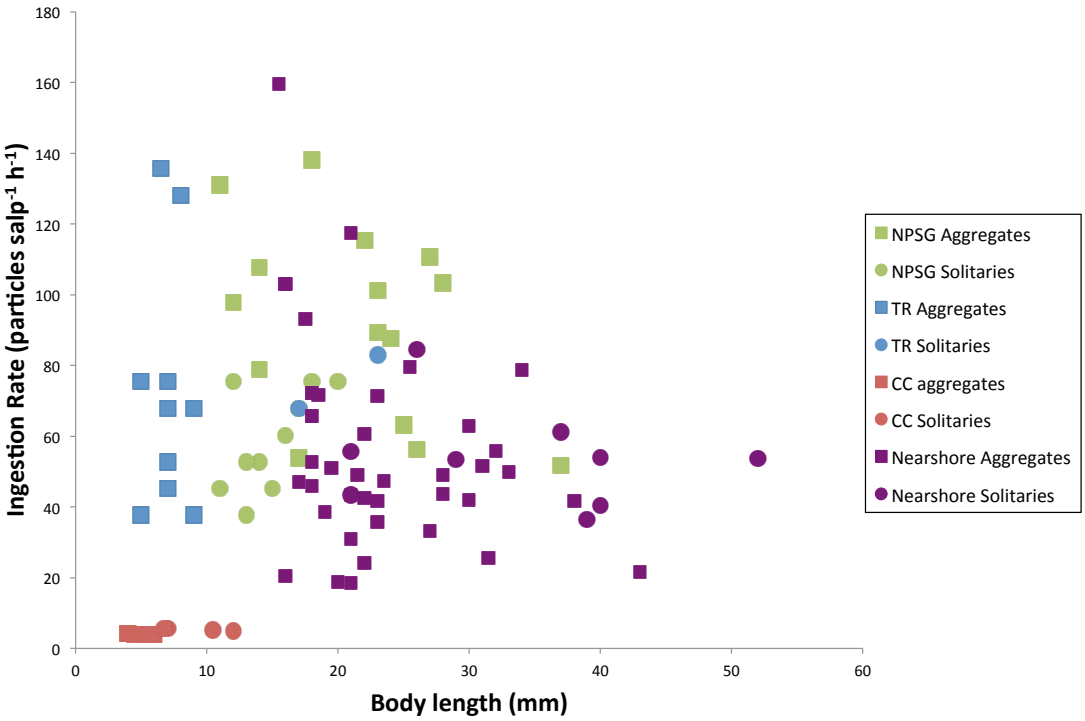

Figure 4.4: Ingestion rate vs. Body length, from epifluorescence microscopy of salp gut contents. TR=transition region, CC=California Current, NPSG=North Pacific Subtropical Gyre. Squares=aggregates, Circles=solitaries.

Figure 4.4 illustrates salp ingestion rates against body length by region, for all salps combined. The California Current salps were both the smallest salps by size, and showed the lowest ingestion rate. Transition region salps were also small, and showed medium to high ingestion rates of plastic particles. NPSG salps were larger but showed ingestion rates in the

same ranges as transition region salps. Nearshore salps (from SKrillEx I) were often the largest, but showed a broad range of ingestion rates. There was no significant effect of region of collection on ingestion rate of plastics ($p > 0.05$, Kruskal-Wallis).

Length and Surface Area of Consumed Particles

During epifluorescence microscopy analysis, every particle enumerated on the slides was categorized as a fiber or fragment, and measured for length and width. Fibers made up 91% of the total particles counted. The surface areas and lengths of fibers ingested by NPSG salps differed significantly from those ingested by California Current and nearshore salps, but not transition region salps (Fig. 4.5a, 4.5c; $p < 0.05$, Dunn's post-hoc test with Benjamini-Hochberg adjustment; asterisks on figures). For fibers ingested by transition region salps, the surface areas and lengths differed significantly from those ingested by California Current and nearshore salps but not of NPSG salps (Fig. 4.5a, 4.5c; $p < 0.05$, Dunn's post-hoc test with Benjamini-Hochberg adjustment; asterisks on figures). The surface areas of plastic fragments ingested by transition region salps differed from those ingested by NPSG salps and California Current salps, but not nearshore salps (Fig. 4.5b; $p < 0.05$, Dunn's post-hoc test with Benjamini-Hochberg adjustment; asterisk on figure); the surface areas of the fragments ingested by the California Current salps differed from those ingested by the transition region salps and the nearshore salps but not the NPSG salps ($p < 0.05$, Dunn's post-hoc test with Benjamini-Hochberg adjustment; cross on figure). The lengths of ingested plastic fragments were heterogeneous (Fig. 4.5d, $p < 0.05$, Kruskal-Wallis) but post-hoc tests did not find any one region to be consistently different from another.

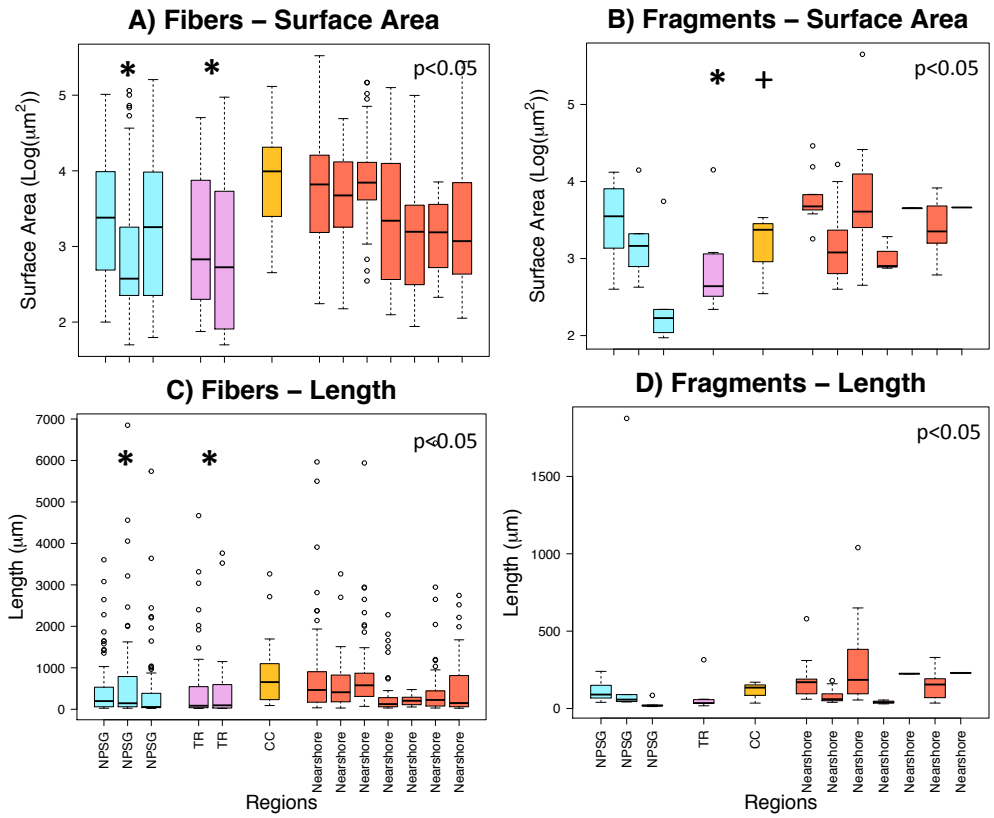

Figure 4.5: Size distribution of ingested plastics. A) Fibers surface area, B) Fragments surface area, C) Fibers length, D) Fragments length. Blue= North Pacific Subtropical Gyre. Purple= transition region. Yellow = California Current. Orange = Nearshore. Box and Whisker plots: middle lines= medians, box edges = first and third quartiles, whiskers = 3/2 times the outer quartile, circles = outliers beyond 3/2 outer quartiles.

Dimensions of Ingested vs. Ambient Microplastics

Figure 4.6 compares the average size (as surface area) of plastic particles ingested by salps with the average size of all particles collected in surface nanoplastic bucket tows, and analyzed via epifluoresence microscopy (Brandon and Freibott 2017). These tows, in adjacent or similar water as the salps, are indications of the ambient nanoplastic concentrations of surface water the salps would be swimming through. Figure 4.6 also compares the average size of 333-µm net-collected microplastics reported by Goldstein et al. (2013), most from the same SEAPLEX cruise as the current study's salps. These net-collected particles still fall in the size range of potential salp prey particles (Vargas and

Madin 2004). Salps consumed smaller plastic than what was available to them in the ambient water. For both nearshore and open ocean (CC, TR, NPSG combined) salps, the average size of particles consumed was significantly smaller than the size of ambient plastic available ($p < 0.05$, Dunn's post-hoc test with Benjamini-Hochberg adjustment; asterisks on figures).

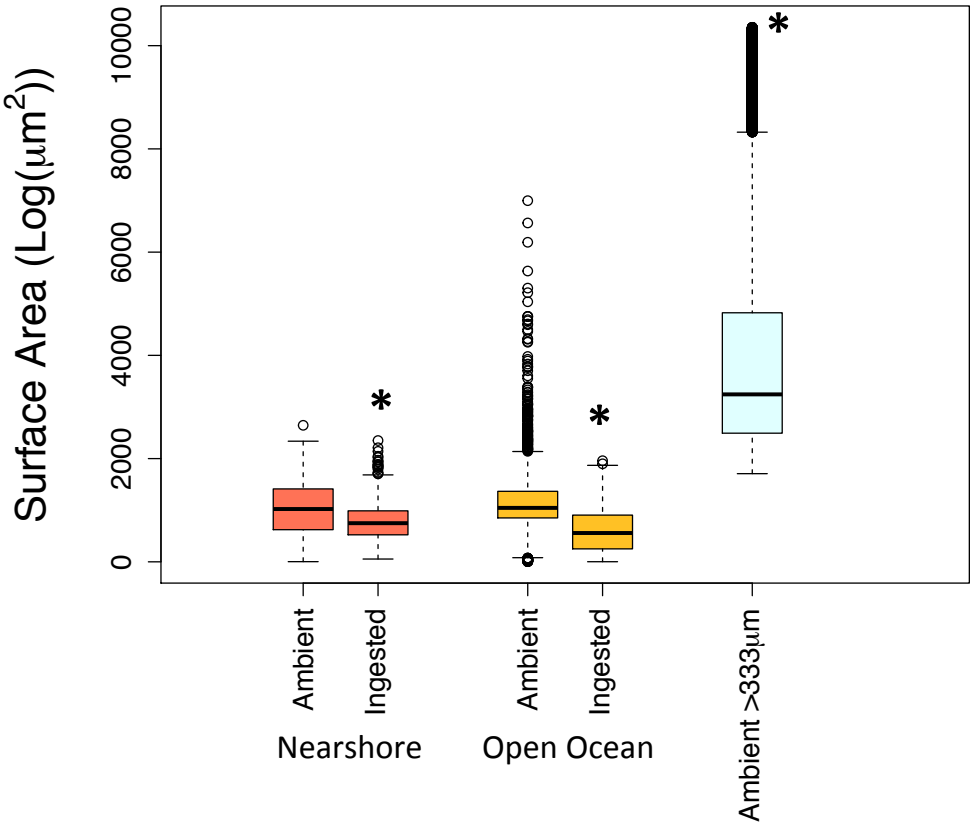

Figure 4.6: Area of salp-ingested particles compared to area of ambient surface seawater particles. Ambient: nanoplastic particles measured by epifluorescence microscopy for ambient surface seawater concentrations, both fibers and fragments (Brandon and Freibott 2017). Ingested: particles ingested by salps, measured in this study, both fibers and fragments. Yellow: nearshore, Blue: open ocean, Orange: Microplastics larger than 333 μm sampled in the open ocean (Goldstein et al. 2013).

DISCUSSION:

Every salp dissected had plastic in its gut, regardless of species, life history stage or region of the ocean sampled. This is the first record of salp ingestion of microplastic *in situ*. Since salp gut clearance times are on the order of 2-7 hours (Madin and Cetta 1984, Perissinottoab and Pakhomov 1998, Huskin et al. 2003), we are confident that by only analyzing the gut, not the mucus net or gill bar, we avoided artifacts of net feeding or other sources of contamination. Airborne contamination is a major concern in modern microplastic work (Davison and Asch 2011, Foekema et al. 2013), especially when samples are so dominated by fibers, as in this study (91% of the particles). However, our process of dissection of the salps limited contamination, by keeping the salps in sealed sample jars until dissection. Dissection was done carefully with salps out of sealed jars for as short of time as possible, salps were dissected in clean glass labware, exposed to continual ventilating air to avoid airborne fiber contamination, then dissected guts were immediately placed in sealed scintillation vials until the point of slide making. Our slide making process could introduce a few airborne fibers, as illustrated by Brandon and Freibott (2017), but exactly the same slidemaking apparatus in the same lab space was used in both that and the present study. We found markedly higher plastic fiber concentrations in our seawater samples than in our Milli-Q control water in that study, leading us to believe that airborne contamination in our slidemaking is not of major concern.

There is little agreement between the literature clearance rate-estimated ingestion rates and our direct measures of ingestion based on epifluorescence microscopy. There are multiple possible reasons for this disparity. The length-dependent literature clearance rates make many assumptions, including that salps' filtration rates are only dependent on body

length and that they are completely non-selective feeders, neither of which may be consistently true. The literature values were often calculated in experimental studies, with multiple replicates of different body sizes and food concentrations; although these studies saw variability in those replicates, they prescribe only a length-dependent clearance rate calculation, thus assuming a consistent filtration rate otherwise (Harbison and Gilmer 1976). We did not correct the literature values for *in situ* temperatures in the present study, which has been shown to increase or decrease salp swimming and ingestion rates, but assuming a Q_{10} value of 2, such a correction would have a minor effect and would not resolve the discrepancy observed. All of these considerations would lead the literature values to be an overestimation of clearance rate. There is also an issue with our slide methodology that creates a bias for underestimation; in regions of a slide with opaque gut tissue it can be difficult to detect all pieces of plastic.

However, more importantly, unlike the plastic particles, these salps are not primarily neustonic; they were caught in a net between 200-0 m depth and they do not feed continuously at the surface. Some salps even exhibit diel vertical migration; though relatively rare in salps (Purcell and Madin 1991), DVM has been shown in *Salpa thompsoni* (Mackintosh 1934, Hardy and Gunther 1935, Foxton 1966), *Salpa aspera* (Harbison and Campenot 1979, Wiebe et al. 1979), *Salpa fusiformis* (Franqueville 1971, Harbison and Campenot 1979), and *Cyclosalpa bakeri* (Miller et al. 1988, Purcell and Madin 1991). In contrast, the nanoplastic concentrations used in the clearance rate-derived ingestion method reflect buoyant nanoplastics collected with a bucket at the surface of the water. These plastics are known to be buoyant and not be at these high concentrations throughout the water column. There has been some wind-mixing of plastics measured down into the mixed

layer, but at much lower concentrations (Kukulka et al. 2012, Goldstein et al. 2013). Thus the salps are interacting with plastic at these high concentrations primarily when they feed at the surface, but they are not swimming through this highly concentrated water all day. The literature-derived ingestion rates assuming relatively constant clearance rates and constant high nanoplastic concentrations are an extreme overestimation compared to the actual salp gut contents.

An extreme case of overestimation is with *Cyclosalpa bakeri*, which Purcell and Madin (1991) found are not at rest at depth during the day and eating at the surface at night, like most diel vertical migrators. In contrast, they are eating at depth during the day and coming to the surface at night to spawn; their filter-feeding mechanism is turned off at the surface to not ingest motile sperm before fertilization. Thus, even though the literature-based clearance rate is only for daytime clearance values (Madin and Purcell 1992), the literature-based clearance rate would be an even larger overestimate than for other salps, because when *C. bakeri* would be in the most contact with high concentrations of neustonic plastic, they are not feeding at all.

All salps had ingested plastic. Aggregate life history zooids had much higher ingestion rates than solitaries. We detected no regional differences in plastic ingestion by salps, excluding the much lower values of the California Current salps. The latter effect is most likely attributable to the very small zooid size of the small number of salps we happened to sample at this time. This relative lack of spatial heterogeneity in plastic ingestion rate is reminiscent of the results in Brandon and Freibott (2017), who detected no spatial heterogeneity in the open ocean concentrations of surface nanoplastics. Here the California Current salps have a lower ingestion rate and the nearshore salps are more similar

in ingestion rate to the other open ocean regions, whereas in Brandon and Freibott, concentrations of nanoplastics in the nearshore environment were significantly different from the entire open ocean.

Also somewhat mirroring the trends seen in Brandon and Freibott (2017), the dimensions of the particles consumed by the transition region salps differ from the other regions, perhaps because that region has smaller particles for the salps to ingest. However, for fiber length and surface area, the NPSG and transition region particles consumed did not differ in dimensions, so the patterns do not correspond exactly.

Salps are thought to be non-selective feeders, not selecting food on a qualitative basis, i.e., whether their food is alive or dead, the cell type, or condition of their food (Fedele 1933b, a, Madin 1990, Bone 1998). Their selectivity is thought to be based primarily on particle size, with the ability to ingest particles from < 1 μm to 1 mm (Madin 1974, Vargas and Madin 2004) or perhaps even smaller (Sutherland et al. 2010). The ambient plastic collected in the surface seawater in the open ocean, both in Brandon and Freibott (2017) and in Goldstein et al. (2013), excepting a few large pieces in Goldstein et al. (2013), fall within the possible prey range of salps. Yet the salps sampled here ate significantly smaller pieces of plastic than were available in the ambient water. This result may be related to the fact that salps do not feed in the neustonic layer all day; perhaps some of the largest plastic is more buoyant and thus the salps are not consistently in contact with it as a potential ingestion source. This is most likely due to the higher surface area:volume ratio of smaller plastics, which leads to faster biofouling, and thus faster loss of buoyancy due to heavy biofilms, of smaller plastic (Fazey and Ryan 2016).

Although salps ate smaller plastic than the plastic that was available to them in surface water, every salp dissected for gut content analysis had consumed plastic in its stomach. It is reasonable to believe that salps are consistently consuming and processing plastic, and are thus a key vector of the transport of plastic from the surface of the ocean to the benthos, via their fast-sinking fecal pellets. This study, the first to show salps' ingestion of microplastics *in situ*, illustrates the possibility that salps could be a key transport mechanism of plastic to the benthos, and a key part of the plastic missing when comparing surface plastic abundances with estimates of plastic production.

CONCLUSIONS:

This study is the first to show ingestion of microplastics by salps *in situ*. Every salp dissected for gut content analysis had ingested plastic, regardless of species, life history stage, or the oceanic region in which they were collected. Aggregates had higher ingestion rates than solitaries. In comparing ambient seawater nanoplastic and microplastic available for ingestion, salps in this study ingested significantly smaller plastic than that observed in their environment. Literature-derived values of ingestion rates, based on literature clearance rates and ambient surface nanoplastic concentrations, were determined to not be realistic estimates for salp ingestion. Our evidence for geographically widespread consumption of plastic debris by salps in different oceanic provinces leads us to believe that salps are a vector of marine debris transport from the surface of the ocean to the benthos, via their fast-sinking pellets and sinking carcasses, and that salps could be a key missing factor in plastic abundance equations.

ACKNOWLEDGEMENTS:

Funding for the SEAPLEX cruise was provided by University of California Ship Funds, Project Kaisei/ Ocean Voyages Institute, AWIS-San Diego, and NSF IGERT Grant No. 0333444. We express thanks to CCE-LTER for funding SKrillEx I. Thank you to Linsey Sala for your help with salp dissections, literature, and knowledge. Thank you to Mark Ohman for your guidance, extended discussions, and assistance throughout this study. Thank you to Kayla Blincow for help with R. I thank the entire M.R. Landry lab for their patience and assistance with the epifluorescence microscope and software. Thank you to Samantha Albotra for volunteering her time in lab to help with the slide preparations.

Chapter 4, in part is currently being prepared for submission for publication of the material. Brandon, Jennifer. The dissertation author was the primary investigator and author of this material.

Table 4.1: Salps analyzed in this study

Cruise	Station	Species	Number in sample Total (agg, sol)
SKrillEx I	Tr. 1, St. 2	*Cyclosalpa affinis*	10 (10,0)
SKrillEx I	Tr. 1, St. 6	*Salpa aspera*	1 (0,1)
SKrillEx I	Tr. 2, St. 6	*Cyclosalpa affinis*	10 (8,2)
SKrillEx I	Tr. 2, St. 7	*Cyclosalpa affinis*	10 (7,3)
SKrillEx I	Tr. 2, St. 8	*Cyclosalpa affinis*	10 (8,2)
SKrillEx I	Tr. 3, St. 1	*Cyclosalpa affinis*	10 (8,2)
SKrillEx I	Tr. 3, St. 3	*Cyclosalpa affinis*	10 (10,0)
SKrillEx I	Tr. 3, St. 4	*Cyclosalpa affinis (4), Ritteriella retracta (1)*	5 (3,2)
SEAPLEX	U3-11 (CC)	*Thalia democratica*	10 (6,4)
SEAPLEX	S1-7 (CC)	*Salpa fusiformis*	1 (0,1)
SEAPLEX	S1-8 (CC)	*Salpa fusiformis*	2 (2,0)
SEAPLEX	U46-127 (TR)	*Iasis cylindrical*	2 (1,1)
SEAPLEX	U4-12 (TR)	*Iasis cylindrical*	10 (9,1)
SEAPLEX	U5-15 (TR)	*Iasis cylindrica (2), Ihlea punctata (2), Ritteriella retracta (4)*	8 (4,4)
SEAPLEX	S3-54 (NPSG)	*Cyclosalpa pinnata*	10 (10,0)
SEAPLEX	U32-67 (NPSG)	*Iasis cylindrical*	10 (0,10)
SEAPLEX	U45-126 (NPSG)	*Cyclosalpa pinnata*	10 (10,0)
SEAPLEX	U26-186 (NPSG)	*Cyclosalpa pinnata*	10 (10,0)
SEAPLEX	G18-78 (NPSG)	*Salpa aspera*	9 (6,3)
SEAPLEX	U40-99 (NPSG)	*Cyclosalpa bakeri (5), Cyclosalpa pinnata (4)*	9 (4,5)
SEAPLEX	U40-121 (NPSG)	*Salpa fusiformis (2), Iasis cylindrica (3), Cyclosalpa pinnata (4), Ihlea punctata (1)*	10 (6,4)
HOT	ZP1005 (NPSG)	*Salpa maxima*	1
HOT	ZP1002 (NPSG)	*Thalia democratica*	2
HOT	ZP1012 (NPSG)	*Cyclosalpa pinnata*	2

REFERENCES:

Alldredge, A., and L. Madin. 1982. Pelagic tunicates: unique herbivores in the marine plankton. Bioscience **32**:655-663.

Ayukai, T. 1987. Discriminate feeding of the calanoid copepod *Acartia clausi* in mixtures of phytoplankton and inert particles. Marine Biology **94**:579-587.

Berner, L. D. 1967. Distributional atlas of Thaliacea in the California Current region. California Cooperative Oceanic Fisheries Investigations Atlas **8**:1-322.

Bone, Q. 1998. The biology of pelagic tunicates. Oxford University Press, Oxford.

Bone, Q., C. Carre, and P. Chang. 2003. Tunicate feeding filters. Journal of the Marine Biological Association of the UK **83**:907-919.

Brandon, J. A., and A. Freibott. 2017. Patterns of suspended microplastic debris in the California Current and North Pacific Subtropical Gyre, imaged by epifluorescence microscopy.

Browne, M. A., P. Crump, S. J. Niven, E. Teuten, A. Tonkin, T. Galloway, and R. Thompson. 2011. Accumulation of microplastic on shorelines worldwide: sources and sinks. Environmental science & technology **45**:9175-9179.

Browne, M. A., A. Dissanayake, T. S. Galloway, D. M. Lowe, and R. C. Thompson. 2008. Ingested microscopic plastic translocates to the circulatory system of the mussel, *Mytilus edulis* (L.). Environmental science & technology **42**:5026-5031.

Browne, Mark A., Stewart J. Niven, Tamara S. Galloway, Steve J. Rowland, and Richard C. Thompson. 2013. Microplastic moves pollutants and additives to worms, reducing functions linked to health and biodiversity. Current Biology **23**:2388-2392.

Bruland, K., and M. Silver. 1981. Sinking rates of fecal pellets from gelatinous zooplankton (salps, pteropods, doliolids). Marine Biology **63**:295-300.

Carlton, J. T., J. W. Chapman, J. B. Geller, J. A. Miller, D. A. Carlton, M. I. McCuller, N. C. Treneman, B. P. Steves, and G. M. Ruiz. 2017. Tsunami-driven rafting: Transoceanic species dispersal and implications for marine biogeography. Science **357**:1402-1406.

Caron, D. A. 1983. Technique for enumeration of heterotrophic and phototrophic nanoplankton, using epifluorescence microscopy, and comparison with other procedures. Applied and Environmental Microbiology **46**:491-498.

Caron, D. A., L. P. Madin, and J. J. Cole. 1989. Composition and degradation of salp fecal pellets: implications for vertical flux in oceanic environments. Journal of Marine Research **47**:829-850.

Carpenter, E. J., and K. Smith. 1972. Plastics on the Sargasso Sea surface. Science **175**:1240-1241.

Cole, M., P. Lindeque, E. Fileman, C. Halsband, R. Goodhead, J. Moger, and T. S. Galloway. 2013. Microplastic ingestion by zooplankton. Environmental science & technology **47**:6646-6655.

Cózar, A., F. Echevarría, J. I. González-Gordillo, X. Irigoien, B. Úbeda, S. Hernández-León, Á. T. Palma, S. Navarro, J. García-de-Lomas, and A. Ruiz. 2014. Plastic debris in the open ocean. Proceedings of the National Academy of Sciences **111**:10239-10244.

Davison, P., and R. G. Asch. 2011. Plastic ingestion by mesopelagic fishes in the North Pacific Subtropical Gyre. Marine Ecology Progress Series **432**:173-180.

Defossez, J.-M., and A. Hawkins. 1997. Selective feeding in shellfish: size-dependent rejection of large particles within pseudofaeces from *Mytilus edulis*, *Ruditapes philippinarum* and *Tapes decussatus*. Marine Biology **129**:139-147.

Derraik, J. G. B. 2002. The pollution of the marine environment by plastic debris: a review. Marine Pollution Bulletin **44**:842-852.

Desforges, J.-P. W., Moira Galbraith, and Peter S. Ross 2015. Ingestion of microplastics by zooplankton in the Northeast Pacific Ocean. Archives of environmental contamination and toxicology **69**:320-330.

Donohue, M. J., R. C. Boland, C. M. Sramek, and G. A. Antonelis. 2001. Derelict fishing gear in the northwestern Hawaiian Islands: Diving surveys and debris removal in 1999 confirm threat to coral reef ecosystems. Marine Pollution Bulletin **42**:1301-1312.

Eriksen, M., L. C. Lebreton, H. S. Carson, M. Thiel, C. J. Moore, J. C. Borerro, F. Galgani, P. G. Ryan, and J. Reisser. 2014. Plastic pollution in the world's cceans: More than 5 trillion plastic pieces weighing over 250,000 tons afloat at sea. PloS one **9**:e111913.

Fazey, F. M., and P. G. Ryan. 2016. Biofouling on buoyant marine plastics: An experimental study into the effect of size on surface longevity. Environmental Pollution **210**:354-360.

Fedele, M. 1933a. Sul complesso delle funzioni che intervengono nel meccanismo ingestivo dei Salpidae. Atti della Accademia Nazionale dei Lincei Rc **17**:241-245.

Fedele, M. 1933b. Sulla nutrizione degli animali pelagici III. Richerche sui Salpidae. Bollettino della Societa dei Naturalisti in Napoli **45**:49-118.

Foekema, E. M., C. De Gruijter, M. T. Mergia, J. A. van Franeker, A. J. Murk, and A. A. Koelmans. 2013. Plastic in North sea fish. Environmental science & technology **47**:8818-8824.

Foxton, P. 1966. The distribution and life-history of *Salpa thompsoni* Foxton with observations on a related species, *Salpa gerlachei* Foxton. Discovery Rep. **34**:1-116.

Franqueville, C. 1971. Macroplancton profond (invertébrés) de la Méditerranée nord-occidentale. Tethys **3**:11-56.

Fraser, J. H. 1947. Thaliacea: I. Family: Salpidae. Pages 1-4 *in* Conseil International pour L'Exploration de La Mer.

Freibott, A., L. Linacre, and M. R. Landry. 2014. A slide preparation technique for light microscopy analysis of ciliates preserved in acid Lugol's fixative. Limnology and Oceanography: Methods **12**:54-62.

Frost, B. W. 1977. Feeding behavior of *Calanus pacificus* in mixtures of food particles1. Limnology and Oceanography **22**:472-491.

Goldstein, M. C., and D. S. Goodwin. 2013. Gooseneck barnacles (*Lepas* spp.) ingest microplastic debris in the North Pacific Subtropical Gyre. PeerJ **1**:e184.

Goldstein, M. C., A. J. Titmus, and M. Ford. 2013. Scales of spatial heterogeneity of plastic marine debris in the northeast Pacific ocean. PloS one **8**:e80020.

Goldstein, M. C., H. S. Carson, and M. Eriksen. 2014. Relationship of diversity and habitat area in North Pacific plastic-associated rafting communities. Marine Biology **161**:1441-1453.

Govindarajan, A. F., A. Bucklin, and L. P. Madin. 2011. A molecular phylogeny of the Thaliacea. Journal of Plankton Research **33**:843-853.

Hall, N. M., K. L. E. Berry, L. Rintoul, and M. O. Hoogenboom. 2015. Microplastic ingestion by scleractinian corals. Marine Biology **162**:725-732.

Harbison, G., and R. Gilmer. 1976. The feeding rates of the pelagic tunicate *Pegea confederata* and two other salps. Limnology and Oceanography **21**:517-528.

Harbison, G., and R. Campenot. 1979. Effects of temperature on the swimming of salps (Tunicata, Thaliacea): Implications for vertical migration. Limnology and Oceanography **24**:1081-1091.

Harbison, G., and V. McAlister. 1979. The filter‐feeding rates and particle retention efficiencies of three species of *Cyclosalpa* (Tunicata, Thaliacea). Limnology and Oceanography **24**:875-892.

Harbison, G., V. L. McAlister, and R. Gilmer. 1986. The response of the salp, *Pegea confoederata*, to high levels of particulate material: Starvation in the midst of plenty. Limnology and Oceanography **31**:371-382.

Hardy, A. C., and E. R. Gunther. 1935. The plankton of the South Georgia whaling grounds and adjacent waters, 1926-1927. Discovery Rep. **8**:1-456.

Hart, M. W. 1991. Particle captures and the method of suspension feeding by echinoderm larvae. The Biological Bulletin **180**:12-27.

Henderson, J. R. 2001. A pre- and post-MARPOL Annex V summary of Hawaiian monk seal entanglements and marine debris accumulation in the northwestern Hawaiian Islands, 1982–1998. Marine Pollution Bulletin **42**:584-589.

Henschke, N., D. A. Bowden, J. D. Everett, S. P. Holmes, R. J. Kloser, R. W. Lee, and I. M. Suthers. 2013. Salp-falls in the Tasman Sea: a major food input to deep-sea benthos. Marine Ecology Progress Series **491**:165-175.

Hidalgo-Ruz, V., L. Gutow, R. C. Thompson, and M. Thiel. 2012. Microplastics in the marine environment: a review of the methods used for identification and quantification. Environmental science & technology **46**:3060-3075.

Huskin, I., M. J. Elices, and R. Anadón. 2003. Salp distribution and grazing in a saline intrusion off NW Spain. Journal of Marine Systems **42**:1-11.

Jambeck, J. R., R. Geyer, C. Wilcox, T. R. Siegler, M. Perryman, A. Andrady, R. Narayan, and K. L. Law. 2015. Plastic waste inputs from land into the ocean. Science **347**:768-771.

Jang, M., W. J. Shim, G. M. Han, M. Rani, Y. K. Song, and S. H. Hong. 2016. Styrofoam debris as a source of hazardous additives for marine organisms. Environmental science & technology **50**:4951-4960.

Katija, K., C. A. Choy, R. E. Sherlock, A. D. Sherman, and B. H. Robison. 2017. From the surface to the seafloor: How giant larvaceans transport microplastics into the deep sea. Science Advances **3**:e1700715.

Kemp, P. F., J. J. Cole, B. F. Sherr, and E. B. Sherr. 1993. Handbook of methods in aquatic microbial ecology. CRC press.

Kremer, P., and L. P. Madin. 1992. Particle retention efficiency of salps. Journal of Plankton Research **14**:1009-1015.

Kukulka, T., G. Proskurowski, S. Morét-Ferguson, D. Meyer, and K. Law. 2012. The effect of wind mixing on the vertical distribution of buoyant plastic debris. Geophysical Research Letters **39:** L07601.

Lavaniegos, B. E., and M. D. Ohman. 2003. Long-term changes in pelagic tunicates of the California Current. Deep Sea Research Part II: Topical Studies in Oceanography **50**:2473-2498.

Law, K. L., S. Morét-Ferguson, N. A. Maximenko, G. Proskurowski, E. E. Peacock, J. Hafner, and C. M. Reddy. 2010. Plastic accumulation in the North Atlantic subtropical gyre. Science **329**:1185-1188.

Law, K. L., S. E. Morét-Ferguson, D. S. Goodwin, E. R. Zettler, E. DeForce, T. Kukulka, and G. Proskurowski. 2014. Distribution of surface plastic debris in the eastern Pacific Ocean from an 11-Year data set. Environmental science & technology **48**:4732-4738.

Lozano, R., and J. Mouat. 2009. Marine Litter in the North-East Atlantic Region: Assessment and Priorities for Response. KIMO International. 9781906840266.

Mackintosh, N. A. 1934. Distribution of the macroplankton in the Atlantic sector of the Antarctic. Discovery Rep. **9**:65-160.

Madin, L. 1974. Field observations on the feeding behavior of salps (Tunicata: Thaliacea). Marine Biology **25**:143-147.

Madin, L. 1982. Production, composition and sedimentation of salp fecal pellets in oceanic waters. Marine Biology **67**:39-45.

Madin, L. 1990. Aspects of jet propulsion in salps. Canadian Journal of Zoology **68**:765-777.

Madin, L., and C. Cetta. 1984. The use of gut fluorescence to estimate grazing by oceanic salps. Journal of Plankton Research **6**:475-492.

Madin, L. P., and J. E. Purcell. 1992. Feeding, metabolism. and growth of *Cyclosalpa bakeri* in the subarctic Pacific. Limnology and Oceanography **37**:1236-1251.

Miller, C. B., K. Denman, A. Gargett, D. Mackas, P. Wheeler, B. Booth, B. Frost, M. Landry, J. Lewin, and C. Lorenzen. 1988. Lower trophic level production dynamics in the oceanic subarctic Pacific Ocean. Bulletin of the Ocean Research Institute-University of Tokyo (Japan) **26**:1-26.

Moore, C. J., S. L. Moore, M. K. Leecaster, and S. B. Weisberg. 2001. A comparison of plastic and plankton in the North Pacific Central Gyre. Marine Pollution Bulletin **42**:1297-1300.

Ogata, Y., H. Takada, K. Mizukawa, H. Hirai, S. Iwasa, S. Endo, Y. Mato, M. Saha, K. Okuda, A. Nakashima, M. Murakami, N. Zurcher, R. Booyatumanondo, M. P. Zakaria, L. Q. Dung, M. Gordon, C. Miguez, S. Suzuki, C. Moore, H. K. Karapanagioti, S. Weerts, T. McClurg, E. Burres, W. Smith, M. V. Velkenburg, J. S. Lang, R. C. Lang, D. Laursen, B. Danner, N. Stewardson, and R. C. Thompson. 2009. International Pellet Watch: Global monitoring of persistent organic pollutants (POPs) in coastal waters. 1. Initial phase data on PCBs, DDTs, and HCHs. Marine Pollution Bulletin **58**:1437-1446.

Pasulka, A. L., M. R. Landry, D. A. Taniguchi, A. G. Taylor, and M. J. Church. 2013. Temporal dynamics of phytoplankton and heterotrophic protists at station ALOHA. Deep Sea Research Part II: Topical Studies in Oceanography **93**:44-57.

Perissinottoab, R., and E. A. Pakhomov. 1998. The trophic role of the tunicate *Salpa thompsoni* in the Antarctic marine ecosystem. Journal of Marine Systems **17**:361-374.

Purcell, J. E., and L. P. Madin. 1991. Diel patterns of migration, feeding, and spawning by salps in the subarctic Pacific. Marine Ecology Progress Series **73**:211-217.

Rochman, C. M., E. Hoh, T. Kurobe, and S. J. Teh. 2013. Ingested plastic transfers hazardous chemicals to fish and induces hepatic stress. Scientific Reports **3**:3263.

Samo, T. J., F. Malfatti, and F. Azam. 2008. A new class of transparent organic particles in seawater visualized by a novel fluorescence approach. Aquatic Microbial Ecology **53**:307-321.

Schlining, K., S. von Thun, L. Kuhnz, B. Schlining, L. Lundsten, N. J. Stout, L. Chaney, and J. Connor. 2013. Debris in the deep: Using a 22-year video annotation database to survey marine litter in Monterey Canyon, central California, USA. Deep Sea Research Part I: Oceanographic Research Papers **79**:96-105.

Silver, M., and K. Bruland. 1981. Differential feeding and fecal pellet composition of salps and pteropods, and the possible origin of the deep-water flora and olive-green "cells". Marine Biology **62**:263-273.

Silver, M. W. 1975. The habitat of *Salpa fusiformis* in the California Current as defined by indicator assemblages. Limnology and Oceanography **20**:230-237.

Small, L., S. Fowler, and M. Ünlü. 1979. Sinking rates of natural copepod fecal pellets. Marine Biology **51**:233-241.

Smith, K., A. Sherman, C. Huffard, P. McGill, R. Henthorn, S. Von Thun, H. Ruhl, M. Kahru, and M. Ohman. 2014. Large salp bloom export from the upper ocean and benthic community response in the abyssal northeast Pacific: Day to week resolution. Limnology and Oceanography **59**:745-757.

Stone, J. P., and D. K. Steinberg. 2016. Salp contributions to vertical carbon flux in the Sargasso Sea. Deep Sea Research Part I: Oceanographic Research Papers **113**:90-100.

Sutherland, K. R., L. P. Madin, and R. Stocker. 2010. Filtration of submicrometer particles by pelagic tunicates. Proceedings of the National Academy of Sciences **107**:15129-15134.

Taylor, A. G., R. Goericke, M. R. Landry, K. E. Selph, D. A. Wick, and M. J. Roadman. 2012. Sharp gradients in phytoplankton community structure across a frontal zone in the California Current Ecosystem. Journal of Plankton Research **34**:778-789.

Thompson, R. C., Y. Olsen, R. P. Mitchell, A. Davis, S. J. Rowland, A. W. John, D. McGonigle, and A. E. Russell. 2004. Lost at sea: where is all the plastic? Science **304**:838-838.

Van Sebille, E., C. Wilcox, L. Lebreton, N. Maximenko, B. D. Hardesty, J. A. Van Franeker, M. Eriksen, D. Siegel, F. Galgani, and K. L. Law. 2015. A global inventory of small floating plastic debris. Environmental Research Letters **10**:124006.

Van Soest, R. 1974. A revision of the genera *Salpa* Forskål, 1775, *Pegea* Savigny, 1816 and *Ritteriella* Metcalf, 1919 (Tunicata, Thaliacea). Beaufortia **22**:153-191.

Van Soest, R. 1975. Zoogeography and speciation in the Salpidae (Tunicata, Thaliacea). Beaufortia **23**:181-215.

Vargas, C. A., and L. P. Madin. 2004. Zooplankton feeding ecology: clearance and ingestion rates of the salps *Thalia democratica*, *Cyclosalpa affinis* and *Salpa cylindrica* on naturally occurring particles in the Mid-Atlantic Bight. Journal of Plankton Research **26**:827-833.

Wiebe, P. H., L. P. Madin, L. R. Haury, G. R. Harbison, and L. M. Philbin. 1979. Diel vertical migration by *Salpa aspera* and its potential for large-scale particulate organic matter transport to the deep-sea. Marine Biology **53**:249-255.

Wilson, D. S. 1973. Food size selection among copepods. Ecology **54**:909-914.

Wright, S. L., R. C. Thompson, and T. S. Galloway. 2013. The physical impacts of microplastics on marine organisms: a review. Environmental Pollution **178**:483-492.

Yount, J. L. 1954. The taxonomy of the Salpidae (Tunicata) of the central Pacific Ocean. Pacific Salpidae **8**:276-330.

Yount, J. L. 1958. Distribution and ecologic aspects of central Pacific Salpidae (Tunicata). Pacific Science **12**:111-130.

CHAPTER 5: Multi-Decadal Changes in Plastic Particles in the Santa Barbara Basin

Jennifer A. Brandon, William Jones

ABSTRACT:

We sampled Santa Barbara Basin sediments for historical changes in rates of microplastic deposition using a box core that spanned 1834-2009. The sediment was visually sorted for plastic and then a subset was confirmed as plastic via FTIR (Fourier Transform Infrared) spectroscopy. After correcting for contamination introduced during processing, we found an exponential increase in plastic deposition from 1945-2009. This increase tightly correlated with Southern California population increases and worldwide plastic production over the same time period. Overall, plastic deposition does not correlate with rainfall or ENSO in the region. This exponential increase in plastic deposition in the post-WWII years could be used as a geological proxy for the Great Acceleration of the Anthropocene in the sedimentary record.

Keywords: Microplastic, Santa Barbara Basin, FTIR, Anthropocene

INTRODUCTION:

Plastic over time

Plastic is a relatively new material. The first fully synthetic plastic, Bakelite, was invented in 1907 (American Chemistry Council 2014). Although new plastics like polyvinyl chloride, polyethylene, and polystyrene were invented and produced in small quantities in the 1920s and 1930s (Andrady and Neal 2009, Freinkel 2011), plastics truly began to grow in prevalence during the 1940s, as World War II required the substitution of plastics for other needed materials (Freinkel 2011, Jambeck et al. 2015). In the 72 years since World

War II, plastic consumption has steadily risen in America and worldwide, and it is showing no signs of slowing (Jambeck et al. 2015). In 1950, worldwide plastic production was only 1.7 million tons (PlasticsEurope 2012); by 2014 annual global plastic production had reached 311 million tons (GESAMP 2016).

Plastic production is increasing, but plastic is also increasingly becoming part of the waste stream: from < 1% of American municipal solid waste by mass in 1960 to 12.9% in 2014 (Jambeck et al. 2015, EPA 2016). An estimated 4.8-12.7 million metric tons of mismanaged plastic waste is entering the ocean every year (Jambeck et al. 2015, EPA 2016). Higher populations produce more waste, and the world population is predicted to increase disproportionately in coastal regions (Browne et al. 2011). These coupled issues of a growing coastal population and growing plastic production will likely combine to create more marine debris.

This accumulation of marine debris in coastal regions is already documented, as coastal regions of high population density show significantly more plastic in their local marine sediments than areas of lower population density (Browne et al. 2011). Browne et al. (2011) identified the majority of the plastics they found as synthetic clothing fibers from wastewater effluent. They also found 250% more microplastic pieces in areas of sewage disposal. Synthetic fabrics, such as nylon and acrylic, are also rising in production (Browne et al. 2011). A single synthetic fleece jacket can release an average of 1,174 mg of microfibers per washing (Hartline et al. 2016), or an average of 300 microfibers L^{-1} (Browne et al. 2011). As coastal populations grow and clothes are increasingly produced from synthetic substances, effluent-derived fibers are becoming a larger concern in nearshore areas (Browne et al. 2011).

Determining how quickly this plastic is accumulating in sediments is challenging. Because plastic is a relatively new material and a very new area of study, few time series exist that can show temporal changes in either rates of coastal discharge or accumulation in sediments. The studies that have shown accumulation of plastic over time have focused on buoyant plastics collected at the sea surface, and have compared current samples with older preserved samples (Goldstein et al. 2012, Law et al. 2014). They have shown between a one and two order of magnitude increase in abundance from 1972-1987 to 1999-2010 in surface marine debris in the Northeast Pacific (Goldstein et al. 2012, Law et al. 2014), but no significant increase in plastic in the subtropical latitudes of the Northeast Atlantic from 1986 to 2008 (Law et al. 2010). There is a clear need for more accumulation studies, and means to assess longer term rates of accumulation in coastal ecosystems apart from surface waters.

The Anthropocene

In the early 2000s, Crutzen (2002) coined the term "Anthropocene" as the modern geological epoch that has been impacted by human activity (Steffen et al. 2007). Although Crutzen (2002) marked the Anthropocene as the last ~200 years, or since the invention of the steam engine in 1784, later work has shown that there was a steep post-WWII shift not only in atmospheric carbon dioxide (C. D. Keeling 2001), but other potential geological proxies as well, such as anthropogenic radionuclides, coal fly ash, altered carbon isotope patterns, and plastics (Steffen et al. 2007, Waters et al. 2016, Zalasiewicz et al. 2016, Zalasiewicz et al. 2017). This post-1945 "Great Acceleration," as the Working Group on the Anthropocene calls it (Steffen et al. 2015, Zalasiewicz et al. 2017), is likely to provide a more striking shift in sedimentary proxies than starting the Anthropocene in the 1800s, but showing trends in

sedimentation over only the last few decades requires sediment layers that can be analyzed on a precise temporal scale (Zalasiewicz et al. 2017).

Santa Barbara Basin

Although there have been many studies of marine microplastics in sediments, including in the deep sea (Thompson et al. 2004, Ryan et al. 2009, Browne et al. 2011, Hidalgo-Ruz et al. 2012, Van Cauwenberghe et al. 2013, Woodall et al. 2014), all have sampled surficial sediments and not compared these samples to older ones. Corcoran et al. (2015) did analyze 8 cm of a box core from the bottom of Lake Ontario and showed that plastics have been accumulating there for approximately the last 38 years, but their chronology is not precise.

In the North Pacific, one of the most well studied sedimentary systems useful for reconstructing paleoclimate variability lies within the Santa Barbara Basin (SBB). The SSB is a semi-enclosed basin south of Point Conception with conditions ideal for paleoclimate reconstructions. To the north of the basin lies the Santa Barbara coastline and to the south, the Channel Islands, with eastern (230 m) and western (475 m) sill depths restricting intermediate water movement. As a result, and due to high surface water productivity, most water below approximately 500 m is anaerobic, minimizing bioturbation and allowing for the preservation of millimeter-scale seasonal laminae couplets (Kennett and Ingram 1995, Reimers et al. 1996, Goericke et al. 2015). Sedimentation on the order of 140 cm ky^{-1} (Inman and Jenkins 1999) is seasonal and dominated by river-delivered siliciclastic sediments (dark laminae) in winter months and biogenic sedimentation (light laminae) during productive non-winter months (Thunell 1998). These dark-light varve couplet pairs have been counted to assign dates to the sediment core stratigraphy (Schimmelmann et al.

2006).

Since the Santa Barbara Basin varved sediment record is sensitive to changes in the overlying water column, researchers have studied the SBB to understand natural and human induced climate variability in the California Current System (CCS) over a wide range of time scales, including the glacial-interglacial, millennial, multidecadal, and subdecadal; researchers have used microfossil assemblages, oxygen and carbon isotopes, biomarkers, and other proxies to generate high-resolution records of climate variability (Baumgartner 1992, Kennett and Ingram 1995, Biondi et al. 1997, Kennett and Kennett 2000, Field et al. 2006, Field et al. 2009, Grelaud et al. 2009, Barron et al. 2010). The SBB is useful for the present study because the varved couplets span 1-2 years, and can thus be used to test for decadal-to-centennial changes. In contrast, sediment cores from aerobic, bioturbated regions can only resolve changes on the multidecadal or millennial scale (Zalasiewicz et al. 2007).

Ecosystem consequences

Understanding the accumulation trends of microplastics in sediments is important for multiple reasons. It is important to know how much plastic is accumulating in the sediment as a proxy for the overlying water column, just as sedimentary microfossils permit reconstruction of abundance patterns for the water column (Baumgartner 1992, Field et al. 2006, Field et al. 2009). However, it is also important because this plastic is entering the sedimentary ecosystem. Benthic animals have been shown to ingest and be entangled in plastic (Donohue et al. 2001, Browne et al. 2008, Graham and Thompson 2009, Murray and Cowie 2011, Hall et al. 2015), and microplastics are being found in sediments at high rates, especially in urban, populated areas (Browne et al. 2011). These plastics entering the benthic ecosystem are not just naked hydrocarbon chains, but contain harmful additives and

colorants (Browne et al. 2013, Jang et al. 2016), and can adsorb persistent organic pollutants like PAHs (polycyclic aromatic hydrocarbons), PCBs (polychlorinated biphenyls) and DDT (Dichlorodiphenyltrichloroethane), from the environment around them (Ogata et al. 2009, Rochman et al. 2013b). These microplastics are ingested by small animals near the base of the food web and, along with their harmful additives, have the potential to accumulate in the food web, affecting much larger animals (Farrell and Nelson 2013, Mattsson et al. 2017). Ingested plastics have been shown to cause liver toxicity (Rochman et al. 2013b) and brain damage to animals (Mattsson et al. 2017), among other ailments, and for these ecological and toxicological reasons, it is essential to know how much plastic is in coastal sediments, and how long it has been accumulating there.

Types of marine microplastics

The appearance of microplastics can reveal something about their source. Synthetic clothing fibers are often brightly colored and elongate, while many other microplastics are transparent or more neutrally colored (Browne et al. 2011). If microplastics derive mostly from macroplastics (> 5 mm) that have been physically and photo-degraded into this size range, they will have more jagged, irregular edges (Browne et al. 2010) and are more likely to match the relative percentages of consumer plastics - i.e., the most commonly produced consumer plastics (polystyrene, polyethylene, polypropylene; Andrady and Neal 2009) being most abundant (Browne et al. 2010). If the microplastics originate from round 'microscrubbers' or 'microbeads' in cleaning products and cosmetics, they will be mostly polyethylene or polystyrene spheres or fragments (Gregory 1996, Browne et al. 2011, Eriksen et al. 2013). Microplastic particles can enter the ecosystem from discrete point sources, such as plastic processing plants, or from diffuse sources, like populated rivers and

beaches (GESAMP 2016). Particles from discrete point sources will often be all of the same plastic type and similar in appearance to each other.

Many microplastics, especially in sediment, are covered in a biofilm and resemble biotic material. Although Browne et al. (2011) found mostly synthetic clothing fibers in their sewage effluent and near-shore sediment samples, they admit that they probably under-sampled other plastics due to their visual sampling techniques. In order to properly identify plastics, it is important to identify plastic by another characteristic besides just visual inspection.

Identifying plastics by their buoyancy is sometimes possible, as Law et al. (2010) found 99% of plastic in neuston tows in the North Atlantic Subtropical Gyre to be less dense than seawater, but nearshore plankton tows (using a continuous plankton recorder) contained both positively and negatively buoyant plastics (Thompson et al. 2004). Positively buoyant plastics can also be found in bottom sediments, although at lower percentages than negatively buoyant plastics (Browne et al. 2011). Negatively buoyant plastics have also been found in low frequencies in beach sediments and surface tows (Hidalgo-Ruz et al. 2012).

One approach for spectral identification of plastic particles, used in this study, is Fourier Transform Infrared (FTIR) Spectroscopy (Browne et al. 2011, Hidalgo-Ruz et al. 2012, Brandon et al. 2016).

Contamination

Microplastics can also originate from contamination during sample processing. During sample collection at sea and sample processing in the lab, airborne fibers from the ship, room, and scientists' clothing can enter samples. The sediment core in the present study was stored in a trilaminate bag, which is plastic, and 2 cm of the core was cut off with

a saw while in its plastic core liner box in order to create the core chronology. Thus, it is likely that the core processing itself released plastic into the sample. Airborne contamination has become a recent concern in microplastic research (Davison and Asch 2011, Foekema et al. 2013, Brandon and Freibott 2017) , with some studies (Foekema et al. 2013) discounting all microplastic fibers since some are most likely contaminants. However, Brandon and Freibott (2017) found that even though there was some microplastic in their control sample, there was a significant difference between the control and environmental samples, and most plastic originated from environmental samples.

MATERIALS AND METHODS:

Sediment core sampling

A box core was collected from the Santa Barbara Basin off the coast of California in October 2010 during the Scripps Institution of Oceanography Cal-ECHOES research cruise (Fig. 5.1). It was collected at 34°17.228' N, 120°02.135' W, at approximately 580 m water depth. Site 1, the site of the box core MV1012-ST46.9-BC1 (BC1), was chosen as a re-occupation of Ocean Drilling Program Site 893.

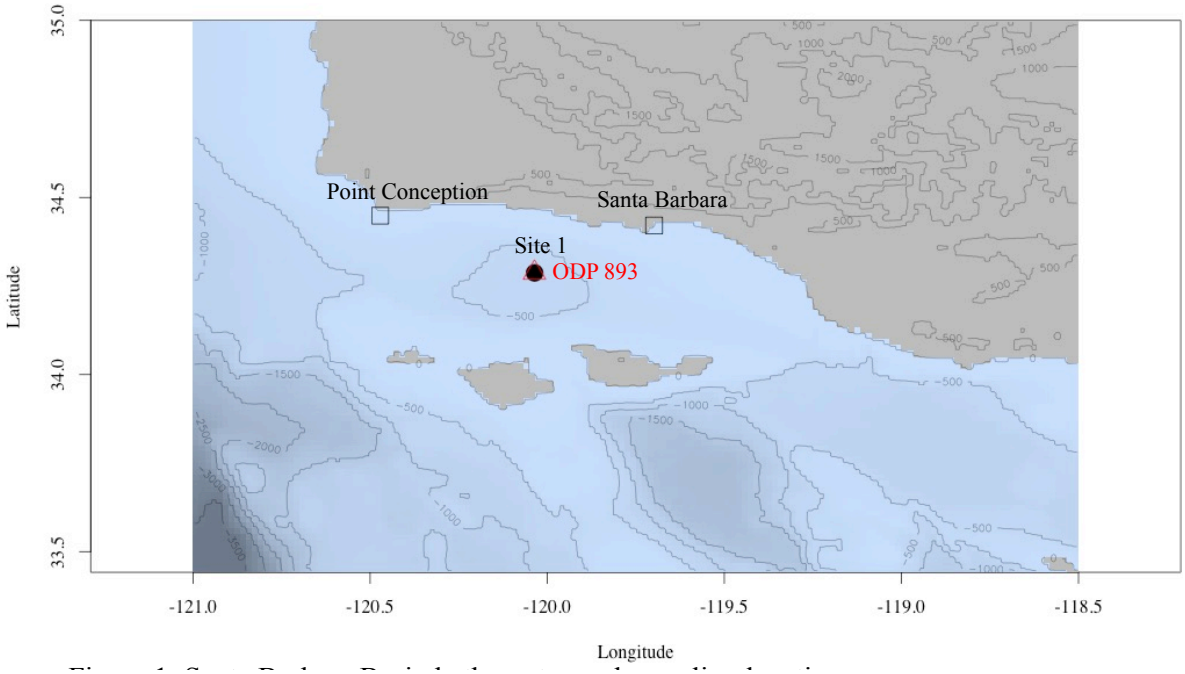

Figure 5.1: Santa Barbara Basin bathymetry and sampling locations. Box core 1 (BC1) was collected from Site 1 (black circle; 34.387133, 120.035583; 580 m water depth). Location of ODP 893 used in chronology development also shown (red triangle; 34.2875, -120.036; 577 m water depth).

Color photographs of the core were taken on the deck of the ship before subcoring occurred. The box core was removed from the coring equipment on deck by subcoring with rectangular plastic core liners of length 76 cm and 15 cm width. The box core was subcored with only one plastic core liner. All subcore sections housed in the plastic core liners were placed into Hybar trilaminate membrane bags with oxygen absorbers, flushed with nitrogen, vacuum-sealed, and stored at 4°C. This storage method was successful in maintaining anoxic conditions within the sediments for several months after sampling and before cores were processed.

Core chronology

One thin vertical slab (2 cm thick) was trimmed off the side of each subcore section with a saw. Vertical core slabs were X-radiographed at the Scripps Institution of

Oceanography Geological Collections using the Geotek MSCL-XR core scanner, which combined individual 2-dimensional images to make the composite x-radiograph images. The core slabs were scanned at 1mm intervals in a linear, non-rotational scan.

X-radiographs and color photographs were used to develop a high-resolution chronology for the core. Several age models have been developed to assign dates to the SBB varved stratigraphy. The traditional age model relied on counting seasonal varve couplets and was used to establish a chronology for the top 35 cm of the box core (Fig. 5.2; Schimmelmann et al. 2006).

Hendy et al. (2013) and Schimmelmann et al. (2013) used ^{14}C dates from planktonic foraminiferal carbonate and terrestrial-derived organic carbon from Kasten core SPR0901-06KC to show that accuracy of the traditional varve counting method decreases prior to approximately 1700 AD due to under-counting of varves. The present box core was sufficiently shallow that it did not necessitate this correction.

Microplastic removal and identification

The 76 cm subcore was cut transversely every 0.5 cm to create transverse samples, which were stored frozen before further processing. Transverse samples were oven-dried overnight at 50°C, washed and then wet-sieved in metal sieves using a 104 μm mesh over a 65 μm mesh. The > 104 μm fraction was first sorted under a dissecting scope by William Jones for fish otoliths (Jones 2016) before being sorted for microplastics. Core chronology was resolved to the upper and lower edges of the 0.5 cm transverse samples; the dates assigned to the upper and lower edges were averaged and used to assign dates to samples found within the transverse section. The samples used in the present analysis were the > 104 μm fraction from the box core. Samples were visually sorted under a Wild M-5 dissecting

microscope at 12x magnification for likely microplastic pieces, which were photographed with either a Canon Powershot S5 IS or Canon E05 Rebel T5i camera. Measurements were made to 66 μm resolution with a calibrated ocular micrometer.

Sediment was sorted in small aliquots on a black sediment sorting tray, with gridded squares. Sorted pieces of plastic were removed from the sediments, counted, measured for length with an ocular micrometer, and photographed for length and shape. In some cases, plastic fibers were so curved or twisted that a feret maximum length was measured instead of a true length. A description of the particles' physical appearance, color, amount and location of fouling, and whether they were agglomerated with other particles was recorded. They were sorted into categories: Fiber, Film, Fragment, and Spherical (Fig. 5.3). Sorted plastic pieces were stored in four-cavity paleontological slides with glass covers until later analysis by FTIR. Whenever sorting was not actively in progress, the sorting tray was covered to limit airborne contamination of microplastics from the laboratory space.

Plastic particles were initially visually differentiated from biological or sedimentary particles by their color and shape; the sediment was predominantly comprised of foraminifera tests, shells, and biological film that had striations that made it appear as if it was once living. The natural material had a few shapes that seemed to dominate the sample. Plastic, in contrast, was predominately comprised of elongate fibers or sharp-edged fragments that did not all look similar. It has been shown that brightly colored plastics are often over-counted in comparison to duller, more biological colored pieces of plastic (Browne et al. 2011), so the sediments were sorted against a black background to reduce that bias. Potential microspheres were examined under 50x magnification to see if the matrix of pores common to foraminifera tests could be discerned; often the matrix was visible on

higher magnification and the sphere was deemed biological. If films had striations that made them look like they may have once been living (e.g., part of a molt), they were also not counted, so this may have decreased film abundance numbers. In general, if a particle's origin was in question, it was deemed part of the sediment and not removed for further FTIR analysis or counted as part of the plastic abundance numbers. To reduce sampling bias between multiple sorters, all images of plastic pieces were personally examined by the senior author to assess whether it was likely plastic or likely biological. Images in question were removed from the plastic abundance numbers.

Fourier-Transform Infrared spectroscopy

To determine whether these visually identified plastics were in fact plastic, a subset of particles was analyzed with a Fourier-Transform Infrared (FTIR) Spectrometer with an attenuated total reflectance (ATR) diamond crystal attachment (Nicolet 6700 with Smart-iTR). All spectra were recorded at 4 cm^{-1} resolution. The FTIR spectra for particles collected from the ocean were compared to published standards (NICODOM 1998, Forrest et al. 2007, Browne et al. 2011, Hidalgo-Ruz et al. 2012) to attempt to identify whether the particles were plastic, biological material, or sedimentary material. The spectra were analyzed via eFTIR software (www.essentialFTIR.com). The plastic was further sorted to plastic type when possible. At least 10% of particles from every fifth 0.5 cm transverse sediment layer from the box core were identified by FTIR. The trilaminate bag and core liner in which the core was stored were also tested via FTIR, to identify sources of contamination.

Calculating deposition rates

The box core had a surface area of approximately 174 cm^2. To calculate plastic deposition rates, the number of plastic particle pieces in a 0.5 cm transverse layer was

divided by the time interval represented by the transverse layer and normalized to 100 cm^2 of seafloor during one year (No. particles*100 cm^{-2} yr^{-1}).

Baseline contamination

After the deposition rate was calculated, the number of particles in layers corresponding to 1836-1945 were averaged, as an indication of baseline contamination of plastic particles. The deepest sample of the core, corresponding to 1834, was removed from analysis, due to previous knowledge that it would have high levels of contamination from contact with the bottom of the box core liner during processing, and would thus skew the average. That average was then subtracted from all other cores' totals, to correct for baseline contamination.

Calculating plastic deposition residuals and trends

Baseline-corrected deposition rates from 1945-2009 were plotted against time. An exponential function was fitted to those new plotted values. Residuals of plastic deposition were calculated from the exponential function.

Correlating deposition rates

The residuals of plastic deposition from the exponential fit were compared to the residuals of rainfall for the urban watershed that feeds into the Santa Barbara Basin. Rainfall records from downtown Los Angeles and downtown Santa Barbara were recorded annually for 1 July -30 June, 1877-2017 for Los Angeles (LA Almanac) and September-August, 1899-2017 for Santa Barbara (Santa Barbara County). Residuals from the 50-year means of rainfall data were compared to the residuals of plastic deposition. The residuals of plastic deposition were also compared to the ONI index (National Weather Service 2017) for correlation with the El Niño-Southern Oscillation.

The Santa Barbara coastal population (Santa Barbara and Ventura counties) from 1950-2010 (US Census Bureau 1995, 2010) and worldwide plastic production from 1950-2010 (PlasticsEurope 2012) were also compared to plastic deposition rates.

RESULTS:

Core chronology

The varve chronology of BC1 is presented in Fig. 5.2. A bacterial mat 1-2 cm thick was present at the top of BC1 indicating that surface sediments were intact. The varved couplets of BC1 were counted from 2009 back to 1871 AD and correlated well with the chronology of sediment cores in Schimmelmann et al. (2006) upon visual cross-dating. To assign dates to the sediment stratigraphy prior to 1871 a regression model was used (Hendy et al. 2013), extending the chronology to approximately 1841 AD.

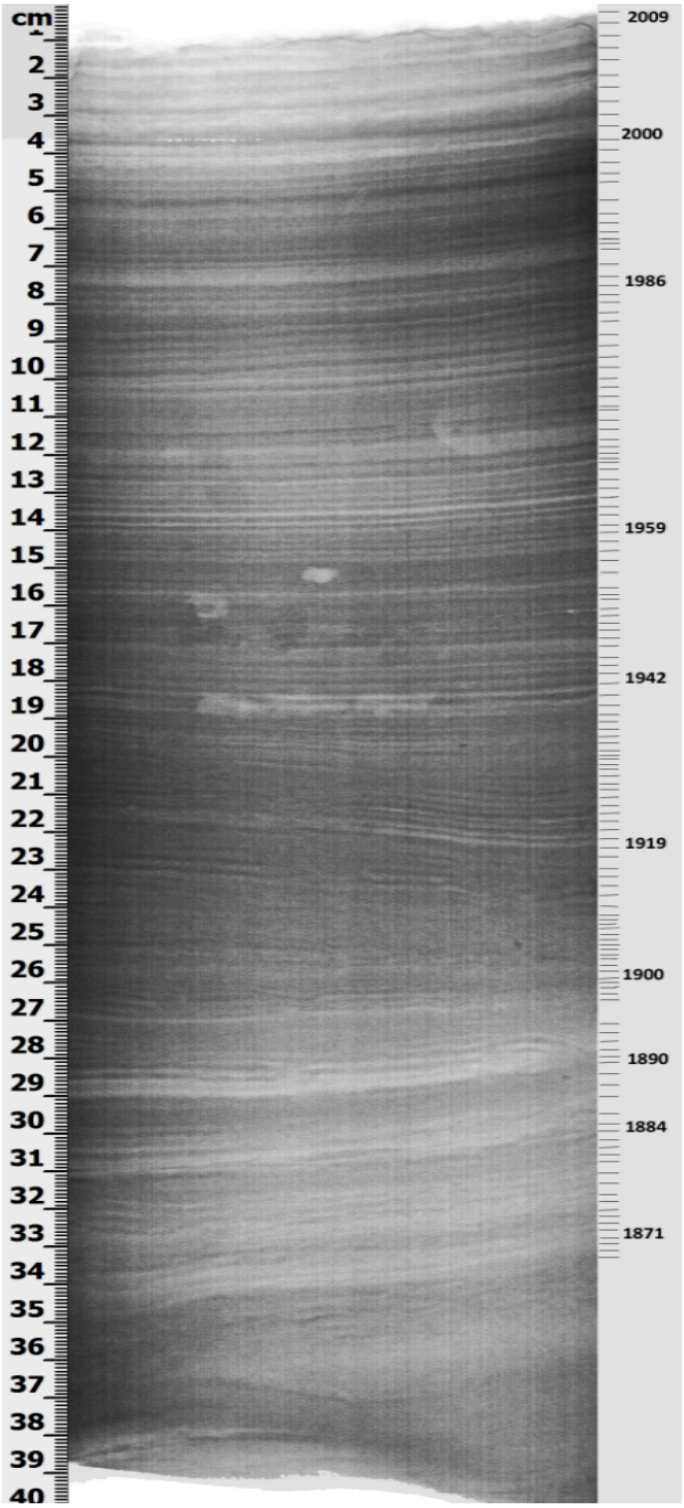

Figure 5.2: X-radiograph of box core. Bacterial mat 1-2 cm thick at top of core indicates that surface sediments were intact. Dates were assigned by counting individual varve couplets.

Plastic particle identification and baseline contamination

Plastics were visually identified in every 0.5 cm transverse layer of the core, including in the transverse layers before 1945, when plastic became popular (Freinkel 2011, Jambeck et al. 2015). Plastic particles were categorized as fibers, fragments, film pieces, and spherical particles (Fig. 5.3). The majority of plastics found in the core were fibers (Fig. 5.4a), which formed 77% of the particles. The contamination samples, from 1841-1945, were even more dominated by fibers, at 89.1% of total particles; 67.5% of the particles in the post-1945 layers were fibers (Fig. 5.4b). Although previous literature has reported mostly bright-colored fibers, and potentially overlooked many neutral-colored fibers (Browne et al. 2011), here the most common fiber color found was white. The next most common particle category was fragments, at 14% of the overall particles, although there were many more in the post-1945 samples than pre-1945 (20.8% vs. 5.8%, respectively; Fig. 5.4b). 9.7% of the post-1945 samples were film, compared to 4.9% of the pre-1945 samples. Almost no spherical plastic particles were found in the core.

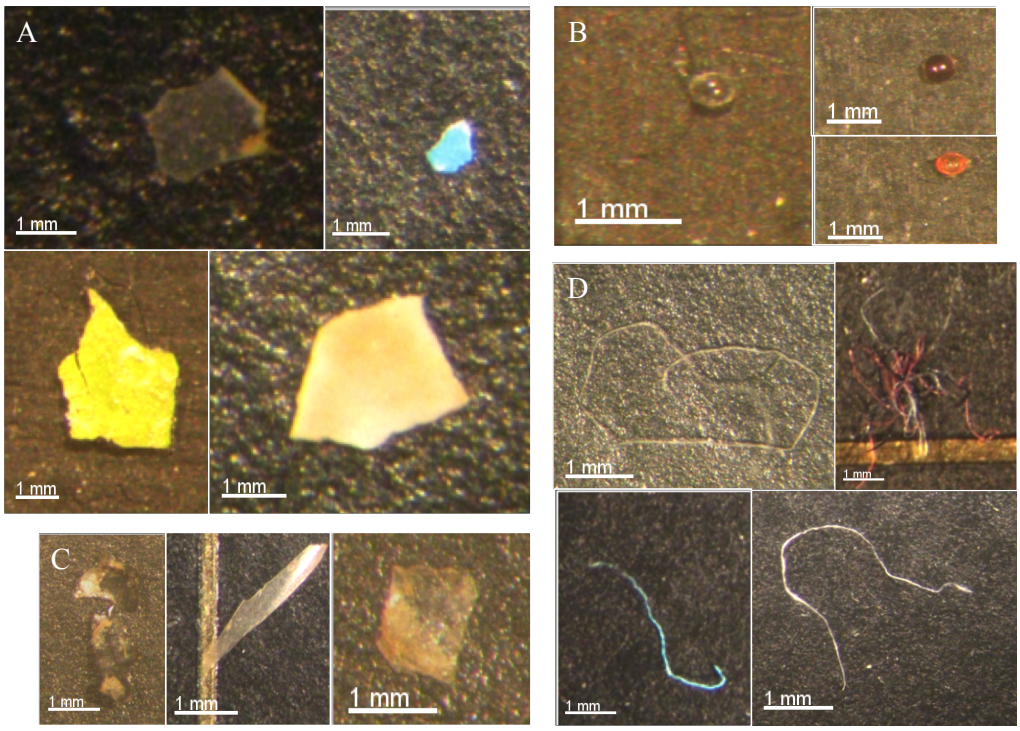

Figure 5.3: Plastic particles from box core. Examples of A) fragments, B) spherical particles, C) film, D) fibers.

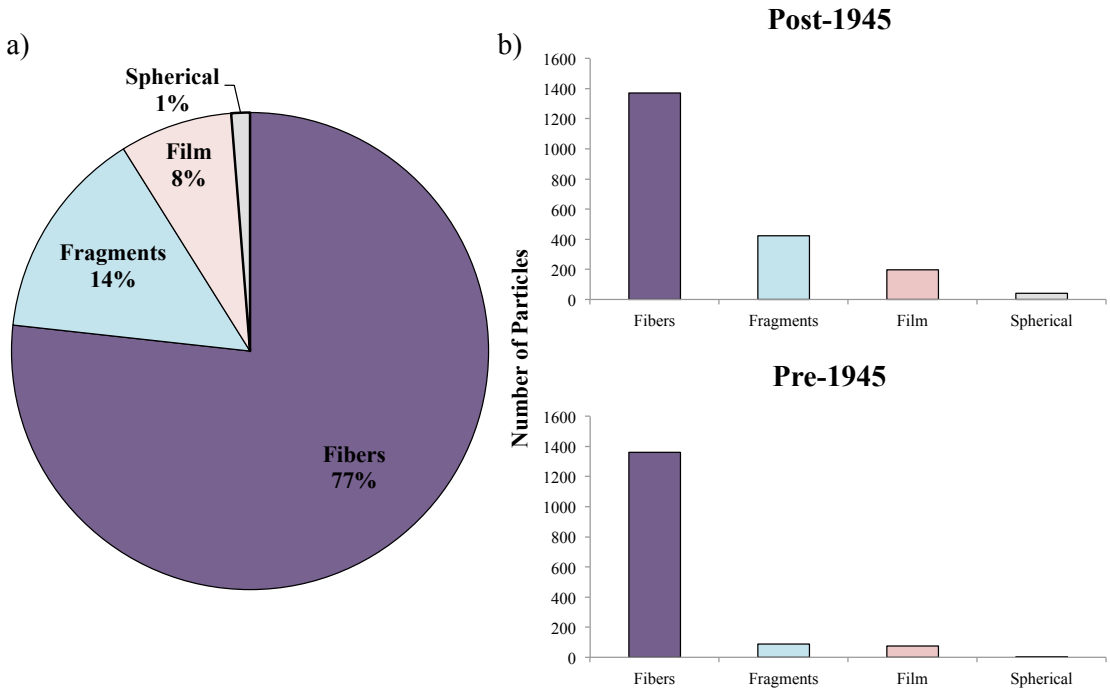

Figure 5.4: Particle types in box core. A) Particle types in entire core (by percentage of total). B) Particle types in the core before and after 1945 (by total number of particles). Dark purple = fibers, teal = fragments, pink = film, grey = spherical particles.

The length distributions of particles (Fig. 5.5a) show that there was a dominance of particles in the size range of 500-1000 μm (35.8% of the overall particles), with a right-skewed distribution. As the core moved back in time, there was little change in the distribution of particle sizes (Fig. 5.5b); post-1945 samples had 36.0% of the particles in the size range of 500-1000 μm, while pre-1945 samples had 35.5%.

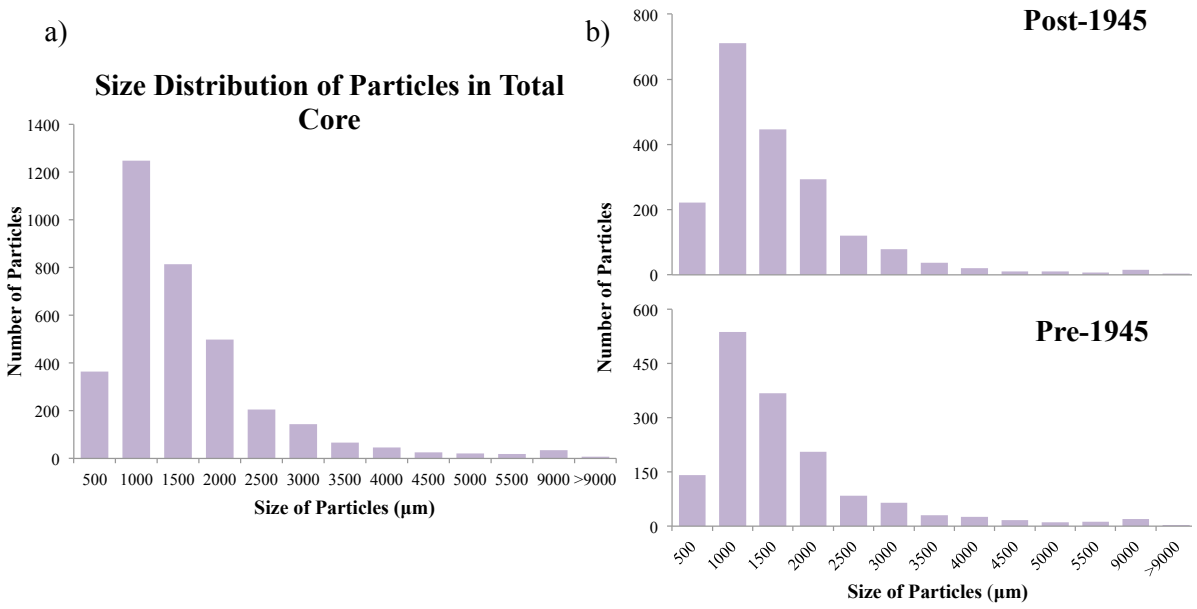

Figure 5.5: Size distribution of particles. A) Distribution of particles in whole core. X axis: upper bound of size bin (μm). B) Size distribution in layers pre- and post-1945.

Identifying plastic pieces via FTIR

Identifications of plastic particles (Table 5.1) were difficult due to the small size of the particles, and the small width of the fibers specifically, but 87.5% of particles were definitively or likely plastic particles. 87.5% of particles likely matched a standard plastic reference spectrum, with 53.0% identifiable to plastic type (Table 5.1; Fig. 5.6a-e). The plastics that could not be identified to plastic type were generally similar to two plastic types' spectra, but could not be clearly differentiated between the two (e.g. Fig. 5.6f). The particles identified as bad reads (column 6, Table 5.1) were often too small to give good FTIR spectra

or had uncertain spectra that were not conclusive enough to ascribe as plastic or not. The particles in column 7 (Table 5.1) had spectra that were high quality but did not look like plastic. They resembled the spectra of calcium carbonate, aragonite, or clay (NICODOM 1998).

Overall, the plastics that were identified to type were polystyrene (PS), polyethylene (PE) including low-density polyethylene (LDPE), PVC, nylon (polyamide), polyester, polyethylene terephthalate (PET), and the box core liner. The plastics that were most likely identified were PS, PE, PET, PVC, polyester, nylon, acrylic, and polypropylene (PP). LDPE was differentiated from HDPE by the presence of a small peak at 1377 cm^{-1}, and if its presence/absence was not clear from the spectra, the piece was recorded as PE (Lobo and Bonilla 2003, Brandon et al. 2016). The trilaminate bag in which the core was stored was PET, as identified by FTIR, and any contamination from the bag could not be differentiated from other PET unless the fragments were large enough to see whether they were metallic silver (like the trilaminate bag) or another color (Fig. 5.6b). However the bag was removed before the core was cut, and so any trilaminate bag contamination would be incidental. Contamination was found from the plastic core liner box that was cut with a saw to make the core chronology; un-aged, identical fragments of that unique spectrum were found throughout the core (Fig. 5.6e). Those fragments were included in Column 4 and 5 of Table 5.1, because these fragments were known to be plastic and identified to type (type = core liner, though its unique plastic spectrum is not identical to any published standard). These fragments were obviously contamination, as were all particles older than 1945 in Table 5.1, and were thus accounted for in the baseline contamination subtraction.

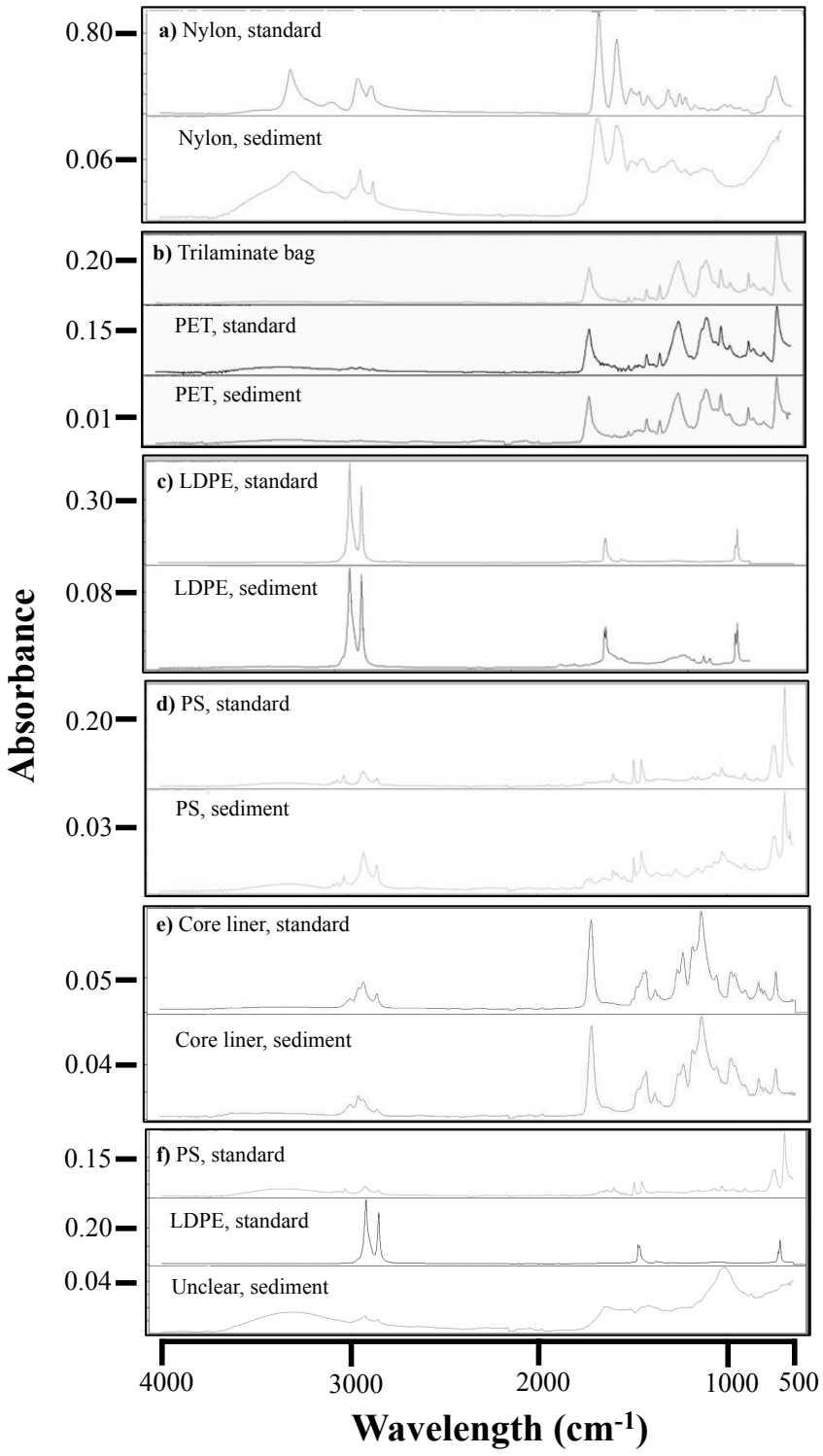

Figure 5.6: FTIR (Fourier Transform Infrared) spectra of plastic standards and sediment samples.

Particles were also assessed for aging/degradation, according to the methods of Brandon et al. (2016). Brandon et al. (2016) found signs of aging and degradation in plastics at the hydroxyl peak (broad peaks from 3100 to 3700, centered at 3300–3400 cm^{-1}), alkenes, or carbon-oxygen bonds (1600-1680 cm^{-1}), and carbonyls (1690-1810, centered at 1715 cm^{-1}). The plastic spectra here were not quantified for degree of aging/degradation, as in Brandon et al. (2016), but only for presence/absence of aging/degradation. If there were only small peaks above the baseline, those samples were not counted as degraded, due to the quality of some of the spectra.

Deposition rate of microplastics

Plastic deposition rate (Particles*100 cm^{-2} $year^{-1}$) was calculated for four individual particle types, between 1834-2010 (Fig. 5.7). Pieces of core liner, identified via FTIR, were separated from the fragment curve, and graphed separately. Fibers dominated the numerical abundance and the shape of the particle accumulation seen in Fig. 5.7.

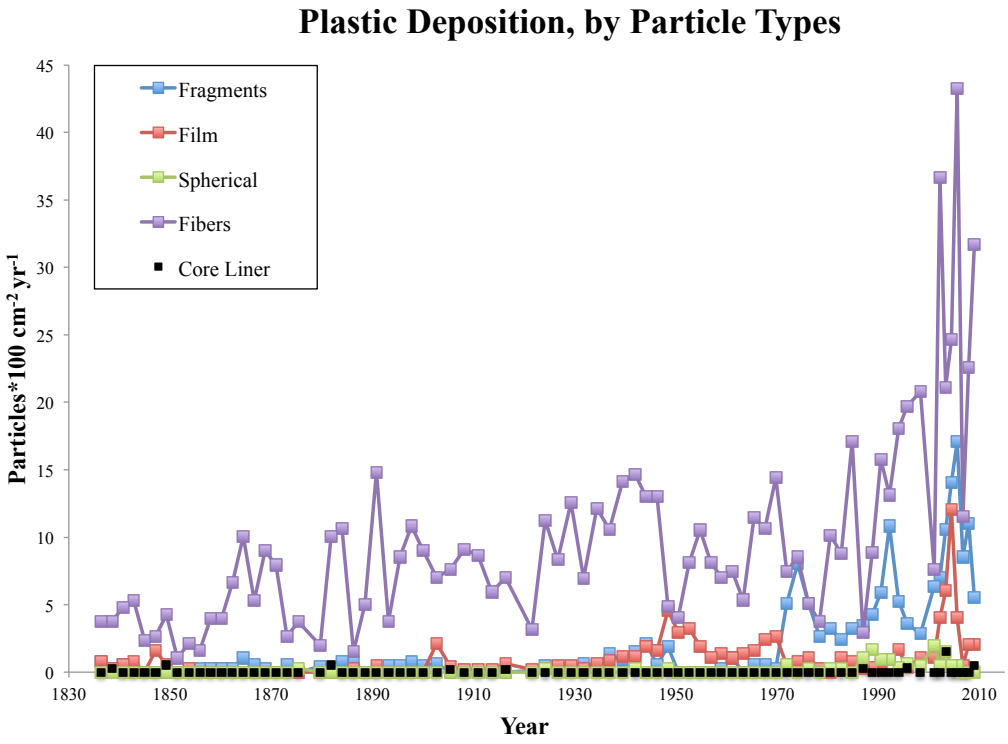

Figure 5.7: Plastic deposition of individual particle types. 1836-2009.

All plastics recorded before 1945 were treated as contamination, because of the low amount of plastic in production at that time (Freinkel 2011, PlasticsEurope 2012). The majority of these pre-1945 plastic pieces were fibers of 500-1000 µm length. The deposition rate of all plastics in each 0.5 cm transverse layer was calculated, and then the average contamination value of 7.8 particles 100 cm^{-2} yr^{-1} from all pre-1945 samples was subtracted from all post-1945 samples (Fig. 5.8). Plastic deposition rates in the Santa Barbara Basin from 1945-2009 have been increasing exponentially, with an approximate doubling time of 16 years.

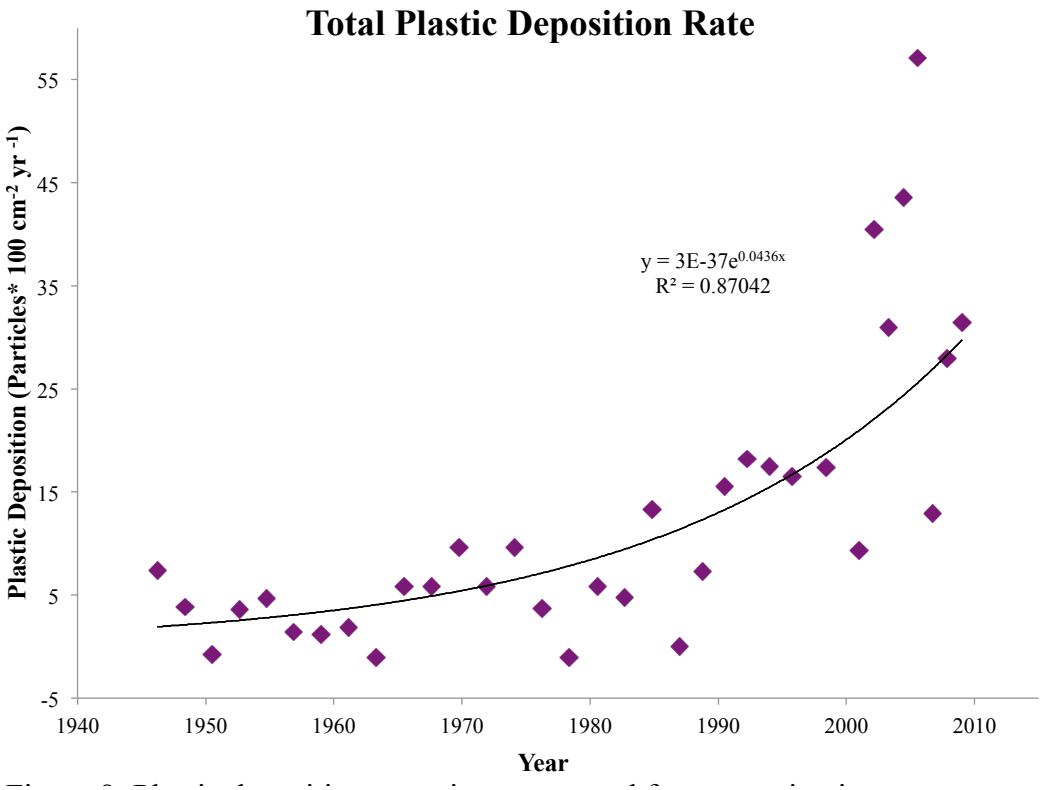

Figure 5.8: Total plastic deposition rate over time, corrected for contamination. All four plastic types combined. 1945-2009, with average value from 1836-1945 subtracted. Exponential curve fitted to deposition values.

Because fibers dominate numerically, the particle deposition rate of only fibers, and just fragments, film, and spherical particles are shown in Fig. 5.9 and Fig. 5.10, respectively. The rate of fiber deposition was better explained by an exponential curve ($r^2 = 0.82$) than that of fragments, films, and spherical particles ($r^2 = 0.57$).

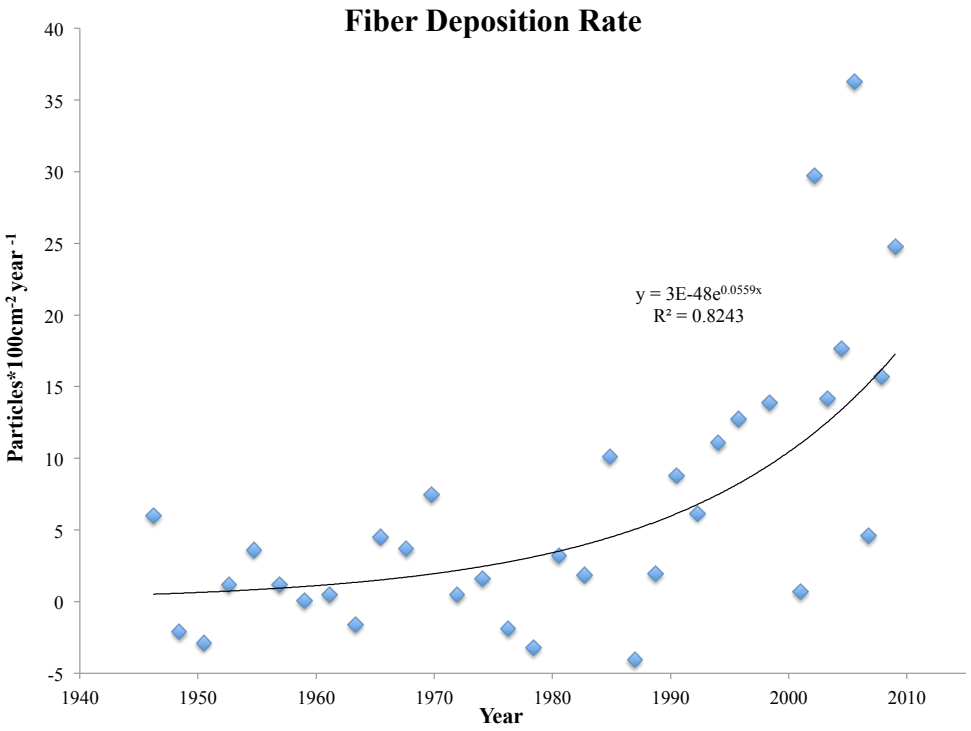

Figure 5.9: Fiber deposition rate, 1945-2009, minus contamination value.

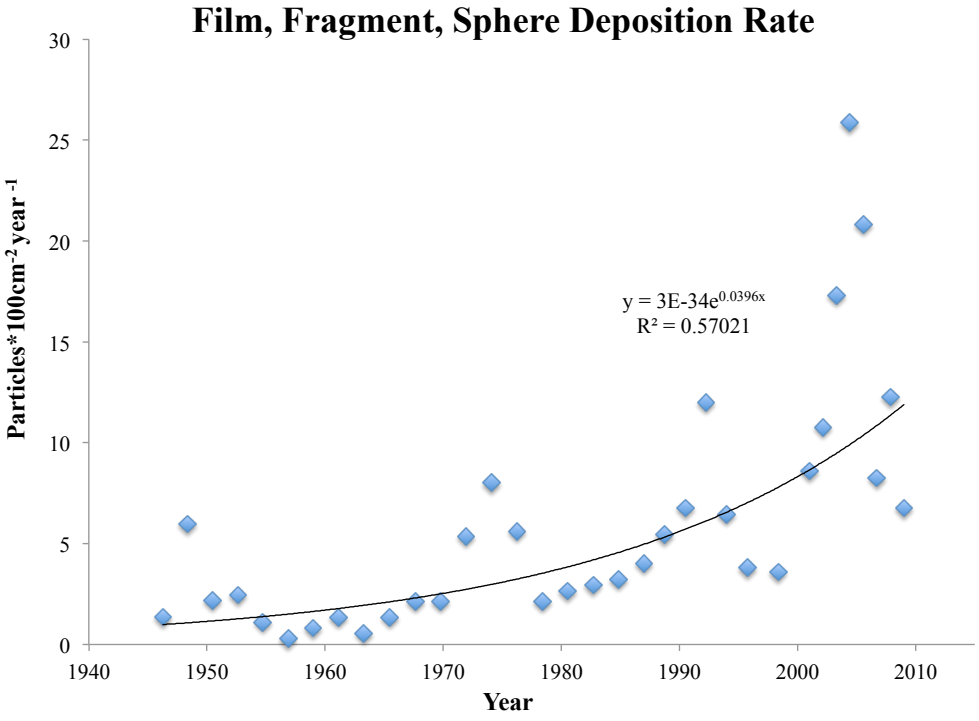

Figure 5.10: Film, fragment, and spherical particle deposition rate, 1945-2009, minus contamination value. Fragments do not include box core liner values.

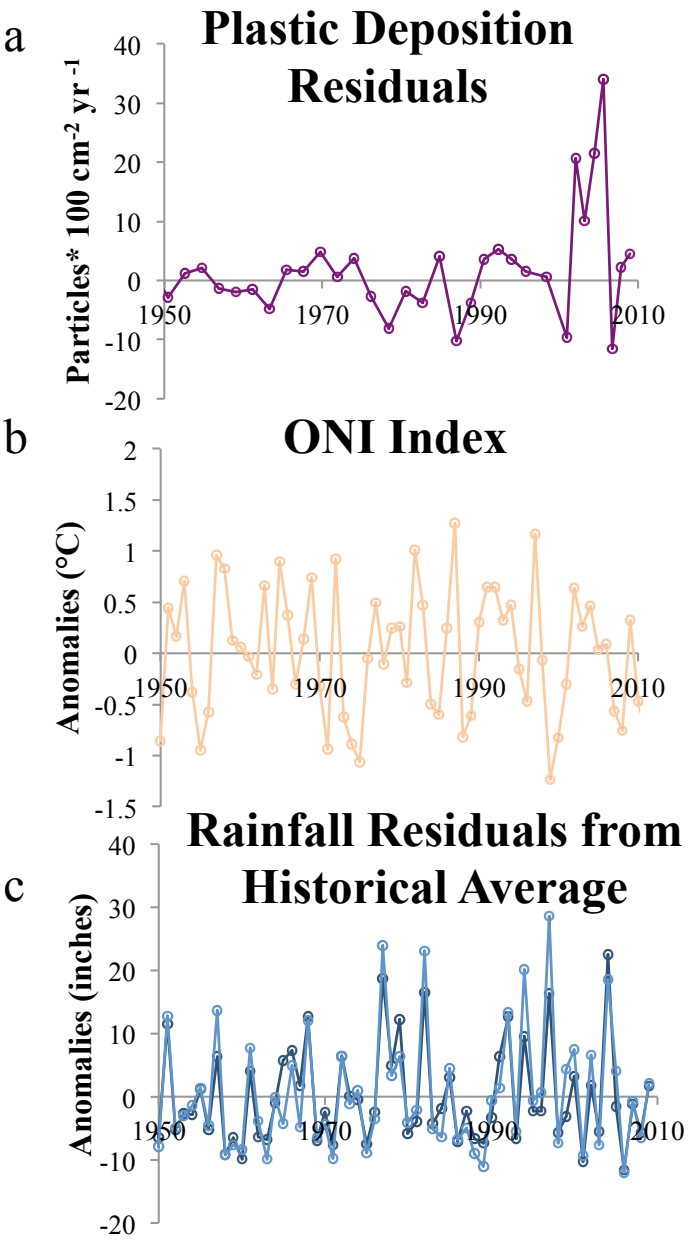

Figure 5.11: Plastic deposition and weather residuals. A) Plastic residuals calculated from exponential fit of all particles. B) ONI residuals calculated from yearly averages. C) Rainfall residuals calculated from 50-year mean. Dark blue: Santa Barbara rainfall. Light blue: Los Angeles rainfall.

Residuals of plastic deposition rate of all plastics from the fitted exponential of Fig. 5.8 show that 1984, 1994, and 2002-5 had anomalously high plastic deposition rates, and 1978, 1985, 1998 and 2007 were years of anomalously low deposition (Fig. 5.11a). Attempts

to relate these anomalies to years of anomalous rainfall showed that plastic deposition residuals were not related to residuals of rainfall in Santa Barbara or Los Angeles County (Fig. 5.11b; LA Almanac, Santa Barbara County; $p > 0.05$), or to the Oceanic Niño index (Fig. 5.11c; ONI; $p > 0.05$).

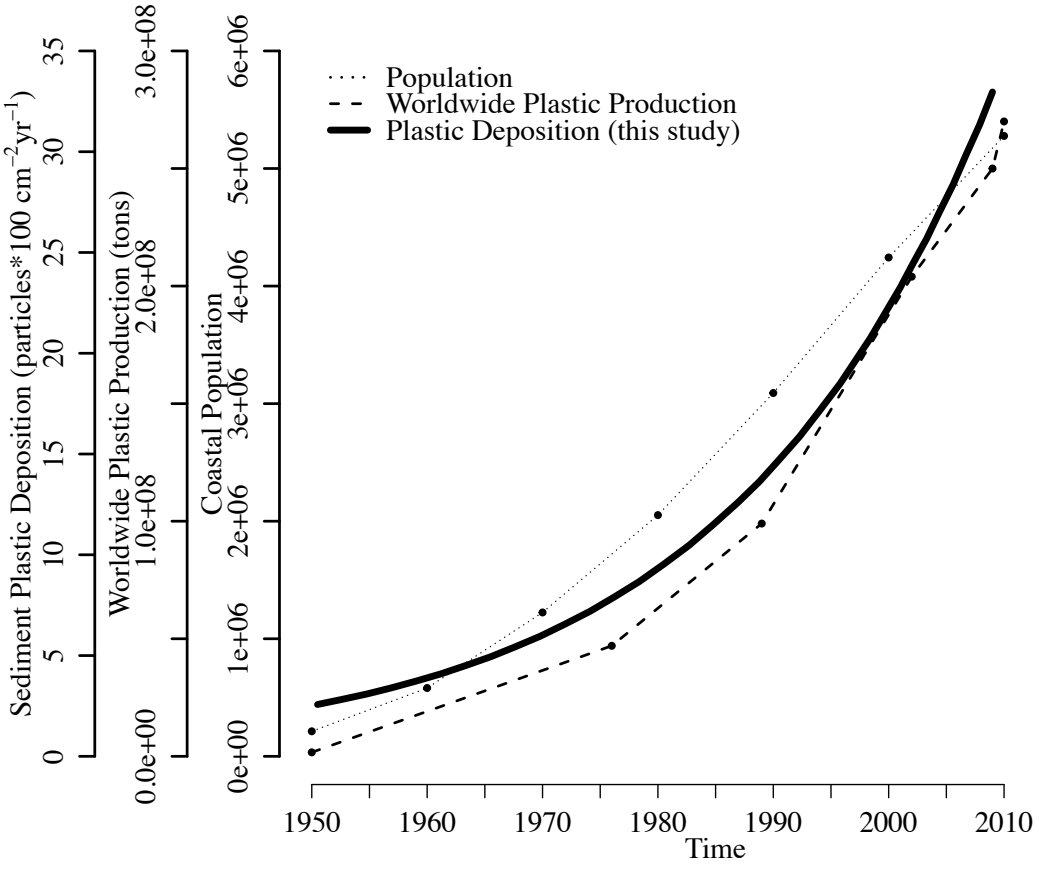

Figure 5.12: Plastic deposition rate in sediment compared to Santa Barbara coastal population and worldwide plastic production, 1950-2010.

Temporal changes in plastic deposition rates in the Santa Barbara Basin correlate strongly with human population increase in Santa Barbara and Ventura counties ($r^2=0.954$, $p < 0.0005$, Fig. 5.12), which have the most direct effect on the Santa Barbara Basin watershed. Plastic deposition rates are also directly correlated with increases in world plastic production ($r^2=0.996$, $p < 0.000001$, Fig. 5.12).

DISCUSSION:

Core chronology

The Santa Barbara Basin is a unique place to answer questions of plastic's accumulation in the benthic ecosystem and in the sedimentary record, because its varved structure allows 1-2 year resolution. This core extends back to 1834, before the advent of plastic, thus this early period provides a control for baseline processing contamination, which is a problem of increasing importance in microplastic research today.

The Anthropocene

In calling for a new geological epoch, the Anthropocene, Zalasiewicz et al. (2017) identified the need for more geological proxies in the sediment record to mark the change from pre-1945 to post-1945, the dawn of the Great Acceleration of modern civilization. Although they pinpointed the release of plutonium in New Mexico in 1945 as perhaps the easiest to identify, they declared that plastic, especially in non-bioturbated sediment, will likely be a very useful stratigraphic marker (Zalasiewicz et al. 2016, Zalasiewicz et al. 2017). After taking into account airborne and processing plastic contamination, we believe our results clearly show this Great Acceleration, by revealing a tightly coupled relationship between worldwide plastic production and the plastic deposited in the sedimentary record.

Plastic particle identification and baseline contamination

Plastics were visually identified in every 0.5 cm transverse layer of the sediment core, including in the layers before 1945. Any plastic before 1945 was treated as contamination due to the low amounts of plastic in production at that time. Contamination is most likely overestimated, as plastic was invented in 1907 (American Chemistry Council 2014), and did exist in small amounts before World War II (Andrady and Neal 2009, Freinkel 2011). So it

is possible that a few of the pieces treated as contamination were in fact deposited in the core. But we assume nearly all of these pieces were added during core processing.

The majority of plastics found in the core overall were fibers, including in the contamination samples, from 1834-1945, where 89.1% of the samples were fibers. This result agrees with both Browne et al. (2011) and Thompson et al. (2004) who found high densities of fibers in sediments, but also Foekema et al. (2013) and Davison and Asch (2011) who found fibers as sources of contamination in their samples. We expected most of the contamination to be airborne fibers, as was found. But the fact that the core spans years before and after the prevalence of plastic allows us to subtract the contamination values and determine that there are still numerous fibers buried in the sediment itself, which agrees with earlier literature (Thompson et al. 2004, Browne et al. 2011). There was an average of 40.3 fibers/layer in post-1945 transverse layers, and 29.6 fibers/layer in pre-1945 layers, so not all fibers in the post-1945 samples were attributable to contamination.

Fourteen percent of the particles in the core were plastic fragments, although many more in the post-1945 samples than pre-1945 samples (Fig. 5.4b). This relative prevalence of fragments post-1945 gives credence to the idea that fibers are more likely to be contamination than fragments, although some of the fragments throughout the core were identified as core liner contamination. Almost no spherical plastics were found in the core, despite the fact that microbeads in consumer products have a diameter of ~400-500 μm and so could have been retained in the 104 μm sieve (Derraik 2002, Eriksen et al. 2013). Although Gregory (1996) found polyethylene microscrubbers in cosmetics in sizes ranging from < 100 μm to > 200 μm in length, which may have passed through the 104 μm sieve, and Fendall and Sewell (2009) found the mode of plastic particles from three cleanser brands

to be < 100 μm, these were irregularly shaped exfoliating microscrubbers, not perfectly spherical microbeads. One of the only perfectly spherical microbeads we found was an un-aged polystyrene microbead from an early sample (circa 1893, before the advent of plastic) and was thus contamination.

The core was sieved through a 104 μm mesh, so the smallest particles caught were > 104 μm. The vast majority of particles was between 500-1000 μm in length, and this trend was remarkably consistent throughout the core, which could be related to visually sorting the core and perhaps missing some smaller particles. But the noteworthy part of these measurements is that these prevalent particles, from 104-1000 μm, are some of the smallest recorded particles in any sediment study (Hidalgo-Ruz et al. 2012) and show that small microplastics are making their way to the marine benthos.

Identifying plastic pieces via FTIR

Overall, FTIR was successful at identifying 53.0% of the visually identified microplastics to plastic type, and identifying an additional 34.5% as plastic. Some of the particles that could not be definitively identified to plastic type had spectra that looked similar to two plastic types but could not be differentiated between the two. This problem was common with particles that showed the triplicate diagnostic peak of polyvinyl chloride (PVC) and polyethylene terephthalate (PET) and particles that showed the doublet peak of polyethylene (PE) and polystyrene (PS), but could not be differentiated further, either because of the quality of the spectra, particle weathering that occluded differentiating regions of the spectra (Brandon et al. 2016), or because the real-world sediment particles contained additives, colorants, etc. that are known to change the shape of FTIR spectra from pure standards (Stark and Matuana 2004, Muasher and Sain 2006). The particles that could

not be identified at all were often too small to give good FTIR spectra or had readings that were not conclusive. Some of those particles were visually recorded at the time of FTIR reading as “thin white fiber” or “reddish black fragment,” so they are likely to still be plastic, but this cannot be confirmed. A few particles had clear spectra similar to the spectra of calcium carbonate, aragonite, or clay (NICODOM 1998). These particles were visually recorded at the time of FTIR reading as “filmy fragment,” “tiny off-white fragment,” “fragment/sediment, looks biological”, and “really thin fiber with sediment still stuck to it.” It is likely then that these particles were biological or sedimentary, and that these particles may have already been removed from the plastic abundance numbers during the secondary proofing of the images by the senior author, but not physically removed from the paleontological sorting tray; thus their sedimentary FTIR readings would not have any effect on the plastic abundance numbers. It is also of note that the FTIR reading of the “really thin fiber with sediment still stuck to it” was likely a FTIR reading of the sediment, and not the thin fiber, giving argument for cleaning all particles before spectral identification, in case of misidentification.

In the future, to improve the identification success, standards of sediment common to the Santa Barbara Basin should be analyzed concurrently with the plastic samples. A micro-FTIR, which can identify very small particles, would also be advisable, for identifying a subset of plastic particles. Despite the uncertainty of some of the spectra, FTIR improved upon the visual identification technique, and definitively identified polystyrene (PS), polyethylene (PE) including low-density polyethylene (LDPE), nylon (polyamide), polyethylene terephthalate (PET), and the core liner within the samples.

It is of note that PE is less dense than seawater, and so would not logically be found

in the sediment. One piece of plastic was also most likely identified as polypropylene (PP), which is also less dense than seawater. However, Browne et al. (2011) found polypropylene and polyethylene (buoyant plastic types) in sediment samples near areas of sewage and wastewater effluent, and it is likely that our samples contain particles from the effluent off the Santa Barbara coastline. These buoyant plastics could have also have sunk to the bottom through fecal or marine snow transport (Cole et al. 2013, Setälä et al. 2014, Zalasiewicz et al. 2016), or via biofouling (Thiel and Gutow 2005, Kaiser et al. 2017). It is also possible that these buoyant pieces were airborne or processing contamination.

We attempted to use the spectral signatures of plastic degradation (Brandon et al. 2016) to assess which pieces were more likely to be contamination. We expected all contamination plastics to be new and pristine, and plastics that were deposited in the sediment to be aged and degraded, but in reality, a marked trend in aging was not seen between layers of the core denoting contamination and non-contamination plastics.

We expected most pristine, un-aged particles to be clothing fibers. Instead, most of the un-aged particles were contaminant fragments of plastic core liner, mixed with only a few un-aged fibers of PET, PVC, and PE.

Deposition rate of microplastics

In previous analysis of fish otoliths from the Cal-ECHOES cores, Jones (2016) used a 3-bin moving average filter in his time series analyses to reduce the effect of alignment errors. Since we only used one core in this analysis and had many more plastic particles than otoliths (44.5 vs. 1 per layer, on average), we did not bin our data. Furthermore, we attempted 3-year data binning, and the exponential fit barely changed.

We assume that this single sediment core is representative of the variability in

deposition rate over the basin. The close alignment of stratigraphic events between the Cal-ECHOES sediment cores and with SPR0901-06KC, the most recently and accurately dated SBB sediment core, indicates similar conditions among cores (Schimmelmann et al. 1990, Hendy et al. 2013, Schimmelmann et al. 2013). Nevertheless, some variability exists between sediment cores. It is likely that a core in a different location compared to the urban watershed would have created a different deposition rate; however, we expect the exponential increase from 1945-2009 to be a robust result.

Correlation of plastic deposition rate

The close correlation between plastic deposition and worldwide plastic production suggests a direct link between the exponential increase in our plastic production and consumption and its effect on ocean ecosystems. Such an increase is now detected not only in surface water but also in a benthic ecosystem and recorded in the sedimentary record. This result calls for limiting our plastic waste stream from entering the ocean, since it is directly mirroring our ever-increasing production trends.

Furthermore, the tightly coupled relationship between the increase in coastal population of the Santa Barbara drainage basin and plastic deposition agrees with Browne et al. (2011), who found more marine microdebris in sediments in areas of high population density, and Eriksen et al. (2013) , who sampled microplastic particles in the Great Lakes and found more microplastic particles km^{-2} at the sampling station directly downstream of Cleveland, OH and Erie, PA than all other stations combined. However these studies use current spatial trends in population to show the effects of population increase on microplastic population, while our study appears to be the first to analyze continuous temporal trends. This tight coupling leads us to predict, barring marked changes in policy or

waste management, that this growing rate of plastic deposition will continue to increase in the future.

CONCLUSIONS:

We sampled sediments of the anaerobic Santa Barbara Basin for plastic particle deposition over time, from 1834-2009. After correcting the plastic deposition values for contamination, we found that in the post-WWII era of heavy plastic consumption, there has been an exponential increase in plastic deposited in sediments of the Santa Barbara Basin. This exponential increase closely correlates with the exponential increase in worldwide plastic production in the last 75 years, and the increase in Southern California population. Although most of this plastic is coming from coastal effluent, there was no correlation found between rain and plastic deposition. Rather, these data show a linkage between plastic production, human coastal population, and plastic deposition in a coastal benthic ecosystem.

ACKNOWLEDGEMENTS:

We thank the captain, crew, and science parties of the Cal-ECHOES research cruise aboard the R/V *Melville*, which was funded through the UC Ship Funds Program and provided the sediment core for this research. We thank Benjamin Fissel, Richard Norris, and Alexandra Hangsterfer for help with processing and imaging the sediment cores. Daniel Hartsook helped process sediment cores sections and sediment material. We thank India Dove, Eliya Baron Lopez, and Sara Higgs for extracting, measuring, and photographing the microplastics in the core. We thank Kayla Blincow for help with R and Linsey Sala for help with microscope photography and editing. Michael Sailor and the Sailor Lab Group made the FTIR work possible. This research was supported by California Sea Grant (Award

NOAA NA14OAR4170075 to David Checkley), the National Science Foundation (NSF Graduate Research Fellowship to William Jones), the National Science Foundation California Current Ecosystem Long Term Ecological Research Site, and private donors.

Chapter 5, in part is currently being prepared for submission for publication of the material. Brandon, Jennifer; Jones, William. The dissertation author was the primary investigator and author of this material.

Table 5.1: Fourier Transform Infrared (FTIR) Spectroscopy Survey of Box Core

Particles from every fifth transect layer measured via FTIR for spectral identification.

Layer number (Year)	Number (%) of particles sampled for FTIR	Ratio of Fibers:Fragments:Film:Spherical	Particles likely plastic	Plastics identified to type	Bad reads	May be sediment
1 (2009.0)	9 (11.5%)	5:1:3:0	5	2	4	0
6 (2003.3)	10 (13.0%)	4:4:2:0	9	3	1	0
11 (1995.8)	8 (10.8%)	3:4:1:0	8	3	0	0
16 (1987.0)	7 (24.1%)	1:5:1:0	5	2	2	0
21 (1976.2)	12 (48.8%)	9:3:0:0	12	5	0	0
26 (1965.5)	12 (23.5%)	8:1:3:0	11	8	1	0
31 (1954.8)	11 (23.9%)	8:1:2:0	7	3	4	0
36 (1944.1)	12 (19.0%)	6:4:2:0	10	8	1	1
41 (1931.8)	7 (20%)	6:1:0:0	6	3	0	1
47 (1916.3)	12 (33.3%)	10:2:0:0	12	7	0	0
51 (1905.4)	12 (31.6%)	8:3:1:0	12	5	0	0
56 (1893.1)	5 (29.4%)	3:1:0:1	4	4	1	0
61 (1881.8)	8 (20.5%)	5:2:1:0	8	5	0	0
66 (1871.0)	6 (20%)	5:1:0:0	6	5	0	0
71 (1860.2)	6 (37.5%)	3:3:0:0	6	5	0	0
76 (1849.3)	8 (44.4%)	5:2:1:0	8	5	0	0
81 (1838.5)	6 (37.5%)	5:1:0:0	4	4	0	2

REFERENCES:

Almanac, L.A. 2017. Total Seasonal Rainfall (Precipitation) Downtown Los Angeles, 1877-2016. National Weather Service, Los Angeles Almanac.

Andrady, A. L., and M. A. Neal. 2009. Applications and societal benefits of plastics. Philosophical Transactions of the Royal Society B: Biological Sciences **364**:1977-1984.

Barron, J. A., D. Bukry, and D. Field. 2010. Santa Barbara Basin diatom and silicoflagellate response to global climate anomalies during the past 2200 years. Quaternary International **215**:34-44.

Baumgartner, T. 1992. Reconstruction of the history of Pacific sardine and Northern anchovy over the past two millennia from sediments of the Santa Barbara Basin, California. California Cooperative Ocean Fisheries Reports **33**:24-40.

Biondi, F., C. Lange, M. Hughes, and W. Berger. 1997. Interdecadal signals during the last millennium (AD 1117–1992) in the varve record of Santa Barbara Basin, California. Geophysical Research Letters **24**:193-196.

Brandon, J., M. Goldstein, and M. D. Ohman. 2016. Long-term aging and degradation of microplastic particles: Comparing in situ oceanic and experimental weathering patterns. Marine Pollution Bulletin **110**:299-308.

Brandon, J. A., Freibott, A. 2017. Patterns of suspended microplastic debris in the California Current and North Pacific Subtropical Gyre, imaged by epifluorescence microscopy. In prep.

Browne, M. A., P. Crump, S. J. Niven, E. Teuten, A. Tonkin, T. Galloway, and R. Thompson. 2011. Accumulation of microplastic on shorelines worldwide: sources and sinks. Environmental science & technology **45**:9175-9179.

Browne, M. A., A. Dissanayake, T. S. Galloway, D. M. Lowe, and R. C. Thompson. 2008. Ingested microscopic plastic translocates to the circulatory system of the mussel, *Mytilus edulis* (L.). Environmental science & technology **42**:5026-5031.

Browne, M. A., T. S. Galloway, and R. C. Thompson. 2010. Spatial patterns of plastic debris along estuarine shorelines. Environmental science & technology **44**:3404-3409.

Browne, M. A., S. J. Niven, T. S. Galloway, S. J. Rowland, and R. C. Thompson. 2013. Microplastic moves pollutants and additives to worms, reducing functions linked to health and biodiversity. Current Biology **23**:2388-2392.

Bureau, U.S. Census. 1995. California: Population of Counties by Decennial Census: 1900 to 1990.

Bureau, U.S. Census. 2010. Population and Housing Units: 1970 to 2010.

C. D. Keeling, S. C. P., R. B. Bacastow, M. Wahlen, T. P. Whorf, M. Heimann, and H. A. Meijer. 2001. Exchanges of atmospheric CO_2 and $^{13}CO_2$ with the terrestrial biosphere and oceans from 1978 to 2000. Scripps Institution of Oceanography, San Diego.

Cole, M., P. Lindeque, E. Fileman, C. Halsband, R. Goodhead, J. Moger, and T. S. Galloway. 2013. Microplastic ingestion by zooplankton. Environmental science & technology **47**:6646-6655.

Corcoran, P. L., T. Norris, T. Ceccanese, M. J. Walzak, P. A. Helm, and C. H. Marvin. 2015. Hidden plastics of Lake Ontario, Canada and their potential preservation in the sediment record. Environmental Pollution **204**:17-25.

Council, American Chemistry 2014. History of Polymers & Plastics for Teachers. http://www.americanchemistry.com/hops/intro_to_plastics/teachers.html.

County, Santa Barbara. Official Monthly and Yearly Rainfall Record: Santa Barbara (Downtown- County Building). Page 3. Santa Barbara County - Flood Control District.

Crutzen, P. J. 2002. Geology of mankind. Nature **415**:23-23.

Davison, P., and R. G. Asch. 2011. Plastic ingestion by mesopelagic fishes in the North Pacific Subtropical Gyre. Marine Ecology Progress Series **432**:173-180.

Derraik, J. G. B. 2002. The pollution of the marine environment by plastic debris: a review. Marine Pollution Bulletin **44**:842-852.

Donohue, M. J., R. C. Boland, C. M. Sramek, and G. A. Antonelis. 2001. Derelict fishing gear in the northwestern Hawaiian Islands: Diving surveys and debris removal in 1999 confirm threat to coral reef ecosystems. Marine Pollution Bulletin **42**:1301-1312.

EPA. 2016. Advancing sustainable materials management: 2014 fact sheet. Advancing Sustainable Materials Management. U.S. Environmental Protection Agency.

Eriksen, M., S. Mason, S. Wilson, C. Box, A. Zellers, W. Edwards, H. Farley, and S. Amato. 2013. Microplastic pollution in the surface waters of the Laurentian Great Lakes. Marine Pollution Bulletin **77**:177-182.

Farrell, P., and K. Nelson. 2013. Trophic level transfer of microplastic: *Mytilus edulis* (L.) to *Carcinus maenas* (L.). Environmental Pollution **177**:1-3.

Fendall, L. S., and M. A. Sewell. 2009. Contributing to marine pollution by washing your face: microplastics in facial cleansers. Marine Pollution Bulletin **58**:1225-1228.

Field, D. B., T. R. Baumgartner, C. D. Charles, V. Ferreira-Bartrina, and M. D. Ohman. 2006. Planktonic foraminifera of the California Current reflect 20th-century warming. Science **311**:63-66.

Field, D. B., T. R. Baumgartner, V. Ferreira, D. Gutierrez, H. Lozano-Montes, R. Salvatteci, and A. Soutar. 2009. Variability from scales in marine sediments and other historical records. Climate change and small pelagic fish. Cambridge University Press, Cambridge, UK:45-63.

Foekema, E. M., C. De Gruijter, M. T. Mergia, J. A. van Franeker, A. J. Murk, and A. A. Koelmans. 2013. Plastic in North sea fish. Environmental science & technology **47**:8818-8824.

Forrest, M., Y. Davies, and J. Davies. 2007. The Rapra collection of infrared spectra of rubbers, plastics and thermoplastic elastomers. Smithers Rapra Publishing.

Freinkel, S. 2011. Plastic: A Toxic Love Story. Houghton Mifflin Harcourt Publishing Company, U.S.A.

GESAMP. 2016. Sources, fates, and effects of microplastics in the marine environment: part two of a global assessment. IMO/FAO/UNESCO-IOC/UNIDO/WMO/IAEA/UN/ UNEP/UNDP Joint Group of Experts on the Scientific Aspects of Marine Environmental Protection.

Goericke, R., S. J. Bograd, and D. S. Grundle. 2015. Denitrification and flushing of the Santa Barbara Basin bottom waters. Deep Sea Research Part II: Topical Studies in Oceanography **112**:53-60.

Goldstein, M. C., M. Rosenberg, and L. Cheng. 2012. Increased oceanic microplastic debris enhances oviposition in an endemic pelagic insect. Biology Letters **8**:817-820.

Graham, E. R., and J. T. Thompson. 2009. Deposit- and suspension-feeding sea cucumbers (Echinodermata) ingest plastic fragments. Journal of Experimental Marine Biology and Ecology **368**:22-29.

Gregory, M. R. 1996. Plastic 'scrubbers' in hand cleansers: a further (and minor) source for marine pollution identified. Marine Pollution Bulletin **32**:867-871.

Grelaud, M., A. Schimmelmann, and L. Beaufort. 2009. Coccolithophore response to climate and surface hydrography in Santa Barbara Basin, California, AD 1917–2004. Biogeosciences **6**:2025-2039.

Hall, N. M., K. L. E. Berry, L. Rintoul, and M. O. Hoogenboom. 2015. Microplastic ingestion by scleractinian corals. Marine Biology **162**:725-732.

Hartline, N. L., N. J. Bruce, S. N. Karba, E. O. Ruff, S. U. Sonar, and P. A. Holden. 2016. Microfiber masses recovered from conventional machine washing of new or aged garments. Environmental science & technology **50**:11532-11538.

Hendy, I. L., L. Dunn, A. Schimmelmann, and D. Pak. 2013. Resolving varve and radiocarbon chronology differences during the last 2000 years in the Santa Barbara Basin sedimentary record, California. Quaternary International **310**:155-168.

Hidalgo-Ruz, V., L. Gutow, R. C. Thompson, and M. Thiel. 2012. Microplastics in the marine environment: a review of the methods used for identification and quantification. Environmental science & technology **46**:3060-3075.

Inman, D. L., and S. A. Jenkins. 1999. Climate change and the episodicity of sediment flux of small California rivers. The Journal of Geology **107**:251-270.

Jambeck, J. R., R. Geyer, C. Wilcox, T. R. Siegler, M. Perryman, A. Andrady, R. Narayan, and K. L. Law. 2015. Plastic waste inputs from land into the ocean. Science **347**:768-771.

Jang, M., W. J. Shim, G. M. Han, M. Rani, Y. K. Song, and S. H. Hong. 2016. Styrofoam debris as a source of hazardous additives for marine organisms. Environmental science & technology **50**:4951-4960.

Jones, W. A. 2016. The Santa Barbara Basin fish assemblage in the last two millennia inferred from otoliths in sediment cores. University of California San Diego.

Kaiser, D., N. Kowalski, S. Oberbeckmann, and J. J. Waniek. 2017. Proving a paradigm: biofilms enhance microplastic deposition.*in* ASLO 2017: Mountains to the Sea, Honolulu, HI.

Kennett, D. J., and J. P. Kennett. 2000. Competitive and cooperative responses to climatic instability in coastal southern California. American Antiquity **65**:379-395.

Kennett, J. P., and B. L. Ingram. 1995. A 20,000-year record of ocean circulation and climate change from the Santa Barbara basin. Nature **377**:510-514.

Law, K. L., S. Morét-Ferguson, N. A. Maximenko, G. Proskurowski, E. E. Peacock, J. Hafner, and C. M. Reddy. 2010. Plastic accumulation in the North Atlantic Subtropical Gyre. Science **329**:1185-1188.

Law, K. L., S. E. Morét-Ferguson, D. S. Goodwin, E. R. Zettler, E. DeForce, T. Kukulka, and G. Proskurowski. 2014. Distribution of surface plastic debris in the eastern Pacific Ocean from an 11-year data set. Environmental science & technology **48**:4732-4738.

Lobo, H., and J. V. Bonilla. 2003. Handbook of plastics analysis. CRC Press.

Mattsson, K., E. V. Johnson, A. Malmendal, S. Linse, L.-A. Hansson, and T. Cedervall. 2017. Brain damage and behavioural disorders in fish induced by plastic nanoparticles delivered through the food chain. Scientific Reports **7:**11452.

Muasher, M., and M. Sain. 2006. The efficacy of photostabilizers on the color change of wood filled plastic composites. Polymer Degradation and Stability **91**:1156-1165.

Murray, F., and P. R. Cowie. 2011. Plastic contamination in the decapod crustacean *Nephrops norvegicus* (Linnaeus, 1758). Marine Pollution Bulletin **62**:1207-1217.

NICODOM. 1998. Inorganic Library of FTIR Spectra. Version 2.0 edition. Nicolet

Ogata, Y., H. Takada, K. Mizukawa, H. Hirai, S. Iwasa, S. Endo, Y. Mato, M. Saha, K. Okuda, A. Nakashima, M. Murakami, N. Zurcher, R. Booyatumanondo, M. P. Zakaria, L. Q. Dung, M. Gordon, C. Miguez, S. Suzuki, C. Moore, H. K. Karapanagioti, S. Weerts, T. McClurg, E. Burres, W. Smith, M. V. Velkenburg, J. S. Lang, R. C. Lang, D. Laursen, B. Danner, N. Stewardson, and R. C. Thompson. 2009. International Pellet Watch: Global monitoring of persistent organic pollutants (POPs) in coastal waters. 1. Initial phase data on PCBs, DDTs, and HCHs. Marine Pollution Bulletin **58**:1437-1446.

PlasticsEurope. 2012. Plastics- The Facts 2012: An analysis of European plastics production, demand and waste data for 2011. http://www.plasticseurope.org/.

Reimers, C. E., K. C. Ruttenberg, D. E. Canfield, M. B. Christiansen, and J. B. Martin. 1996. Porewater pH and authigenic phases formed in the uppermost sediments of the Santa Barbara Basin. Geochimica et Cosmochimica Acta **60**:4037-4057.

Rochman, C. M., E. Hoh, T. Kurobe, and S. J. Teh. 2013. Ingested plastic transfers hazardous chemicals to fish and induces hepatic stress. Scientific Reports **3:**3263.

Ryan, P. G., C. J. Moore, J. A. van Franeker, and C. L. Moloney. 2009. Monitoring the abundance of plastic debris in the marine environment. Philosophical Transactions of the Royal Society of London B: Biological Sciences **364**:1999-2012.

Schimmelmann, A., I. L. Hendy, L. Dunn, D. K. Pak, and C. B. Lange. 2013. Revised~ 2000-year chronostratigraphy of partially varved marine sediment in Santa Barbara Basin, California. GFF **135**:258-264.

Schimmelmann, A., C. B. Lange, and W. H. Berger. 1990. Climatically controlled marker layers in Santa Barbara Basin sediments and fine-scale core-to-core correlation. Limnology and Oceanography **35**:165-173.

Schimmelmann, A., C. B. Lange, E. B. Roark, and B. L. Ingram. 2006. Resources for paleoceanographic and paleoclimatic analysis: a 6,700-year stratigraphy and regional

radiocarbon reservoir-age (ΔR) record based on varve counting and 14C-AMS dating for the Santa Barbara Basin, offshore California, USA. Journal of Sedimentary Research **76**:74-80.

Service, National Weather. 2017. Cold & warm episodes by season. NOAA National Weather Service Climate Prediction Center.

Setälä, O., V. Fleming-Lehtinen, and M. Lehtiniemi. 2014. Ingestion and transfer of microplastics in the planktonic food web. Environmental Pollution **185**:77-83.

Stark, N. M., and L. M. Matuana. 2004. Surface chemistry changes of weathered HDPE/wood-flour composites studied by XPS and FTIR spectroscopy. Polymer Degradation and Stability **86**:1-9.

Steffen, W., W. Broadgate, L. Deutsch, O. Gaffney, and C. Ludwig. 2015. The trajectory of the Anthropocene: the Great Acceleration. The Anthropocene Review **2**:81-98.

Steffen, W., P. J. Crutzen, and J. R. McNeill. 2007. The Anthropocene: are humans now overwhelming the great forces of nature? AMBIO: A Journal of the Human Environment **36**:614-621.

Thiel, M., and L. Gutow. 2005. The ecology of rafting in the marine environment. II. The rafting organisms and community. Oceanography and Marine Biology: an annual review **43**:279-418.

Thompson, R. C., Y. Olsen, R. P. Mitchell, A. Davis, S. J. Rowland, A. W. John, D. McGonigle, and A. E. Russell. 2004. Lost at sea: where is all the plastic? Science **304**:838-838.

Thunell, R. C. 1998. Seasonal and annual variability in particle fluxes in the Gulf of California: A response to climate forcing. Deep Sea Research Part I: Oceanographic Research Papers **45**:2059-2083.

Van Cauwenberghe, L., A. Vanreusel, J. Mees, and C. R. Janssen. 2013. Microplastic pollution in deep-sea sediments. Environmental Pollution **182**:495-499.

Waters, C. N., J. Zalasiewicz, C. Summerhayes, A. D. Barnosky, C. Poirier, A. Gałuszka, A. Cearreta, M. Edgeworth, E. C. Ellis, and M. Ellis. 2016. The Anthropocene is functionally and stratigraphically distinct from the Holocene. Science **351**:aad2622.

Woodall, L. C., A. Sanchez-Vidal, M. Canals, G. L. Paterson, R. Coppock, V. Sleight, A. Calafat, A. D. Rogers, B. E. Narayanaswamy, and R. C. Thompson. 2014. The deep sea is a major sink for microplastic debris. Royal Society open science **1**:140317.

Zalasiewicz, J., A. Smith, M. Hounslow, M. Williams, A. Gale, J. Powell, C. Waters, T. L. Barry, P. R. Bown, and P. Brenchley. 2007. The scale-dependence of strata-time relations: implications for stratigraphic classification. Stratigraphy **4**:139-144.

Zalasiewicz, J., C. N. Waters, J. A. I. do Sul, P. L. Corcoran, A. D. Barnosky, A. Cearreta, M. Edgeworth, A. Gałuszka, C. Jeandel, and R. Leinfelder. 2016. The geological cycle of plastics and their use as a stratigraphic indicator of the Anthropocene. Anthropocene **13**:4-17.

Zalasiewicz, J., C. N. Waters, C. P. Summerhayes, A. P. Wolfe, A. D. Barnosky, A. Cearreta, P. Crutzen, E. Ellis, I. J. Fairchild, and A. Gałuszka. 2017. The Working Group on the Anthropocene: Summary of evidence and interim recommendations. Anthropocene **19**:55-60.

CHAPTER 6: Conclusion of the Dissertation

This chapter summarizes the key findings of my dissertation, and puts these findings in broader context of their significance for our understanding of the ecological effects of marine microplastic, and how these findings can help shape future mitigation and policy decisions.

The age of marine debris can be approximated by its chemical structure

Chapter 2 addresses a pertinent issue in marine debris research and mitigation, the fact that is very hard to tell the point of origin of marine debris, or how long it has been traversing the ocean (Stefatos et al. 1999, Goldstein et al. 2014). Especially with respect to marine microdebris (< 5 mm), tracing these particles to their source is almost impossible (Jambeck et al. 2015). This chapter used a combination of a controlled long-term (3 year) experiment and analyses of field-collected plastic debris to understand temporal changes in chemical structure of plastic polymers and to attempt to approximate their duration at sea.

Chapter 2 utilized Fourier Transform Infrared (FTIR) spectroscopy to analyze the chemical structure and spectral signature of microplastics, and thus identify a given microplastic particle to plastic type, and to attempt to determine the degree of aging the particle had undergone. By conducting an aging experiment with three degradation treatments: sunlight/seawater, sunlight/no seawater, and darkness/seawater, I was able to measure the aging of common consumer plastics (HDPE, LDPE, and PP) that had been exposed to these treatments for a known amount of time. I measured the changes in bonds that are likely to show weather-related change (Albertsson et al. 1987, Lacoste and Carlsson 1992, Socrates 2004, Pavia et al. 2008, Rajakumar et al. 2009). I then compared these

changes in controlled treatments to spectral changes in oceanic plastics collected by Miriam Goldstein on SEAPLEX in 2009, in an attempt to assess the degree of degradation of plastics found in the California Current, North Pacific Subtropical Gyre, and the transition region in between. Chapter 2 found patterns in the aging and degradation of plastics, by examining the changes in hydroxyl, carbonyl, and carbon-oxygen bonds. We found that these bonds changed with aging and weathering, but not linearly, most likely due to the most aged plastic on the outside of particles sloughing off over time, exposing newer, un-aged plastic underneath. This nonlinear aging pattern does not allow an exact timeline of plastic age to be created, but rather an approximate one; I can place plastics in relative time intervals of younger (0-18 months) or older (> 18-30 months). I found plastics in the California Current and transition region were, in general, younger (< 18 months) than plastics found in the center of the North Pacific Subtropical Gyre (> 18 months). This agrees with previous modeled marine debris trajectories (Kubota 1994, Maximenko et al. 2012).

Chapter 2 allows scientists to differentiate from un-weathered and weathered plastics, based on changes in their chemical structure, and allows the amount of time the particles have been weathering in the ocean to be approximated. This has important policy and mitigation implications because it allows scientists to approximate the trajectories and thus, points of origins, of particles, and approximately differentiate the weathering times of particles in different regions of the ocean. This can help assess where cleanup and mitigation efforts should be focused, and whether policy has been effective at curbing new plastic from entering a region. This chapter allows a first step in deciphering the origins of particles of marine microdebris.

There is much more plastic in the ocean than recorded in previous estimates

Chapter 3 quantified a size class of plastic that had been overlooked by the vast majority of previous plastic abundance estimates (Hidalgo-Ruz et al. 2012, Goldstein et al. 2013, Van Sebille et al. 2015), which is plastic smaller than 333 μm. This plastic is known to be ecologically important, because it overlaps with the prey range of so many suspension-feeding animals (Wilson 1973, Harbison and McAlister 1979, Hart 1991, Defossez and Hawkins 1997, Browne et al. 2008, Katija et al. 2017), and is likely to be the most abundant size-class of plastic, because plastic continues to degrade into smaller and smaller pieces (Gilfillan et al. 2009), and smaller plastic degrades faster than larger plastic (Gerritse 2015). This chapter, by quantifying this < 333 μm size class, also attempted to obtain comprehensive, quantitative estimates of oceanic plastic by including the entire size range of plastic. However, these small particles cannot be confirmed as plastic by only visual methods. Therefore, in Chapter 3 my coauthor and I developed a new approach using epifluorescence microscopy to exploit the autofluorescence of plastic in order to quantify nanoplastic suspended in surface seawater. I also created a new sampling protocol that sampled for this smallest plastic and also limited plastic contamination within the sampling scheme.

By utilizing this new technique on surface water samples across a spatial gradient of the NE Pacific, I determined that nanoplastic concentrations are 5-7 orders of magnitude higher than concentrations of microplastics. This result shows that previous net-based sampling severely underestimates the numerical abundance of plastic in the ocean. However, by surface area, microplastics > 333 μm still dominate. While larger plastics may impact the food web at higher trophic levels by interacting directly with large animals, nanoplastics

may have direct impacts on the lower levels of the food web, and their high concentrations may have the most deleterious effect on ecosystems by affecting basal consumers and by bioaccumulating up the food web.

We found the highest abundances of nanoplastic in the extreme nearshore environment, but unlike previous marine debris studies, we found no accumulation of nanoplastics in the North Pacific Subtropical Gyre. However, we found lower plankton: plastic ratios in oligotrophic versus eutrophic ocean regions, which shows that these highly abundant nanoplastics will have differential effects on the plankton communities and food webs in different regions of the ocean, and may have an even stronger ecological effect in the oligotrophic gyre than the eutrophic California Current where there are more alternative prey available. This chapter has important ecological implications for understanding which levels of the food web encounter the most plastic and which regions of the ocean are disproportionately influenced by plastic debris. These results also have important policy implications, because the marine debris community is underestimating the numerical amount of plastic by 5-7 orders of magnitude and must adjust our estimates.

Zooplankton ingest nanoplastic in situ

In Chapter 4, I utilized the same new epifluorescence microscopy approach as Chapter 3 to examine the understudied question of zooplankton ingestion of plastic *in situ*. Salps were dissected as a model species of neustonic filter-feeding zooplankton. Salps are high-throughput, non-selective filter-feeders and are known to have fast-sinking fecal pellets and tunics, and as such, could be key to the transport of plastic from the surface ocean to the benthos. This study is the first to show ingestion of microplastics by salps *in situ*. Every salp

dissected for gut content analysis had ingested plastic, regardless of species, life history stage, or the oceanic region in which they were collected. Aggregates had higher ingestion rates than solitaries. There were no significant differences among ocean regions in nanoplastic ingestion rates. In comparing ambient seawater nanoplastic and microplastic available for ingestion, salps ingested significantly smaller plastic than that observed in their environment. Literature-derived values of ingestion rates, based on literature clearance rates and ambient surface nanoplastic concentrations, were determined to not be realistic estimates for salp ingestion. Our evidence for geographically widespread consumption of plastic debris by salps, regardless of species or body size, leads us to believe that salps are a vector of marine debris transport from the surface of the ocean to the benthos, via their fast-sinking pellets and sinking carcasses, and that salps could be a key missing factor in plastic abundance equations.

Plastic is accumulating in the ocean sedimentary record at an exponential rate

Chapter 5 examines the amount of microplastic in the understudied benthos, and analyzes the temporal distribution of plastic in the sedimentary record. Plastic should only be detected in the sediment in noticeable quantities from 1945-onward, when it became a popular consumer product. The sediment core that was used in this chapter also allowed us to address the research question of airborne processing contamination. Perhaps most importantly, it provides a geological proxy in a varved basin to help determine the sedimentary signature of the new Anthropocene geological epoch (Zalasiewicz et al. 2007, Zalasiewicz et al. 2017).

Chapter 5 examined microplastic deposition in a box core taken in the varved Santa Barbara Basin, an intermittently anoxic basin that allows us to separate layers on the timescale needed to see a pattern within the last 72 years, since the end of WWII. After correcting for airborne processing contamination with values from before 1945, we found plastic deposition rates within the Santa Barbara Basin sediments to increase exponentially post-1945. These changes were tightly correlated with Southern California population increases and worldwide plastic production over the same time period. As future population increases are expected to occur mainly on the coasts worldwide (Browne et al. 2011), and plastic consumption is showing no signs of stopping or slowing (Jambeck et al. 2015), this trend will likely continue into the near future, with potentially serious ecological consequences. These findings have extremely important policy and mitigation implications, because our reliance on plastic is directly mirrored in our sedimentary footprint. It is not just seen in surface microplastics, but is affecting the entire ocean, making it all the way to the benthos. Our plastic consumption habits are also leaving their footprint on sedimentary time; plastic marine debris has been proposed as a good sedimentary proxy for the beginning of the new geological epoch called the Anthropocene (Zalasiewicz et al. 2016, Zalasiewicz et al. 2017). This chapter was able to show that plastic shows an exponential rise right at the beginning of the Great Acceleration (Steffen et al. 2015, Zalasiewicz et al. 2017).

Filling the gaps in abundance estimates

There are large gaps in many predicted estimates of how much plastic should be in the ocean and the amount of plastic that has previously been recorded in the surface ocean (Cózar et al. 2014, Jambeck et al. 2015). However these abundance estimates do not sample

the benthos, which Chapter 5 here shows is a coastal sink for plastic. They do not sample nanoplastics, which Chapter 3 shows are 5-7 orders of magnitude more numerically abundant than larger microplastics. And they do not take into account animal consumption and fecal transport out of surface water, which is addressed in Chapter 4. This thesis argues that all of these variables must be included for a truly comprehensive abundance estimate.

Future Directions

We are seeing many animals capable of eating plastic (Derraik 2002, Thompson et al. 2004, Browne et al. 2008, Graham and Thompson 2009), finding more and more animals eating plastic *in situ*, including salps, and alarmingly, in this thesis, discovering there is more plastic than we believed in the ocean and it is accumulating at an exponential rate. But there is still a lot we do not know.

Chapter 4 illustrated that a model zooplankter ingests microplastic *in situ*, but it only evaluated one type of zooplankton, salps, and provided only preliminary answers about salps' effect on "the plastic cycle". Salps are known to be patchy, and live in "boom and bust" cycles that can dominate ecosystems like the California Current when they are present and outcompete the other zooplankton present for phytoplankton present in surface waters (Alldredge and Madin 1982). Future work would do well to analyze species that are constantly present in surface waters and are known to be outcompeted by salps, like neustonic copepods, and to inspect their plastic and alternative prey ingestion at times of salp presence and absence. It is of note that although salps are thought to be capable of outcompeting other animals for food, which is deleterious to the other species, outcompeting them for suspended plastic nanodebris may actually be harmful to the salps and beneficial to

the other species. A study examining salps' and other zooplankton's toxicity before and after ingestion could be very useful to determine whether salps are actually benefitting the ecosystem by clearing the water of plastic debris.

Salps are known to contribute to the oceanic carbon cycle, by their fecal pellets and dead tunics acting as a vector for moving carbon from the surface water to the benthos (Bruland and Silver 1981, Smith et al. 2014). Although Chapter 4 touched on this issue by noting which salps' guts included visible forming fecal pellets, this is an area that deserves further study. Salp fecal pellets in sediment traps and preserved samples should be dissected and examined for microplastic. Dead tunics on the seafloor should also be dissected, especially after bloom events when they coat the seafloor in high densities (Smith et al. 2014). ROVs could also be used to catch salp fecal pellets or tunics as they sink, in a fashion similar to how individual larvacean houses are caught for microplastic research (Katija et al. 2017). In order to fully parse out whether salp transport is one of the key vectors of the missing plastic in calculated plastic abundance estimates (Cózar et al. 2014, Jambeck et al. 2015), fecal pellets and tunics need to be examined, not just live animals caught in the upper water column.

Although these questions of plastic ingestion and plastic cycling in the water column are essential to understand, perhaps the biggest unanswered questions of microplastic research are in the area of toxicology and bioaccumulation. We know plastic is almost never a simple hydrocarbon chain, but almost always contain BPA, phthalates, and other additives and colorants (Browne et al. 2013, Rochman et al. 2013a, Jang et al. 2016), as well as sorbed persistent organic pollutants, or POPs (Ogata et al. 2009). And we know that animals, including animals sold for human consumption (Rochman 2015), are consuming these

plastic particles. But what we are just starting to understand is how the plastic being consumed by these animals is affecting them, and how, as consumers of marine resources, these plastic residues might affect us. There are many toxicology questions that are still not answered concerning how POPs and other chemicals within plastic harm the consumers. There is also the pressing question of how, or whether, plastic particles are bioaccumulated up the food web. Though some studies are showing that nanoplastics are bioaccumulated up steps of the food web or translocated into muscle tissue (Browne et al. 2008, Mattsson et al. 2017), it is not known whether this always happens, or what the upper size limit of a microplastic piece has to be to pass up the food web. It is also not known whether, when plastic pieces are ingested and passed through the digestive tract, chemicals are still absorbed by the animal and bioaccumulated.

These toxicological questions of bioaccumulation and reduced ecological fitness are of even greater importance when put in the context of this thesis, which shows there are 5-7 orders of magnitude more pieces of plastic than previously estimated, that plastic is extremely small (< 333 μm) and thus easy to ingest by animals at the bottom of the food web, that plastic is often old (> 18-30 months) and thus degraded and more likely to have adsorbed hydrophobic environmental pollutants (Browne et al. 2011), and that plastic is accumulating in the ocean at an exponential rate, tied to our exponential plastic production. This thesis revealed important patterns concerning the temporal and spatial abundances of microplastic, but it is now important to understand the extent of the deleterious effects these plastic pieces may be having on marine ecosystems.

REFERENCES:

Abu-Hilal, A. H., and T. H. Al-Najjar. 2009. Plastic pellets on the beaches of the northern Gulf of Aqaba, Red Sea. Aquatic Ecosystem Health & Management **12**:461-470.

Ahmad, S. R. 1983. UV laser induced fluorescence in high-density polyethylene. Journal of Physics D: Applied Physics **16**:L137.

Albertsson, A.-C., S. O. Andersson, and S. Karlsson. 1987. The mechanism of biodegradation of polyethylene. Polymer Degradation and Stability **18**:73-87.

Alldredge, A., and L. Madin. 1982. Pelagic tunicates: unique herbivores in the marine plankton. Bioscience **32**:655-663.

Alldredge, A. L., U. Passow, and B. E. Logan. 1993. The abundance and significance of a class of large, transparent organic particles in the ocean. Deep Sea Research Part I: Oceanographic Research Papers **40**:1131-1140.

Allen, V., J. H. Kalivas, and R. G. Rodriguez. 1999. Post-consumer plastic identification using Raman spectroscopy. Applied spectroscopy **53**:672-681.

Almanac, L.A. 2017. Total Seasonal Rainfall (Precipitation) Downtown Los Angeles, 1877-2016. National Weather Service, Los Angeles Almanac.

Andrady, A. L. 2011. Microplastics in the marine environment. Marine Pollution Bulletin **62**:1596-1605.

Andrady, A. L., and M. A. Neal. 2009. Applications and societal benefits of plastics. Philosophical Transactions of the Royal Society B: Biological Sciences **364**:1977-1984.

Arthur, C., Baker, J., and Bamford, H. (Eds.). 2009. Proceedings of the International Research Workshop on the Occurrence, Effects, and Fate of Microplastic Marine Debris, September 9-11, 2008, University of Washington Tacoma, Tacoma, WA, USA. U.S. Dept. of Commerce, National Oceanic and Atmospheric Administration, National Ocean Service, Office of Response & Restoration, Silver Spring, Md.

Ayukai, T. 1987. Discriminate feeding of the calanoid copepod *Acartia clausi* in mixtures of phytoplankton and inert particles. Marine Biology **94**:579-587.

Azam, F., and F. Malfatti. 2007. Microbial structuring of marine ecosystems. Nature Reviews Microbiology **5**:782-791.

Backhurst, M. K., and R. G. Cole. 2000. Subtidal benthic marine litter at Kawau Island, north-eastern New Zealand. Journal of Environmental Management **60**:227-237.

Badr, Y., Z. Ali, and R. Khafagy. 1999. UV laser induced fluorescence of unirradiated and irradiated low density polyethylene. Journal of Photochemistry and Photobiology A: Chemistry **124**:35-40.

Barnes, D. K., F. Galgani, R. C. Thompson, and M. Barlaz. 2009. Accumulation and fragmentation of plastic debris in global environments. Philosophical Transactions of the Royal Society B: Biological Sciences **364**:1985-1998.

Barron, J. A., D. Bukry, and D. Field. 2010. Santa Barbara Basin diatom and silicoflagellate response to global climate anomalies during the past 2200 years. Quaternary International **215**:34-44.

Baumgartner, T. 1992. Reconstruction of the history of Pacific sardine and Northern anchovy over the past two millennia from sediments of the Santa Barbara Basin, California. CalCOFI Reports. **33**:24-40.

Berner, L. D. 1967. Distributional atlas of Thaliacea in the California Current region. California Cooperative Oceanic Fisheries Investigations Atlas **8**:1-322.

Besseling, E., A. Wegner, E. M. Foekema, M. J. Van Den Heuvel-Greve, and A. A. Koelmans. 2012. Effects of microplastic on fitness and PCB bioaccumulation by the lugworm *Arenicola marina* (L.). Environmental science & technology **47**:593-600.

Biondi, F., C. Lange, M. Hughes, and W. Berger. 1997. Interdecadal signals during the last millennium (AD 1117–1992) in the varve record of Santa Barbara Basin, California. Geophysical Research Letters **24**:193-196.

Bocklitz, T., A. Walter, K. Hartmann, P. Rösch, and J. Popp. 2011. How to pre-process Raman spectra for reliable and stable models. Analytica chimica acta **704**:47-56.

Bone, Q. 1998. The biology of pelagic tunicates. Oxford University Press, Oxford.

Bone, Q., C. Carre, and P. Chang. 2003. Tunicate feeding filters. Journal of the Marine Biological Association of the UK **83**:907-919.

Bowley, H. J., D. L. Gerrard, J. D. Louden, G. Turrell, D. J. Gardiner, and P. R. Graves. 2012. Practical Raman Spectroscopy. Springer Science & Business Media.

Brandon, J., M. Goldstein, and M. D. Ohman. 2016. Long-term aging and degradation of microplastic particles: Comparing in situ oceanic and experimental weathering patterns. Marine Pollution Bulletin. **110**:299-308.

Brandon, J. A., and A. Freibott. 2017. Patterns of suspended microplastic debris in the California Current and North Pacific Subtropical Gyre, imaged by epifluorescence microscopy. In prep.

Browne, M. A., P. Crump, S. J. Niven, E. Teuten, A. Tonkin, T. Galloway, and R. Thompson. 2011. Accumulation of microplastic on shorelines worldwide: sources and sinks. Environmental science & technology **45**:9175-9179.

Browne, M. A., A. Dissanayake, T. S. Galloway, D. M. Lowe, and R. C. Thompson. 2008. Ingested microscopic plastic translocates to the circulatory system of the mussel, *Mytilus edulis* (L.). Environmental science & technology **42**:5026-5031.

Browne, M. A., T. S. Galloway, and R. C. Thompson. 2010. Spatial patterns of plastic debris along estuarine shorelines. Environmental science & technology **44**:3404-3409.

Browne, M. A., S. J. Niven, T. S. Galloway, S. J. Rowland, and R. C. Thompson. 2013. Microplastic moves pollutants and additives to worms, reducing functions linked to health and biodiversity. Current Biology **23**:2388-2392.

Bruland, K., and M. Silver. 1981. Sinking rates of fecal pellets from gelatinous zooplankton (salps, pteropods, doliolids). Marine Biology **63**:295-300.

Bureau, U.S. Census. 1995. California: Population of counties by decennial census: 1900 to 1990.

Bureau, U.S. Census. 2010. Population and housing units: 1970 to 2010.

C. D. Keeling, S. C. P., R. B. Bacastow, M. Wahlen, T. P. Whorf, M. Heimann, and H. A. Meijer. 2001. Exchanges of atmospheric CO_2 and $^{13}CO_2$ with the terrestrial biosphere and oceans from 1978 to 2000. Scripps Institution of Oceanography, San Diego.

Carlton, J. T., J. W. Chapman, J. B. Geller, J. A. Miller, D. A. Carlton, M. I. McCuller, N. C. Treneman, B. P. Steves, and G. M. Ruiz. 2017. Tsunami-driven rafting: Transoceanic species dispersal and implications for marine biogeography. Science **357**:1402-1406.

Caron, D. A. 1983. Technique for enumeration of heterotrophic and phototrophic nanoplankton, using epifluorescence microscopy, and comparison with other procedures. Applied and Environmental Microbiology **46**:491-498.

Caron, D. A., L. P. Madin, and J. J. Cole. 1989. Composition and degradation of salp fecal pellets: implications for vertical flux in oceanic environments. Journal of Marine Research **47**:829-850.

Carpenter, E. J., and K. Smith. 1972. Plastics on the Sargasso Sea surface. Science **175**:1240-1241.

CCE-LTER. LTER Process Cruises. California Current Ecosystem Long Term Ecological Research.

Chan, W. Y., and J. Witting. 2012. The impact of microplastics on salp feeding in the tropical Pacific. Australian National University Undergraduate Research Journal **4**.

Cole, M., P. Lindeque, E. Fileman, C. Halsband, R. Goodhead, J. Moger, and T. S. Galloway. 2013. Microplastic ingestion by zooplankton. Environmental science & technology **47**:6646-6655.

Colton, J. B., F. D. Knapp, and B. R. Burns. 1974. Plastic particles in surface waters of the northwestern Atlantic. Science **185**:491-497.

Connection, Population. 2003. World Population: A Graphic Simulation of the History of Human Population Growth. PBS NOVA, http://www.pbs.org/wgbh/nova/earth/global-population-growth.html.

Conservancy, Ocean. 2010. Trash Travels. International Coastal Cleanup 25th Anniversary report.

Corcoran, P. L., T. Norris, T. Ceccanese, M. J. Walzak, P. A. Helm, and C. H. Marvin. 2015. Hidden plastics of Lake Ontario, Canada and their potential preservation in the sediment record. Environmental Pollution **204**:17-25.

Council, American Chemistry. 2014a. History of Polymers & Plastics for Teachers. http://www.americanchemistry.com/hops/intro_to_plastics/teachers.html.

Council, American Chemistry. 2014b. Life Cycle of a Plastic Product. http://www.americanchemistry.com/s_plastics/doc.asp?CID=1571&DID=5972.

Council, American Chemistry. 2014c. Resin Identification Codes. http://plastics.americanchemistry.com/Plastic-Resin-Codes-PDF.

County, Santa Barbara. Official Monthly and Yearly Rainfall Record: Santa Barbara (Downtown- County Building). Page 3. Santa Barbara County - Flood Control District.

Cózar, A., F. Echevarría, J. I. González-Gordillo, X. Irigoien, B. Úbeda, S. Hernández-León, Á. T. Palma, S. Navarro, J. García-de-Lomas, and A. Ruiz. 2014. Plastic debris in the open ocean. Proceedings of the National Academy of Sciences **111**:10239-10244.

Crutzen, P. J. 2002. Geology of mankind. Nature **415**:23-23.

Davison, P., and R. G. Asch. 2011. Plastic ingestion by mesopelagic fishes in the North Pacific Subtropical Gyre. Marine Ecology Progress Series **432**:173-180.

Defossez, J.-M., and A. Hawkins. 1997. Selective feeding in shellfish: size-dependent rejection of large particles within pseudofaeces from *Mytilus edulis*, *Ruditapes philippinarum* and *Tapes decussatus*. Marine Biology **129**:139-147.

Derraik, J. G. B. 2002. The pollution of the marine environment by plastic debris: a review. Marine Pollution Bulletin **44**:842-852.

Desforges, J.-P. W., Moira Galbraith, and Peter S. Ross 2015. Ingestion of microplastics by zooplankton in the Northeast Pacific Ocean. Archives of environmental contamination and toxicology **69**:320-330.

DiraMED. Raman Applications. Research of non-invasive Raman spectroscopy based diagnostic systems and application to medical and narcotic screening, monitoring, and therapeutic treatment of substances *in vivo.* *http://www.diramed.com/raman_applications.html*

Donohue, M. J., R. C. Boland, C. M. Sramek, and G. A. Antonelis. 2001. Derelict fishing gear in the northwestern Hawaiian Islands: Diving surveys and debris removal in 1999 confirm threat to coral reef ecosystems. Marine Pollution Bulletin **42**:1301-1312.

Dotmar. 2014. Density of Plastics. http://www.dotmar.com.au/density.html.

Dupont. 2014a. Dupont Heritage Timeline: 1939 Nylon. History, http://www2.dupont.com/Phoenix_Heritage/en_US/1939_c_detail.html.

Dupont. 2014b. Dupont Heritage Timeline: 1941 Orlon. History, http://www2.dupont.com/Phoenix_Heritage/en_US/1941_detail.html.

EPA. 2016. Advancing Sustainable Materials Management:2014 Fact Sheet. Advancing Sustainable Materials Management. U.S. Environmental Protection Agency.

EPA, U. S. 2012. Rapid method for acid digestion of glass-fiber and organic/polymeric composition filters and swipes prior to isotopic uranium, plutonium, americium, strontium, and radium analyses for environmental remediation following homeland security events. *in* Office of Air and Radiation, editor. U.S. Environmental Protection Agency, Montgomery, AL.

Eriksen, M., L. C. Lebreton, H. S. Carson, M. Thiel, C. J. Moore, J. C. Borerro, F. Galgani, P. G. Ryan, and J. Reisser. 2014. Plastic pollution in the world's oceans: More than 5 trillion plastic pieces weighing over 250,000 tons afloat at sea. PloS one **9**:e111913.

Eriksen, M., S. Mason, S. Wilson, C. Box, A. Zellers, W. Edwards, H. Farley, and S. Amato. 2013. Microplastic pollution in the surface waters of the Laurentian Great Lakes. Marine Pollution Bulletin **77**:177-182.

Everall, N. 2008. The influence of out-of-focus sample regions on the surface specificity of confocal Raman microscopy. Applied spectroscopy **62**:591-598.

Farrell, P., and K. Nelson. 2013. Trophic level transfer of microplastic: *Mytilus edulis* (L.) to *Carcinus maenas* (L.). Environmental Pollution **177**:1-3.

Fedele, M. 1933a. Sul complesso delle funzioni che intervengono nel meccanismo ingestivo dei Salpidae. Atti della Accademia Nazionale dei Lincei Rc **17**:241-245.

Fedele, M. 1933b. Sulla nutrizione degli animali pelagici III. Richerche sui Salpidae. Bollettino della Societa dei Naturalisti in Napoli **45**:49-118.

Fendall, L. S., and M. A. Sewell. 2009. Contributing to marine pollution by washing your face: microplastics in facial cleansers. Marine Pollution Bulletin **58**:1225-1228.

Field, D. B., T. R. Baumgartner, C. D. Charles, V. Ferreira-Bartrina, and M. D. Ohman. 2006. Planktonic foraminifera of the California Current reflect 20th-century warming. Science **311**:63-66.

Field, D. B., T. R. Baumgartner, V. Ferreira, D. Gutierrez, H. Lozano-Montes, R. Salvatteci, and A. Soutar. 2009. Variability from scales in marine sediments and other historical records. Climate change and small pelagic fish. Cambridge University Press, Cambridge, UK:45-63.

Foekema, E. M., C. De Gruijter, M. T. Mergia, J. A. van Franeker, A. J. Murk, and A. A. Koelmans. 2013. Plastic in North Sea fish. Environmental science & technology **47**:8818-8824.

Forrest, M., Y. Davies, and J. Davies. 2007. The Rapra collection of infrared spectra of rubbers, plastics and thermoplastic elastomers. Smithers Rapra Publishing.

Fraser, J. H. 1947. Thaliacea: I. Family: Salpidae. Pages 1-4 *in* Conseil International pour L'Exploration de La Mer, editor.

Freibott, A., L. Linacre, and M. R. Landry. 2014. A slide preparation technique for light microscopy analysis of ciliates preserved in acid Lugol's fixative. Limnology and Oceanography: Methods **12**:54-62.

Freinkel, S. 2011. Plastic: A Toxic Love Story. Houghton Mifflin Harcourt Publishing Company, U.S.A.

Frost, B. W. 1977. Feeding behavior of *Calanus pacificus* in mixtures of food particles. Limnology and Oceanography **22**:472-491.

Fry, D. M., S. I. Fefer, and L. Sileo. 1987. Ingestion of plastic debris by Laysan albatrosses and wedge-tailed shearwaters in the Hawaiian Islands. Marine Pollution Bulletin **18**:339-343.

Gerritse, L. J., and D.Vethaak. 2015. CLEANSEA Special Newsletter. CLEANSEA.

GESAMP. 2015. Sources, fate and effects of microplastics in the marine environment: a global assessment. IMO/FAO/UNESCO-IOC/UNIDO/WMO/IAEA/UN/ UNEP/UNDP Joint Group of Experts on the Scientific Aspects of Marine Environmental Protection.

GESAMP. 2016. Sources, fates, and effects of microplastics in the marine environment: part two of a global assessment. IMO/FAO/UNESCO-IOC/UNIDO/WMO/IAEA/UN/ UNEP/UNDP Joint Group of Experts on the Scientific Aspects of Marine Environmental Protection.

Gilfillan, L. R., M. D. Ohman, M. J. Doyle, and W. Watson. 2009. Occurrence of plastic micro-debris in the southern California Current system. California Cooperative Oceanic Fisheries Investigations Reports **50**:123-133.

Goericke, R., S. J. Bograd, and D. S. Grundle. 2015. Denitrification and flushing of the Santa Barbara Basin bottom waters. Deep Sea Research Part II: Topical Studies in Oceanography **112**:53-60.

Goldstein, M. C., H. S. Carson, and M. Eriksen. 2014. Relationship of diversity and habitat area in North Pacific plastic-associated rafting communities. Marine Biology **161**:1441-1453.

Goldstein, M. C., and D. S. Goodwin. 2013. Gooseneck barnacles (*Lepas* spp.) ingest microplastic debris in the North Pacific Subtropical Gyre. PeerJ **1**:e184.

Goldstein, M. C., M. Rosenberg, and L. Cheng. 2012. Increased oceanic microplastic debris enhances oviposition in an endemic pelagic insect. Biology Letters **8**:817-820.

Goldstein, M. C., A. J. Titmus, and M. Ford. 2013. Scales of spatial heterogeneity of plastic marine debris in the northeast Pacific ocean. PloS one **8**:e80020.

Govindarajan, A. F., A. Bucklin, and L. P. Madin. 2011. A molecular phylogeny of the Thaliacea. Journal of Plankton Research **33**:843-853.

Graham, E. R., and J. T. Thompson. 2009. Deposit- and suspension-feeding sea cucumbers (Echinodermata) ingest plastic fragments. Journal of Experimental Marine Biology and Ecology **368**:22-29.

Grasselli, J. G., and B. J. Bulkin. 1991. Analytical Raman Spectroscopy. Wiley.

Gregory, M. R. 1996. Plastic 'scrubbers' in hand cleansers: a further (and minor) source for marine pollution identified. Marine Pollution Bulletin **32**:867-871.

Gregory, M. R. 2009. Environmental implications of plastic debris in marine settings—entanglement, ingestion, smothering, hangers-on, hitch-hiking and alien invasions.

Philosophical Transactions of the Royal Society B: Biological Sciences **364**:2013-2025.

Grelaud, M., A. Schimmelmann, and L. Beaufort. 2009. Coccolithophore response to climate and surface hydrography in Santa Barbara Basin, California, AD 1917–2004. Biogeosciences **6**:2025-2039.

Hall, N. M., K. L. E. Berry, L. Rintoul, and M. O. Hoogenboom. 2015. Microplastic ingestion by scleractinian corals. Marine Biology **162**:725-732.

Harbison, G., and R. Campenot. 1979. Effects of temperature on the swimming of salps (Tunicata, Thaliacea): Implications for vertical migration. Limnology and Oceanography **24**:1081-1091.

Harbison, G., and V. McAlister. 1979. The filter-feeding rates and particle retention efficiencies of three species of *Cyclosalpa* (Tunicata, Thaliacea). Limnology and Oceanography **24**:875-892.

Harbison, G., V. L. McAlister, and R. Gilmer. 1986. The response of the salp, *Pegea confoederata*, to high levels of particulate material: Starvation in the midst of plenty. Limnology and Oceanography **31**:371-382.

Harrison, J. P., J. J. Ojeda, and M. E. Romero-González. 2012. The applicability of reflectance micro-Fourier-transform infrared spectroscopy for the detection of synthetic microplastics in marine sediments. Science of the Total Environment **416**:455-463.

Hart, M. W. 1991. Particle captures and the method of suspension feeding by echinoderm larvae. The Biological Bulletin **180**:12-27.

Hartline, N. L., N. J. Bruce, S. N. Karba, E. O. Ruff, S. U. Sonar, and P. A. Holden. 2016. Microfiber masses recovered from conventional machine washing of new or aged garments. Environmental science & technology **50**:11532-11538.

Henderson, J. R. 2001. A pre- and post-MARPOL Annex V summary of Hawaiian monk seal entanglements and marine debris accumulation in the Northwestern Hawaiian Islands, 1982–1998. Marine Pollution Bulletin **42**:584-589.

Hendy, I. L., L. Dunn, A. Schimmelmann, and D. Pak. 2013. Resolving varve and radiocarbon chronology differences during the last 2000 years in the Santa Barbara Basin sedimentary record, California. Quaternary International **310**:155-168.

Henschke, N., D. A. Bowden, J. D. Everett, S. P. Holmes, R. J. Kloser, R. W. Lee, and I. M. Suthers. 2013. Salp-falls in the Tasman Sea: a major food input to deep-sea benthos. Marine Ecology Progress Series **491**:165-175.

Hewes, C. D., and O. Holm-Hansen. 1983. A method for recovering nanoplankton from filters for identification with the microscope: the filter-transfer-freeze (FTF) technique. Limnology and Oceanography **28**:389-394.

Hidalgo-Ruz, V., L. Gutow, R. C. Thompson, and M. Thiel. 2012. Microplastics in the marine environment: a review of the methods used for identification and quantification. Environmental science & technology **46**:3060-3075.

Hoffman, D. L. 1989. Settlement and recruitment patterns of a pedunculate barnacle, *Pollicipes polymerus* (Sowerby), off La Jolla, California. Journal of Experimental Marine Biology and Ecology **125**:83-98.

Huskin, I., M. J. Elices, and R. Anadón. 2003. Salp distribution and grazing in a saline intrusion off NW Spain. Journal of Marine Systems **42**:1-11.

Inman, D. L., and S. A. Jenkins. 1999. Climate change and the episodicity of sediment flux of small California rivers. The Journal of Geology **107**:251-270.

Jambeck, J. R., R. Geyer, C. Wilcox, T. R. Siegler, M. Perryman, A. Andrady, R. Narayan, and K. L. Law. 2015. Plastic waste inputs from land into the ocean. Science **347**:768-771.

Jang, M., W. J. Shim, G. M. Han, M. Rani, Y. K. Song, and S. H. Hong. 2016. Styrofoam debris as a source of hazardous additives for marine organisms. Environmental science & technology **50**:4951-4960.

Jones, W. A. 2016. The Santa Barbara Basin fish assemblage in the last two millennia inferred from otoliths in sediment cores. University of California San Diego. Thesis, unpublished.

Kaiser, D., N. Kowalski, S. Oberbeckmann, and J. J. Waniek. 2017. Proving a paradigm: Biofilms enhance microplastic deposition. *in* ASLO 2017: Mountains to the Sea, Honolulu, HI.

Karl, D. M. 1999. A sea of change: biogeochemical variability in the North Pacific Subtropical Gyre. Ecosystems **2**:181-214.

Katija, K., C. A. Choy, R. E. Sherlock, A. D. Sherman, and B. H. Robison. 2017. From the surface to the seafloor: How giant larvaceans transport microplastics into the deep sea. Science Advances **3**:e1700715.

Kemp, P. F., J. J. Cole, B. F. Sherr, and E. B. Sherr. 1993. Handbook of methods in aquatic microbial ecology. CRC press.

Kennett, D. J., and J. P. Kennett. 2000. Competitive and cooperative responses to climatic instability in coastal southern California. American Antiquity **65**:379-395.

Kennett, J. P., and B. L. Ingram. 1995. A 20,000-year record of ocean circulation and climate change from the Santa Barbara basin. Nature **377**:510-514.

Koelmans, A. A., E. Besseling, and W. J. Shim. 2015. Nanoplastics in the aquatic environment. Critical review. Pages 325-340 Marine anthropogenic litter. Springer.

Kremer, P., and L. P. Madin. 1992. Particle retention efficiency of salps. Journal of Plankton Research **14**:1009-1015.

Kubota, M. 1994. A Mechanism for the Accumulation of Floating Marine Debris North of Hawaii. Journal of Physical Oceanography **24**:1059-1064.

Lacoste, J., and D. Carlsson. 1992. Gamma-, photo-, and thermally-initiated oxidation of linear low density polyethylene: A quantitative comparison of oxidation products. Journal of Polymer Science Part A: Polymer Chemistry **30**:493-500.

Langhals, H., D. Zgela, and T. Schlücker. 2015. Improved High Performance Recycling of Polymers by Means of Bi-Exponential Analysis of Their Fluorescence Lifetimes. Green and Sustainable Chemistry **5**:92.

Lavaniegos, B. E., and M. D. Ohman. 2003. Long-term changes in pelagic tunicates of the California Current. Deep Sea Research Part II: Topical Studies in Oceanography **50**:2473-2498.

Law, K. L., S. Morét-Ferguson, N. A. Maximenko, G. Proskurowski, E. E. Peacock, J. Hafner, and C. M. Reddy. 2010. Plastic accumulation in the North Atlantic subtropical gyre. Science **329**:1185-1188.

Law, K. L., S. E. Morét-Ferguson, D. S. Goodwin, E. R. Zettler, E. DeForce, T. Kukulka, and G. Proskurowski. 2014. Distribution of surface plastic debris in the eastern Pacific Ocean from an 11-year data set. Environmental science & technology **48**:4732-4738.

Lechner, A., H. Keckeis, F. Lumesberger-Loisl, B. Zens, R. Krusch, M. Tritthart, M. Glas, and E. Schludermann. 2014. The Danube so colourful: A potpourri of plastic litter outnumbers fish larvae in Europe's second largest river. Environmental Pollution **188**:177-181.

Lobo, H., and J. V. Bonilla. 2003. Handbook of plastics analysis. CRC Press.

Lozano, R., and J. Mouat. 2009. Marine litter in the North-East Atlantic region: Assessment and priorities for response. KIMO International. 9781906840266.

Lynn, R. J., and J. J. Simpson. 1987. The California Current System: The seasonal variability of its physical characteristics. Journal of Geophysical Research: Oceans (1978–2012) **92**:12947-12966.

Madin, L. 1974. Field observations on the feeding behavior of salps (Tunicata: Thaliacea). Marine Biology **25**:143-147.

Madin, L. 1982. Production, composition and sedimentation of salp fecal pellets in oceanic waters. Marine Biology **67**:39-45.

Madin, L. 1990. Aspects of jet propulsion in salps. Canadian Journal of Zoology **68**:765-777.

Madin, L., and C. Cetta. 1984. The use of gut fluorescence to estimate grazing by oceanic salps. Journal of Plankton Research **6**:475-492.

Markwort, L., and B. Kip. 1996. Micro-Raman imaging of heterogeneous polymer systems: General applications and limitations. Journal of Applied Polymer Science **61**:231-254.

Masterson, K. 2009. The history of plastic: From billiards to bibs. Plastic Peril? NPR, http://www.npr.org/templates/story/story.php?storyId=114331762.

Mattsson, K., E. V. Johnson, A. Malmendal, S. Linse, L.-A. Hansson, and T. Cedervall. 2017. Brain damage and behavioural disorders in fish induced by plastic nanoparticles delivered through the food chain. Scientific Reports **7**:11452.

Maximenko, N., J. Hafner, and P. Niiler. 2012. Pathways of marine debris derived from trajectories of Lagrangian drifters. Marine Pollution Bulletin **65**:51-62.

Meehl, G. A. 1982. Characteristics of surface current flow inferred from a global ocean current data set. Journal of Physical Oceanography **12**:538-555.

Moody, S. 2010. Washed Up: The curious journeys of flotsam and jetsam. Sasquatch Books.

Moore, C. J., S. L. Moore, M. K. Leecaster, and S. B. Weisberg. 2001. A comparison of plastic and plankton in the North Pacific Central Gyre. Marine Pollution Bulletin **42**:1297-1300.

Muasher, M., and M. Sain. 2006. The efficacy of photostabilizers on the color change of wood filled plastic composites. Polymer Degradation and Stability **91**:1156-1165.

Murray, F., and P. R. Cowie. 2011. Plastic contamination in the decapod crustacean *Nephrops norvegicus* (Linnaeus, 1758). Marine Pollution Bulletin **62**:1207-1217.

NICODOM. 1998. Inorganic Library of FTIR Spectra. Version 2.0 edition. Nicolet

Niiler, P. P., and R. W. Reynolds. 1984. The three-dimensional circulation near the eastern North Pacific Subtropical Front. Journal of Physical Oceanography **14**:217-230.

Nurmukhametov, R., L. Volkova, and S. Kabanov. 2006. Fluorescence and absorption of polystyrene exposed to UV laser radiation. Journal of Applied Spectroscopy **73**:55-60.

Ogata, Y., H. Takada, K. Mizukawa, H. Hirai, S. Iwasa, S. Endo, Y. Mato, M. Saha, K. Okuda, A. Nakashima, M. Murakami, N. Zurcher, R. Booyatumanondo, M. P. Zakaria, L. Q. Dung, M. Gordon, C. Miguez, S. Suzuki, C. Moore, H. K. Karapanagioti, S. Weerts, T. McClurg, E. Burres, W. Smith, M. V. Velkenburg, J. S. Lang, R. C. Lang, D. Laursen, B. Danner, N. Stewardson, and R. C. Thompson. 2009. International Pellet Watch: Global monitoring of persistent organic pollutants (POPs) in coastal waters. 1. Initial phase data on PCBs, DDTs, and HCHs. Marine Pollution Bulletin **58**:1437-1446.

Pasulka, A. L., M. R. Landry, D. A. Taniguchi, A. G. Taylor, and M. J. Church. 2013. Temporal dynamics of phytoplankton and heterotrophic protists at station ALOHA. Deep Sea Research Part II: Topical Studies in Oceanography **93**:44-57.

Pavia, D., G. Lampman, G. Kriz, and J. Vyvyan. 2008. Introduction to Spectroscopy. Cengage Learning.

Perissinottoab, R., and E. A. Pakhomov. 1998. The trophic role of the tunicate *Salpa thompsoni* in the Antarctic marine ecosystem. Journal of Marine Systems **17**:361-374.

PerkinElmer. 2005. FT-IR Spectroscopy Attenuated Total Reflectance (ATR).*in* Perkin Elmer Life and Analytical Sciences, http://www.perkinelmer.com.

PlasticsEurope. 2012. Plastics- The Facts 2012: An analysis of European plastics production, demand and waste data for 2011. http://www.plasticseurope.org.

Potgieter-Vermaak, S., B. Horemans, W. Anaf, C. Cardell, and R. V. Grieken. 2012. Degradation potential of airborne particulate matter at the Alhambra monument: a Raman spectroscopic and electron probe X-ray microanalysis study. Journal of Raman Spectroscopy **43**:1570-1577.

Rajakumar, K., V. Sarasvathy, A. T. Chelvan, R. Chitra, and C. Vijayakumar. 2009. Natural weathering studies of polypropylene. Journal of Polymers and the Environment **17**:191-202.

Reimers, C. E., K. C. Ruttenberg, D. E. Canfield, M. B. Christiansen, and J. B. Martin. 1996. Porewater pH and authigenic phases formed in the uppermost sediments of the Santa Barbara Basin. Geochimica et Cosmochimica Acta **60**:4037-4057.

Rochman, C. M., M. A. Browne, B. S. Halpern, B. T. Hentschel, E. Hoh, H. K. Karapanagioti, L. M. Rios-Mendoza, H. Takada, S. Teh, and R. C. Thompson. 2013a. Policy: Classify plastic waste as hazardous. Nature **494**:169-171.

Rochman, C. M., et al. 2015. Anthropogenic debris in seafood: Plastic debris and fibers from textiles in fish and bivalves sold for human consumption. Scientific Reports **5**:14340.

Rochman, C. M., E. Hoh, T. Kurobe, and S. J. Teh. 2013b. Ingested plastic transfers hazardous chemicals to fish and induces hepatic stress. Scientific Reports **3**:3263.

Roden, G. I. 1980. On the subtropical frontal zone north of Hawaii during winter. Journal of Physical Oceanography **10**:342-362.

Rose, A. 1948. The sensitivity performance of the human eye on an absolute scale. JOSA **38**:196-208.

Ryan, P. G., C. J. Moore, J. A. van Franeker, and C. L. Moloney. 2009. Monitoring the abundance of plastic debris in the marine environment. Philosophical Transactions of the Royal Society of London B: Biological Sciences **364**:1999-2012.

Samo, T. J., F. Malfatti, and F. Azam. 2008. A new class of transparent organic particles in seawater visualized by a novel fluorescence approach. Aquatic Microbial Ecology **53**:307-321.

Sato, H., M. Shimoyama, T. Kamiya, T. Amari, S. Šašic, T. Ninomiya, H. W. Siesler, and Y. Ozaki. 2002. Raman spectra of high-density, low-density, and linear low-density polyethylene pellets and prediction of their physical properties by multivariate data analysis. Journal of Applied Polymer Science **86**:443-448.

Schimmelmann, A., I. L. Hendy, L. Dunn, D. K. Pak, and C. B. Lange. 2013. Revised ~2000-year chronostratigraphy of partially varved marine sediment in Santa Barbara Basin, California. GFF **135**:258-264.

Schimmelmann, A., C. B. Lange, and W. H. Berger. 1990. Climatically controlled marker layers in Santa Barbara Basin sediments and fine-scale core-to-core correlation. Limnology and Oceanography **35**:165-173.

Schimmelmann, A., C. B. Lange, E. B. Roark, and B. L. Ingram. 2006. Resources for paleoceanographic and paleoclimatic analysis: a 6,700-year stratigraphy and regional radiocarbon reservoir-age (ΔR) record based on varve counting and 14C-AMS dating for the Santa Barbara Basin, offshore California, USA. Journal of Sedimentary Research **76**:74-80.

Schlining, K., S. von Thun, L. Kuhnz, B. Schlining, L. Lundsten, N. J. Stout, L. Chaney, and J. Connor. 2013. Debris in the deep: Using a 22-year video annotation database to

survey marine litter in Monterey Canyon, central California, USA. Deep Sea Research Part I: Oceanographic Research Papers **79**:96-105.

Scordato, A., S. Schwartz, J. D. Griffin, N. S. Claxton, M. J. Parry-Hill, T. J. Fellers, K. M. Vogt, I. D. Johnson, S. H. Neaves, O. Alvarado, J. Parsons, Lionel , M. A. Sodders, R. L. Ludlow, and M. W. Davidson. 2016. Blue Excitation: B-1A (Longpass Emission) MicroscopyU: The Source for Microscopy Education. Nikon Instruments, Inc.

Service, National Weather. 2017. Cold & Warm Episodes by Season. NOAA National Weather Service, National Weather Service Climate Prediction Center.

Setälä, O., V. Fleming-Lehtinen, and M. Lehtiniemi. 2014. Ingestion and transfer of microplastics in the planktonic food web. Environmental Pollution **185**:77-83.

Shlaer, S., E. L. Smith, and A. M. Chase. 1942. Visual acuity and illumination in different spectral regions. The Journal of general physiology **25**:553-569.

Silver, M., and K. Bruland. 1981. Differential feeding and fecal pellet composition of salps and pteropods, and the possible origin of the deep-water flora and olive-green "cells". Marine Biology **62**:263-273.

Silver, M. W. 1975. The habitat of *Salpa fusiformis* in the California Current as defined by indicator assemblages. Limnology and Oceanography **20**:230-237.

Small, L., S. Fowler, and M. Ünlü. 1979. Sinking rates of natural copepod fecal pellets. Marine Biology **51**:233-241.

Smith, K., A. Sherman, C. Huffard, P. McGill, R. Henthorn, S. Von Thun, H. Ruhl, M. Kahru, and M. Ohman. 2014. Large salp bloom export from the upper ocean and benthic community response in the abyssal northeast Pacific: Day to week resolution. Limnology and Oceanography **59**:745-757.

Socrates, G. 2004. Infrared and Raman characteristic group frequencies: tables and charts. Third Edition edition. John Wiley & Sons, Ltd., Chichester, England.

Stark, N. M., and L. M. Matuana. 2004. Surface chemistry changes of weathered HDPE/wood-flour composites studied by XPS and FTIR spectroscopy. Polymer Degradation and Stability **86**:1-9.

Stefatos, A., M. Charalampakis, G. Papatheodorou, and G. Ferentinos. 1999. Marine debris on the seafloor of the Mediterranean Sea: Examples from two enclosed gulfs in western Greece. Marine Pollution Bulletin **38**:389-393.

Steffen, W., W. Broadgate, L. Deutsch, O. Gaffney, and C. Ludwig. 2015. The trajectory of the Anthropocene: the Great Acceleration. The Anthropocene Review **2**:81-98.

Steffen, W., P. J. Crutzen, and J. R. McNeill. 2007. The Anthropocene: are humans now overwhelming the great forces of nature. AMBIO: A Journal of the Human Environment **36**:614-621.

Stone, J. P., and D. K. Steinberg. 2016. Salp contributions to vertical carbon flux in the Sargasso Sea. Deep Sea Research Part I: Oceanographic Research Papers **113**:90-100.

Supply, Freund Container. 2010. Plastic Properties. Guide to Plastics.

Sutherland, K. R., L. P. Madin, and R. Stocker. 2010. Filtration of submicrometer particles by pelagic tunicates. Proceedings of the National Academy of Sciences **107**:15129-15134.

Taylor, A. G., R. Goericke, M. R. Landry, K. E. Selph, D. A. Wick, and M. J. Roadman. 2012. Sharp gradients in phytoplankton community structure across a frontal zone in the California Current Ecosystem. Journal of Plankton Research **34**:778-789.

Thiel, M., and L. Gutow. 2005. The ecology of rafting in the marine environment. II. The rafting organisms and community. Oceanography and Marine Biology: an annual review **43**:279-418.

Thompson, R. C., Y. Olsen, R. P. Mitchell, A. Davis, S. J. Rowland, A. W. John, D. McGonigle, and A. E. Russell. 2004. Lost at sea: where is all the plastic? Science **304**:838-838.

Thunell, R. C. 1998. Seasonal and annual variability in particle fluxes in the Gulf of California: A response to climate forcing. Deep Sea Research Part I: Oceanographic Research Papers **45**:2059-2083.

Turner, A., S. Fitzer, and G. A. Glegg. 2008. Impacts of boat paint chips on the distribution and availability of copper in an English ria. Environmental Pollution **151**:176-181.

USEPA. 1992. Plastic pellets in the aquatic environment: Sources, and recommendations. Washington, DC.

Van Cauwenberghe, L., A. Vanreusel, J. Mees, and C. R. Janssen. 2013. Microplastic pollution in deep-sea sediments. Environmental Pollution **182**:495-499.

Van Sebille, E., C. Wilcox, L. Lebreton, N. Maximenko, B. D. Hardesty, J. A. Van Franeker, M. Eriksen, D. Siegel, F. Galgani, and K. L. Law. 2015. A global inventory of small floating plastic debris. Environmental Research Letters **10**:124006.

Van Soest, R. 1974. A revision of the genera *Salpa* Forskål, 1775, *Pegea* Savigny, 1816 and *Ritteriella* Metcalf, 1919 (Tunicata, Thaliacea). Beaufortia **22**:153-191.

Van Soest, R. 1975. Zoogeography and speciation in the Salpidae (Tunicata, Thaliacea). Beaufortia **23**:181-215.

Vargas, C. A., and L. P. Madin. 2004. Zooplankton feeding ecology: clearance and ingestion rates of the salps *Thalia democratica*, *Cyclosalpa affinis* and *Salpa cylindrica* on naturally occurring particles in the Mid-Atlantic Bight. Journal of Plankton Research **26**:827-833.

Venrick, E., T. Backman, W. Bartram, C. Platt, M. Thornhill, and R. Yates. 1973. Man-made objects on the surface of the central North Pacific Ocean. Nature **241**:271-271.

Verdugo, P., A. L. Alldredge, F. Azam, D. L. Kirchman, U. Passow, and P. H. Santschi. 2004. The oceanic gel phase: a bridge in the DOM–POM continuum. Marine Chemistry **92**:67-85.

Waters, C. N., J. Zalasiewicz, C. Summerhayes, A. D. Barnosky, C. Poirier, A. Gałuszka, A. Cearreta, M. Edgeworth, E. C. Ellis, and M. Ellis. 2016. The Anthropocene is functionally and stratigraphically distinct from the Holocene. Science **351**:aad2622.

Wilson, D. S. 1973. Food size selection among copepods. Ecology **54**:909-914.

Wong, C., D. R. Green, and W. J. Cretney. 1974. Quantitative tar and plastic waste distributions in the Pacific Ocean. Nature **247**:30-32.

Woodall, L. C., A. Sanchez-Vidal, M. Canals, G. L. Paterson, R. Coppock, V. Sleight, A. Calafat, A. D. Rogers, B. E. Narayanaswamy, and R. C. Thompson. 2014. The deep sea is a major sink for microplastic debris. Royal Society open science **1**:140317.

Wright, S. L., R. C. Thompson, and T. S. Galloway. 2013. The physical impacts of microplastics on marine organisms: a review. Environmental Pollution **178**:483-492.

Yount, J. L. 1954. The taxonomy of the Salpidae (Tunicata) of the central Pacific Ocean. Pacific Salpidae **8**:276-330.

Yount, J. L. 1958. Distribution and ecologic aspects of central Pacific Salpidae (Tunicata). Pacific Science **12**:111-130.

Zalasiewicz, J., A. Smith, M. Hounslow, M. Williams, A. Gale, J. Powell, C. Waters, T. L. Barry, P. R. Bown, and P. Brenchley. 2007. The scale-dependence of strata-time relations: implications for stratigraphic classification. Stratigraphy **4**:139-144.

Zalasiewicz, J., C. N. Waters, J. A. I. do Sul, P. L. Corcoran, A. D. Barnosky, A. Cearreta, M. Edgeworth, A. Gałuszka, C. Jeandel, and R. Leinfelder. 2016. The geological cycle of plastics and their use as a stratigraphic indicator of the Anthropocene. Anthropocene **13**:4-17.

Zalasiewicz, J., C. N. Waters, C. P. Summerhayes, A. P. Wolfe, A. D. Barnosky, A. Cearreta, P. Crutzen, E. Ellis, I. J. Fairchild, and A. Gałuszka. 2017. The Working Group on the Anthropocene: Summary of evidence and interim recommendations. Anthropocene. **19**:55-60.

Zettler, E. R., T. J. Mincer, and L. A. Amaral-Zettler. 2013. Life in the "plastisphere": microbial communities on plastic marine debris. Environmental science & technology **47**:7137-7146.

Zubris, K. A. V., and B. K. Richards. 2005. Synthetic fibers as an indicator of land application of sludge. Environmental Pollution **138**:201-211.